

Phenolic and petrochemical wastewater treatment in AnMBR under extreme conditions High salinity, high temperature, and high concentration of toxic compounds

Garcia Rea, V.S.

DOI

[10.4233/uuid:71b4a574-184e-4b4d-929b-11f7c1e1b2db](https://doi.org/10.4233/uuid:71b4a574-184e-4b4d-929b-11f7c1e1b2db)

Publication date

2023

Document Version

Final published version

Citation (APA)

Garcia Rea, V. S. (2023). *Phenolic and petrochemical wastewater treatment in AnMBR under extreme conditions: High salinity, high temperature, and high concentration of toxic compounds*. [Dissertation (TU Delft), Delft University of Technology]. <https://doi.org/10.4233/uuid:71b4a574-184e-4b4d-929b-11f7c1e1b2db>

Important note

To cite this publication, please use the final published version (if applicable).
Please check the document version above.

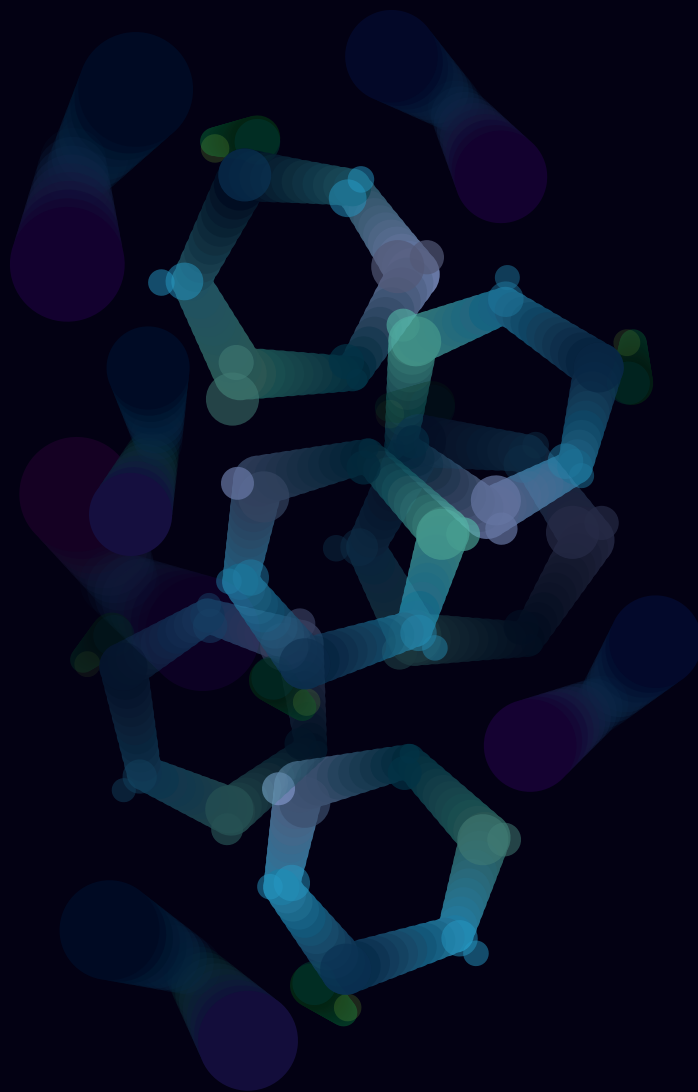
Copyright

Other than for strictly personal use, it is not permitted to download, forward or distribute the text or part of it, without the consent of the author(s) and/or copyright holder(s), unless the work is under an open content license such as Creative Commons.

Takedown policy

Please contact us and provide details if you believe this document breaches copyrights.
We will remove access to the work immediately and investigate your claim.

Phenolic and petrochemical wastewater treatment in AnMBR under extreme conditions



Víctor Servando García Rea

Phenolic and petrochemical wastewater treatment in AnMBR under extreme conditions

**High salinity, high temperature, and high concentration of
toxic compounds**

Víctor Servando GARCIA REA

Phenolic and petrochemical wastewater treatment in AnMBR under extreme conditions

High salinity, high temperature, and high concentration of toxic compounds

Dissertation

for the purpose of obtaining the degree of doctor
at Delft University of Technology
by the authority of the Rector Magnificus Prof.dr.ir. T.H.J.J. van der Hagen,
chair of the Board for Doctorates
to be defended publicly on
Thursday 7th December 2023 at 15:00 o'clock

by

Víctor Servando GARCIA REA

Master of Science in Biological Sciences,
Universidad Nacional Autónoma de México, México,
born in Mexico City, Mexico

This dissertation has been approved by the promotor:

Prof. dr. ir. J. B. van Lier

Dr. ir. H. L. F. M. Spanjers

Composition of the doctoral committee:

Rector Magnificus, chairperson

Prof. dr. ir. J. B. van Lier Delft University of Technology, promotor

Dr. ir. H.L.F.M. Spanjers Delft University of Technology, promotor

Independent members:

Prof. dr. J.A. Field University of Arizona, USA

Prof. dr. F. Cervantes Universidad Nacional Autónoma de México, Mexico

Prof. dr. ir. D. Weissbrodt Norwegian University of Science and
Technology, Norway

Prof. dr. H.M. Jonkers Delft University of Technology

Dr. ir. R. Kleerebezem Delft University of Technology

Reserve member:

Prof. dr. ir. L.C. Rietveld Delft University of Technology

This research was supported by the Dutch Technology Foundation (STW, Project No.13348), which is part of the Netherlands Organization for Scientific Research (NWO), partly funded by the Dutch Ministry of Economic Affairs. This research was co-sponsored by Evides Industrierwater B.V and Paques B.V.

The Mexican National Council of Science and Technology (CONACyT) granted V.S. Garcia Rea the PhD Scholarship No. 410669.

Keywords: Anaerobic digestion, AnMBR, salinity, phenol, phenolic compounds, acetate, thermophilic, *p*-cresol, syntrophic acetate oxidation, resorcinol, carbon and energy sources, bitumen fume condensate, IC₅₀, microbial community.

Cover page and chapter pages design: Flor Armina García Rea.

The cover page and the chapter pages are an abstract representation of the phenolic compounds and microorganisms present in the anaerobic membrane bioreactor. The decrease in the quantity of phenolic compounds represents the anaerobic biodegradation occurring in the reactor.

ISBN: 978-94-93353-44-2

To my country

To my people

To my University

“Por mi raza hablará el espíritu”

Table of contents

Summary	15
Samenvatting	19
Rsumen	25
Abbreviations	30
Chapter I	
Introduction	35
1.1 General introduction and scope of the PhD project	36
1.2 Theoretical framework	39
1.2.1 Anaerobic digestion: microbiological and biochemical aspects	39
1.2.2 Anaerobic digestion for industrial (petro)chemical wastewater treatment	41
1.2.3 Anaerobic membrane bioreactors	45
1.2.4 Application of AnMBRs for industrial (petro)chemical wastewater treatment	47
1.2.5 Thermophilic AD for industrial chemical wastewater	48
1.2.6 Anaerobic treatment of phenolic wastewater	49
1.2.6.1 Anaerobic treatment of phenolic wastewater under thermophilic conditions	50
1.2.7 Biochemical aspects of anaerobic phenol and aromatic compounds degradation	52
1.2.7.1 Anaerobic phenol degradation	52
1.2.7.2 Anaerobic phenol degradation under thermophilic conditions	55
1.2.7.3 Anaerobic degradation of (complex) aromatic compounds	56
1.2.8 Phenol degradation under anaerobic conditions with the addition of external carbon and energy sources	57
1.2.9 Thermodynamic state analysis of microbial biochemical processes in environmental systems	59
1.2.9.1 Microbial metabolism and growth thermodynamics	60
1.2.10 Microbial community dynamics in the anaerobic digestion of industrial wastewater	61
1.3 Outline of the thesis	62
1.4 References	66

Chapter 2

Enhancing phenol conversion rates in saline anaerobic membrane bioreactor using acetate and butyrate as additional carbon and energy sources

	73
2.1 Introduction	75
2.2 Materials and methods	76
2.2.1 Analytical techniques	76
2.2.1.1 Chemical oxygen demand	76
2.2.1.2 Phenol, volatile fatty acids, and benzoate concentrations	76
2.2.2 Batch tests	76
2.2.2.1 Specific methanogenic activity inhibition by phenol	76
2.2.2.2 Phenol degradation tests	77
2.2.3 Experimental setup and reactors operation	77
2.2.3.1 Anaerobic membrane bioreactor setup	77
2.2.3.2 AnMBRs operation and model wastewater composition	78
2.2.4 Microbial community analysis	80
2.2.4.1 DNA extraction, quantification, and amplification	80
2.2.4.2 DNA data processing	80
2.2.4.3 Canonical correspondence analysis	81
2.3 Results and Discussion	81
2.3.1 Acetoclastic SMA inhibition by phenol, and butyrate degradation tests	81
2.3.2 Phenol degradation in batch assays	83
2.3.3 AnMBR operation	83
2.3.3.1 AnMBR operation towards phenol as the main carbon and energy source	83
2.3.3.2 Effect of the addition of acetate on the specific phenol conversion rate	85
2.3.3.3 Effect of the addition of the acetate-butyrate on the specific phenol conversion rate	88
2.3.4 Analysis of the microbial community dynamics during the operation of the reactors	90
2.3.4.1 Microbial community dynamics in the AnMBR towards phenol as the main carbon and energy source	90
2.3.4.2 Microbial community dynamics in the AnMBR with acetate as additional carbon and energy source	91
2.3.4.3 Microbial community dynamics in the AnMBR with the acetate-butyrate mixture	92
2.3.4.4 Canonical correspondence analysis	93
2.3.5 Discussion on the possible phenol-degrading-enhancing mechanisms	93
2.4 Conclusions	97

Chapter 3

Syntrophic acetate oxidation having a key role in thermophilic phenol conversion in anaerobic membrane bioreactor under saline conditions

	103
3.1 Introduction	105
3.2 Materials and methods	106
3.2.1 Anaerobic membrane bioreactor	106
3.2.2 Feeding solution during the different reactor operation stages	106
3.2.3 Chemical and physicochemical analysis	107
3.2.4 Syntrophic acetate oxidation activity in the AnMBR biomass	107
3.2.5 DNA extraction and microbial community dynamics study	107
3.2.6 Targeted Amplicon libraries construction	108
3.2.7 DNA sequencing	108
3.2.8 Statistics and bioinformatics for the analysis of sequences	108
3.2.9 Stoichiometry and thermodynamics of anaerobic growth on phenol under thermophilic conditions	109
3.3 Results and Discussion	109
3.3.1 AnMBR operation for phenol degradation and its simultaneous conversion with acetate	109
3.3.2 Syntrophic acetate oxidation determination by ^{13}C isotope labeling in the continuous operation	112
3.3.3 Phenol degradation intermediates	112
3.3.4 Contribution of the membrane-attached biomass to phenol conversion	114
3.3.5 Membrane analysis	114
3.3.6 Microbial community dynamics	115
3.3.7 Stoichiometry and thermodynamics of anaerobic growth on phenol under thermophilic conditions: effects of hydrogen partial pressure and syntrophic relationships	119
3.4 Conclusions	121
3.5 Outlook, recommendations, and further applications	122
3.6 References	124

Chapter 4

Degradation of *p*-cresol, resorcinol, and phenol in anaerobic membrane bioreactors under saline conditions

	129
4.1 Introduction	131
4.2 Materials and Methods	132
4.2.1 Analytical techniques	132
4.2.1.1 Phenol, <i>p</i> -cresol, and resorcinol concentrations measurement	132
4.2.1.2 COD, volatile fatty acids, and biogas composition determination	133
4.2.2 Batch tests	133
4.2.2.2 Anerobic biodegradability tests for <i>p</i> -cresol and resorcinol by phenol-degrading biomass	133
4.2.2.3 Specific methanogenic activity inhibition and cellular membrane damage	134
4.2.3 Simultaneous degradation of phenol with <i>p</i> -cresol or resorcinol	135
4.2.3.1 Anaerobic membrane bioreactors operation	135
4.2.3.2 DNA extraction for microbial community composition analysis	136
4.2.3.3 16S rRNA gene amplification, sequencing, and data processing	136
4.2.4 Thermodynamic state analysis	137
4.3 Results	137
4.3.1 Anaerobic biodegradability of <i>p</i> -cresol and resorcinol by phenol-degrading biomass	137
4.3.2 Specific methanogenic activity inhibition and cell viability	138
4.3.2.1 Simultaneous degradation of phenol and resorcinol	143
4.3.3 Thermodynamic state analysis	146
4.3.3.1 <i>p</i> -Cresol	146
4.3.3.2 Resorcinol	146
4.4 Discussion	146
4.5 Conclusions	154
4.6 References	156

Chapter 5

Chemical characterization and anaerobic treatment of bitumen fume condensate using a membrane bioreactor

	161
5.1 Introduction	163
5.2 Materials and Methods	164
5.2.1 Chemical oxygen demand and volatile suspended solids	164
5.2.2 Characterization of the organic compounds in the BFC	164
5.2.2.1 Targeted analysis: gas chromatography-tandem mass spectrometry	165
5.2.2.2 Non-targeted analysis: gas chromatography-mass spectrometry quadrupole time of flight	165
5.2.3 Elemental analysis by inductively coupled plasma mass spectrometry	168
5.2.4 Precipitation of the metals in the BFC	168
5.2.5 Effect of the BFC on the specific methanogenic activity and cell membrane integrity of anaerobic biomass	168
5.2.5.1 Specific methanogenic activity inhibition	168
5.2.5.2 Cell membrane integrity determination	169
5.2.6 AnMBR operation	169
5.2.6.1 AnMBR setup	169
5.2.6.2 AnMBR feeding medium and operational conditions	170
5.2.7 Microbial community dynamics	170
5.2.7.1 Biomass sampling, DNA extraction, 16S rRNA gene amplification, and DNA data processing	170
5.3 Results and Discussion	171
5.3.1 Bitumen fume condensate characterization	171
5.3.1.1 COD	171
5.3.1.2 Phenol and volatile fatty acids	172
5.3.1.3 Organic compounds targeted analysis: GC-MS/MS	172
5.3.1.4 Organic compound non-targeted analysis: GC-MS QTOF	173
5.3.1.5 Elemental analysis by inductively coupled plasma mass spectrometry	173
5.3.2 Biochemical tests	173
5.3.2.1 Specific methanogenic activity inhibition	173
5.3.2.3 Microbial community structure of the three biomass sources	178
5.3.3 BFC biodegradation in AnMBR	180
5.3.3.1 Conversion rates and COD & phenol removal efficiencies	180
5.3.3.2 Microbial community dynamics in the AnMBR	186
5.4 References	190

Chapter 6

Conclusions, outlook, and recommendations	197
6.1 Conclusions	198
6.2 Outlook and research recommendations	200
6.2.1 Safety recommendations for working with toxic compounds	201
6.2.1.1 Safety at work	201
6.2.1.2 Chemicals	201
6.2.1.3 Guidelines in case of chemical spill	202
6.2.2 Guidance for practical application: results implication	202
6.2.3 Guidance for practical application: full-scale implementation	205
6.2.4 Research recommendations	206
6.3 References	209
 Appendix A1	
Supplementary material Chapter 1	211
 Appendix A2	
Supplementary material Chapter 2	215
 Appendix A3	
Supplementary material Chapter 3	223
 Appendix A4	
Supplementary material Chapter 5	229
 Professional acknowledgments	242
Personal acknowledgments	245
About the author	250
List of publications	252

Summary

Anaerobic digestion (AD) is a biochemical process in which organic matter is converted into biogas in a series of biochemical reactions. The development of high-rate anaerobic reactors (HRAR) led to the breakthrough of full-scale applications of AD for the treatment of industrial wastewater. HRARs, such as the upflow anaerobic sludge blanket (UASB) or the expanded granular sludge bed (EGSB) reactors are characterized by long solids retention times obtained by the gravitational separation of the solids from the liquid. Enhanced biomass retention is facilitated by the formation and growth of granular methanogenic biomass in EGSB and, most commonly also, in UASB reactors treating industrial wastewaters.

Since the late 1970's anaerobic technology has been increasingly applied for the treatment of several types of industrial wastewater. AD was initially and successfully used for the treatment of wastewater coming from agro-food industries and related sectors. Hereafter, AD was also applied for the treatment of more complex wastewater, such as those coming from chemical and petrochemical industries. Full-scale applications on these types of wastewater, however, were less successful because of operational problems caused by biomass degranulation, biomass loss, and prevailing toxicity, for instance. As a result, the total number of full-scale installations used for the treatment of (petro)chemical effluents remained limited. Particularly, the more extreme chemical characteristics of these types of wastewaters such as high content of toxic and inhibitory compounds, high salt concentration, and sometimes high temperature, led to reluctance in the (petro)chemical sector to use AD as a wastewater treatment alternative. Both high salinity and high temperature may cause poor granulation or even disruption of the granular structure of the sludge, which may result in biomass washout and eventually reactor failure.

Anaerobic membrane bioreactors (AnMBR) offer the possibility of full biomass retention. In an AnMBR, a microfiltration (MF) or ultrafiltration (UF) membrane is coupled to the bioreactor. Therefore, independently of the characteristics of the wastewater to be treated, all biomass will be kept inside the bioreactor. Full biomass retention is especially important for the development of a proper microbiome, commonly consisting of slow-growing microorganisms that are needed for the degradation of the toxic and inhibitory compounds, as well as the ultimate conversion of the organics into methane. Because of the presence of an “absolute” barrier, AnMBRs are regarded as a viable option for the treatment of chemical and petrochemical wastewater.

The goal of this PhD research was to achieve stable, and enhanced, anaerobic biodegradation of synthetic phenolic (phenol, *p*-cresol, and resorcinol) wastewater under saline conditions and efficient treatment of real petrochemical wastewater using AnMBR technology. Furthermore, the potentials for thermophilic conditions (55°C) for phenol degradation were also assessed. The overall research question of this thesis was: “Is it possible to enhance the anaerobic treatment of phenolics-containing wastewater under saline conditions, applying a wide temperature range using AnMBRs?”

Therefore, in this PhD study the degradation under saline anaerobic conditions of the three model aromatic compounds phenol, *p*-cresol, and resorcinol was researched using bench scale AnMBRs (7 L). Furthermore, the treatability of a petrochemical wastewater, namely bitumen fume condensate (BFC), was assessed using the same AnMBR reactors.

Phenol, and other phenolic compounds, can be present in several types of (petro) chemical wastewater in concentrations ranging from few milligrams to several grams per liter. Moreover, (petro)chemical wastewater is often characterized by high salinity, owing to the characteristics of the raw material and the industrial production processes. Phenol conversion at 8 gNa⁺·L⁻¹ was studied using both phenol as the sole carbon and energy source (CES) and in the presence of easily biodegradable CES, namely, acetate and butyrate, that are compounds commonly found in petrochemical wastewater. Acetate is a compound which can be directly used by acetoclastic methanogens, whereas butyrate is firstly oxidized to acetate and H₂, prior to methanogenesis. As such, the presence of butyrate is expected to promote both acetoclastic and hydrogenotrophic methanogenesis. The reactor fed with phenol as the sole CES could not sustain continuous phenol degradation. Specific phenol conversion rates (sPhCR) of 115 and 210 mgPh·gVSS⁻¹·d⁻¹ were determined in the AnMBR fed with acetate [2 gCOD·L⁻¹] or a 2:1 acetate-butyrate [2 gCOD·L⁻¹] mixture as additional CES, respectively. The microbial community study of the reactor's biomass performed by the analysis of specified regions of the 16S rRNA gene revealed that the syntrophic phenol degrader *Syntrophorhabdus* sp. and the acetoclastic methanogen *Methanosaeta* sp. were the most abundant microorganisms. In the reactors fed with acetate or the acetate-butyrate mixture, the relative abundance of *Syntrophorhabdus* sp. reached values of up to 63% and 55%, respectively. A canonical correspondence analysis (CCA) showed that the microbial community structure had a direct correlation with the specific phenol loading rate (sPhLR) and sPhCR.

Since petrochemical wastewaters are often characterized by high temperatures, thermophilic (55 °C) saline [6.5 gNa⁺·L⁻¹] phenol degradation was also studied using the AnMBR. The research focused on the enhancement of the sPhCR using acetate as additional CES, identification of possible biochemical conversion routes of phenol and acetate, thermodynamic considerations, presence of syntrophic associations, and study of the microbial community dynamics in the thermophilic AnMBR biomass. The results revealed that phenol degradation was limited when phenol [0.5 g·L⁻¹] was the sole substrate. However, phenol removal efficiency increased significantly ($p < 0.001$) to 80%, which corresponded to a sPhCR of 29 mgPh·gVSS⁻¹·d⁻¹ when acetate was simultaneously fed to the reactor. A microbial community analysis of the reactor's biomass and a ¹³C isotopic study using ¹²CH₃¹³COO⁻ for the reactor feeding strongly suggested that acetate was converted via syntrophic acetate oxidation (SAO) coupled to hydrogenotrophic methanogenesis. In addition, the data showed that phenol conversion under saline thermophilic conditions followed the benzoyl-CoA pathway, similarly as under mesophilic conditions. Notably, no sound phenol degraders such as *Syntrophorhabdus* sp. were found; a result opposite to the findings in the mesophilic reactor. Nevertheless, the biofilm developed on the membrane that was rich in hydrogenotrophic methanogens and putative SAO bacteria showed to have a high phenol-catabolic activity, leading to the appearance of benzoate in the permeate.

Once the phenol degradation experiments were completed, the degradation of more complex phenolic mixtures comprising phenol-*p*-cresol and phenol-resorcinol were studied. Batch experiments showed that the phenol-degrading AnMBR-biomass had a broader metabolic capacity than expected, since it was able to degrade the *p*-cresol and resorcinol without a previous exposure to these compounds. Emphasis was placed on the determination of the inhibitory and toxic effects of the phenolic compounds on the previously phenol-adapted biomass and the specific phenolic conversion rates achieved in the membrane bioreactors using the phenol-adapted biomass as seed material. Half maximal inhibitory concentrations (IC₅₀) of 0.73 g_{*p*-cresol}·L⁻¹ and 3.00 g_{resorcinol}·L⁻¹ were estimated for the acetoclastic methanogens of the AnMBR-cultivated phenol-degrading biomass, whereas IC₅₀ values of 0.60 g_{*p*-cresol}·L⁻¹ and 0.25 g_{resorcinol}·L⁻¹ were estimated for the non-adapted biomass. In both biomass sources, flow cytometry analysis showed that *p*-cresol caused a higher decrease in the non-damaged cell counts in comparison to resorcinol. Therefore, it was concluded that *p*-cresol displayed a rather biocidal inhibition, whereas for resorcinol it was defined as biostatic inhibition. Subsequently, two AnMBRs were fed with phenol-*p*-cresol or phenol-resorcinol under saline conditions [8.0 gNa⁺·L⁻¹]. Maximum conversion rates of 22 mg_{*p*-cresol}·gVSS⁻¹·d⁻¹ and 16 mg_{resorcinol}·gVSS⁻¹·d⁻¹ were found.

For the last experiment, the use of an AnMBR for the degradation of real petrochemical wastewater produced during the reclaimed asphalt pavement process was studied. BFC wastewater coming from an asphalt and road industry located in the Netherlands was chemically characterized. The non-targeted analyses identified approximately 900 organic and inorganic compounds, including polycyclic aromatic hydrocarbons, phenolic compounds, and metallic ions. Experiments for the determination of the toxic and inhibitory effects of the wastewater on three different anaerobic biomass types were conducted. The different biomass types were harvested from a municipal wastewater treatment plant digester, a granular-biomass reactor treating benzoate, and a phenol-degrading AnMBR. The IC_{50} values were determined for each of the biomass sources. The AnMBR-cultivated phenol-degrading biomass showed to be less inhibited with an IC_{50} of $990 \text{ mgCOD}\cdot\text{L}^{-1}$. Subsequently, a mesophilic AnMBR was operated for 180 days and was fed with a mixture of BFC, phenol, acetate, and nutrients. The COD concentration in the reactor feeding varied between 0.6 and $2.4 \text{ gCOD}\cdot\text{L}^{-1}$. The reactor showed a maximum COD removal efficiency of 88% that corresponded to a sludge conversion rate (SCR) of $286 \pm 71 \text{ mgCOD}\cdot\text{L}^{-1}\cdot\text{d}^{-1}$.

The results described in this thesis showed the feasibility of the application of AnMBRs for the treatment of phenolic wastewater at high sodium concentrations and the positive effects of the simultaneous digestion of phenol with easily degradable CES on the sPhCRs. Furthermore, the prerequisite presence of acetate as additional CES for phenol conversion in AnMBR under saline thermophilic conditions was shown. However, lower sPhCR rates were found in comparison to the mesophilic operation. Moreover, with the help of ^{13}C isotopic ($^{12}\text{CH}_3^{13}\text{COO}^-$), analytical, and microbial community analyses, a clearer picture of the degradation pathway of phenol and acetate under thermophilic conditions was obtained. It was also shown that AnMBR-cultivated phenol-degrading methanogenic biomass had a broader catabolic activity than expected and was more resilient to the inhibition or toxicity caused by compounds such as, *p*-cresol, resorcinol, or BFC. Finally, this research was the first to report the successful treatment of BFC wastewater under anaerobic conditions.

The results obtained in this thesis open the possibilities for the application of AnMBRs for the treatment of (petro)chemical wastewater under extreme biological conditions, which expands the limits of the applicability of anaerobic digestion.

Samenvatting

Anaërobe vergisting (AD) is een biochemisch proces waarbij organisch materiaal in een reeks biochemische reacties wordt omgezet in biogas. De ontwikkeling van high-rate anaerobe reactoren (HRAR) leidde tot de doorbraak van full-scale toepassingen van AD voor de behandeling van industrieel afvalwater. HRAR's, zoals de upflow anaerobic sludge blanket (UASB) of de expanded granular sludge bed (EGSB) reactors, worden gekenmerkt door lange verblijftijden van vaste stoffen die worden verkregen door de scheiding van vaste stoffen en vloeistoffen op basis van verschillen in dichtheid. Verbeterde retentie van biomassa wordt vergemakkelijkt door de vorming en groei van korrelvormige methanogene biomassa in EGSB en, meestal ook, in UASB-reactoren die industrieel afvalwater behandelen.

Sinds het einde van de jaren 1970 wordt anaërobe technologie in toenemende mate toegepast voor de behandeling van verschillende soorten industrieel afvalwater. AD werd aanvankelijk met succes gebruikt voor de behandeling van afvalwater afkomstig van de agrovoedingsindustrie en aanverwante sectoren. Hierna werd AD ook toegepast voor de behandeling van complexere stromen, zoals afvalwater dat afkomstig is van de chemische en petrochemische industrie. Voor dit type afvalwater waren echter niet veel toepassingen succesvol vanwege problemen zoals degranulatie van biomassa, verlies van biomassa of lage CZV-verwijderingsefficiënties. Als gevolg was er slechts een beperkt aantal full-scale installaties die werd gebruikt voor de behandeling van dit complexer afvalwater. De terughoudendheid voor het gebruik van AD werd voornamelijk veroorzaakt door problemen die verband houden met de extremere chemische eigenschappen van dit soort afvalwater, zoals een hoog gehalte aan giftige en remmende verbindingen, een hoge zoutconcentratie en soms een hoge temperatuur. Zowel een hoog zoutgehalte als een hoge temperatuur kunnen leiden tot slechte korrelvorming of zelfs verstoring van de korrelstructuur van het slib, wat kan leiden tot verlies van biomassa met een slecht functionerende anaerobe reactor tot gevolg.

Anaërobe membraanbioreactoren (AnMBR) bieden de mogelijkheid om biomassa volledig te behouden. In een AnMBR wordt een microfiltratie (MF) of ultrafiltratie (UF) membraan gekoppeld aan de bioreactor. Daarom zal alle biomassa, onafhankelijk van de kenmerken van het te behandelen afvalwater, in de bioreactor worden vastgehouden. Volledige retentie van biomassa is vooral belangrijk voor de ontwikkeling van een goed microbioom, dat gewoonlijk bestaat uit langzaam groeiende micro-organismen die nodig zijn voor de afbraak van de toxische en remmende verbindingen, evenals de uiteindelijke omzetting van de organische stoffen in methaan. Vanwege de

aanwezigheid van een “absolute” barrière worden AnMBR's beschouwd als een geschikte optie voor de behandeling van chemisch en petrochemisch afvalwater.

Het doel van dit promotieonderzoek was om zowel stabiele en verbeterde anaërobe biologische afbraak van synthetisch fenolhoudend (fenol, *p*-cresol en resorcinol) afvalwater onder zoute omstandigheden als efficiënte behandeling van echt petrochemisch afvalwater te bereiken met behulp van AnMBR-technologie. Bovendien werden ook de mogelijkheden voor de afbraak van fenol onder thermofiele omstandigheden (55°C) onderzocht. De hoofdvraag van dit proefschrift was: is het mogelijk om de anaerobe behandeling van fenolhoudend afvalwater onder zoute omstandigheden te verbeteren met behulp van AnMBR's?

Om deze vraag te kunnen beantwoorden werd in dit promotieonderzoek de afbraak van de drie aromatische verbindingen fenol, *p*-cresol en resorcinol onder zoute en anaërobe omstandigheden onderzocht met behulp van AnMBR's op laboratoriumschaal (7 L). Daarnaast werd de behandelbaarheid van een petrochemisch afvalwater, namelijk condensaat van bitumendamp (BFC), onderzocht met behulp van dezelfde AnMBR-reactoren.

Fenol en andere fenolverbindingen kunnen in verschillende soorten (petro)chemisch afvalwater aanwezig zijn in concentraties variërend van enkele milligrammen tot enkele grammen per liter. Bovendien wordt (petro)chemisch afvalwater vaak gekenmerkt door hoge zoutconcentraties voortkomend uit zowel de eigenschappen van de grondstoffen als ook het industriële productieproces. Fenolomzetting onder zoute omstandigheden [8 gNa⁺·L⁻¹] werd zowel bestudeerd met fenol als enige koolstof- en energiebronnen (CES) als ook in aanwezigheid van gemakkelijk afbreekbare CES's die vaak worden aangetroffen in petrochemisch afvalwater, zoals acetaat en butyraat. Acetaat is een verbinding die rechtstreeks door de (acetoclastische) methanogenen wordt gebruikt, terwijl butyraat een substraat is waarvan wordt verwacht dat het zowel acetoclastische als hydrogenotrofe methanogenese bevordert. De reactor die met fenol als enige CES werd gevoed kon de continue afbraak van fenol niet volhouden. Specific phenol conversion rates (sPhCR) van 115 en 210 mgPh·gVSS⁻¹·d⁻¹ werden bepaald in de AnMBR met respectievelijk acetaat [2 gCOD·L⁻¹] en een 2:1 acetaat-butyraat [2 gCOD·L⁻¹] mengsel als extra CES. De microbiomstudie van de biomassa in de reactor, uitgevoerd door de analyse van gespecificeerde regio's van het 16S rRNA-gen, liet zien dat de syntrofische fenolafbreker *Syntrophorhabdus* sp. en het acetoclastische methanogeen *Methanosaeta* sp. de meest voorkomende micro-organismen waren. In de reactoren die werden gevoed met acetaat en het acetaat-butyraatmengsel als extra CES bereikte de relatieve talrijkheid van *Syntrophorhabdus* sp. waarden tot respectievelijk 63% en

55%. Een canonical correspondence analysis (CCA) toonde aan dat de structuur van de microbiële gemeenschap een directe correlatie had met de specific phenol loading rate (sPhLR) en sPhCR.

Aangezien petrochemisch afvalwater vaak wordt gekenmerkt door hoge temperaturen werd fenolafbraak in thermofiele (55 °C) en zoute omstandigheden [6.5 gNa⁺·L⁻¹] ook bestudeerd met behulp van de AnMBR. Het onderzoek richtte zich op de verbetering van de sPhCR met acetaat als aanvullende CES, identificatie van mogelijke biochemische omzettingroutes van fenol en acetaat, thermodynamische overwegingen, aanwezigheid van syntrofische associaties en studie van de dynamiek van de microbiële gemeenschap in de thermofiele AnMBR-biomassa. De resultaten toonden aan dat de afbraak van fenol beperkt was wanneer fenol [0.5 g·L⁻¹] het enige substraat was. De efficiëntie van de fenolverwijdering nam echter aanzienlijk toe ($p < 0.001$) tot 80%, wat overeenkomt met een sPhCR van 29 mgPh·gVSS⁻¹·d⁻¹, wanneer acetaat tegelijkertijd aan de reactor werd toegevoerd. Een microbiële gemeenschapsanalyse van de biomassa van de reactor en een ¹³C-isotopenstudie met ¹²CH₃¹³COO voor de reactorvoeding suggereerden sterk dat acetaat werd omgezet via syntrofische acetaatoxidatie (SAO) gekoppeld aan hydrogenotrofe methanogenese. Bovendien toonden de gegevens aan dat omzetting van fenol onder zoute en thermofiele omstandigheden de benzoyl-CoA-route volgde, op dezelfde manier als onder mesofiele omstandigheden. Opmerkelijk is dat er geen fenolafbrekers zoals *Syntrophorhabdus* sp. werden gevonden, een resultaat dat tegengesteld is aan de bevindingen in de mesofiele reactor. Niettemin bleek de biofilm die zich ontwikkelde op het membraan, dat rijk was aan hydrogenotrofe methanogenen en vermeende SAO-bacteriën, een hoge fenol-katabole activiteit te hebben, wat leidde tot de aanwezigheid van benzoaat in het permeaat.

Na voltooiing van de experimenten voor afbraak van fenol werd de afbraak van complexere fenolmengsels, bestaande uit fenol-*p*-cresol en fenol-resorcinol, bestudeerd. Batch-experimenten toonden aan dat de fenolafbrekende AnMBR-biomassa een bredere metabolische capaciteit had dan verwacht, omdat het in staat was om *p*-cresol en resorcinol af te breken zonder eerdere blootstelling aan deze stoffen. De nadruk werd gelegd op de bepaling van de remmende en toxische effecten van de fenolverbindingen op de reeds aan fenol aangepaste biomassa en op de specifieke fenol omzettingssnelheden die werden bereikt in de membraanbioreactoren met behulp van de aan fenol aangepaste biomassa als entmateriaal. Half maximal inhibitory concentrations (IC₅₀) van 0.73 g_{p-cresol}·L⁻¹ en 3.00 g_{resorcinol}·L⁻¹ werden geschat voor de acetoclastische methanogenen van de AnMBR-gekweekte fenolafbrekende biomassa, terwijl IC₅₀-waarden van 0.60 g_{p-cresol}·L⁻¹ en 0.25 g_{resorcinol}·L⁻¹ werden geschat voor de niet-aangepaste biomassa. In beide biomassabronnen veroorzaakte *p*-cresol een hogere afname van het aantal niet-

beschadigde cellen in vergelijking met resorcinol, zoals blijkt uit de resultaten van de flowcytometrie-analyse. Daarom werd geconcludeerd dat *p*-cresol biocideremming vertoonde, terwijl het voor resorcinol werd gedefinieerd als biostatische remming. Vervolgens werden twee AnMBR's gevoed met fenol-*p*-cresol of fenol-resorcinol onder zoute omstandigheden [8.0 g·Na⁺·L⁻¹]. Er werden maximale omzettingssnelheden van 22 mg_{*p*-cresol}·gVSS⁻¹·d⁻¹ en 16 mg_{resorcinol}·gVSS⁻¹·d⁻¹ gevonden.

Voor het laatste experiment werd het gebruik bestudeerd van een AnMBR voor de afbraak van petrochemisch afvalwater dat wordt geproduceerd tijdens het teruggewinnen van asfaltbeton. BFC-afvalwater afkomstig van de asfalt- en wegenindustrie in Nederland werd chemisch en fysisch-chemisch gekarakteriseerd. De niet gerichte analyses identificeerden ongeveer 900 organische en anorganische verbindingen, waaronder polycyclische aromatische koolwaterstoffen, fenolverbindingen en metaalionen. Er werden experimenten uitgevoerd voor de bepaling van de toxische en remmende effecten van het afvalwater op drie verschillende soorten anaerobe biomassa. De verschillende soorten biomassa werden onttrokken uit een vergister van een communale rioolwaterzuiveringsinstallatie, een korrelslibreactor die benzoaat behandelt en de fenolafbrekende AnMBR. Voor elk van de biomassabronnen zijn de IC₅₀-waarden bepaald. De AnMBR-gekweekte fenolafbrekende biomassa bleek met een IC₅₀ van 990 mgCOD·L⁻¹ minder geremd te zijn door het BFC-afvalwater dan de biomassa uit de overige bronnen. Vervolgens was gedurende 180 dagen een mesofiele AnMBR in werking welke werd gevoed met een mengsel van BFC, fenol, acetaat en voedingsstoffen. De CZV-concentratie in de reactorvoeding varieerde tussen 2.4 en 0.6 gCOD·L⁻¹. De reactor vertoonde een maximale CZV-verwijderingsefficiëntie van 88%, wat overeenkomt met een slib omzettingssnelheid (SCR) van 286 ± 71 mgCOD·L⁻¹·d⁻¹.

De in dit proefschrift beschreven resultaten toonden de haalbaarheid aan van de toepassing van AnMBR's voor de behandeling van fenolhoudend afvalwater bij hoge natriumconcentraties en de positieve effecten van de gelijktijdige vergisting van fenol met gemakkelijk afbreekbare CES op de sPhCR's. Bovendien werd de vereiste aanwezigheid van acetaat als extra CES voor fenolomzetting onder zoute en thermofiele omstandigheden aangetoond. Er werden echter lagere sPhCR-percentages gevonden in vergelijking met de mesofiele omstandigheden. Bovendien werd met behulp van ¹³Cisotopen (¹²CH₃¹³COO⁻), analytische en microbioomanalyses een duidelijker beeld verkregen van de afbraakroute van fenol en acetaat onder thermofiele omstandigheden. Er werd ook aangetoond dat AnMBR-gekweekte fenolafbrekende methanogene biomassa een bredere katabole activiteit had dan verwacht en beter bestand was tegen de remming of toxiciteit veroorzaakt door verbindingen zoals *p*-cresol, resorcinol, of BFC. Ten slotte

was dit onderzoek het eerste dat melding maakte van de succesvolle behandeling van BFC-afvalwater onder anaërobe omstandigheden.

De resultaten van dit proefschrift tonen de mogelijkheden voor de toepassing van AnMBR's voor de behandeling van (petro)chemisch afvalwater onder extreme biologische omstandigheden, waardoor de grenzen van de toepasbaarheid van anaerobe vergisting worden verlegd.

Resumen

La digestión anaerobia (DA) es un proceso bioquímico en el que la materia orgánica se convierte en biogás en una serie de reacciones bioquímicas. El desarrollo de los reactores anaerobios de alta tasa, o HRAR por sus siglas en inglés, condujo al avance de las aplicaciones a gran escala de la DA para el tratamiento de aguas residuales industriales. Los HRAR, como los reactores de manto de lodos anaerobios de flujo ascendente (UASB) o de lecho de lodos granulares expandidos (EGSB), se caracterizan por largos tiempos de retención de sólidos obtenidos por la separación gravitacional de los sólidos del líquido. El aumento en la retención de la biomasa se ve facilitado por la formación y el crecimiento de biomasa metanogénica granular en los EGSB y, comúnmente, también en los reactores UASB que tratan aguas residuales industriales.

Desde finales de la década de 1970, la tecnología anaerobia se ha aplicado cada vez más para el tratamiento de varios tipos de aguas residuales industriales. La DA se utilizó inicialmente y con éxito para el tratamiento de aguas residuales procedentes de industrias agroalimentarias y sectores afines. A partir de entonces, la DA también se trató de aplicar para el tratamiento de aguas residuales más complejas, como las procedentes de las industrias química y petroquímica. Sin embargo, las aplicaciones a gran escala (full-scale) en estos tipos de aguas residuales tuvieron menos éxito debido a problemas operativos causados, por ejemplo, por la degranulación y pérdida de biomasa, y la toxicidad inherente de las mismas aguas. Como resultado, el número total de instalaciones a gran escala utilizadas para el tratamiento de efluentes (petro) químicos ha sido limitado. En particular, las características químicas extremas de este tipo de aguas residuales, como el alto contenido de compuestos tóxicos e inhibitorios, la alta concentración de sal y, a veces, la alta temperatura, llevaron a la reticencia en el sector (petro)químico a utilizar la DA como alternativa para el tratamiento de aguas residuales. Tanto la alta salinidad como la alta temperatura pueden causar una granulación deficiente o incluso la pérdida de la estructura granular del lodo, lo que puede provocar el lavado de la biomasa fuera del reactor y, por lo tanto, inminente la falla del reactor.

Los biorreactores anaerobios de membrana (AnMBR) ofrecen la posibilidad de una retención total de la biomasa. En un AnMBR, una membrana de microfiltración (MF) o ultrafiltración (UF) es acoplada al biorreactor. Por lo tanto, toda la biomasa se mantendrá dentro del biorreactor independientemente de las características de las aguas residuales a tratar. La retención total de la biomasa es especialmente importante para el desarrollo de un microbioma adecuado, que suele consistir en microorganismos de crecimiento lento, mismos que son necesarios para la degradación de los

compuestos tóxicos e inhibitorios, así como para la conversión final en metano de los compuestos orgánicos presentes en las aguas residuales. Debido a la presencia de una barrera “absoluta”, los AnMBR se consideran una opción viable para el tratamiento de aguas residuales químicas y petroquímicas.

El objetivo de esta investigación doctoral fue lograr una biodegradación anaerobia estable e incrementada de aguas residuales fenólicas sintéticas (fenol, *p*-cresol y resorcinol) en condiciones salinas y un tratamiento eficiente de aguas residuales petroquímicas reales utilizando la tecnología AnMBR. Además, se evaluaron el potencial de la degradación de fenol en condiciones termofílicas (55 °C). La pregunta principal de investigación de esta tesis fue: “¿Es posible mejorar el tratamiento anaerobio de aguas residuales que contienen compuestos fenólicos en condiciones salinas, aplicando un amplio rango de temperatura, utilizando AnMBR?”

Por lo tanto, en este estudio de doctorado se investigó la degradación anaerobia y en condiciones salinas de los tres compuestos aromáticos modelo fenol, *p*-cresol, y resorcinol utilizando AnMBRs a escala laboratorio (7 L). Además, se evaluó la capacidad de tratamiento de un agua residual petroquímica como es el condensado de humos del bitumen (BFC) utilizando los mismos reactores AnMBR.

El fenol, y otros compuestos fenólicos, pueden estar presentes en varios tipos de aguas residuales (petro)químicas en concentraciones que van desde unos pocos miligramos hasta varios gramos por litro. Además, las aguas residuales (petro)químicas suelen caracterizarse por una alta salinidad, debido a las características de la materia prima y los procesos de producción industrial. La degradación de fenol se estudió en un medio con una concentración de 8 gNa⁺·L⁻¹. El experimento se realizó utilizando tanto fenol como única fuente de carbono y energía (CES) como en presencia de CES fácilmente biodegradables, por ejemplo, acetato y butirato, que son compuestos que se encuentran comúnmente en las aguas residuales petroquímicas. El acetato es un compuesto que puede ser utilizado directamente por los metanógenos acetoclásticos, mientras que el butirato se oxida a acetato e hidrógeno (H₂) antes de la metanogénesis. Como tal, se esperaba que la presencia de butirato promoviera la metanogénesis acetoclástica e hidrogenotrófica. El reactor alimentado con fenol como única CES no pudo mantener una degradación continua del fenol. En cambio, se determinaron tasas específicas de conversión de fenol (sPhCR) de 115 y 210 mgPh·gVSS⁻¹·d⁻¹ en el AnMBR alimentado con acetato [2 gCOD·L⁻¹] o con una mezcla acetato-butirato 2:1 [2 gCOD·L⁻¹] como CES adicionales, respectivamente. El estudio de la comunidad microbiana de la biomasa del reactor realizado mediante el análisis de regiones específicas del gen 16S rRNA reveló que el degradador sintrófico de fenol *Syntrophorhabdus* sp. y el metanógeno

acetoclástico *Methanosaeta* sp. fueron los microorganismos más abundantes. En los reactores alimentados con acetato o la mezcla acetato-butirato, la abundancia relativa de *Syntrophorhabdus* sp. alcanzó valores de hasta 63% y 55%, respectivamente. Un análisis de correspondencias canónicas (CCA) mostró que la estructura de la comunidad microbiana tenía una correlación directa con la tasa de carga específica de fenol (sPhLR) y la sPhCR.

Dado que las aguas residuales petroquímicas a menudo se caracterizan por estar a altas temperaturas, se estudió también la degradación del fenol usando AnMBR en condiciones salinas [6,5 gNa⁺·L⁻¹] y termofílicas (55 °C). La investigación se centró en la mejora de la sPhCR utilizando acetato como CES adicional, la identificación de posibles rutas de conversión bioquímica de fenol y acetato, consideraciones termodinámicas de las conversiones, presencia de asociaciones sintróficas en el (micro)bioma del reactor, y el estudio de la dinámica de la comunidad microbiana en la biomasa termofílica del AnMBR. Los resultados revelaron que la degradación del fenol estuvo en exceso limitada cuando el fenol [0.5 g·L⁻¹] se utilizó como único sustrato. Sin embargo, la eficiencia de remoción de fenol aumentó significativamente ($p < 0,001$) a 80% cuando se alimentó simultáneamente acetato al reactor. El aumento de remoción correspondió a una sPhCR de 29 mgPh·gVSS⁻¹·d⁻¹. Un análisis de la comunidad microbiana de la biomasa del reactor y un estudio isotópico de ¹³C utilizando ¹²CH₃¹³COO⁻ para la alimentación del reactor sugirieron fuertemente que el acetato fue convertido a través del proceso conocido como oxidación sintrófica del acetato (SAO, por sus siglas en inglés) acoplado a la metanogénesis hidrogenotrófica. Además, los datos mostraron que la conversión de fenol en condiciones termófilas salinas siguió la vía del benzoil-CoA, de manera similar a como lo hace en condiciones mesófilas. Cabe destacar que no se encontraron claros degradadores de fenoles como *Syntrophorhabdus* sp., un resultado opuesto a los hallazgos obtenidos en el reactor mesófilo. Sin embargo, la biopelícula desarrollada en la membrana era abundante en metanógenos hidrogenotróficos y bacterias SAO putativas. La biopelícula mostró tener una alta actividad catabólica (degradación de fenol) lo que llevó a la aparición de benzoato en el permeado del reactor.

Una vez finalizados los experimentos de degradación de fenol, se estudió la degradación de mezclas fenólicas más complejas, por ejemplo, fenol-*p*-cresol y fenol-resorcinol. Los experimentos por lotes mostraron que la biomasa degradadora de fenol cultivada en el AnMBR tenía una capacidad metabólica más amplia de lo esperado, ya que fue capaz de degradar el *p*-cresol y el resorcinol sin haber tenido una exposición previa a estos compuestos. De igual manera, se hizo hincapié en, a) la determinación de los efectos inhibitorios y tóxicos de los compuestos fenólicos sobre la biomasa previamente adaptada al fenol y b), la determinación de las tasas

específicas de conversión de los fenólicos alcanzadas en los biorreactores de membrana cuando se utilizó la biomasa adaptada al fenol como material semilla. Concentraciones inhibitorias medias (IC_{50}) de $0,73 \text{ g}_{\text{p-cresol}} \cdot \text{L}^{-1}$ y $3,00 \text{ g}_{\text{resorcinol}} \cdot \text{L}^{-1}$ fueron estimadas para los metanógenos acetoclásticos de la biomasa degradadora de fenol cultivada con AnMBR, mientras que valores de IC_{50} de $0,60 \text{ g}_{\text{p-cresol}} \cdot \text{L}^{-1}$ y $0,25 \text{ g}_{\text{resorcinol}} \cdot \text{L}^{-1}$ se estimaron para la biomasa no adaptada. El análisis de citometría de flujo mostró que en ambos tipos de biomasa, el *p*-cresol causó una mayor disminución en los recuentos de células no dañadas en comparación con el resorcinol. Por lo tanto, se concluyó que el *p*-cresol mostró una inhibición biocida, mientras que para el resorcinol, la inhibición se definió como biostática. Posteriormente, dos AnMBRs fueron alimentados con mezclas de fenol-*p*-cresol o fenol-resorcinol en condiciones salinas [$8,0 \text{ gNa}^+ \cdot \text{L}^{-1}$]. Se encontraron tasas máximas de conversión de $22 \text{ mg}_{\text{p-cresol}} \cdot \text{gVSS}^{-1} \cdot \text{d}^{-1}$ y $16 \text{ mg}_{\text{resorcinol}} \cdot \text{gVSS}^{-1} \cdot \text{d}^{-1}$.

Para el último experimento, se estudió el uso de un AnMBR para la degradación de aguas residuales petroquímicas producidas durante el proceso de recuperado de pavimento. Por lo tanto, se caracterizaron químicamente las aguas residuales de BFC procedentes de una industria de asfalto situada en los Países Bajos. Los análisis químicos no-dirigidos (non-targeted) identificaron aproximadamente 900 compuestos orgánicos e inorgánicos, incluidos hidrocarburos aromáticos policíclicos, compuestos fenólicos e iones metálicos. Así mismo, se realizaron experimentos para la determinación de los efectos tóxicos e inhibitorios de las aguas residuales petroquímicas sobre tres tipos diferentes de biomasa anaerobia. Los diferentes tipos de biomasa se recolectaron de a) un digestor de de lodos en una planta de tratamiento de aguas residuales municipales, b) un reactor de biomasa granular que trata benzoato y c) un AnMBR degradador de fenol. Los valores de IC_{50} fueron determinados para cada una de las fuentes de biomasa. La biomasa degradadora de fenol cultivada en el AnMBR mostró ser más resistente a la inhibición por el BFC, mostrando un valor de IC_{50} de $990 \text{ mgDQO} \cdot \text{L}^{-1}$. Posteriormente, se operó un AnMBR mesofílico durante 180 días, mismo que se alimentó con una mezcla de BFC, fenol, acetato y nutrientes. La concentración de DQO en la alimentación del reactor varió entre $0,6$ y $2,4 \text{ gDQO} \cdot \text{L}^{-1}$. El reactor mostró una eficiencia máxima de remoción de DQO del 88% que correspondió a una tasa de conversión de lodos (SCR) de $286 \pm 71 \text{ mgDQO} \cdot \text{L}^{-1} \cdot \text{d}^{-1}$.

Los resultados descritos en esta tesis mostraron la viabilidad de la aplicación de los AnMBRs para el tratamiento de aguas residuales fenólicas a altas concentraciones de sodio y los efectos positivos de la digestión simultánea de fenol(icos) con CES fácilmente biodegradables sobre las tasas específicas de conversión de fenol(icos). Además, se demostró que la presencia de acetato como CES adicional es un requisito para la conversión de fenol en AnMBR en condiciones termofílicas salinas. Sin embargo,

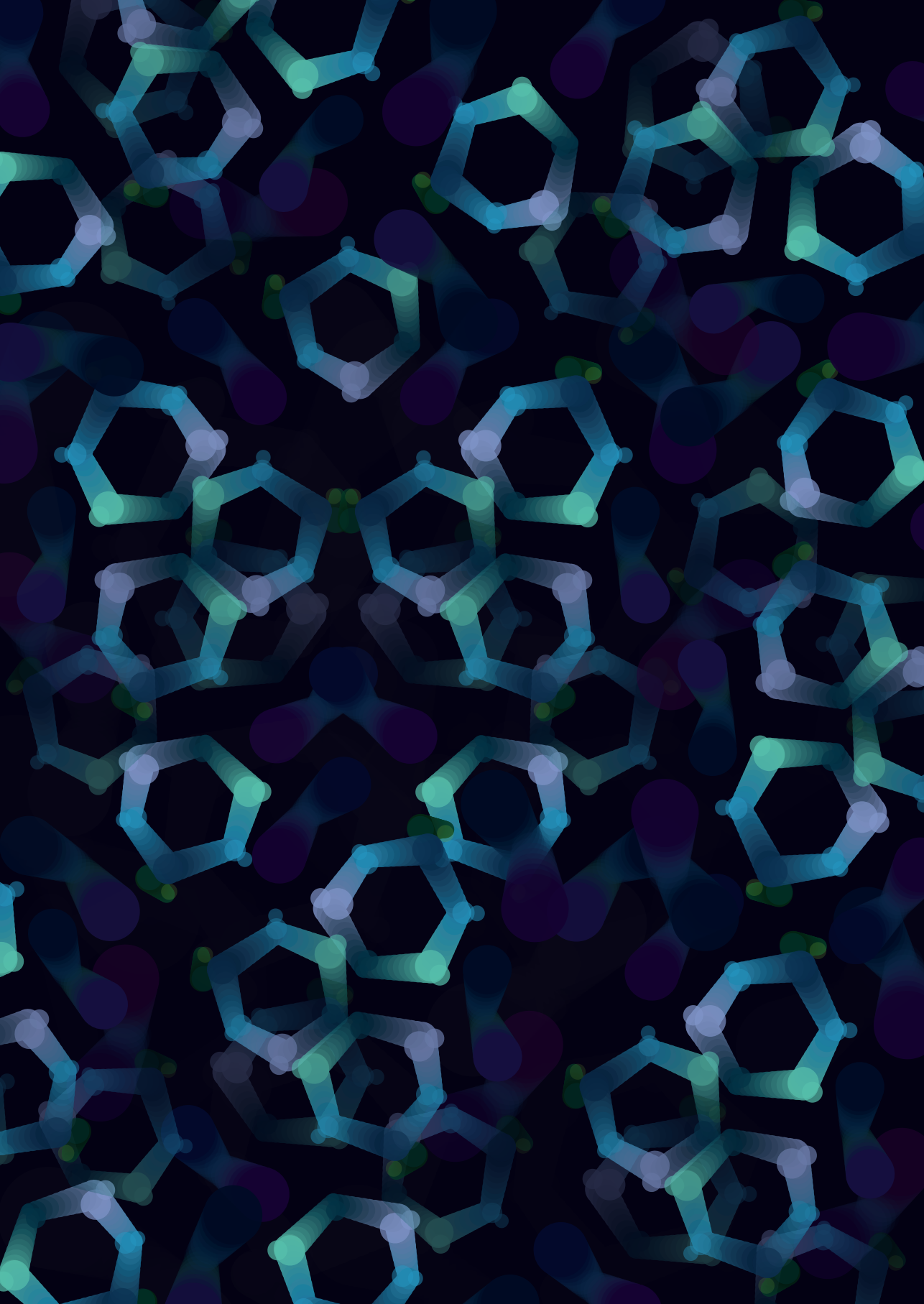
se encontraron tasas específicas de conversión de fenol más bajas en comparación con la operación mesofílica. Además, con la ayuda de los análisis isotópicos de ^{13}C ($^{12}\text{CH}_3^{13}\text{COO}^-$), de química analítica, y de la comunidad microbiana, se obtuvo una imagen más clara de la vía de degradación del fenol y el acetato en condiciones termofílicas. También se demostró que la biomasa metanogénica degradadora de fenol y cultivada en el AnMBR tenía una actividad catabólica más amplia de lo esperado y era más resistente a la inhibición o toxicidad causada por compuestos como *p*-cresol, resorcinol, o BFC. Finalmente, esta investigación fue la primera en reportar el tratamiento exitoso de aguas residuales de BFC en condiciones anaerobias.

Los resultados obtenidos en esta tesis abren las posibilidades de la aplicación de AnMBRs para el tratamiento de aguas residuales (petro)químicas en condiciones biológicas extremas, lo que amplía los límites de la aplicabilidad de la digestión anaerobia.

Abbreviations

PH ₂	Hydrogen partial pressure
ABR	Anaerobic baffled reactor.
AD	Anaerobic Digestion
AFFT	Multiple alignment using fast Fourier transform.
AnMBR	Anaerobic membrane bioreactor.
ANOVA	Analysis of variance.
BFC	Bitumen fume condensate.
BTEX	Benzene, toluene, ethylbenzene, xylene.
CES	Carbon and energy source.
CGWW	Coal gasification wastewater.
COD	Chemical oxygen demand.
DNA	Deoxyribonucleic acid.
EGSB	Expanded granular sludge bed.
ESEM	Environmental scanning electron microscope.
FCM	Flow cytometry.
GC	Gas chromatography.
GC-FIC	Gas chromatography with flame ionization detector.
GC-QTOF	Gas chromatography quadrupole-time-of-flight.
GC-TCD	Gas chromatography with a thermal conductivity detector.
HAIB	Horizontal flow anaerobic immobilized.
HM	Hydrogenotrophic methanogenesis.
HPLC	High-performance liquid chromatography.
HRT	Hydraulic retention time.
IC ₅₀	Half maximal inhibitory concentration.
ICP-MS	Inductively coupled plasma mass spectrometry.
MWWTP	Municipal wastewater treatment plant.
NIST	National Institute of Standards and Technology.
OCR	Organic conversion rate.
OLR	Organic loading rate.
PAH	Polycyclic aromatic compounds.
PCoA	Principal coordinate analysis.
PDB	Pee Dee Belemnite.
PTA	Purified terephthalic acid.
PVDF	Polyvinylidene fluoride.
qPCR	Real-time polymerase chain reaction.
RAP	Reclaimed asphalt pavement.
rRNA	Ribosomal ribonucleic acid.

$r_{s,s}$	Specific substrate uptake rate.
$r_{s,v}$	Volumetric substrate uptake rate.
SAO	Syntrophic acetate oxidation.
SAOB	Syntrophic acetate-oxidizing bacteria.
SBBR	Sequencing batch biofilm reactor.
SCR	Sludge conversion rate.
SLR	Sludge loading rate.
SMA	Specific methanogenic activity.
$s_{p\text{-cresol}}^{CR}$	Specific <i>p</i> -Cresol conversion rate.
$sPhCR$	Specific phenol conversion rate.
$sPhLR$	Specific phenol loading rate.
$s_{resorcinol}^{CR}$	Specific resorcinol conversion rate.
SRT	Solids retention time.
TOC	Total organic carbon.
TSS	Total suspended solids.
UASB	Upflow anaerobic sludge blanket reactor.
VFA	Volatile fatty acids.
VOC	Volatile organic compounds.
$vOLR$	Volumetric organic loading rate.
$v_{p\text{-cresol}}^{LR}$	Volumetric <i>p</i> -Cresol loading rate.
$v_{resorcinol}^{LR}$	Volumetric resorcinol loading rates.
VSS	Volatile suspended solids.
ΔG_R°	Standard Gibbs free energy change.
ΔG_R^{O1}	Gibbs free energy change under standard conditions but pH = 7.
$\Delta G_R^{1,T}$	Gibbs free energy change with corrections for temperature and concentrations/partial pressures.
$\delta^{13}C_{PDB}(CH_4)$	¹³ C delta in methane.
γ	Degree of reduction.



Chapter I

Introduction

This chapter is partially based on: Garcia Rea Víctor S., Muñoz Sierra Julian D., Fonseca Aponte Laura M., Cerqueda-Garcia Daniel, Quchani Kiyan M., Spanjers Henri, van Lier Jules B. (2020). Enhancing Phenol Conversion Rates in Saline Anaerobic Membrane Bioreactor Using Acetate and Butyrate as Additional Carbon and Energy Sources. *F. Microbiol.*, 11. DOI: 10.3389/fmicb.2020.604173.

Garcia Rea Víctor S., Muñoz Sierra Julian D., El-Kalliny Amer S., Cerqueda-Garcia Daniel, Lindeboom Ralph E.F., Spanjers Henri, van Lier Jules B. (2023). Syntrophic acetate oxidation having a key role in thermophilic phenol conversion in anaerobic membrane bioreactor under saline conditions, *Chem. Eng. J.*, 455. DOI: <https://doi.org/10.1016/j.cej.2022.140305>.

Garcia Rea Víctor S., Egerland Bueno B., Cerqueda-Garcia Daniel, Muñoz Sierra Julian D., Spanjers Henri, van Lier Jules B. (2022). Degradation of p-cresol, resorcinol, and phenol in anaerobic membrane bioreactors under saline conditions. *Chem. Eng. J.*, 430. DOI: <https://doi.org/10.1016/j.cej.2021.132672>.

Garcia Rea Víctor S., Egerland Bueno B., Muñoz Sierra Julian D., Nair Athira, Lopez Prieto Israel J., Cerqueda-Garcia Daniel, van Lier Jules B., Spanjers Henri. (2023). Chemical characterization and anaerobic treatment of bitumen fume condensate using a membrane bioreactor. *J. Hazard. Mater.*, 477. DOI: <https://doi.org/10.1016/j.jhazmat.2022.130709>.

1.1 General introduction and scope of the PhD project

The application of anaerobic digestion (AD) for the treatment of wastewater has been studied for several decades (Lettinga, 2014; Van Lier et al., 2020). Important developments were obtained in the Netherlands, mainly at Wageningen University & Research and Delft University of Technology (Lettinga, 2014). Anaerobic technology was, however, initially considered to be unsuitable for the treatment of all types of industrial wastewater (van Lier et al., 2001); for example, it was commonly accepted that anaerobic biomass, mainly the methanogens, would not be able to withstand all adverse conditions that can be expected with chemical industrial wastewater. Nevertheless, some studies have shown that for the treatment of chemical compounds anaerobic technologies can be as robust as the aerobic technologies (Kleerebezem et al., 1999; van Lier et al., 2001). For some compounds, anaerobic or sequenced anaerobic-aerobic conversions are required to achieve a complete degradation of the organic pollutants (van Lier et al., 2001). For example, the double azo bond ($-N=N-$) in the azo dyes of textile wastewater requires reductive conditions for breaking the oxidized atomic bond. Likewise, poly-nitro-aromatics and polyols are refractory under aerobic conditions (Macarie, 2000; van Lier et al., 2001).

The presence of active biomass and its efficient retention is one of the most important factors for the proper functioning of anaerobic reactors. A constraint in anaerobic wastewater treatment is that anaerobic biomass is characterized by a low growth rate and low growth yield. Moreover, anaerobic biomass may grow dispersedly, which makes the poor settling biomass prone to wash-out from the continuous flow reactor systems. Therefore, the occurrence of biomass granulation represented a major advance in the application of AD for (industrial) wastewater treatment (van Lier et al., 2001), which allowed the implementation of high-rate “sludge bed” reactors, such as the upflow anaerobic sludge blanket (UASB) reactor, or the expanded granular sludge bed (EGSB) reactors. These types of reactors, including others, are known as high-rate anaerobic reactors (HRAR). HRAR are characterized by a high concentration of active biomass ($> 40 \text{ kgVSS}\cdot\text{m}^{-3}$) and thus a high volumetric metabolic conversion capacity that notably improves the reactor's performance and the quality of the treated effluent. However, the extremely adverse characteristics of some industrial wastewater continued to be a problem even for these types of reactors causing, for example, inhibition of the biomass or biomass washout from the reactor, following after granular sludge disintegration (Dereli et al., 2012).

Characteristics such as the presence of toxic or inhibitory compounds, high temperature, and high dissolved-salts concentrations are typical of (petro)chemical wastewater and are considered biologically extreme for the anaerobic digestion

process (de Oliveira Souza et al., 2015; Díaz et al., 2002; Kong et al., 2019; Zhao and Liu, 2016). Furthermore, the combination of these characteristics may cause biomass degranulation that results in the washout of the biomass. The use of membrane units in the so-called anaerobic membrane bioreactor (AnMBR) technology, was proposed as a way to prevent possible biomass loss by the adverse effects of these types of wastewater (Dereli et al., 2012). Moreover, the concentration of any biodegradable toxic compound can be kept below the inhibitory concentrations because of the completely mixed flow behavior in AnMBRs; therefore, preventing possible disruptions in the biochemical processes, like the sensitive methanogenesis step.

An AnMBR is a bioreactor that is coupled to a membrane module that acts as a filter. Commonly, the used bioreactor can be characterized as a completely stirred tank reactor (CSTR) whereas the membranes can be classified as micro- (MF), ultra (UF), or nanofiltration (NF) membranes depending on their nominal pore size. A membrane with an adequate pore size must be employed to effectively retain the required biomass in the reactor. For example, full biomass retention is required in the case of slowly growing, suspended toxicant-degrading anaerobic microorganisms that only manifest at long solids retention times (SRTs). Their retention in the bioreactor ensures the proper performance of the reactor regardless of the settling capacity of the biomass. However, too narrow pore sizes result in operational difficulties such as low membrane porosity, low fluxes, and high transmembrane pressures (TMP). It should be noted that in AnMBR systems, UF membranes are commonly applied. The resulting quality of the AnMBR effluent or permeate is much higher than in systems without membranes. In fact, the suspended solids free permeate is ideal feed water for any subsequent water reclamation process. Currently, water reclamation is a common target for many companies in search for closing water loops in the production process.

The development of high-rate anaerobic reactor technology, and specifically the granular sludge bed technology, allowed for a rapid increase in the implementation of anaerobic treatment systems for industrial wastewater, particularly those coming from the food and beverage industries. As a result, the number of full-scale installations steadily grew in the past decades (Van Lier et al., 2020). Next to food processing wastewater, AD also showed to be applicable to wastewater generated by chemical and petrochemical industries (Macarie, 2000). However, the wastewater characteristics of the latter industries, such as, presence of toxicity, high salinity, and high temperatures, negatively affect the performance of the anaerobic treatment process (Dereli et al., 2012). Effective biomass retention using biofilms or granular sludge require long start-up periods, while due to the mentioned extreme conditions, such biomass retention is not always possible to achieve. However, in an AnMBR, complete biomass

retention can be accomplished because of the use of MF or UF membrane modules. AnMBR technology has been applied more frequently for the treatment of industrial wastewater (Dvořák et al., 2015); however, there are only a few laboratory studies on the treatment of (petro)chemical wastewater under extreme conditions, for example, high salinity and high temperature (Muñoz Sierra, 2022).

The goal of this PhD research was to achieve stable, and enhanced, anaerobic biodegradation of synthetic phenolic (phenol, *p*-cresol, and resorcinol) wastewater under saline conditions, in addition to efficient treatment of real petrochemical wastewater using AnMBR technology. The research addressed the main research question: “Is it possible to enhance the anaerobic treatment of phenolics-containing wastewater under saline conditions, applying a wide temperature range using AnMBRs?”

Addition of external and easily biodegradable carbon and energy sources (CES), such as the volatile fatty acids butyrate and acetate, were expected to increase the specific conversion rates of phenol and the phenolics under saline mesophilic conditions. The use of these compounds was aimed to promote and sustain the methanogenic populations, both acetoclastic (using acetate or butyrate), and hydrogenotrophic (using butyrate). The use of acetate as additional CES was also expected to increase the specific phenol conversion rate under thermophilic conditions, although to a lower extent. It was hypothesized that phenol-degrading biomass would be capable to also degrade *p*-cresol, because *p*-cresol and phenol share the same biochemical degradation pathway. However, the capacity of phenol degrading sludge to degrade resorcinol was thought to be non-existent, as resorcinol has its own degradation route. Therefore, it was expected that the microbial communities degrading mixtures of phenol-*p*-cresol or phenol-resorcinol would be different. Similarly, it was expected that the phenol-degrading biomass grown in the AnMBR would exhibit higher tolerance to the toxic effects of another toxic phenolic compound, including those found in petrochemical wastewater. Lastly, it was expected that AnMBR conditions, characterized by long SRTs, would allow for the development of slow-growing biomass, capable of treating toxic or inhibitory petrochemical wastewater.

The knowledge acquired in this research may be applied for a variety of (petro)chemical industries. Furthermore, the possibility of water reclamation after AnMBR treatment provides a solution to the depletion of freshwater sources in industrialized areas. The key topics considered for the thesis are:

- Assessment of the degradation performance of the AnMBR biomass when treating toxic compounds, such as phenol and phenolic compounds, under saline mesophilic

conditions. For example, determination of specific loading and conversion rates [$\text{mg}_{\text{phenolic}} \cdot \text{gVSS}^{-1} \cdot \text{d}^{-1}$].

- Assessment of degradation performance of phenol in an AnMBR under saline and thermophilic conditions and gaining insight into the required microbial interactions when the reactor is operated at high temperatures.
- Study on the effects of additional carbon and energy sources on 1) the phenol removal efficiency and phenol conversion rates in AnMBRs under saline and mesophilic or thermophilic conditions, and 2) on the microbial population dynamics of the AnMBRs' biomass.
- Assessment of reactor performance during the simultaneous degradation of multiple phenolic compounds under saline mesophilic conditions.
- Investigation of inhibition and toxicity phenomena caused by phenolic compounds or real petrochemical wastewater on anaerobic biomass.
- Research on the feasibility of AnMBR for the treatment of real (petro)chemical wastewater (pilot studies).

1.2 Theoretical framework

1.2.1 *Anaerobic digestion: microbiological and biochemical aspects*

Anaerobic digestion (AD) is a biochemical process that consists of a series of redox reactions, performed in the absence of molecular oxygen, in which complex organic matter is converted into simpler gaseous compounds. The end product, named biogas, is a mixture of mainly methane (CH_4), carbon dioxide (CO_2), hydrogen sulfide (H_2S), hydrogen (H_2), nitrogen (N_2), and water vapor.

AD is conducted by a variety of microorganisms, namely bacteria and archaea, that share a complex metabolic, trophic, and energetic network (Figure. 1.1). The microorganisms in AD are usually classified into four main physiological groups that perform subsequent conversion phases or stages:

1. Hydrolysis

The first stage in AD is hydrolysis; in this stage macromolecules such as polysaccharides, proteins, and fats are broken down mainly by the action of enzymes that are secreted by hydrolytic bacteria or attached to their membrane. During hydrolysis less complex (monomeric or dimeric) compounds are formed. These simple compounds can be solubilized and metabolized by fermentative microorganisms.

2. Acidogenesis

In the second stage, the soluble compounds that are taken up by fermentative microorganisms are further degraded into more simple compounds such as volatile fatty acids (VFA), alcohols, lactic acid, CO_2 , H_2 , and new biomass.

3. Acetogenesis

In the third stage of AD, acetogenesis, the compounds that were formed during acidogenesis are further fermented into acetate with H_2 and CO_2 as byproducts. Acetate is the main precursor for the subsequent stage.

4. Methanogenesis

In the last stage of the AD, methane (the most reduced compound of carbon) is formed. Only a few species of microorganism are involved in methane production during AD: the methanogens. These are comprised solely by archaea, and depending on the substrate that is converted into methane, they can be classified in acetoclastic (acetate), hydrogenotrophic (mainly CO_2 and H_2), or methylotrophic (C_1 compounds) methanogens.

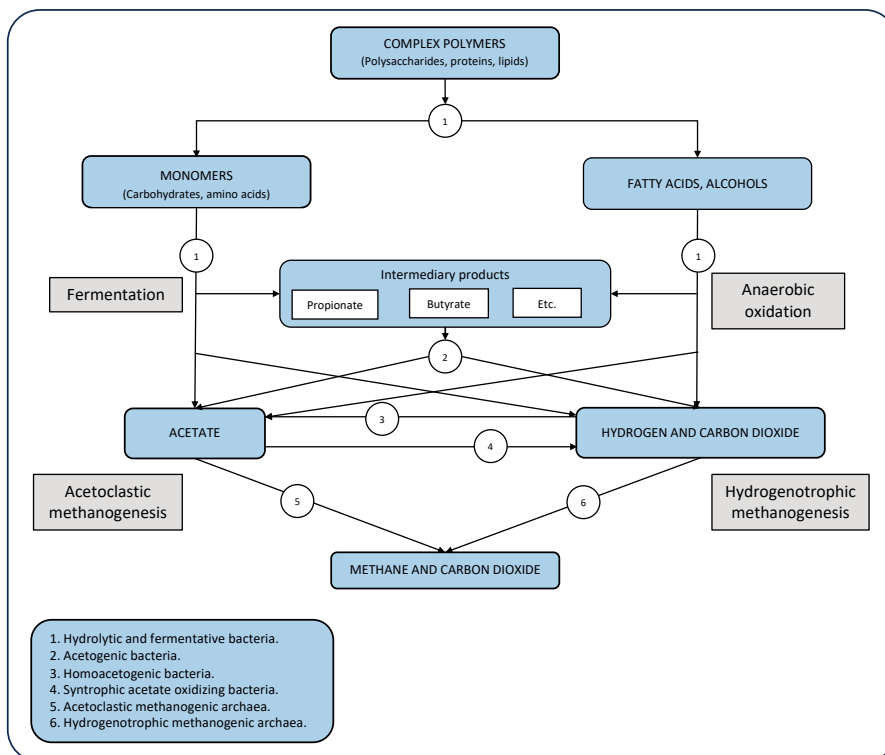


Figure 1.1. Stages in the AD process and the involved physiological microbial groups (van Lier et al., 2023).

1.2.2 *Anaerobic digestion for industrial (petro)chemical wastewater treatment*

AD has become a mature and robust technology for the treatment of industrial wastewater (Van Lier et al., 2015). The application of anaerobic wastewater technology has expanded over the last 40 to 50 years, treating effluents that were considered not viable for this type of process, for example chemical and petrochemical wastewater (Macarie, 2000; Van Lier et al., 2015).

One of the major breakthroughs in the application of AD to industrial wastewater was the development of a new generation of reactors also known as high-rate anaerobic reactors (HRARs). HRARs are based on a high biomass retention capacity, which allows them to overcome drawbacks implicit to anaerobic digestion such as the low growth rate of biomass (Macarie, 2000; Van Lier et al., 2015). In the HRARs, the sludge retention time (SRT) became independent of the hydraulic retention time (HRT), which allows HRTs of several hours with SRTs of months and volumetric organic loading rates (vOLR) ranging from 4 to 40 kgCOD·m³·d⁻¹ (Van Lier et al., 2015). AD was applied mainly for the treatment of foodindustry wastewater, for example, bakery, brewery, cannery, dairy, distillery, and fish and potatoes processing (van Lier et al., 2001). However, it was shown that AD is also useful for the treatment of wastewater coming from industries such as the chemical and petrochemical (Kleerebezem et al., 1999; Macarie, 2000).

The first studies for the application of AD for the treatment of chemical and petrochemical wastewater were performed in the 1970s. However, 1980s saw an increase in the installation of reactors that treated what could be considered as non-conventional wastewater for anaerobic technology (Macarie, 2000). These reactors included the UASB reactor of Shell, Moerdijk, The Netherlands, which degraded benzoate-polluted wastewater; the Celanese reactor in Texas, USA which degraded wastewater with a mixture of VFA, polyesters and acrylic esters; or the Capco reactor of Amoco, which treated purified terephthalic acid (PTA) wastewater in Taiwan (Macarie, 2000).

Currently, industries favor high-rate reactor technology, with the UASB and EGSB reactors as the most implemented (Van Lier et al., 2015). Nevertheless, the last decades have seen a development of high-rate anaerobic reactors that depend less on the granulation process for biomass retention and several of these reactors were successfully applied (Van Lier et al., 2015; Van Lier et al., 2020).

Previous research studies investigated the anaerobic treatment of (petro)chemical wastewater (Table 1.1), but most of these studies focused on the degradation of specific compounds such as purified terephthalic acid (PTA) (Guyot et al., 1990; Kleerebezem

et al., 2005; Noyola et al., 2000), benzene, toluene, ethylbenzene, and xylenes (BTEX) (Ribeiro et al., 2013). AD indeed showed to be a feasible option for the treatment of those types of wastewater with reactors that achieved COD removal efficiencies exceeding 80%. However, poor reactor performances with low COD removal efficiencies (45%) were also reported (Guyot et al., 1990).

Table 1.1. Research studies using AD for the degradation of petrochemical wastewater.

Reference	Reactor	Temp (°C)	HRT	vOLR	Operation time
(Guyot et al., 1990).	UASB	33	3 d	2.6 kg COD·m ⁻³ d ⁻¹	194 d
(Kennes et al., 1997).	UASB	35	0.67 d	2-4 g COD·L ⁻¹ d ⁻¹	50 d
(Kleerebezem et al., 1997).	UASB	30	24 h	4.5 g COD·L ⁻¹ d ⁻¹	160 d
(Noyola et al., 2000).	UASB (real scale)	40	-	5.9 kg COD·m ⁻³ d ⁻¹	10 m
(Kleerebezem and Lettinga, 2000).	Hybrid and UASB	37	UASB: 2-5 h Two-stages reactor: 10-15 h	-	300 d
(Kleerebezem et al., 2005).	UASB	37	First stage: 4.7-5.3 d Second Stage: 2.9-5.2 d Third Stage: 2.2-2.9 d	1.6 g COD·L ⁻¹ d ⁻¹	398 d
(Almendariz et al., 2005).	EGSB	30	2 d	1.5 g COD·L ⁻¹ d ⁻¹	344 d
(Ji et al., 2009).	ABR	20-30	60 h	0.5 kg COD·m ⁻³ d ⁻¹	212 d (first 164 d was the start-up period)
(Wang et al., 2010).	UASB	37	24 h	3.5 g COD·m ⁻³ d ⁻¹	Start-up: 1-227 d Operation: 228-359 d
(Wang, Wei et al., 2011).	UASB	37	48 h	1.0 kg COD·m ⁻³ d ⁻¹	Single feed mode: 168 d Step feed mode: 120 d
(Gasim et al., 2012).	UASB	25-29	40 h	1.21 kg COD·m ⁻³ d ⁻¹	170 d
(Garcia-Mancha et al., 2012).	EGSB	20 and 25	-	0.5/10.5 g COD·L ⁻¹ d ⁻¹	80 d
(Jafarzadeh et al., 2012)	UASB/ Filter	35	4-48 h	0.5-24 kg COD·m ⁻³ d ⁻¹	Start-up: 60 d Operation: 160 d

Substrate	Concentration	Removal percentage	Additional carbon/energy source
Effluent from a petrochemical plant producing terephthalic acid	6 g·L ⁻¹	46%	No
p-Cresol	650 ppm	80%	VFA
Terephthalate	720 mg COD·L ⁻¹	89%	Sucrose
Terephthalic acid production wastewater	10.3 g COD·L ⁻¹	47%	No
Terephthalic acid production wastewater	3 g COD·L ⁻¹		Acetate/benzoate
Terephthalate	2.5 g COD·L ⁻¹	90%	Acetate/benzoate
Refinery spent caustics (SC, from desulfurization units) diluted with sour water (SW, from discharge pipeline)	SC : 364.1 g·L ⁻¹ SW: 1.6 g·L ⁻¹	90%	Phenol/Cresols
Heavy oil-produced water from Liaohe Oilfield, China	TN: 7.8 mg·L ⁻¹ TP: 0.4 mg·L ⁻¹	65%	No
Raw CGWW	2-3.5 g COD·L ⁻¹	71%	Methanol
Raw CGWW	2.5 g COD·L ⁻¹	50%	Phenol/Sodium Acetate
Petroleum refinery wastewater	356 mg·L ⁻¹ 2048 mg COD·L ⁻¹	83%	No
Used industrial oils recovery plant wastewater (mainly ethylene-glycol)	94 g COD·L ⁻¹ 27.6 ± 0.9 g ethylene-glycol L ⁻¹	75%	No
Petrochemical wastewater collected from a petroleum refinery	1 - 4 g·L ⁻¹	42-85%	No

Table 1.1. Continued

Reference	Reactor	Temp (°C)	HRT	vOLR	Operation time
(Wang et al., 2013).	AnMBR	28-30	2,5,7,10 d	11, 4.4, 3.1 and 2.2 kg COD·m ⁻³ d ⁻¹	160 d
(Bhattacharyya et al., 2013).	AnMBR	35	25 d	1.5 - 3.4 kg COD·m ⁻³ d ⁻¹	45 d
(Ribeiro et al., 2013).	HAIB	30	13.5 -20 h	-	200 d
(Siddique et al., 2014).	CSTR	37	10 d	6.3 kg COD·m ⁻³ d ⁻¹	145 d

Fewer studies have dealt with complex and real petrochemical wastewater (Table 1.1). Coal gasification wastewater (CGWW) is a typical toxic/inhibitory matrix with similar compounds as those reported in BFC, such as phenolics and polycyclic aromatic hydrocarbons (PAH). (Wang et al., 2010) reported the application of AD to treat this wastewater, either with the dosage of methanol (500 mg·L⁻¹) as an additional carbon and energy source or by using a step-feed strategy (Wang, Wei et al., 2011). These studies reported enhanced COD and phenol removal efficiencies between 55% and 75%, when an OLR of 3.5 kgCOD·m⁻³d⁻¹ was applied for the former study (Wang et al., 2010), and with influent concentrations of 2,500 mgCOD·L⁻¹ and 500 mgPhenol·L⁻¹ for the latter (Wang, Wei et al., 2011). (Gasim et al., 2012) reported the degradation of petroleum refinery wastewater using UASB reactors, under six OLRs between 0.6 and 4.1 kgCOD·m⁻³d⁻¹. The conclusion of their study was that AD in UASB reactors is suitable to treat the petroleum refinery wastewater. The UASB reactor achieved a COD removal efficiency of 83% (effluent COD = 350 mg·L⁻¹) at an OLR of 1.2 kgCOD·m⁻³d⁻¹. (Jafarzadeh et al., 2012) reported the treatment of petrochemical wastewater with pollutants such as ethylene, propylene, benzene, among others. The hybrid reactor (UASB/Filter) treated OLRs between 0.5 and 24 kgCOD_{total}·m⁻³d⁻¹, with an HRT of 4-48 h and removal efficiencies between 42-86%. Most of the studies conducted for the anaerobic treatment of petrochemical wastewater have reported the usage of sludge bed reactors, such as UASB and EGSB reactors, even when petrochemical wastewater may hamper the anaerobic granulation process (Table 1.1).

In addition to granulation, biomass retention can be achieved through other methods.. An example is separation facilitated by a physical barrier, which acts as a biomass filter. This concept is applied in anaerobic membrane bioreactors or AnMBRs.

Substrate	Concentration	Removal percentage	Additional carbon/energy source
Bamboo industry wastewater (alkenes, benzenes, esters, phenolics)	22 mg·L ⁻¹	93% (1.5 gCOD·L ⁻¹ effluent)	No
Simulated high-strength wastewater: acrylic acid, acetic acid, and formaldehyde	85 g·L ⁻¹	> 99% of COD and formaldehyde	No
BTEX/gasoline	1.8 g COD·L ⁻¹	99%	Ethanol
Petrochemical wastewater collected from a petroleum refinery	15 g COD·L ⁻¹	98%	Beef and dairy cattle manure

1.2.3 *Anaerobic membrane bioreactors*

According to (Judd and Judd, 2011) the term membrane bioreactor defines a (waste) water treatment process that integrates a permselective membrane with a biological conversion process. An AnMBR is, therefore, an anaerobic reactor that is coupled to a membrane module. AnMBRs may have two main configurations depending on the location of the membrane: external cross-flow (side stream) and submerged (Figure 1.2) (Dvořák et al., 2015; Robles et al., 2018). An external cross-flow configuration makes use of a powerful cross-flow feed pump sending the feedwater alongside the membrane surface. The high pressure at the feed-side is the driving force for permeation of the treated water across the membrane. In the submerged configuration the membrane module can be located directly inside the bioreactor or in a separate membrane tank that is only dedicated to solids separation. Permeate extraction in the submerged configuration is usually achieved by vacuum extraction using a permeate pump (Dvořák et al., 2015; Robles et al., 2018).

In the external cross-flow configuration, the trans membrane pressure is generated by the feed/recirculation pump and sometimes by a second permeate pump that extracts the permeate. In addition, the feed/recirculation flow generates a constant cross-flow that scours the membrane and continuously disrupts the formation of a thick biomass cake layer on the membrane feed-side (Dvořák et al., 2015). Typical cross-flow velocity values range between 1-3 m·s⁻¹ (Judd and Judd, 2011). Higher values distinctly increase the energy costs while they may promote sludge flocs disintegration that decrease the sludge particle size and may increase the membrane clogging or fouling potential. Physical or chemical membrane cleaning, inspection, or replacement are easier to accomplish in an external membrane tank (submerged configuration) or membrane skid (cross-flow configuration), as the membranes are better accessible (Dvořák et al.,

2015; Judd and Judd, 2011). Therefore, a separate membrane tank or membrane skid is usually preferred at full-scale applications. Conversely, the single tank submerged membrane configuration, in which the membranes are mounted in the bioreactor, has the advantage that less energy is needed for the reactor operation, as no recirculation pump is used; however, to avoid clogging of the membranes, a biogas sparging pump is commonly applied (Robles et al., 2018).

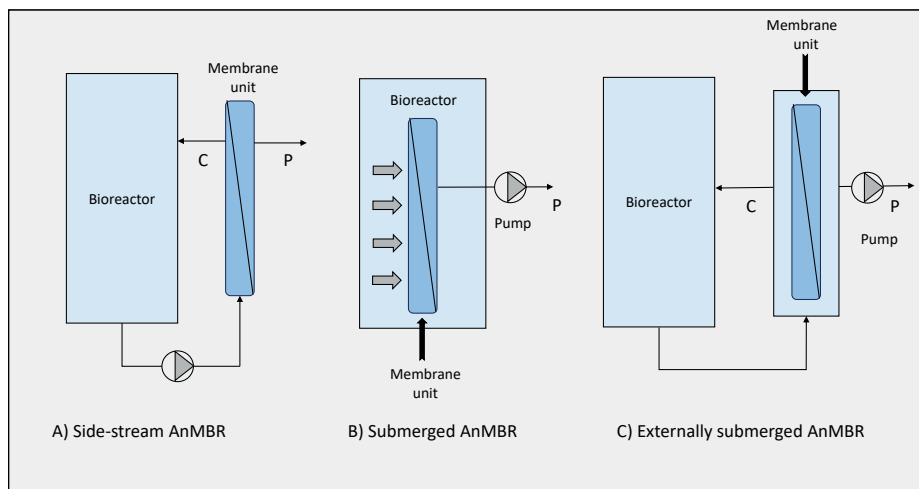


Figure 1.2. Main AnMBR configurations depending on the membrane unit location. Modified from (van Lier et al., 2019). P: Permeate; C: concentrate or retentate.

Membrane materials might be classified in two major types: polymeric and ceramic (Judd and Judd, 2011). Ceramic membranes provide superior resistance (chemical, thermal, hydraulic) in comparison to polymeric; however, due to their high costs, its use is limited. In (anaerobic) MBRs polymeric membranes are commonly used (Judd and Judd, 2011). Polymeric membranes may consist of hydrophilic materials, for example, cellulose acetate (although not commercially used), or fully hydrophobic materials such as polypropylene (PP), polyethylene (PE) and polytetrafluoroethylene (PTFE). Other materials such as polysulfone (PS)/polyethersulfone (PES), polyacrylonitrile (PAN), and polyvinylidene difluoride (PVDF) are also used. Currently, the most commonly found membranes are made of PES, PVDF, or PE derivative membranes. In general, PVDF membranes provide excellent strength and flexibility with a robust chemical resistance. PVDF can tolerate acidic pH down to 1 and basic pH up to 11 and it has a high tolerance to chlorine, allowing a less complicated cleaning process (Judd and Judd, 2011).

Membranes can also be classified according to their configuration. Six different configurations are currently available and are classified depending on the membrane's geometry and the way the membranes are orientated in relation to the flow: 1) flat sheet (FS), 2) hollow fiber (HF), 3) multi tubular (MT), 4) capillary tube (CT), 5) pleated filter cartridge (FC), 6) spiral-wound (SW). It should be noted that in (anaerobic) MBRs only the first three configurations are used (Judd and Judd, 2011).

The flux (J) is one of the key parameters in the operation of an AnMBR. The flux is defined as the quantity of liquid (permeate) passing through a unit of the membrane area per unit time [$L \cdot m^{-2} \cdot h^{-1}$] also known as Lmh. The flux is directly related to the driving force, which is a function of the transmembrane pressure (TMP) and the total hydraulic resistance created by the membrane and the interfacial region adjacent to it (Judd and Judd, 2011).

1.2.4 Application of AnMBRs for industrial (petro)chemical wastewater treatment

High toxicity, high salinity, and high temperature represent characteristics of industrial wastewater that may be considered as (biologically) extreme and which may negatively affect the anaerobic conversion process (Dereli et al., 2012). Low biomass retention, or washout of specific biomass, are some of the problems faced when anaerobic technology is applied for the treatment of chemical industrial wastewater (Rajeshwari et al., 2000). Strategies to increase biomass retention, such as biofilm or granule formation, require long start-up periods and sometimes are not possible under biologically extreme conditions (Dereli et al., 2012). However, the use of microfiltration or ultrafiltration modules in AnMBRs can provide a complete retention of all microorganisms, especially those responsible for the degradation of specific pollutants (Dereli et al., 2012).

The full biomass retention offered by the filtration unit gives important advantages to AnMBRs in comparison to sludge bed systems. For example, a) the effluent or permeate is of high quality as it is free of suspended solids, thus offering the possibility of water reclamation, and b) specific microbial populations (besides methanogens) that are needed for the degradation of particular substrates, e.g. toxic or inhibitory compounds, are retained regardless their settling or adherence ability or low growth rate (Mutamim et al., 2013). Therefore AnMBRs represent an attractive option for the treatment of wastewater characterized by extreme conditions that hamper biomass granulation such as high concentration of salt and toxic compounds, or high temperature, characteristics commonly found in wastewater produced by the (petro) chemical industries (Dereli et al., 2012). Besides, since many industries foresee a distinct reduction in the water consumption, pursuing cleaner industrial production

processes, it is very well possible that these biologically-extreme effluents will become more common in the (near) future (Dereli et al., 2012). However, the costs related to operation and cleaning of the membranes are still a drawback in the application of AnMBRs (Mutamim et al., 2013; Van Lier et al., 2015) as flux decline due to membrane fouling is one of the main constraints for the application of AnMBR technology (Dereli et al., 2012). However, the primary challenge in the treatment of (petro) chemical wastewater is the effective degradation of pollutants rather than achieving high operational fluxes. Therefore, the fouling problem may not represent the major obstacle for the application of AnMBR technology in this specific niche.

1.2.5 *Thermophilic AD for industrial chemical wastewater*

Thermophilic anaerobic treatment of industrial/toxic wastewater continues to be a challenge for the AD process. Unsatisfactory biomass immobilization is one of the main drawbacks in the treatment of industrial effluents at high temperature (Dereli et al., 2012). Moreover, changes in process water temperature will exert diverse effects on the different microbial subpopulations.

Despite the aforementioned constraints, thermophilic anaerobic operation may improve process economics in some industrial wastewater since less cooling is required and less re-heating when process water recovery is envisaged.. Thermophilic yields of methane obtained are equivalent to that of mesophilic operation (Dereli et al., 2012). Furthermore, thermophilic operation offers other advantages such as an increase in substrate utilization rates (hydrolysis), lower viscosity and thus potential solids-liquid separation improvement.

The vast majority of anaerobic industrial wastewater treatment systems are based on sludge bed technology, making use of granular sludge (Van Lier et al., 2015). However, prevailing saline-thermophilic conditions will constrain biomass granulation even more, whilst treating wastewater with toxic or inhibitory compounds that likely result in increased biomass decay rates. Under such extreme conditions, the washout of viable microorganisms is likely to occur, ultimately leading to poor reactor performance (Muñoz Sierra et al., 2019). Anaerobic membrane bioreactors, (AnMBR) have been proposed to overcome these problems (Dereli et al., 2012; Lin et al., 2012; Mutamim et al., 2013) as the filtration process ensures that all the biomass, including specialized microbial groups, is retained inside the reactor.

Coal gasification wastewater (CGWW) is an example of a petrochemical industrial effluent characterized by temperatures > 45 °C, total dissolved solids concentrations ranging between 0.5 and 2.5 g·L⁻¹, phenol and aromatic compounds in concentrations

ranging from 80 to $\text{mg}\cdot\text{L}^{-1}$, carboxylic acids from 200 to $600\text{ mg}\cdot\text{L}^{-1}$, pH values from 6.5 to 11.5, and alkalinity between 220 and $17,000\text{ mg}\cdot\text{L}^{-1}$ (Ji et al., 2016; Macarie, 2000; Maiti et al., 2019; Singer et al., 1978; Wang, W. et al., 2011; Zhao and Liu, 2016). Because these streams are produced in large flows on a global scale, e.g. 1 ton of coke production generates approximately 1 m^3 of coke oven wastewater (Maiti et al., 2019), anaerobic conversion of phenolic compounds at the prevalent process temperature would offer substantial energy recovery potential, while presenting a cost-effective solution for treating the wastewater and possibly providing reclaimed process water for reuse.

Thus far, only few studies of AnMBRs with toxic or recalcitrant compounds under thermophilic conditions are reported (Muñoz Sierra et al., 2017). Furthermore, AnMBR technology has not been fully introduced neither fully challenged with thermophilic conditions for the degradation of phenolic wastewater. It still needs to be determined if the results achieved under thermophilic operation are worth, or if the stress imposed to the AnMBR biomass makes the reactor operation unstable and thus non-feasible.

1.2.6 *Anaerobic treatment of phenolic wastewater*

Various authors have published research on the anaerobic treatment of phenolic wastewater in the literature (Table 1.2). Phenol degradation in UASB reactors and upflow sludge bed filters has been reported, but long acclimation times and granulation problems at high loading rates are common drawbacks. Although the applied specific phenol loading rate (sPhLR) [$\text{gPh}\cdot\text{gVSS}^{-1}\cdot\text{d}^{-1}$] or specific phenol conversion rate (sPhCR) [$\text{gPh}\cdot\text{gVSS}^{-1}\cdot\text{d}^{-1}$] gives more precise information about the biomass performance in the phenolic degradation, most of the studies only report influent phenol concentrations. In general, influent values between 500 and $750\text{ mg phenol}\cdot\text{L}^{-1}$ are stated as inhibitory in the UASB processes (Dereli et al., 2012; Tay et al., 2000). Table 1.2 presents phenol loading rates found in the literature.

Phenolic compounds, and mostly phenol, are the main components of the CGWW (Ji et al., 2016). Coal Gasification is a high water-consuming activity, and the wastewater produced contain a high concentration of toxic compounds (Zhao and Liu, 2016). Phenol and phenolic compounds could reach concentrations between 2,000 to $8,000\text{ mg}\cdot\text{L}^{-1}$, representing 40-50% of the COD in the CGWW (Gai et al., 2008; Ji et al., 2016; Zhao and Liu, 2016). Cresols correspond in average to 30% of the other phenolics (Veeresh et al., 2005) and the biodegradation of these compounds represent an extra challenge because of its recalcitrant and toxic properties (Fang and Zhou, 2000; Hwang and Cheng, 1991). Resorcinol is found in a concentration range from 10- $1,000\text{ mg}\cdot\text{L}^{-1}$ in the CGWW effluents. Any possible anaerobic treatment method for phenolic wastewater is preferred over physicochemical processes owing to its cost-

effectiveness and despite the toxicity and inhibition posed by the phenolic compounds to the anaerobic microorganisms (Fang et al., 2006; Zhao and Liu, 2016). Research on anaerobic phenol conversion is mostly conducted under mesophilic conditions (Fang et al., 2006). However, some wastewater (e.g. CGWW) leaves the process at high temperatures (40-60°C), raising the interest for thermophilic operation.

Table 1.2. Research studies on phenol and phenolic degradation under anaerobic conditions

Author	Reactor	Temp (°C)	HRT (h)	Loading rate	Substrate
(Zhou and Fang, 1997)	UASB	37	24	0.27 gPh·gVS ⁻¹ d ⁻¹	Phenol m-Cresol
(Lay and Cheng, 1998)				0.58 gPh·gVS ⁻¹ d ⁻¹	Phenol
(Fang and Zhou, 1999)	UASB (2.8 L)	37	24	0.74 gPh·gVS ⁻¹ d ⁻¹ 0.48 g _m Cr·gVS ⁻¹ d ⁻¹	Phenol and m-cresol
(Swaminathan et al., 1999).	FFFB	25-30	8		Resorcinol and catechol
(Fang and Zhou, 2000)	UASB	37			Phenol <i>p</i> -cresol
(Tay et al., 2000)	UASB	35	12	0.28 gPh·gVSS ⁻¹ d ⁻¹	Phenol
(Guiot et al., 2000)	UASB	29	72	0.007 gPh·gVSS ⁻¹ d ⁻¹	Phenol o-cresol <i>p</i> -cresol
(Tay et al., 2001)	UASB (2 L)	37	12	0.45 gPh·gVSS ⁻¹ d ⁻¹	Phenol
(de Amorim et al., 2015)	AFBR	30	24		Phenol

1.2.6.1 Anaerobic treatment of phenolic wastewater under thermophilic conditions

Previous research showed the feasibility of phenol-, phenolics-, or aromatics-containing wastewater degradation under thermophilic conditions (Table 1.3). Nevertheless, there is a lack of understanding of the biochemical and microbiological aspects such as the degradation pathways, microbial interaction, and syntrophic associations, which is needed for guaranteeing process stability. More insights are required into the maximum attainable conversion rates, the phenol degradation pathway under thermophilic (saline) conditions, and the specialized microbial groups that are required for stable thermophilic conversion of phenol.

Concentration	VSS	Recycling	Removal efficiency	Additional carbon/ energy source
		Yes	98% phenol 20% Cresol	Sucrose in the startup/No
200 mgPh·L ⁻¹ and 100 mgmCres·L ⁻¹	9.6 gVSS·L ⁻¹			Sucrose, nitrate
250 mg·L ⁻¹ Resorcinol 250 mg·L ⁻¹ Catechol				
		Yes	95% phenol 65% <i>p</i> -cresol	No
	5.6 gVSS·L ⁻¹	No	88 phenol	No
500 mg·L ⁻¹ phenol, 150 mg·L ⁻¹ ocresol, 150 mg·L ⁻¹ pcresol	18 gVSS·L ⁻¹	20:01	100 phenol 85 <i>p</i> -cresol 56 <i>o</i> -cresol	Whey
105-1260 mg·L ⁻¹	5.6 gVSS·L ⁻¹	No		Sucrose
50 - 700 mg·L ⁻¹	23.3 gVSS·L ⁻¹		93%	No

1.2.7 Biochemical aspects of anaerobic phenol and aromatic compounds degradation

1.2.7.1 Anaerobic phenol degradation

The anaerobic phenol catabolism has been studied using different model organisms. The first detailed results were obtained with the nitrate reducer *T. aromatica* (Carmona et al., 2009). In this microorganism, the two-step reaction results in a carboxylation of phenol that corresponds to the chemical counterpart of the Kolbe-Schmitt reaction (Carmona et al., 2009; Fuchs, 2008). The first step considers the phosphorylation of phenol into phenylphosphate by the phenylphosphate synthase (Fuchs, 2008) (Figure 1.3). One ATP molecule is used for the phosphorylation. In the second step, the phenylphosphate is carboxylated into 4-hydroxybenzoate in a reaction catalyzed by the enzyme phenylphosphate carboxylase. The carboxylase uses CO₂ as substrate and is highly sensitive to oxygen (Schühle and Fuchs, 2004).

Table 1.3. Research studies on the anaerobic degradation of phenolic and/or aromatic wastewater under thermophilic conditions.

Reference	Reactor	Operation	Temperature	Operation time	Substrate
(Karlsson et al., 1999)	Serum bottles (50 mL)	Mesophilic/ Thermophilic	37 °C/ 55 °C		Phenol
(Leván and Schnürer, 2005)	Medium bottles (500 mL)	Mesophilic/ Thermophilic	37 °C/ 55 °C		Benzoic acid, resorcinol , p-cresol, phenol, PCP, tricBa, phtalic acid, etc.
(Fang et al., 2006)	UASB (2.8 L)	Thermophilic	55 °C	224 d	Synthetic phenol containing wastewater.
(Chen et al., 2008)	Serum bottles (50 mL)	Mesophilic/ Thermophilic	37 °C/ 55 °C	18 month	Phenol
(Sreekanth et al., 2009)	2 Hybrid UASB (7 L)	Thermophilic condition	55 +/- 3 °C		4-chloro-2-nitrophenol (4C-2-NP), 2-chloro-4-nitrophenol (2C-4-NP), 2-chloro-5-methylphenol (2C-5-MP)
Wang W. et al. (Wang, W. et al., 2011)	2 UASB (1 L)	Thermophilic/ Mesophilic	55 °C/ 35 °C	120 d first stage	Lurgi coal gasification. Phenolic compounds, heterocyclic compounds, PAH, LCA, amine compounds, ammonia, sulfide, thiocyanate and cyanide.

In strict anaerobic microorganisms the carboxylation of phenol appears to be performed by an ATP-independent reaction (Carmona et al., 2009). Because of thermodynamic constraints, the phenol and/or aromatic compound degradation under methanogenic conditions requires the development of a syntrophic relationship between the aromatic compound degraders and methanogens (Nobu et al., 2015). Most of the metabolic pathways used by the syntrophic degraders utilize either H^+ or HCO_3^- as electron acceptors and yield H_2 ($E_o' = -414$ mV) or formate ($E_o' = -432$ mV) as product (Nobu et al., 2015). NADH, one of the most common electron donors, however, has a higher redox potential ($E_o' = -320$ mV). Therefore, (Sieber et al., 2012) proposed the ubiquitous presence of processes such as proton motive force (reverse electron transfer) or electron bifurcation and confurcation as energy inputs to overcome thermodynamic constraints.

Concentration	Additional carbon/energy source	Inocula source	Micoorganisms found
0.5 g/L or 1 g/L	No		N/A
0.5 mM	No	Meso/ thermophilic reactor	N/A
630 mgPh/L (1500 mgCOD/L)	Sucrose during the start-up phase [0.6 gCOD/Ld].	Mesophilic phenol-degrading sludge from a UASB (37 °C)	21 OTUs
100 mg/L-750 mg/L	No	Seed sludge for an anaerobic digester at a local WWTP.	Methanosaetaceae (meso and thermo), Methanomicrobiales (meso) and Methanobacteriaceae (meso and thermo)
2-30 mg/L	Yes (1:33.3 to 1:166.6 with an optimal of 1:100)	Digestate of slaughter house	Methanobrevibacter and Methnaothrix like bacteria.
[COD]= 1500 mg/L and [Phenol]= 300 mg/L. Increased to 2500 and 500	No	Full scale anaerobic reactor treating LCGW	N/A

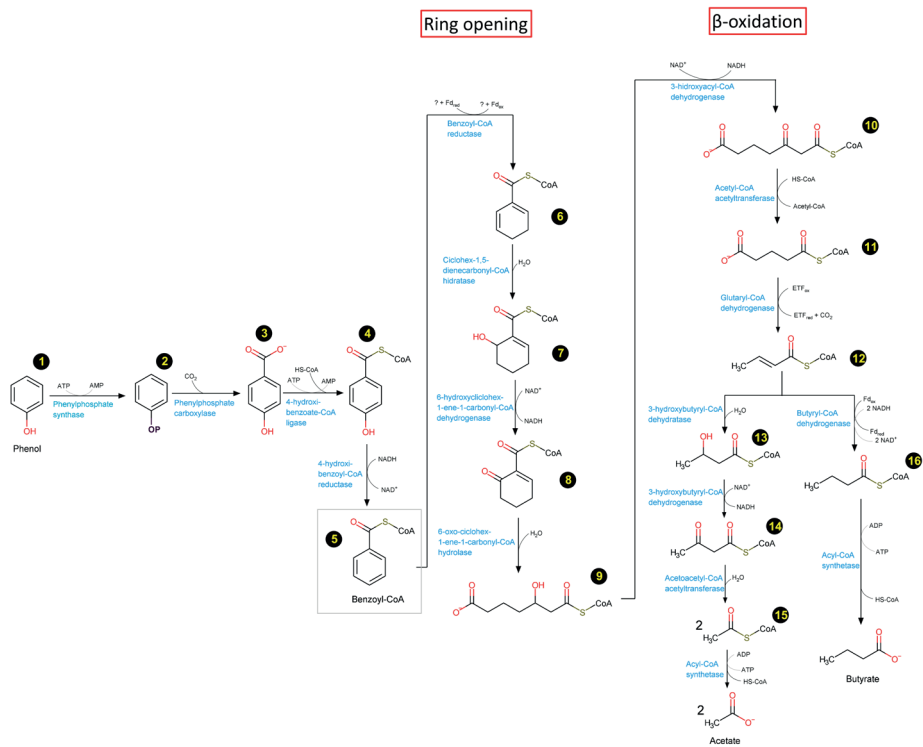


Figure 1.3. Proposed phenol degradation pathway under anaerobic (methanogenic) conditions for *Syntrophorhabdus aromaticivorans* strain UI. The pathway is divided in three main steps, namely, 1) oxygen-independent oxidation of phenol to the central metabolite benzoyl-CoA, 2) aromatic ring opening, and 3) boxidation to form acetate (mainly) or butyrate (adapted from (Nobu et al., 2015)). Molecule names: 1. Phenol; 2. Phenylphosphate; 3. 4-Hydroxybenzoate; 4. 4-Hydroxybenzoyl-CoA; 5. Benzoyl-CoA; 6. Cyclohex-1,5-dienecarbonyl-CoA; 7. 6-Hydroxycyclohex-1-ene-1-carbonyl-CoA; 8. 6-Oxo-cyclohex-1-ene-carbonyl-CoA; 9. 3-Hydroxypimeloyl-CoA; 10. 3-Ketopimeloyl-CoA; 11. Glutaryl-CoA; 12. Crotonyl-CoA; 13. 3-Hydroxybutyryl-CoA; 14. Acetoacetyl-CoA; 15. Acetyl-CoA; 16. Butyryl-CoA (Garmona et al., 2009).

The phenol degrader *Syntrophorhabdus aromaticivorans* strain UI contains genes encoding for a phenylphosphate synthase (PpsAB) and a phenylphosphate carboxylase (PpcBDAC) that are expressed during phenol degradation. Therefore, the activation of phenol can be performed via ATP consumption. Then, the phenol is carboxylated in the para position to form 4-hydroxybenzoate (4-HB) (Nobu et al., 2015). It is hence suggested that due to the presence of the PpsAB and PpcBDAC genes, the strain UI utilizes ATP for phenol activation instead of performing the activation in an ATP-independent way (Nobu et al., 2015). The produced 4-HB is then transformed into benzoyl-CoA due to the action of the enzymes 4-hydroxybenzoyl-ligase and 4-hydroxybenzoyl-CoA reductase (Figure 1.3) (Nobu et al., 2015).

The metabolic conversion of benzoyl-CoA then starts with the reduction of the aromatic ring of benzoyl-CoA to the dienoyl-CoA intermediate in a highly endergonic reaction. *T. aromatica* and *R. palustris* are microorganisms known to perform the same reaction with the use of ATP to drive the aromatic ring reduction (Nobu et al., 2015). Non-ATP dependent benzoyl-CoA reductase (BCR) operons were found in the strain UI; therefore, mechanisms such as membrane potential and electron bifurcation were suggested as alternative input for such BCR system (Nobu et al., 2015). It is likely that heterodisulfide reductase (Hdr) and hydrogenase proteins associated with the BCR participate in the endergonic reaction. The cyclohex-1,5-dienecarbonyl-CoA is further degraded into fatty acids, mainly acetate, H_2 and CO_2 by a series of reactions that involve the hydration of the dienoyl-CoA intermediate, ring hydrolysis, and β -oxidation. Butyrate may be yield as a transient product (Nobu et al., 2015) (Figure 1.3).

1.2.7.2 Anaerobic phenol degradation under thermophilic conditions

Research on the anaerobic degradation of phenol under thermophilic conditions is only scarcely documented (Chen et al., 2008; Fang et al., 2006; Hoyos-Hernandez et al., 2014; Leven et al., 2012; Levén and Schnürer, 2005) as most of the fundamental insights were obtained under mesophilic (nitrate-reducing) conditions (Fuchs et al., 2011; Liang and Fang; Schink et al., 2000). (Levén and Schnürer, 2005), studied the degradation of phenolic compounds and benzoate under mesophilic and thermophilic conditions. They found that under mesophilic conditions 6 out of 13 compounds were converted into methane, whereas under thermophilic conditions (55 °C) only benzoic acid was mineralized. (Karlsson et al., 1999) studied the effects of hydrogen partial pressure on phenol degradation under mesophilic and thermophilic conditions by enriched mixed cultures. They proposed different degradation pathways for phenol degradation depending on the temperature range. In subsequent research, they reported the importance of CO_2 on the phenol fermentation process (Karlsson et al., 2000). Based on the results from continuous thermophilic reactor operation, (Fang et al., 2006) reported the degradation of phenol as the sole CES in a UASB reactor, whereas (Sreekanth et al., 2009) reported the degradation of chloro-nitro phenolic compounds with glucose as additional CES using a hybrid UASB-anaerobic filter reactor. Based on their studies, an alternative phenol degradation pathway via caproate and not benzoyl-CoA as the main intermediate was proposed (Fang et al., 2006; Karlsson et al., 1999).

The feasibility of phenol degradation under saline and thermophilic conditions using acetate as additional CES was previously shown by our research group (Muñoz Sierra et al., 2020; Munoz Sierra et al., 2018). However, to date, the feasibility of the degradation of phenol as sole CES by suspended biomass, the effect of additional CES on the specific phenol conversion rate (sPhCR), and the microbial community

in thermophilic-saline ($[\text{Na}^+] = 6.5 \text{ g}\cdot\text{L}^{-1}$) suspended biomass are not addressed in any scientific research.

1.2.7.3 Anaerobic degradation of (complex) aromatic compounds

Microbial evolution has allowed the development of degradation routes for the commonly present aromatic compounds in nature, in which the strong oxidative enzyme systems of fungi play a central role. Due to the broad microbial enzymatic capability and flexibility, fungi and also bacteria can even degrade xenobiotic aromatic compounds (Carmona et al., 2009; Fuchs et al., 2011). Under anaerobic conditions, bacteria are generally responsible for the bioconversion of aromatic compounds. The catabolic reactions for aromatic compound degradation can proceed through a variety of peripheral pathways. These peripheral, upper, or channeling pathways activate several aromatic substrates into a narrower number of common metabolites (Figure 1.4) (Carmona et al., 2009). Then, the central (or lower) pathways convert the key metabolites into intermediary compounds such as acetyl-CoA or benzoyl-CoA (Fuchs et al., 2011). Other examples of central aromatic intermediates are resorcinol, phloroglucinol, hydroxyhydroquinone, 6-hydroxynicotinate, hydroxybenzoyl-CoA, 3-methylbenzoyl-CoA, and aminobenzoyl-CoA (Carmona et al., 2009) (Figure 1.4).

However, the anaerobic biodegradation of (more complex) aromatic compounds containing more than one aromatic ring has not been fully investigated. Limitations in the study of these conversions are, for example, the low growth rates ($\text{gCOD}_x \cdot \text{gCOD}_s^{-1} \text{d}^{-1}$) and low yields ($\text{gCOD}_x \cdot \text{gCOD}_s^{-1}$) of the microorganisms responsible for the degradation of these compounds. The low growth rates and low yields reflect the low Gibbs-free energy change in the anaerobic conversion reactions of aromatic compounds. As stated by (Heijnen and Kleerebezem, 2010), the energy gained by catabolic conversion of a compound is first used for cell maintenance and secondly for cell growth. However, the capability of strict anaerobic microorganisms to degrade polycyclic aromatic hydrocarbons (PAHs) has been clearly demonstrated in the literature (Carmona et al., 2009; Dhar et al., 2020; Foght, 2008). However, little is known about the degradation routes, biochemical processes, involved microorganisms and required microbial (syntrophic) interactions that are governing the conversion process.

Enzymatic ‘activation’ is suggested as the initial step in the anaerobic conversion of aromatic hydrocarbons, such as PAHs (Foght, 2008). Five main reactions are suggested for the activation of aromatic compounds: a) fumarate addition, b) methylation of unsubstituted aromatics, c) hydroxylation via dehydrogenases, d) direct carboxylation, and e) phosphorylation (Foght, 2008; Ladino-Orjuela et al., 2016). The molecules are directed after the activation via pathways yielding central metabolites, such as the

benzoyl-CoA, which are subsequently metabolized via ring saturation, cleavage, and β -oxidation in the central or lower pathways (Carmona et al., 2009; Ladino-Orjuela et al., 2016).

Although studies have shown the feasibility of anaerobic degradation of compounds, such as acenaphthene, anthracene, fluorene, naphthalene, phenanthrene, and pyrene, further research is needed to determine the capability of AD for the degradation of complex substrates for example high molecular weight PAHs (Dhar et al., 2020).

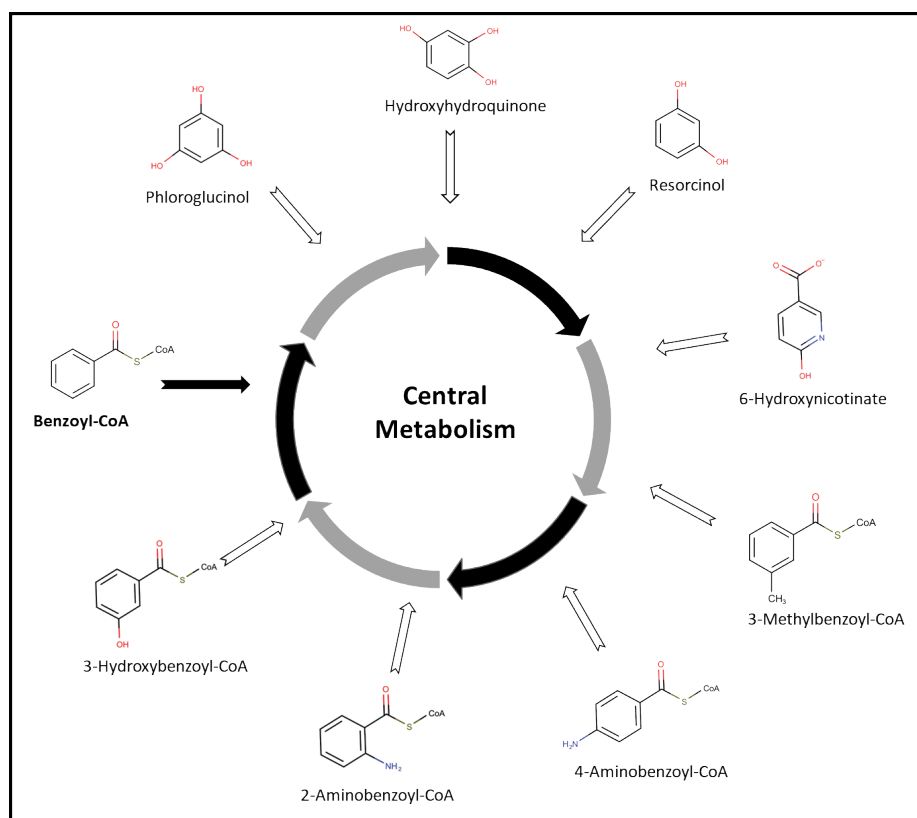


Figure 1.4. Key metabolites in the anaerobic degradation of (mono)aromatic compounds. Modified from (Carmona et al., 2009).

1.2.8 Phenol degradation under anaerobic conditions with the addition of external carbon and energy sources

Different additional CES have been used to promote or enhance the degradation of phenol under anaerobic conditions (Liang and Fang, 2010), namely, glucose (Tay et al., 2001), VFA (Carbajo et al., 2010), or acetate (Muñoz Sierra et al., 2017). Additional CES

also have been used during the reactor start-up, or during the degradation of mixtures of phenolic compounds. In most of these studies, however, it remains unclear how and to what extent these substrates promoted or increased phenol degradation.

The effect of additional CES on the degradation of toxic or inhibitory compounds such as phenol might be explained by four possible mechanisms:

1. Co-metabolism, a process that was initially defined as the catabolic degradation of a recalcitrant substrate without using the generated energy for anabolic purposes (Horvath, 1972). In this process, the degradation of refractory compounds is dependent on the presence of a main substrate, or primary source, which is commonly an easily degradable compound (Bertrand et al., 2015; Horvath, 1972). However, (Wackett, 1996) attributed the enhancement in the conversion rate to an unknown or unidentified effect in the metabolic network between the different microbial populations, which are present in non-defined mixed cultures.

2. Direct usage of additional CES by the toxicant degraders to increase their metabolic capacity (Gali et al., 2006; Kennes et al., 1997; Tay et al., 2001); meaning that: i) toxicant degraders can use the additional CES as substrate to increase their energy gain from catabolism, enhancing microbial maintenance and growth, and thus increasing its net microbial yield and fraction in the biomass. ii) the catabolic activity (i.e. uptake rate) of the toxicant degraders will be increased; or iii) both the fraction of the toxicant-degraders in the biomass and its toxicant-degrading activity are increased. This would imply, for example, that phenol degraders could use another (easily biodegradable) CES for biochemical energy gain besides phenol. The latter contrasts to the general comprehension that in anaerobic digestion (AD), specific (physiological) microbial populations have well-defined narrow substrate ranges (Batstone et al., 2002) (Appendix A.1).

3. The need for effective syntrophic microbial associations to maximize the Gibbs' free energy change of the compound degradation. In the case of phenol conversion, an effective transfer of reducing equivalents, i.e., hydrogen is required for favorable thermodynamics conditions (Qiu et al., 2008). Therefore, the development of a sound hydrogenotrophic methanogenic subpopulation is indispensable for establishing efficient anaerobic oxidation of aromatics and/or their degradation products.

4. An increase in intermediate compounds involved in the conversion of phenolics. Phenol degradation under anoxic conditions occurs via carboxylation of the phenolic ring to form 4-hydroxybenzoate (Fuchs et al., 2011; Gibson and Harwood, 2002; Schink et al., 2000). It has been reported that under strict anaerobic (methanogenic)

conditions, phenol degradation is dependent on a sufficiently high $\text{CO}_2/\text{HCO}_3^-$ and H_2 concentration (Fuchs, 2008; Karlsson et al., 1999; Knoll et al., 1987). Vereesh *et al.* reported that dosage of additional CES increased the phenol-degrading activity of the biomass, hypothesizing that this was due to a higher phenol hydrogenation rate, resulting in a more rapid cleavage of the phenolic ring (Veeresh et al., 2005).

In contrast to these four mechanisms, supply of additional CES, such as acetate, has been shown to inhibit the anaerobic degradation of terephthalic acid (Kleerebezem, 1999.), which even though is not a phenolic compound, shares the same degradation pathway (under anoxic/anaerobic conditions) with phenol (Nobu et al., 2015). Hence, the effect of additional CES' dosage on the degradation of recalcitrant and toxic or inhibitory compounds is not fully understood. Moreover, there is few information of the effect of additional CES dosage on the sPhCR, especially in AnMBRs under saline conditions.

1.2.9 Thermodynamic state analysis of microbial biochemical processes in environmental systems

Ecosystems are characterized as open systems in a thermodynamic perspective, which means energy and matter flows through them. Based on the quantitative analysis of the different energy and matter flows of a biochemical system, a better understanding of such system and better insight into its main processes can be attained. Such state analysis is based on thermodynamic principles and thermodynamics laws with matter and energy balances as the core of the analysis (Heijnen and Kleerebezem, 2010; Kleerebezem and Van Loosdrecht, 2010). The stoichiometric derivation of all involved redox reactions (and sub-reactions) of the prevailing metabolic processes, i.e., catabolic and anabolic reactions, is one of the main objectives of a thermodynamic state analysis (Kleerebezem and Van Loosdrecht, 2010). Hereafter, the value of the different process parameters, such as pH, can be estimated, which may change due to microbial metabolism or nutrients uptake for sustaining microbial growth. Furthermore, Gibbs' free energy balances can be applied to analyze the nonequilibrium situation of the microbial systems (Heijnen and Kleerebezem, 2010). Likewise, it is possible to make predictions of the effects of changing parameters, such as product concentration or temperature, in the redox reactions (Kleerebezem and Van Loosdrecht, 2010). Moreover, after derivation of the redox equations, key reactions can be visualized that require a syntrophic relationship to overcome the reactions' thermodynamic constraints.

1.2.9.1 Microbial metabolism and growth thermodynamics

Metabolism can be defined as a set of biochemical reactions and processes by which a living organism exchanges (bio)chemical energy and matter with the environment. Microbial metabolism can be understood as the interconnection between catabolism and anabolism by means of specific molecules serving as energy carrier (Kleerebezem and Van Loosdrecht, 2010). Figure 1.5 shows the relationship between the substrate, product, and the role of (microbial) metabolism, namely catabolism and metabolism. Energy is harvested and stored in the form of ATP after the substrate is converted in a catabolic reaction. In anabolism, the stored energy is used to generate new building blocks to form the new biomass constituents. During anabolism, a carbon and a nitrogen source is required, and the ATP-stored energy will be used to perform the assimilative reactions. Likewise, also non-growth-related anabolic processes, such as maintenance, are considered for biochemical energy consumption. The catabolic and anabolic reactions are stoichiometrically interconnected depending on the energetic requirements of the cell (Kleerebezem and Van Loosdrecht, 2010).

A clear insight into the redox reactions related to catabolism and anabolism of a microorganism is required to subsequently derive the biochemical reactions describing a microbial metabolism. The general metabolic growth equation is subsequently derived from the coupling of catabolism to anabolism (Heijnen and Kleerebezem, 2010; Kleerebezem and Van Loosdrecht, 2010).

In literature, several methods have been proposed for coupling catabolism and anabolism to microbial metabolism and growth (Kleerebezem and Van Loosdrecht, 2010). The underlying theoretical concept supporting these methods is that one fraction of the generated energy in catabolism will be required for the production of biomass. Three methods have been clearly described (Kleerebezem and Van Loosdrecht, 2010):

- The ATP balancing method.
- The thermodynamic electron equivalent method (TEEM).
- The Gibbs' free energy dissipation method.

Among these methods, the Gibbs energy dissipation method has the advantage that it does not require a detailed biochemical picture of the metabolic process or pathway that is under study, which is information that is commonly not available for most of the environmental processes (Kleerebezem and Van Loosdrecht, 2010). The Gibbs energy dissipation method utilizes a black box model approach like the TEEM. Both methods only require the identification of the carbon and nitrogen source for the anabolic reaction and the donor and acceptor couples of the catabolic reaction

(Kleerebezem and Van Loosdrecht, 2010). The dissipation method considers the degree of reduction (γ) and the carbon chain length of the carbon source. The TEEM assumes a constant Gibbs' free energy dissipation per mole of formed biomass, for all growth systems independently of the carbon source (Kleerebezem and Van Loosdrecht, 2010). Similar biomass yield estimations are obtained with both methods. The Gibbs' free energy dissipation method, however, yields slightly superior results compared to the TEEM method due to its improved description of the relationship between the Gibbs' free energy dissipation and the nature of the carbon source.

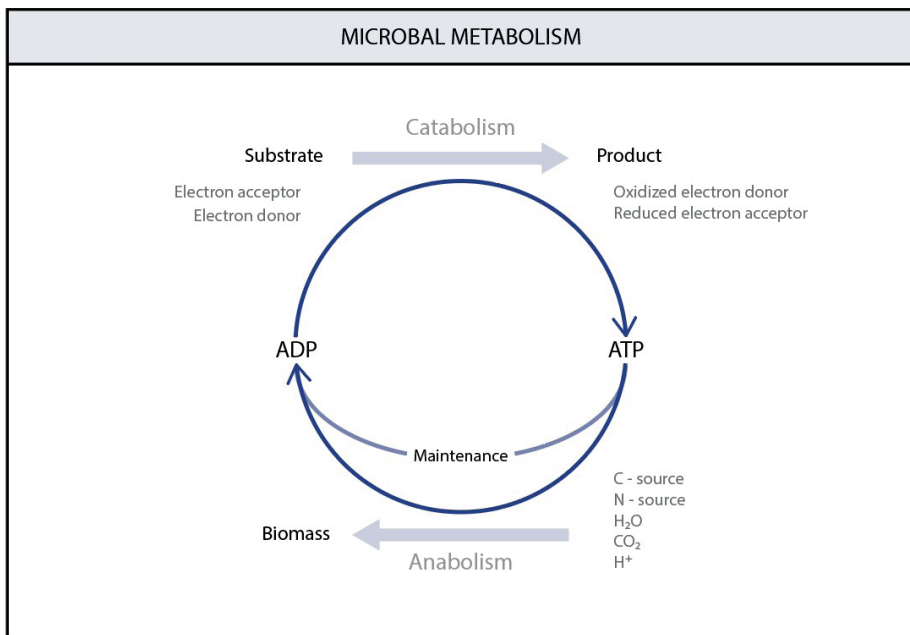


Figure 1.5. Schematic representation of microbial metabolism (grey box). Adapted from (Kleerebezem and Van Loosdrecht, 2010).

1.2.10 *Microbial community dynamics in the anaerobic digestion of industrial wastewater*

The development of new and cheaper molecular biology techniques and technology such as the next generation sequencing (NGS) has allowed an increased and improved analysis of the microbial community in the bioreactors (Vincent et al., 2017). Changes in the microbiome can be related to various operational parameters of the reactor, including configuration, inoculum source, substrate fed, and/or substrate or volumetric loading rates.

Analysis of the 16S ribosomal ribonucleic acid (rRNA) gene is a technique applied for the identification and study of the microorganisms present in the bioreactor. The gene has the three main characteristics that allow it to act as a molecular phylogenetic marker, as 1) it is present in all the prokaryotic forms of life, 2) has a genetic structure that is conserved among time but has enough variations to allow the distinction between different microorganisms, and 3) has a structure long enough (1500 – 1800 pb) for (molecular) analysis (Gabezas et al., 2015). The analysis of the 16S rRNA gene allows the identification of microorganism up to their genus and sometimes even species level.

Microbial communities in bioreactors treating industrial wastewater are expected to be less diverse than in natural ecosystems. The industrial wastewater components and their concentrations may exhibit toxic or inhibitory effects on the biomass and will, therefore, exert a strong selection pressure on the microorganisms, narrowing the microbial community of the bioreactors.

A full biomass retention system such as the AnMBR enables the study of all microbial populations that can develop in the reactor independently of their adherence or immobilization capacity. Therefore, in an AnMBR, it is possible to determine the effects of changing process parameters, such as the (sludge) loading rate, on the entire microbial community dynamics in the reactor. Hereafter, it is possible to correlate the microbial community dynamics with the changing process parameters using statistical analysis, such as the principal coordinate analysis (PCoA) or the canonical correspondence analysis (CCA).

A better knowledge of the microbial composition and its dynamics in the reactor will offer the possibility of an increased understanding of the occurring processes, which may allow for improved reactor operation and performance.

1.3 Outline of the thesis

Figure 1.6 and Figure 1.7 show a schematic or a graphical representation of the thesis outline, respectively. Chapter two discusses the effect of the dosage of additional and easily degradable CES, namely acetate and butyrate, on the phenol degradation rate and AnMBR reactor performance under mesophilic and saline conditions ($8 \text{ g Na}^+ \cdot \text{L}^{-1}$). More specifically, the enhancement of sPhCR and the microbial community dynamics in the reactor's biomass are studied.

Chapter three discusses the role of syntrophic acetate oxidation (SAO) as the key biochemical process for effective phenol degradation under saline ($6 \text{ g Na}^+ \cdot \text{L}^{-1}$) and

thermophilic (55 °C) conditions. Special attention is given to the possible degradation pathways of acetate and phenol.

Chapter four studies the simultaneous degradation of (bi)phenolic mixtures under saline (8 g Na⁺·L⁻¹) and mesophilic conditions. Batch tests, performed with the biomass grown during the conducted research described in Chapter two, showed a broader biomass metabolic potential than expected. The performance of two reactors for the degradation of phenol-*p*-cresol and phenol-resorcinol was assessed and complemented with thermodynamic calculations and microbial community analysis.

In Chapter five, the knowledge acquired during the experiments in the previous chapters was used for the treatment of bitumen fume condensate (BFC), a petrochemical wastewater coming from an asphalt company located in the Netherlands. The organic and inorganic components of the BFC were thoroughly characterized and the toxic and inhibitory effects of the BFC on anaerobic biomass were assessed. An AnMBR was operated for the degradation of BFC wastewater, and a microbial community analysis in the reactor's biomass was performed.

Chapter six presents the conclusions of the thesis. It also summarizes an integrative outlook of the performed investigations. Similarly, the applicability of the results of the project is discussed, and future research topics and possible research directions are suggested.

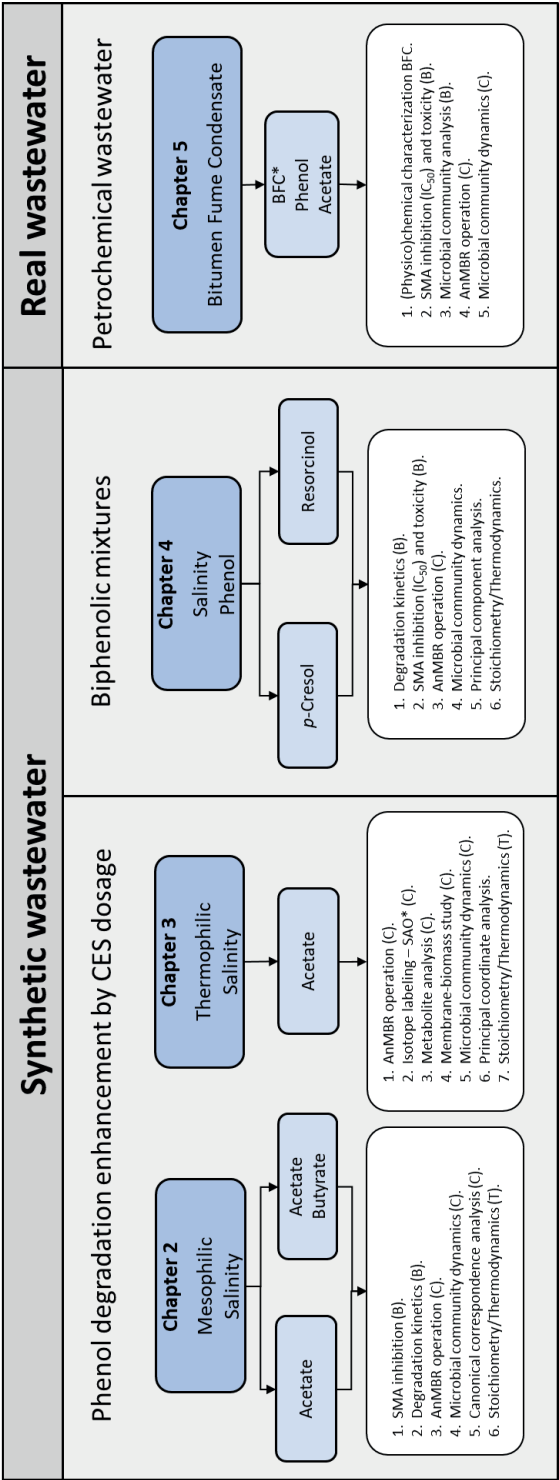


Figure 1.6. Schematic representation of the thesis's outline. *Abbreviations: SAO – syntrophic acetate oxidation; BFC – bitumen fume condensate. (B): Batch experiments; (C): continuous experiments.

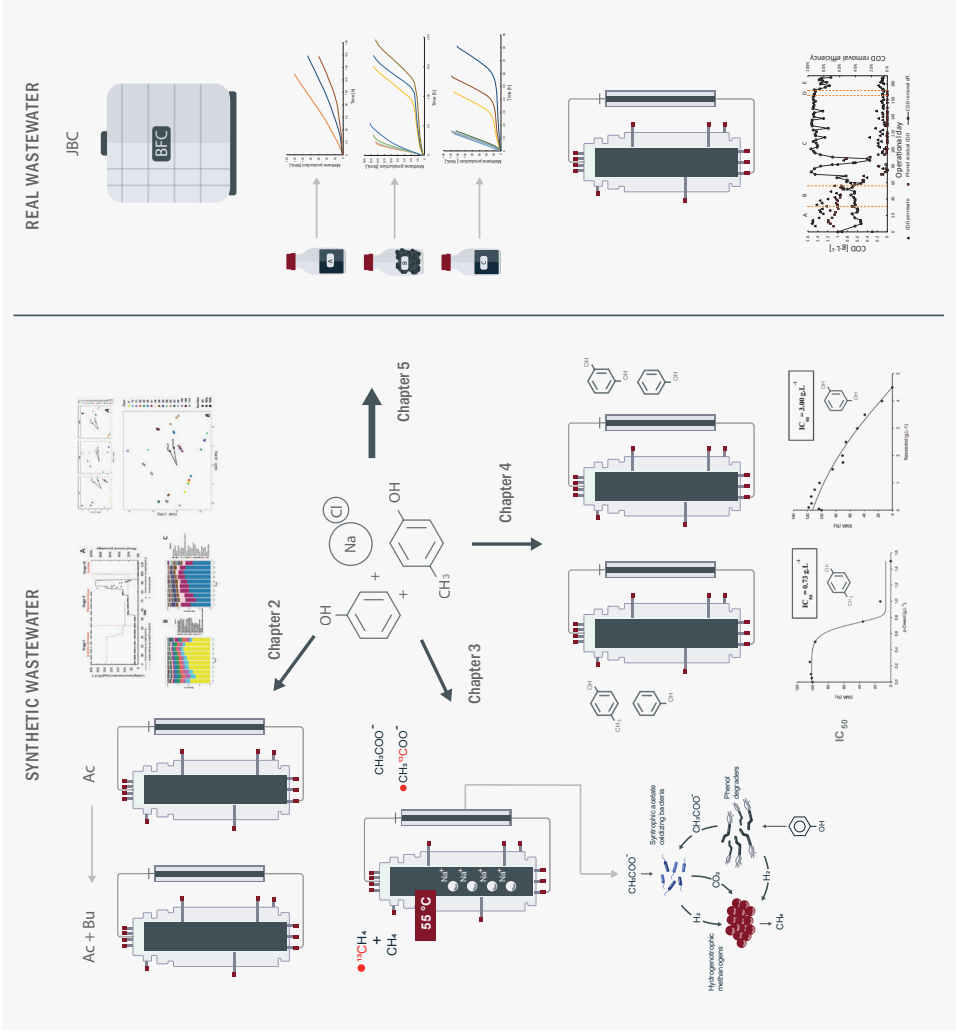


Figure 1.7. Graphical representation of the thesis's outline.

1.4 References

- Almendariz, F.J., Meraz, M., Olmos, A.D., Monroy, O., 2005. Phenolic refinery wastewater biodegradation by an expanded granular sludge bed reactor. *Water Sci. Technol.* 52(1-2), 391-396. <https://doi.org/10.2166/wst.2005.0544> %J Water Science and Technology.
- Batstone, D.J., Keller, J., Angelidaki, I., Kalyuzhnyi, S.V., Pavlostathis, S.G., Rozzi, A., Sanders, W.T.M., Siegrist, H., Vavilin, V.A., 2002. The IWA Anaerobic Digestion Model No 1 (ADM1). *Water Sci. Technol.* 45(10), 65-73. <https://doi.org/10.2166/wst.2002.0292> %J Water Science and Technology.
- Bertrand, J.-C., Doumenq, P., Guyoneaud, R., Marrot, B., Martin-Laurent, F., Matheron, R., Moulin, P., Soulas, G., 2015. Applied Microbial Ecology and Bioremediation, in: Bertrand, J.-C., Caumette, P., Lebaron, P., Matheron, R., Normand, P., Sime-Ngando, T. (Eds.), *Environmental Microbiology: Fundamentals and Applications: Microbial Ecology*. Springer Netherlands, Dordrecht, pp. 659-753. https://doi.org/10.1007/978-94-017-9118-2_16.
- Bhattacharyya, D., Allison, M.J., Webb, J.R., Zanatta, G.M., Singh, K.S., Grant, S.R., 2013. Treatment of an Industrial Wastewater Containing Acrylic Acid and Formaldehyde in an Anaerobic Membrane Bioreactor. *J. Hazard. Toxic Radioact. Waste* 17(1), 74-79. [https://doi.org/doi:10.1061/\(ASCE\)HZ.2153-5515.0000148](https://doi.org/doi:10.1061/(ASCE)HZ.2153-5515.0000148).
- Cabezas, A., de Araujo, J.C., Callejas, C., Galès, A., Hamelin, J., Marone, A., Sousa, D.Z., Trably, E., Etchebehere, C., 2015. How to use molecular biology tools for the study of the anaerobic digestion process? *Reviews in Environmental Science and Bio/Technology* 14(4), 555-593. <https://doi.org/10.1007/s11157-015-9380-8>.
- Carbajo, J.B., Boltes, K., Leton, P., 2010. Treatment of phenol in an anaerobic fluidized bed reactor (AFBR): continuous and batch regime. *Biodegradation* 21(4), 603-613. <https://doi.org/10.1007/s10532-010-9328-1>.
- Carmona, M., Zamarro, M.T., Blázquez, B., Durante-Rodríguez, G., Juárez, J.F., Valderrama, J.A., Barragán, M.J., García, J.L., Díaz, E., 2009. Anaerobic catabolism of aromatic compounds: a genetic and genomic view. *Microbiol Mol Biol Rev* 73(1), 71-133. <https://doi.org/10.1128/mmbr.00021-08>.
- Chen, C.-L., Wu, J.-H., Liu, W.-T., 2008. Identification of important microbial populations in the mesophilic and thermophilic phenol-degrading methanogenic consortia. *Water Res.* 42(8-9), 1963-1976. <https://doi.org/http://dx.doi.org/10.1016/j.watres.2007.11.037>.
- de Amorim, E.L.C., Sader, L.T., Silva, E.L., 2015. Effects of the Organic-Loading Rate on the Performance of an Anaerobic Fluidized-Bed Reactor Treating Synthetic Wastewater Containing Phenol. *Journal of Environmental Engineering* 141(10), 04015022.
- de Oliveira Souza, M., Ribeiro, M.A., Carneiro, M.T.W.D., Athayde, G.P.B., de Castro, E.V.R., da Silva, F.L.F., Matos, W.O., de Queiroz Ferreira, R., 2015. Evaluation and determination of chloride in crude oil based on the counterions Na, Ca, Mg, Sr and Fe, quantified via ICP-OES in the crude oil aqueous extract. *Fuel* 154, 181-187. <https://doi.org/https://doi.org/10.1016/j.fuel.2015.03.079>.
- Dereli, R.K., Ersahin, M.E., Ozgun, H., Ozturk, I., Jeison, D., van der Zee, F., van Lier, J.B., 2012. Potentials of anaerobic membrane bioreactors to overcome treatment limitations induced by industrial wastewaters. *Bioresour. Technol.* 122, 160-170. <https://doi.org/10.1016/j.biortech.2012.05.139>.
- Dhar, K., Subashchandrabose, S.R., Venkateswarlu, K., Krishnan, K., Megharaj, M., 2020. Anaerobic Microbial Degradation of Polycyclic Aromatic Hydrocarbons: A Comprehensive Review, in: de Voegt, P. (Ed.) *Reviews of Environmental Contamination and Toxicology* Volume 251. Springer International Publishing, Cham, pp. 25-108. https://doi.org/10.1007/398_2019_29.
- Díaz, M.P., Boyd, K.G., Grigson, S.J.W., Burgess, J.G., 2002. Biodegradation of crude oil across a wide range of salinities by an extremely halotolerant bacterial consortium MPD-M, immobilized onto polypropylene fibers. *Biotechnol. Bioeng.* 79(2), 145-153. <https://doi.org/https://doi.org/10.1002/bit.10318>.

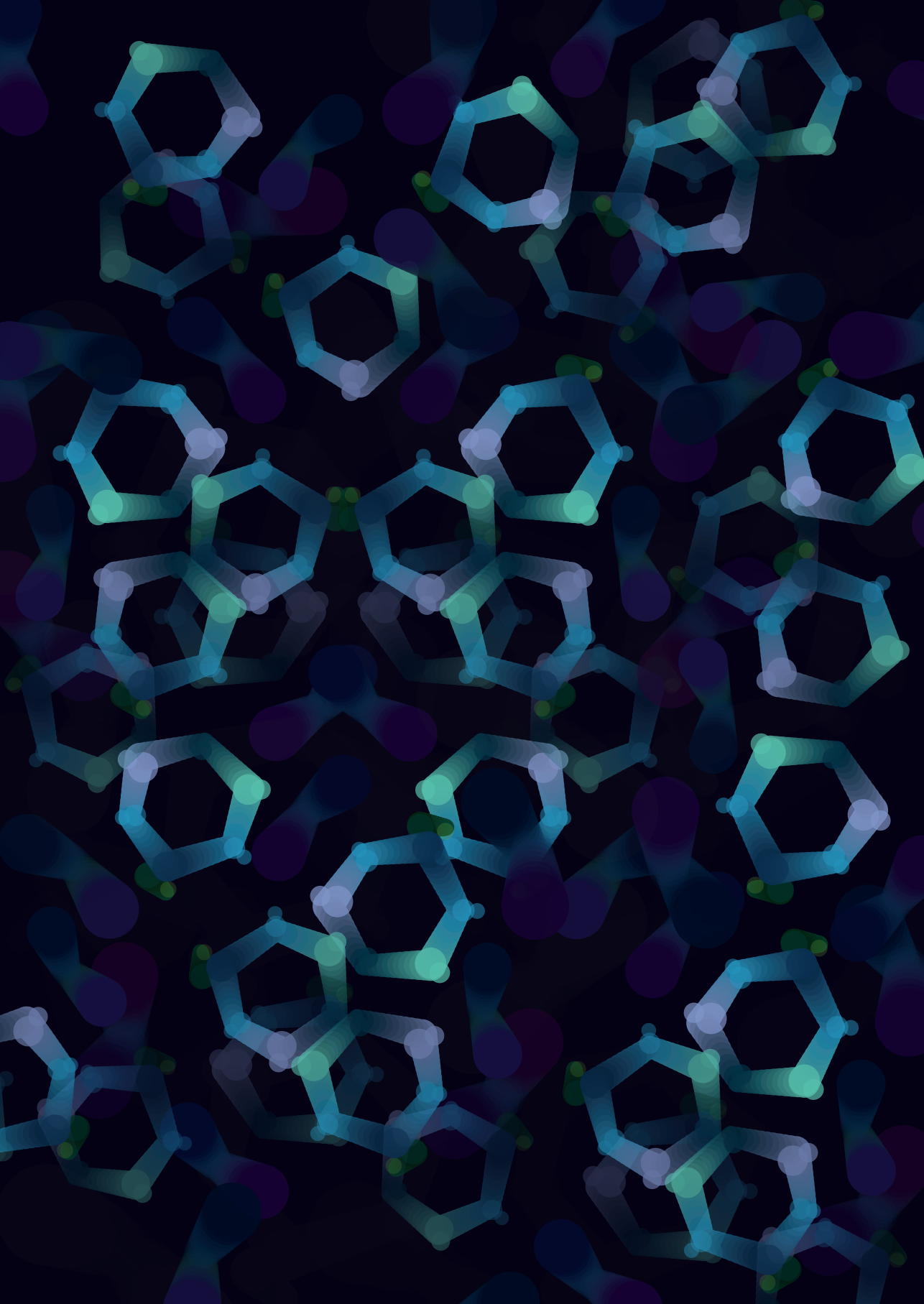
- Dvořák, L., Gómez, M., Dolina, J., Černín, A., 2015. Anaerobic membrane bioreactors—a mini review with emphasis on industrial wastewater treatment: applications, limitations and perspectives. *Desalination Water Treat.*, 1-15. <https://doi.org/10.1080/19443994.2015.1100879>.
- Fang, H., Liang, D., Zhang, T., Liu, Y., 2006. Anaerobic treatment of phenol in wastewater under thermophilic condition. *Water Res.* 40(3), 427-434. <https://doi.org/10.1016/j.watres.2005.11.025>.
- Fang, H.H., Zhou, G.-M., 1999. Interactions of methanogens and denitrifiers in degradation of phenols. *Journal of environmental engineering* 125(1), 57-63.
- Fang, H.H., Zhou, G.-M., 2000. Degradation of phenol and p-cresol in reactors. *Water Sci. Technol.* 42(5-6), 237-244.
- Foght, J., 2008. Anaerobic biodegradation of aromatic hydrocarbons: pathways and prospects. *J. Mol. Microbiol. Biotechnol.* 15(2-3), 93-120. <https://doi.org/10.1159/000121324>.
- Fuchs, G., 2008. Anaerobic metabolism of aromatic compounds. *Ann. N.Y. Acad. Sci.* 1125(1), 82-99.
- Fuchs, G., Boll, M., Heider, J., 2011. Microbial degradation of aromatic compounds - from one strategy to four. *Nat. Rev. Microbiol.* 9(11), 803-816. <https://doi.org/10.1038/nrmicro2652>.
- Gai, H., Jiang, Y., Qian, Y., Kraslawski, A., 2008. Conceptual design and retrofitting of the coal-gasification wastewater treatment process. *Chem. Eng. J.* 138(1), 84-94.
- Gali, V.S., Kumar, P., Mehrotra, I., 2006. Biodegradation of Phenol with Wastewater as a Cosubstrate in Upflow Anaerobic Sludge Blanket. 132(11), 1539-1542. [https://doi.org/10.1061/\(ASCE\)0733-9372\(2006\)132:11\(1539\)](https://doi.org/10.1061/(ASCE)0733-9372(2006)132:11(1539)).
- Garcia-Mancha, N., Puyol, D., Monsalvo, V.M., Rajhi, H., Mohedano, A.F., Rodriguez, J.J., 2012. Anaerobic treatment of wastewater from used industrial oil recovery. *J. Chem. Technol. Biotechnol.* 87(9), 1320-1328. <https://doi.org/10.1002/jctb.3753>.
- Gasim, H., Kutty, S., Isa, M.H., 2012. Anaerobic treatment of petroleum refinery wastewater. *Int. J. Chem. Mol. Eng.* 6(8), 512-515.
- Gibson, J., Harwood, C.S., 2002. Metabolic Diversity in Aromatic Compound Utilization by Anaerobic Microbes. *Annu. Rev. Microbiol.* 56(1), 345-369. <https://doi.org/10.1146/annurev.micro.56.012302.160749>.
- Guiot, S.R., Tawfik-Hájjí, K., Lépine, F., 2000. Immobilization strategies for bioaugmentation of anaerobic reactors treating phenolic compounds. *Water Sci. Technol.* 42(5-6), 245-250. <https://doi.org/10.2166/wst.2000.0520> %J Water Science and Technology.
- Guyot, J.P., Macarie, H., Noyola, A., 1990. Anaerobic digestion Of a Petrochemical Wastewater using the UASB process. *Appl. Biochem. Biotechnol.* 24(1), 579-589. <https://doi.org/10.1007/BF02920280>.
- Heijnen, J.J., Kleerebezem, R., 2010. Bioenergetics of Microbial Growth, *Encyclopedia of Industrial Biotechnology*. pp. 1-66. <https://doi.org/10.1002/9780470054581.eibo84>.
- Horvath, R.S., 1972. Microbial co-metabolism and the degradation of organic compounds in nature. *Bacteriological reviews* 36(2), 146-155.
- Hoyos-Hernandez, C., Hoffmann, M., Guenne, A., Mazeas, L., 2014. Elucidation of the thermophilic phenol biodegradation pathway via benzoate during the anaerobic digestion of municipal solid waste. *Chemosphere* 97, 115-119. <https://doi.org/10.1016/j.chemosphere.2013.10.045>.
- Hwang, P.-C., Cheng, S.-S., 1991. Treatment of p-Cresol with a Recirculating UASB Reactor Using the Concept of Kinetic Control. *Water Sci. Technol.* 24(5), 133-140.

- Jafarzadeh, M.T., Mehrdadi, N., Hashemian, S.J., 2012. Application of an anaerobic hybrid reactor for petrochemical effluent treatment. *Water Sci. Technol.* 65(12), 2098-2105. <https://doi.org/10.2166/wst.2012.088>.
- Ji, G.D., Sun, T.H., Ni, J.R., Tong, J.J., 2009. Anaerobic baffled reactor (ABR) for treating heavy oil produced water with high concentrations of salt and poor nutrient. *Bioresour. Technol.* 100(3), 1108-1114. <https://doi.org/https://doi.org/10.1016/j.biortech.2008.08.015>.
- Ji, Q., Tabassum, S., Hena, S., Silva, C.G., Yu, G., Zhang, Z., 2016. A review on the coal gasification wastewater treatment technologies: past, present and future outlook. *J. Clean. Prod.* 126, 38-55. <https://doi.org/https://doi.org/10.1016/j.jclepro.2016.02.147>.
- Judd, S., Judd, C., 2011. The MBR book. The MBR Book.
- Karlsson, A., Ejlerstsson, J., Nezirevic, D., Svensson, B.H., 1999. Degradation of phenol under meso- and thermophilic, anaerobic conditions. *Anaerobe* 5(1), 25-35. <https://doi.org/10.1006/anae.1998.0187>.
- Karlsson, A., Ejlerstsson, J., Svensson, B.H.J.A.o.M., 2000. CO₂-dependent fermentation of phenol to acetate, butyrate and benzoate by an anaerobic, pasteurised culture. *173(5)*, 398-402. <https://doi.org/10.1007/s002030000160>.
- Kennes, C., Mendez, R., Lema, J.M., 1997. Methanogenic degradation of p-cresol in batch and in continuous UASB reactors. *Water Res.* 31(7), 1549-1554. [https://doi.org/https://doi.org/10.1016/S0043-1354\(96\)00156-X](https://doi.org/https://doi.org/10.1016/S0043-1354(96)00156-X).
- Kleerebezem, R., 1999. Anaerobic treatment of phthalates, microbiological and technological aspects. Wageningen WUR.
- Kleerebezem, R., Beckers, J., Hulshoff Pol, L.W., Lettinga, G., 2005. High rate treatment of terephthalic acid production wastewater in a two-stage anaerobic bioreactor. *Biotechnol. Bioeng.* 91(2), 169-179. <https://doi.org/10.1002/bit.20502>.
- Kleerebezem, R., Ivala, M., Pol, L.W.H., Lettinga, G., 1999. High-Rate Treatment of Terephthalate in Anaerobic Hybrid Reactors. *15(3)*, 347-357. <https://doi.org/10.1021/bp9900561>.
- Kleerebezem, R., Lettinga, G., 2000. High-rate anaerobic treatment of purified terephthalic acid wastewater. *Water Sci. Technol.* 42(5-6), 259-268. <https://doi.org/10.2166/wst.2000.0522> %J Water Science and Technology.
- Kleerebezem, R., Mortier, J., Hulshoff Pol, L.W., Lettinga, G., 1997. Anaerobic pre-treatment of petrochemical effluents: Terephthalic acid wastewater. *Water Sci. Technol.* 36(2), 237-248. [https://doi.org/https://doi.org/10.1016/S0273-1223\(97\)00393-4](https://doi.org/https://doi.org/10.1016/S0273-1223(97)00393-4).
- Kleerebezem, R., Van Loosdrecht, M.C.M., 2010. A Generalized Method for Thermodynamic State Analysis of Environmental Systems. *Crit. Rev. Environ. Sci. Technol.* 40(1), 1-54. <https://doi.org/10.1080/10643380802000974>.
- Knoll, G., Winter, J.J.A.M., 1987. Anaerobic degradation of phenol in sewage sludge. *25(4)*, 384-391. <https://doi.org/10.1007/bf00252552>.
- Kong, Z., Li, L., Xue, Y., Yang, M., Li, Y.-Y., 2019. Challenges and prospects for the anaerobic treatment of chemical-industrial organic wastewater: A review. *J. Clean. Prod.* 231, 913-927. <https://doi.org/https://doi.org/10.1016/j.jclepro.2019.05.233>.
- Ladino-Orjuela, G., Gomes, E., da Silva, R., Salt, C., Parsons, J.R., 2016. Metabolic Pathways for Degradation of Aromatic Hydrocarbons by Bacteria, *Reviews of Environmental Contamination and Toxicology Volume 237*. Springer, pp. 105-121. https://doi.org/https://doi.org/10.1007/978-3-319-23573-8_5.
- Lay, J.-J., Cheng, S.-S., 1998. Influence of hydraulic loading rate on UASB reactor treating phenolic wastewater. *Journal of Environmental Engineering* 124(9), 829-837.
- Lettinga, G., 2014. My Anaerobic Sustainability Story. LeAF.

- Leven, L., Nyberg, K., Schnurer, A., 2012. Conversion of phenols during anaerobic digestion of organic solid waste--a review of important microorganisms and impact of temperature. *J. Environ. Manage.* 95 Suppl, S99-103. <https://doi.org/10.1016/j.jenvman.2010.10.021>.
- Leven, L., Schnurer, A., 2005. Effects of temperature on biological degradation of phenols, benzoates and phthalates under methanogenic conditions. *Int. Biodeterior. Biodegrad.* 55(2), 153-160. <https://doi.org/http://dx.doi.org/10.1016/j.ibiod.2004.09.004>.
- Liang, D., Fang, H.H.P., Anaerobic Treatment of Phenolic Wastewaters, *Environmental Anaerobic Technology*. pp. 185-205. https://doi.org/10.1142/9781848165434_0009.
- Liang, D., Fang, H.H.P., 2010. Anaerobic Treatment of Phenolic Wastewaters, *Environmental Anaerobic Technology*. pp. 185-205. https://doi.org/10.1142/9781848165434_0009.
- Lin, H., Gao, W., Meng, F., Liao, B.-Q., Leung, K.-T., Zhao, L., Chen, J., Hong, H., 2012. Membrane Bioreactors for Industrial Wastewater Treatment: A Critical Review. *Crit. Rev. Environ. Sci. Technol.* 42(7), 677-740. <https://doi.org/10.1080/10643389.2010.526494>.
- Macarie, H., 2000. Overview of the application of anaerobic treatment to chemical and petrochemical wastewaters. *Water Sci. Technol.* 42(5-6), 201-214. <https://doi.org/https://doi.org/10.2166/wst.2000.0515>.
- Maiti, D., Ansari, I., Rather, M.A., Deepa, A., 2019. Comprehensive review on wastewater discharged from the coal-related industries – characteristics and treatment strategies. *Water Sci. Technol.* 79(11), 2023-2035. <https://doi.org/10.2166/wst.2019.195> %J Water Science and Technology.
- Muñoz Sierra, J.D., 2022. Anaerobic Membrane Bioreactors under Extreme Conditions.
- Muñoz Sierra, J.D., García Rea, V.S., Cerqueda-García, D., Spanjers, H., van Lier, J.B., 2020. Anaerobic Conversion of Saline Phenol-Containing Wastewater Under Thermophilic Conditions in a Membrane Bioreactor. *Front. Bioeng. Biotechnol.* 8(1125). <https://doi.org/10.3389/fbioe.2020.565311>.
- Muñoz Sierra, J.D., Lafita, C., Gabaldón, C., Spanjers, H., van Lier, J.B., 2017. Trace metals supplementation in anaerobic membrane bioreactors treating highly saline phenolic wastewater. *Bioresour. Technol.* 234, 106-114. <https://doi.org/http://dx.doi.org/10.1016/j.biortech.2017.03.032>.
- Muñoz Sierra, J.D., Oosterkamp, M.J., Wang, W., Spanjers, H., van Lier, J.B., 2019. Comparative performance of upflow anaerobic sludge blanket reactor and anaerobic membrane bioreactor treating phenolic wastewater: Overcoming high salinity. *Chem. Eng. J.* 366, 480-490. <https://doi.org/https://doi.org/10.1016/j.cej.2019.02.097>.
- Munoz Sierra, J.D., Wang, W., Cerqueda-Garcia, D., Oosterkamp, M.J., Spanjers, H., van Lier, J.B., 2018. Temperature susceptibility of a mesophilic anaerobic membrane bioreactor treating saline phenol-containing wastewater. *Chemosphere* 213, 92-102. <https://doi.org/10.1016/j.chemosphere.2018.09.023>.
- Mutamim, N.S.A., Noor, Z.Z., Hassan, M.A.A., Yuniarto, A., Olsson, G., 2013. Membrane bioreactor: Applications and limitations in treating high strength industrial wastewater. *Chem. Eng. J.* 225, 109-119. <https://doi.org/http://dx.doi.org/10.1016/j.cej.2013.02.131>.
- Nobu, M.K., Narihiro, T., Hideyuki, T., Qiu, Y.L., Sekiguchi, Y., Woyke, T., Goodwin, L., Davenport, K.W., Kamagata, Y., Liu, W.T., 2015. The genome of *Syntrophorhabdus aromaticivorans* strain UI provides new insights for syntrophic aromatic compound metabolism and electron flow. *Environ. Microbiol.* 17(12), 4861-4872. <https://doi.org/10.1111/1462-2920.12444>.
- Noyola, A., Macarie, H., Varela, F., Landrieu, S., Marcelo, R., Rosas, M.A., 2000. Upgrade of a petrochemical wastewater treatment plant by an upflow anaerobic pond. *Water Sci. Technol.* 42(5-6), 269-276. <https://doi.org/10.2166/wst.2000.0523> %J Water Science and Technology.
- Qiu, Y.L., Hanada, S., Ohashi, A., Harada, H., Kamagata, Y., Sekiguchi, Y., 2008. *Syntrophorhabdus aromaticivorans* gen. nov., sp. nov., the first cultured anaerobe capable of degrading phenol to acetate in obligate syntrophic associations with a hydrogenotrophic methanogen. *Appl. Environ. Microbiol.* 74(7), 2051-2058. <https://doi.org/10.1128/aem.02378-07>.

- Rajeshwari, K.V., Balakrishnan, M., Kansal, A., Lata, K., Kishore, V.V.N., 2000. State-of-the-art of anaerobic digestion technology for industrial wastewater treatment. *Renew. Sust. Energ. Rev.* 4(2), 135-156. [https://doi.org/http://dx.doi.org/10.1016/S1364-0321\(99\)00014-3](https://doi.org/http://dx.doi.org/10.1016/S1364-0321(99)00014-3).
- Ribeiro, R., de Nardi, I.R., Fernandes, B.S., Foresti, E., Zaiat, M., 2013. BTEX removal in a horizontal-flow anaerobic immobilized biomass reactor under denitrifying conditions. *Biodegradation* 24(2), 269-278. <https://doi.org/10.1007/s10532-012-9585-2>.
- Robles, Á., Ruano, M.V., Charfi, A., Lesage, G., Heran, M., Harmand, J., Seco, A., Steyer, J.-P., Batstone, D.J., Kim, J., Ferrer, J., 2018. A review on anaerobic membrane bioreactors (AnMBRs) focused on modelling and control aspects. *Bioresour. Technol.* 270, 612-626. <https://doi.org/https://doi.org/10.1016/j.biortech.2018.09.049>.
- Schink, B., Philipp, B., Muller, J., 2000. Anaerobic degradation of phenolic compounds. *Naturwissenschaften* 87(1), 12-23. <https://doi.org/https://doi.org/10.1007/s001140050002>.
- Schühle, K., Fuchs, G., 2004. Phenylphosphate Carboxylase: a New C-C Lyase Involved in Anaerobic Phenol Metabolism in *Thauera aromatica*. 186(14), 4556-4567. <https://doi.org/10.1128/JB.186.14.4556-4567.2004> %J Journal of Bacteriology.
- Siddique, M.N.I., Sakinah Abd Munaim, M., Zularisam, A.W., 2014. Mesophilic and thermophilic biomethane production by co-digesting pretreated petrochemical wastewater with beef and dairy cattle manure. *J. Ind. Eng. Chem* 20(1), 331-337. <https://doi.org/https://doi.org/10.1016/j.jiec.2013.03.030>.
- Sieber, J.R., McInerney, M.J., Gunsalus, R.P., 2012. Genomic insights into syntrophy: the paradigm for anaerobic metabolic cooperation. *Annu. Rev. Microbiol.* 66, 429-452. <https://doi.org/10.1146/annurev-micro-090110-102844>.
- Singer, P.C., Pfaender, F.K., Chinchilli, J., Maciorowski III, A.F., J.C.L, G., R., 1978. Assessment of Coal Conversion Wastewaters: Characterization and Preliminary Biotreatability. , in: EPA, E. (Ed.). U.S. Washington D.C.
- Sreekanth, D., Sivaramakrishna, D., Himabindu, V., Anjaneyulu, Y., 2009. Thermophilic degradation of phenolic compounds in lab scale hybrid up flow anaerobic sludge blanket reactors. *J. Hazard. Mater.* 164(2-3), 1532-1539. <https://doi.org/http://dx.doi.org/10.1016/j.jhazmat.2008.09.070>.
- Swaminathan, K., Chakrabarti, T., Subrahmanyam, P.V.R., 1999. Substrate-substrate interaction of resorcinol and catechol in upflow anaerobic fixed film – fixed bed reactors in mono and multisubstrate matrices. *Bioprocess. Eng.* 20(4), 349-353. <https://doi.org/10.1007/pl00009052>.
- Tay, J.-H., He, Y.-X., Yan, Y.-G., 2000. Anaerobic biogranulation using phenol as the sole carbon source. *Water Environ. Res* 72(2), 189-194.
- Tay, J.-H., He, Y.-X., Yan, Y.-G., 2001. Improved anaerobic degradation of phenol with supplemental glucose. *Journal of environmental engineering* 127(1), 38-45.
- Van Lier, J., Van der Zee, F., Frijters, C., Ersahin, M., 2015. Celebrating 40 years anaerobic sludge bed reactors for industrial wastewater treatment. *Rev. Environ. Sci. Bio.* 14(4), 681-702. <https://doi.org/https://doi.org/10.1007/s11157-015-9375-5>.
- van Lier, J.B., Mahmoud, N., Rea, V.S.G., 2023. Anaerobic wastewater treatment, in: Lopez-Vazquez, C.M., Damir, B., Volcke, E.I.P., van Loosdrecht, M.C.M., Wu, D., Chen, G. (Eds.), *Biological Wastewater Treatment: Examples and Exercises*. IWA Publishing, p. o. https://doi.org/10.2166/9781789062304_0507.
- Van Lier, J.B., Mahmoud, N., Zeeman, G., 2020. Anaerobic wastewater treatment, in: Chen, G., van Loosdrecht, M.C.M., Ekama, G.A.B., D. (Eds.), *Biological wastewater treatment: principles, modelling and design*. IWA Publishing, pp. 701 - 756.
- van Lier, J.B., Seco, A., Jefferson, B., Ersahin, M.E., Robles, A., 2019. Upgrading anaerobic sewage treatment applying membranes: AnMBR and UF post filtration, in: de Lemos Chernicharo, C.A., Bressani-Ribeiro, T. (Eds.), *Anaerobic Reactors for Sewage Treatment: Design, Construction and Operation*. IWA Publishing, p. o. https://doi.org/10.2166/9781780409238_0339.

- van Lier, J.B., Tilche, A., Ahring, B.K., Macarie, H., Moletta, R., Dohanyos, M., Pol, L.W., Lens, P., Verstraete, W., 2001. New perspectives in anaerobic digestion. *Water Sci. Technol.* 43(1), 1-18. <https://doi.org/https://doi.org/10.2166/wst.2001.0001>.
- Veeresh, G.S., Kumar, P., Mehrotra, I., 2005. Treatment of phenol and cresols in upflow anaerobic sludge blanket (UASB) process: a review. *Water Res.* 39(1), 154-170. <https://doi.org/http://dx.doi.org/10.1016/j.watres.2004.07.028>.
- Vincent, A.T., Derome, N., Boyle, B., Culley, A.I., Charette, S.J., 2017. Next-generation sequencing (NGS) in the microbiological world: How to make the most of your money. *J. Microbiol. Methods* 138, 60-71. <https://doi.org/https://doi.org/10.1016/j.mimet.2016.02.016>.
- Wackett, L.P., 1996. Co-metabolism: is the emperor wearing any clothes? *Curr. Opin. Biotechnol.* 7(3), 321-325. [https://doi.org/https://doi.org/10.1016/S0958-1669\(96\)80038-3](https://doi.org/https://doi.org/10.1016/S0958-1669(96)80038-3).
- Wang, W., Han, H., Yuan, M., Li, H., 2010. Enhanced anaerobic biodegradability of real coal gasification wastewater with methanol addition. *J. Environ. Sci. (China)* 22(12), 1868-1874. [https://doi.org/https://doi.org/10.1016/S1001-0742\(09\)60327-2](https://doi.org/https://doi.org/10.1016/S1001-0742(09)60327-2).
- Wang, W., Han, H., Yuan, M., Li, H., Fang, F., Wang, K., 2011. Treatment of coal gasification wastewater by a two-continuous UASB system with step-feed for COD and phenols removal. *Bioresour. Technol.* 102(9), 5454-5460. <https://doi.org/https://doi.org/10.1016/j.biortech.2010.10.019>.
- Wang, W., Ma, W., Han, H., Li, H., Yuan, M., 2011. Thermophilic anaerobic digestion of Lurgi coal gasification wastewater in a UASB reactor. *Bioresour. Technol.* 102(3), 2441-2447. <https://doi.org/10.1016/j.biortech.2010.10.140>.
- Wang, W., Yang, Q., Zheng, S., Wu, D., 2013. Anaerobic membrane bioreactor (AnMBR) for bamboo industry wastewater treatment. *Bioresour. Technol.* 149, 292-300. <https://doi.org/10.1016/j.biortech.2013.09.068>.
- Zhao, Q., Liu, Y., 2016. State of the art of biological processes for coal gasification wastewater treatment. *Biotechnol. Adv.* 34(5), 1064-1072. <https://doi.org/10.1016/j.biotechadv.2016.06.005>.
- Zhou, G.-M., Fang, H.H.P., 1997. Co-degradation of phenol and m-cresol in a UASB reactor. *Bioresour. Technol.* 61(1), 47-52. [https://doi.org/http://dx.doi.org/10.1016/S0960-8524\(97\)84698-6](https://doi.org/http://dx.doi.org/10.1016/S0960-8524(97)84698-6).



Chapter 2

Enhancing phenol conversion rates in saline anaerobic membrane bioreactor using acetate and butyrate as additional carbon and energy sources

This chapter is an adapted version of: García Rea Víctor S., Muñoz Sierra Julian D., Fonseca Aponte Laura M., Cerqueda-García Daniel, Quchani Kiyan M., Spanjers Henri, van Lier Jules B. (2020). Enhancing Phenol Conversion Rates in Saline Anaerobic Membrane Bioreactor Using Acetate and Butyrate as Additional Carbon and Energy Sources. F. Microbiol., 11. DOI: 10.3389/fmicb.2020.604173.

Abstract

Phenolic industrial wastewater, such as those from coal gasification, are considered a challenge for conventional anaerobic wastewater treatment systems because of its extreme characteristics such as presence of recalcitrant compounds, high toxicity, and salinity. However, anaerobic membrane bioreactors (AnMBRs) are considered of potential interest since they retain all micro-organism that are required for conversion of the complex organics. In this study, the degradation of phenol as main carbon and energy source (CES) in AnMBRs at high salinity ($8.0 \text{ g Na}^+ \cdot \text{L}^{-1}$) was evaluated, as well as the effect of acetate and an acetate-butyrate mixture as additional CES on the specific phenol conversion rate and microbial community structure. Three different experiments in two lab-scale (6.5 L) AnMBRs (35°C) were conducted. The first reactor (R1) was fed with phenol as the unique CES, the second reactor was fed with phenol and either acetate [$2 \text{ gCOD} \cdot \text{L}^{-1}$], or a 2:1 acetate-butyrate [$2 \text{ gCOD} \cdot \text{L}^{-1}$] mixture as additional CES. Results showed that phenol conversion could not be sustained when phenol was the sole CES. In contrast, when the reactor was fed with acetate or acetate-butyrate mixture, specific phenol conversion rates of 115 and $210 \text{ mgPh} \cdot \text{gVSS}^{-1} \cdot \text{d}^{-1}$, were found respectively. The syntrophic phenol degrader *Syntrophorhabdus* sp. and the acetoclastic methanogen *Methanosaeta* sp. were the dominant bacteria and archaea, respectively, with corresponding relative abundances of up to 63% and 26%. The findings showed that dosage of additional CES allowed the development of a highly active phenoldegrading biomass, potentially improving the treatment of industrial and chemical wastewaters.

2.1 Introduction

Rapid industrialization has generated many industrial effluents that constitute a major source of pollution (Lin et al., 2013). At present, many of these industrial effluents are successfully treated using anaerobic high-rate treatment processes (Van Lier et al., 2015). However, some industrial wastewaters represent a challenge for conventional anaerobic wastewater treatment systems. Wastewater characteristics that are considered extreme reduce the performance of conventional anaerobic systems, which leads to process imbalance or reactor failure (Dereli et al., 2012). (Dereli et al., 2012), proposed the use of anaerobic membrane bioreactors (AnMBR) to treat industrial wastewater with extreme characteristics, especially because of their effective biomass retention and the production of suspended-solids-free effluents, making them suitable for water reclamation.

Chemical and petrochemical wastewater, such as coal gasification wastewater, is an example of an industrial effluent with toxic phenolics as the major organic pollutants (Li et al., 2017). Nevertheless, other compounds such as acetate or butyrate, which could be used by microorganisms as carbon and energy sources (CES), are also present in coal gasification wastewater as common contaminants (Blum et al., 1986; Ji et al., 2016; Singer et al., 1978). Besides, it has been reported that coal-related industries wastewaters have a high concentration of total dissolved solids, ranging from 174 to 2000 mg·L⁻¹ (Maiti et al., 2019). Furthermore, under closed-water-loops, increasing salinity in the wastewater is expected.

Little is known regarding the microbial community structure and dynamics in AnMBRs under saline conditions treating toxic compounds such as phenol. Furthermore, no study has been conducted to determine how the microbial community is shifted by either the increase in the loading rates and/or the addition of extra CES, especially in suspended biomass systems as the one present in the AnMBR.

This study researched the effect of the addition of acetate or a mixture of acetate-butyrate as additional CES on the sPhCR of AnMBRs and on the microbial community related to the degradation process, with particular focus on the phenol degraders and the methanogens. The effect of phenol on the acetoclastic specific methanogenic activity (SMA) and the sPhCR in batch experiments were assessed as well.

2.2 Materials and methods

2.2.1 Analytical techniques

2.2.1.1 Chemical oxygen demand

During the operation of the reactors, COD in the feed and the permeate was measured using a spectrophotometer (DR3900, Hach Lange, Germany). Hach Lange Kits (Hach Lange, Germany) were used following the instructions of the manufacturer. Proper dilutions were done to avoid Cl^- interference.

2.2.1.2 Phenol, volatile fatty acids, and benzoate concentrations

Phenol, volatile fatty acids (VFAs), and benzoate were measured by a gas chromatograph (GC) (Agilent Technology) equipped with a flame ionization detector (FID) with a capillary column (type HP-PLOT/U) with a size of 25 m x 320 mm x 0.5 mm. Helium was used as carrier gas at a flow rate of 67 mL·min⁻¹ and a split ratio of 25:1. The oven temperature was increased from 80 to 180 °C in 10.5 min. Injector and detector temperatures were 80 and 240 °C, respectively, and the injection volume was 1 µL.

For the preparation of the samples, approximately 1 mL of permeate was filtered through a 0.45 µm filter (Chromafil Xtra PES-45/25). Depending on the dilution required to have phenol, VFAs, and benzoate in the measurable range of the GC, a certain volume of the filtrate was mixed with pentanol [320 mg·L⁻¹] to obtain a final volume of 1.5 mL. Finally, 10 µL of formic acid [95 %] (Merck, New Jersey) were added to the vial. Phenol concentration was double-checked with a spectrophotometer (Merck, Germany) using Merck – Spectroquant® Phenol cell kits (Merck, Germany) following manufacturers' instructions.

2.2.2 Batch tests

2.2.2.1 Specific methanogenic activity inhibition by phenol

Batch tests with initial phenol concentrations of 50 (n = 2), 200 (n = 6), and 500 (n = 6) mg·L⁻¹ were carried out in 250 mL Schott glass (Schott, Germany) reactors. Biomass samples (60-80 mL) were taken from the AnMBR to have a final volume of 200 mL at a VSS concentration of 4 g·L⁻¹ (Inoculum/Substrate = 2 for the control with 2.0 gAc-COD·L⁻¹). Macro- and micronutrients, phosphate buffer solutions, and Na⁺ as NaCl were dosed as specified in Section 2.2.3. A shaker (New Brunswick™, Eppendorf, Germany) at 130 rpm and at 35 °C was used for the incubation. Methane production was continuously measured by an AMPTS (Bioprocess Control, Sweden) following manufacturer's instruction. The tests were stopped when the acetate was completely depleted after 48-72 h approx.

2.2.2.2 Phenol degradation tests

Batch tests with a phenol concentration of $500 \text{ mg}\cdot\text{L}^{-1}$ ($n = 5$) were performed. The batch tests were conducted in 250 mL Schott (Schott, Germany) glass reactors. Biomass was taken from the AnMBR to have a final VSS concentration of $4 \text{ g}\cdot\text{L}^{-1}$. The batch reactors were supplemented with macro- and micronutrient solution, phosphate buffer solutions, and Na^+ (as NaCl) as specified in Section 2.2.3. The bottles were incubated at 35°C and 130 rpm. Samples (1–2 mL) were periodically taken, and phenol concentration was measured.

2.2.3 Experimental setup and reactors operation

2.2.3.1 Anaerobic membrane bioreactor setup

Two AnMBRs (6.5 L working volume) were used for the continuous experiment. Figure 2.1 depicts a scheme of the reactors' setup. The temperature of the reactors was kept at $35.0 \pm 1.0^\circ\text{C}$ by a water bath (Tamson Instruments, The Netherlands) circulating warm water through the reactor double-jacketed wall. Mixing in the reactor was ensured by internal sludge circulation with a reactor turnover of approximately 200 times $\cdot\text{d}^{-1}$. The setup used two peristaltic pumps (Watson Marlow 12 U/DV, 220 Du) for the feeding solution and permeate extraction, respectively, and one pump (Watson Marlow 620U) for the sludge recirculation. Temperature and pH were measured online by pH/temperature probes (Endress & Hauser, Memosens and Mettler Toledo). The biogas production rate was measured by a gas meter counter MGC-1 PMMA (Ritter, Milligas, and MGC-10).

Each reactor was coupled to an external pressure-driven ultrafiltration (nominal pore size of 30 nm) PVDF membrane module (X-Flow, Pentair). Membranes were 64 cm length and 0.52 cm diameter, and were operated at a cross-flow velocity of $0.8 \text{ m}\cdot\text{s}^{-1}$ ($Q \approx 1450 \text{ L}\cdot\text{d}^{-1}$). Reactors worked at a constant flux of $6 \text{ L}\cdot\text{m}^{-2}\cdot\text{h}^{-1}$. The transmembrane pressure (TMP) was measured by three different pressure sensors (AE Sensors, The Netherlands), with a range of -800 to 600 mbar, that were located at the entrance and outlet of the membrane, and at the permeate side. Reactor volume was controlled by two pressure sensors (AE Sensors, The Netherlands) with a range of 0 to 100 mbar, one was located on top of the reactor to measure the gas pressure, and the other at the bottom of the reactor, to measure the hydrostatic pressure plus the gas pressure.

Biomass was already acclimated to high sodium concentration, and phenol and acetate degradation (Muñoz Sierra et al., 2018). Before starting the continuous experiments, the biomass was mixed and then evenly distributed between the two reactors.

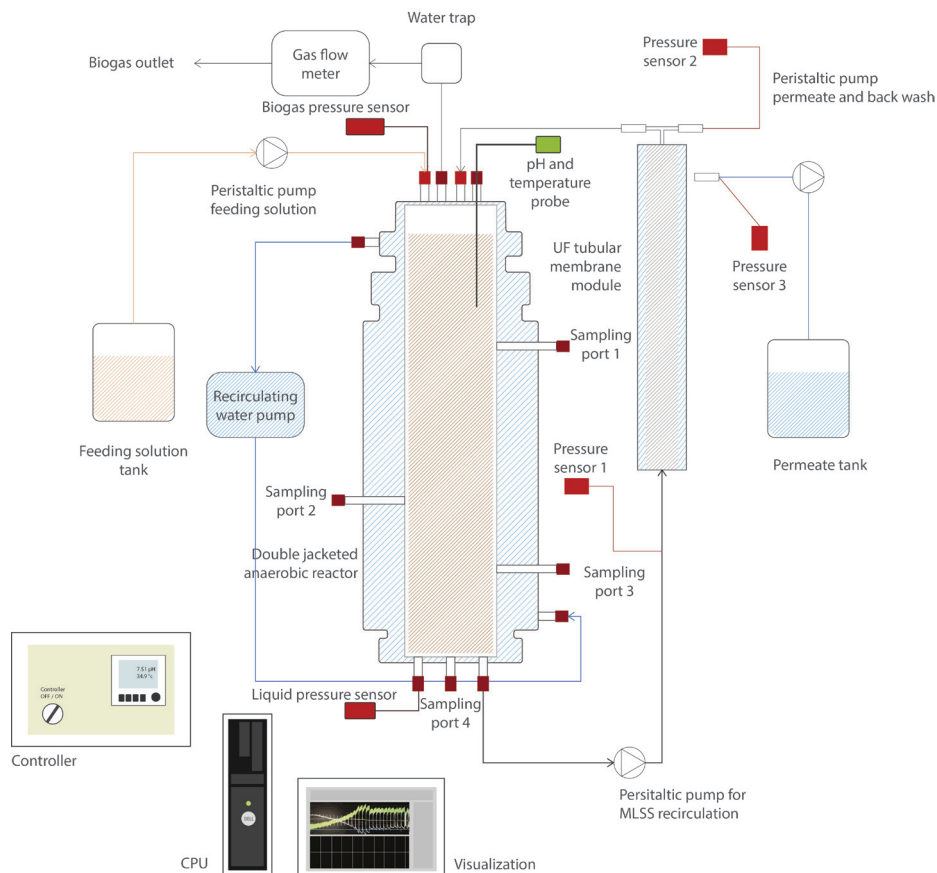


Figure 2.1. Scheme of the side-stream anaerobic membrane bioreactor (AnMBR) setup.

2.2.3.2 AnMBRs operation and model wastewater composition

In the first reactor (R1), phenol was targeted to be the main CES. For the second reactor (R2), acetate and a 2:1 acetate-butyrate mixture were added as additional CES (Table 2.1). Besides the first 10 days of operation of R1 where the HRT was decreased from 7 to 4 d, the HRT in the AnMBRs was maintained at 4 d. The average SRT was calculated as $SRT = X_{\text{reactor}} / X_{\text{removed}}$ [gVSS]/[gVSS·d⁻¹], where X_{removed} resulted from the biomass withdrawn for samplings divided by the days between each determination of solids. SRT values of 4300 ± 1600 (R1), 4500 ± 1700 d (R2a), and 5300 ± 2040 d (R2b) were found.

Table 2.1. Influent concentration and loading rates of the different carbon sources during the operation of the AnMBRs.

Reactor	Stages	Operation day	Phenol [g·L ⁻¹]	Phenol loading rate [mgPh·gVSS ⁻¹ ·d ⁻¹]	Acetate [gCOD·L ⁻¹]	Acetate loading rate [gCOD-Ac·gVSS ⁻¹ ·d ⁻¹]	Butyrate [gCOD·L ⁻¹]	Butyrate loading rate [gCOD-Bu·gVSS ⁻¹ ·d ⁻¹]
R1	I	0 - 59	0.5	10, 28, 42	4.7, 3.5, 1.2, 0.3, 0	100, 76, 25, 7, 0.	N/A	N/A
	II	60 - 99	0.5, 0.9, 0.5	42, 52, 31	0	0	N/A	N/A
	III	100 - 115	0	0	2.5	54	N/A	N/A
R2 (a)	I	0 - 43	0.5	25	4.7, 3.5, 2.3, 2.0	236, 177, 113, 100	N/A	N/A
	II	44 - 100	0.5, 1.5, 3.0, 6.0, 8.2	25, 75, 115, 230, 317	2.0	100, 75	N/A	N/A
	III	101 - 115	0.0	0	9.1	350	N/A	N/A
R2 (b)	I	0 - 30	0.5	≈17	1.33	≈48	0.66	≈24
	II	31 - 110	0.75, 1.0, 1.5, 2.7, 6.5, 11.1	30, 42, 62, 108, 195, 260	1.33	≈48	0.66	≈24

For the model wastewater composition, and based on a modification to Hendriks *et al.* 2017 and Muñoz-Sierra *et al.* 2018, per each gram of COD in the feeding solution, 1.5 mL of macronutrients solution, 0.76 mL of micronutrients solution, 2.2 mL of buffer phosphate solution A, 3.4 mL of buffer phosphate solution B, and 50 mg of yeast extract (Sigma Aldrich) were added, as well, to the feeding solution (Table 2.2). Enough NaCl was added to the feeding solution to keep a Na^+ concentration of 8.0 g/L.

Table 2.2. Micro- & macro nutrient and buffer solutions dosed in the AnMBRs

Solution	Composition
Micronutrient	EDTA- Na_2 [1.0 g·L ⁻¹], H_3BO_3 [0.050 g·L ⁻¹], $\text{MnCl}_2 \cdot 4\text{H}_2\text{O}$ [0.50 g·L ⁻¹], $\text{FeCl}_3 \cdot 6\text{H}_2\text{O}$ [2.0 g·L ⁻¹], ZnCl_2 [0.050 g·L ⁻¹], $\text{NiCl}_2 \cdot 6\text{H}_2\text{O}$ [0.050 g·L ⁻¹], $\text{CuCl}_2 \cdot 2\text{H}_2\text{O}$ [0.030 g·L ⁻¹], Na_2SeO_3 [0.10 g·L ⁻¹], $(\text{NH}_4)_6\text{Mo}_7\text{O}_{24} \cdot 4\text{H}_2\text{O}$ [0.090 g·L ⁻¹], Na_2WO_4 [0.080 g·L ⁻¹], $\text{CoCl}_2 \cdot 6\text{H}_2\text{O}$ [2.0 g·L ⁻¹]
Macronutrient	NH_4Cl 170 g·L ⁻¹ , $\text{CaCl}_2 \cdot 2\text{H}_2\text{O}$ 8 g·L ⁻¹ and $\text{MgSO}_4 \cdot 7\text{H}_2\text{O}$ 9 g·L ⁻¹
Buffer solution A	$\text{K}_2\text{HPO}_4 \cdot 3\text{H}_2\text{O}$ [45.6 g·L ⁻¹]
Buffer solution B	$\text{NaH}_2\text{PO}_4 \cdot 2\text{H}_2\text{O}$ [31.2 g·L ⁻¹]

2.2.4 Microbial community analysis

2.2.4.1 DNA extraction, quantification, and amplification

Biomass samples corresponding to 1.5 – 2.0 mL of MLSS were regularly taken from the AnMBRs during the operation of the reactors. The biomass was transferred to Eppendorf tubes (Eppendorf, Germany) and centrifuged in a microcentrifuge (Eppendorf, Germany) at 10,000 g for 5 min. The supernatant was discarded and the biomass pellets were frozen and stored at -80°C. For the DNA extraction, the biomass pellet were thawed, and the DNA was extracted with the DNeasy UltraClean Microbial Kit (Qiagen, Germany). Qubit3.0 DNA detection (Qubit® dsDNA HS assay kit, Life Technologies, U.S.) was used to verify DNA quality and quantity.

DNA (16S rRNA gene) amplification was done by Illumina Novaseq 6000 platform by Novogene. The hypervariable regions V3-V4 were amplified using the primer set 341F [(5'-3') CCTAYGGGRBGCASCAG] and 806R [(5'-3') GGACTACNNGGGTATCTAAT]. The PCR reactions were carried out with Phusion® High-Fidelity PCR Master Mix (New England Biolabs).

2.2.4.2 DNA data processing

The paired-end reads (2 x 250) were processed in the QIIME2 pipeline (Bolyen *et al.*, 2019). After manual inspection, the forward and reverse reads were truncated in the position 250 in the 3' end, and the forward reads were trimmed in the position 35 in

the 5' end. Then, the reads were denoised, and the amplicon sequences variants were resolved with the DADA2 plugin (Callahan et al., 2016), removing chimeric sequences with the “consensus” method. The taxonomy of the representative sequences of the amplicon sequences variants was assigned with the classify-consensus-vsearch plugin (Rognes et al., 2016), using the SILVA 132 database (Quast et al., 2013) as reference. The feature table was exported to the R environment to perform the statistical analysis with the phyloseq library (McMurdie and Holmes, 2013).

2.2.4.3 Canonical correspondence analysis

A canonical correspondence analysis (CCA) was calculated, using the Weighted Unifrac distance metric and the specific phenol loading rate (sPhLR) and sPhCR as explanatory variables. The statistical significance of the ordination in the CCA was tested with an ANOVA at a p-value < 0.05.

2.3 Results and Discussion

2.3.1 *Acetoclastic SMA inhibition by phenol, and butyrate degradation tests*

Batch tests with initial phenol concentrations of 50, 200, and 500 mg·L⁻¹ were performed to determine a possible inhibition by phenol on the acetoclastic specific methanogenic activity (SMA) of the AnMBR biomass (Figure 2.2) (Appendix A.2, Table A.2.1). At initial phenol concentrations of 50 and 200 mg·L⁻¹, the SMA values were $3.4 \pm 4.8 \%$ and $4.3 \pm 23.6 \%$, respectively, higher than the control (acetate 2.0 gCOD·L⁻¹), meaning that at these concentrations, there was no inhibition in the acetoclastic methanogens due to phenol. On the other hand, the SMA at an initial phenol concentration of 500 mg·L⁻¹ was $27.0 \pm 6.6 \%$ lower than the control SMA, meaning that the methanogens were inhibited by phenol.

AD inhibition by phenol is a phenomenon reported in literature (Liang and Fang, 2010; Olguin-Lora et al., 2003). Although phenol may affect all main physiological microbial populations of the AD process, it is reported, as with other inhibitory or toxic substances (Astals et al., 2015), that the acetoclastic methanogenic population could be the most affected group (Chen et al., 2008). Half maximum inhibitory concentration (IC₅₀) ranges between 50 and 1750 mg·L⁻¹ for non-adapted and phenol-degrading biomass have been reported (Collins et al., 2005; Fang and Chan, 1997; Muñoz Sierra et al., 2017; Olguin-Lora et al., 2003).

Furthermore, we performed all batch experiments at 8.0 g Na⁺·L⁻¹ which might have had an impact as well, even though the biomass was adapted to this Na⁺ concentration. In agreement with literature (Collins et al., 2005; Fang and Chan, 1997; Muñoz Sierra et al., 2017; Olguin-Lora et al., 2003), the results obtained in this research showed that

a phenol concentration of 50 mg·L⁻¹ caused no negative effect on the SMA when compared to the control without phenol. As well, the average SMA at phenol concentration of 200 mg·L⁻¹ was not affected, but phenol concentration of 500 mg·L⁻¹ decreased the SMA with 27%. Butyrate at a concentration up to 3.0 gCOD·L⁻¹ did not cause inhibition problems (Appendix A.2. Section A.2.2).

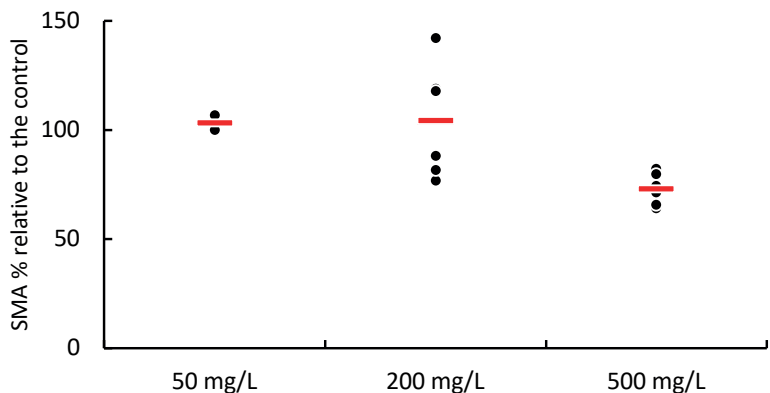


Figure 2.2. Effect of the phenol addition on the percentage of the acetoclastic SMA of the AnMBR sludge. Each point represents the percentage of the SMA value when different phenol concentrations were added in comparison to the value of the control SMA (acetate at 2 gCOD·L⁻¹). The thick red line represents the average SMA value for the different phenol concentrations

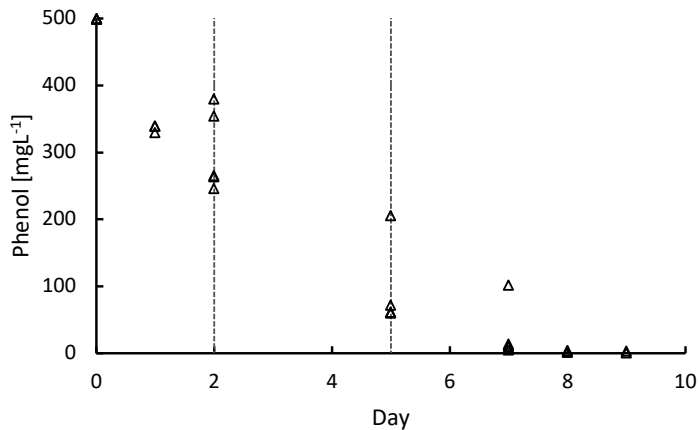


Figure 2.3. Phenol degradation batch assays. The lines represent the period used for the determination of the specific phenol conversion rate

2.3.2 Phenol degradation in batch assays

To further study the phenol degradation kinetics, a series of batch tests with phenol concentrations of $500 \text{ Ph} \cdot \text{L}^{-1}$ were performed (Figure 2.3). For calculating the sPhCR, the period between day 2 and day 5 of the assays was chosen to get the part of the curve that avoids a possible inhibition of the phenol degraders by high phenol concentration. The average sPhCRs calculated during the batch test were $17.8 \pm 2.6 \text{ mgPh} \cdot \text{gVSS}^{-1} \cdot \text{d}^{-1}$.

Several sPhCR values for granular biomass have been reported in batch tests, such as 126 (Tay et al., 2000), 65 (Razo-Flores et al., 2003), and 38-93 (Fang et al., 2004) $\text{mgPh} \cdot \text{gVSS}^{-1} \cdot \text{d}^{-1}$ which are higher than the average value of $16.6 \pm 1.9 \text{ mgPh} \cdot \text{gVSS}^{-1} \cdot \text{d}^{-1}$ that we obtained. However, in our study, the sPhCRs assessed in the batch tests were lower than the sPhCRs determined in the continuous experiment (Section 2.3.3).

2.3.3 AnMBR operation

2.3.3.1 AnMBR operation towards phenol as the main carbon and energy source
R1 was operated to assess whether phenol could serve as the sole CES (Figure 2.4, A) and the maximum sPhCR that could be achieved. During stage I, in which acetate was stepwise decreased, the sPhLR was stepwise increased in ten days from 12 to $42 \text{ mgPh} \cdot \text{gVSS}^{-1} \cdot \text{d}^{-1}$. During this period, the sPhCR remained the same as the sPhLR, i.e., $42 \text{ mgPh} \cdot \text{gVSS}^{-1} \cdot \text{d}^{-1}$, corresponding to a phenol removal efficiency exceeding 99%. In stage II, after the exclusion of acetate from the feeding, the sPhCR decreased to $29 \text{ mgPh} \cdot \text{gVSS}^{-1} \cdot \text{d}^{-1}$ during the days 59-72. When the phenol loading was increased to $62 \text{ mgPh} \cdot \text{gVSS}^{-1} \cdot \text{d}^{-1}$, the sPhCR and the removal percentage started to decrease, and on day 94, the sPhCR and the phenol removal efficiency were 0. During stage III, phenol was excluded from the influent because no phenol conversion was observed, and further intoxication of the reactor biomass was unwanted. Hence, the COD was replaced with acetate.

In our present study, it was not possible to achieve long-time AnMBR operation with phenol as the sole CES. This was confirmed with a second experiment (Appendix A.2, Section A.2.3). Possibly, this inability might be attributed to the applied sodium concentration of $8 \text{ g} \cdot \text{L}^{-1}$, which has been hypothesized to decrease the phenol conversion (Wang et al., 2017). Under saline conditions, more of the catabolically generated energy from the substrate conversion, in this case phenol, will be spent on regulating a higher maintenance energy in the biomass, because of the increased osmotic pressure (He et al., 2017; Russell and Cook, 1995). A maximum sPhCR of $40 \text{ mgPh} \cdot \text{gVSS}^{-1} \cdot \text{L}^{-1}$ was determined from days 49 to 62 (Stage I) when phenol was the main CES, representing 80% of the total COD while acetate contributed to 20% of the COD. However, this sPhCR could not be sustained for more than five days after the acetate was excluded from the influent (Stage II).

For continuous reactor operation, anaerobic degradation of phenol as sole CES at different sPhCRs (6 - 690 mgPh·gVSS⁻¹·d⁻¹) has been reported (Fang et al., 1996; Kennes et al., 1997; Liang and Fang, 2010; Ramakrishnan and Gupta, 2008; Razo-Flores et al., 2003; Zhou and Fang, 1997) (Table 2.3). Most of these studies refer to granular-sludge-based reactors, such as upflow anaerobic sludge blanket (UASB) reactors, under non-saline conditions. As an exception, Suidan *et al.* 1988, reported the successful continuous operation of a chemostat (suspended biomass) with phenol as the only CES.

An anaerobic granule consists of several populations of microorganisms forming an ecosystem, in which the products of a specific population serves as the substrate

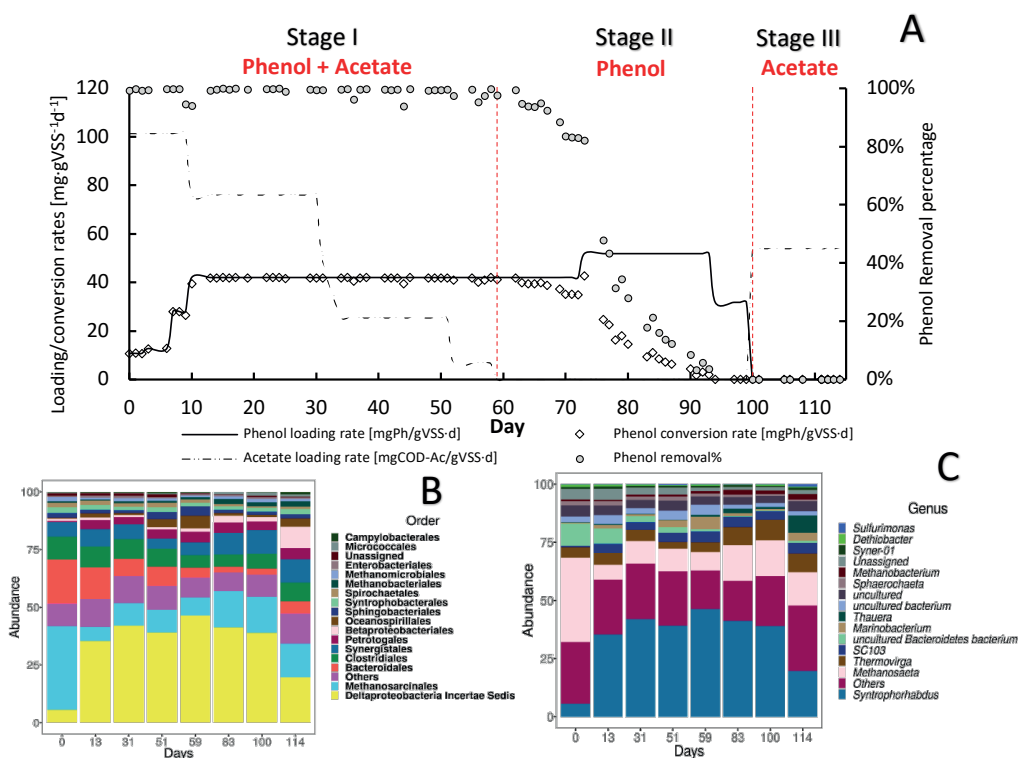


Figure 2.4. Operation (A) and microbial community dynamics (B and C) of the R1 towards the usage of phenol as the main carbon and energy source (CaES). The graph in figure A shows the phenol loading and conversion rates, the acetate loading rate, and the phenol removal percentage during the AnMBR operation. Figures B and C show the microbial community dynamics, as the more abundant microbial orders (B) or genus during the different operational days.

for others in a very close vicinity. Moreover, methanogens and phenol-degraders in the inside are only exposed to very low phenol concentrations when phenol is indeed readily degraded in the continuous system. Subsequent phenol conversion

in the granule interior provides the conversion intermediates as a substrate for the other populations, allowing the use of phenol as the sole CES. In suspended biomass systems, such as an AnMBR, the phenol concentration is the same for all biomass, while distances between microbial species are much larger, making these systems much more sensitive to increased phenol concentrations.

2.3.3.2 Effect of the addition of acetate on the specific phenol conversion rate

R2(a) was operated to determine the effect of the addition of acetate as an extra CES on the sPhCR (Figure 2.5 A). In stage I, the acetate-COD concentration in the influent was decreased from 4.7 to 2.0 gCOD·L⁻¹, corresponding to an acetate loading rate of 100 mgAc-COD·gVSS⁻¹·d⁻¹, while the sPhLR was maintained at 25 mgPh·gVSS⁻¹·d⁻¹, corresponding to a phenol concentration in the influent of 0.5 gPh·L⁻¹. During this stage, the sPhCR was 25 mgPh·gVSS⁻¹·d⁻¹, corresponding to a phenol removal percentage of ≈100%.

In stage II, the sPhLR was stepwise increased from 75 to 230 mgPh·gVSS⁻¹·d⁻¹, corresponding to phenol concentrations in the influent of 1.5 and 8.2 g·L⁻¹, respectively. Phenol removal of 100% was observed with phenol loading rates of 75 and 115 mgPh·gVSS⁻¹·d⁻¹. At a loading rate of 230 mgPh·gVSS⁻¹·d⁻¹, the sPhCR and the removal efficiency decreased to 86 mgPh·gVSS⁻¹·d⁻¹ and 55%, respectively. The further increase in the sPhLR (320 mgPh·gVSS⁻¹·d⁻¹) on day 87 caused an intoxication of the AnMBR, which was observed as a decreased sPhCR that was eventually halted. During days 94 to 100, phenol in the feeding solution was excluded and acetate concentration was kept at 2.0 gCOD·L⁻¹. In stage III, the reactor was fed with only acetate at a concentration of 9.1 gCOD·L⁻¹ to avoid further intoxication of the biomass.

Acetate has been used as an additional CES in the process of biological phenol degradation under anaerobic conditions, either during the reactor start-up (Razo-Flores et al., 2003) or operation (Muñoz Sierra et al., 2018, 2019; Munoz Sierra et al., 2018; Wang et al., 2017) (Table 2.3). Wang et al. reported UASB reactors treating synthetic wastewater with acetate concentration of 3.6 gCOD·L⁻¹ and phenol concentrations ranging from 0.1 to 2.0 g·L⁻¹, operating under saline conditions with Na⁺ concentration of 10 g·L⁻¹. They reported maximum sPhCR of 20 and 13 mgPh·gVSS⁻¹·d⁻¹ for batch and continuous reactors, respectively. Working with AnMBRs, Muñoz Sierra et al. 2019, reported maximum sPhCRs of 87 mgPh·gVSS⁻¹·d⁻¹ at a sodium concentration of 18 g·L⁻¹, corresponding to concentrations in the influent of 5 gPhenol·L⁻¹ and an acetate concentration of approx. 30 gCOD·L⁻¹. For comparison, in this experiment, we found a maximum stable sPhCR of 115 mgPh·gVSS⁻¹·L⁻¹ when acetate was used as additional CES.

Table 2.3. Studies dealing with phenol degradation either as main/unique carbon and energy source or with the dosage of additional carbon and energy sources

Phenol degradation with no additional carbon and energy source				
Substrate [mg·L⁻¹]	Sludge PhLR [gPh·gVSS⁻¹·d⁻¹]	Total Removal	sCH₄ rate [L·gVSS⁻¹·d⁻¹]	CH₄ yield [LCH₄·gCODr⁻¹]
Phenol (400)		90%		0.21
Phenol (420-1260)	0.03-0.09	98%	0.075	0.35
Phenol (2000) After rec (250 to 500)	0.58	99%	0.001	0.47
Phenolics (600)	0.0182	30%	0.001	0.02
Phenol (50 - 700)	0.024	85%	0.024	0.415
Additional carbon and energy source dosage for reactor start-up or biomass reactivation				
Substrate [mg·L⁻¹]	Sludge PhLR [gPh·gVSS⁻¹·d⁻¹]	Total Removal	sCH₄ rate [L·gVSS⁻¹·d⁻¹]	CH₄ yield [LCH₄·gCODr⁻¹]
Phenol (234)	0.006	92%	0.008	0.338
Phenol (1260)	0.26	94%		0.308
Phenol (1260)	0.315	86%	0.304	0.284
Phenol degradation with additional carbon and energy source dosage				
Substrate (mg/L)	Sludge PhLR [gPh·gVSS⁻¹·d⁻¹]	Total Removal	sCH₄ rate [L·gVSS⁻¹·d⁻¹]	CH₄ yield [LCH₄·gCODr⁻¹]
Phenol (105-1260) + Glucose	0.06-0.28	98%		
Phenol (625) +acetate (3850) + Na (10 g·L ⁻¹)	0.1042	100%		
Phenol (1000) +Acetate (1000)		99%		0.39
Phenol (500-1000) + VFAs	0.07-0.14	98%		0.32
Phenol (672) + VFAs		95%		0.28
Phenol (500) + Acetate + Na [4.7 - 20 g·L ⁻¹]	0.012	99%		
Phenol (500)+ NaCl (8gNa ⁺ /L)	0.042	97%	0.036	--

$\text{gCH}_4\text{-COD}\cdot\text{gCODr}^{-1}$	HRT	Vol [L]	Reactor type	Reference
53%	0.14 d	0.66	rUASB	Chang <i>et al.</i> , 1995
89%	12 h	2.8	rUASB	Fang <i>et al.</i> , 1996
117%	6 h	35	rUASB	Lay and Cheng, 1998
5%	24 h	7	UASB	Wang <i>et al.</i> , 2010
69%	24 h	2.8	AFBR	De Amorim <i>et al.</i> , 2015
$\text{gCH}_4\text{-COD}\cdot\text{gCODr}^{-1}$	HRT	Vol [L]	Reactor	Reference
86%	48 h	13.4	rAF	Li <i>et al.</i> , 2016
80%	12 h	2.8	UASB	Fang <i>et al.</i> , 2004
72%	12 h	2	UASB	Tay <i>et al.</i> , 2000
$\text{gCH}_4\text{-COD}\cdot\text{gCODr}^{-1}$	HRT	Vol [L]	Reactor	Reference
	12 h	2	UASB	Tay <i>et al.</i> 2001
	48 h	3.5	rUASB-AF	Wang <i>et al.</i> , 2017
100%	5-2.5h	10	GAC-AFBR	Lao, 2002
87%	12 h	3.5	rEGSB-AF	Scully <i>et al.</i> , 2006
72%	0.43d	1.8	AFBR	Carbajo <i>et al.</i> , 2010
	6.5 d	6.5	AnMBR	Muñoz-Sierra <i>et al.</i> 2018
--	4 d	6	AnMBR	This study

Table 2.3. Continued

Phenol degradation with additional carbon and energy source dosage				
Substrate (mg/L)	Sludge PhLR [gPh·gVSS ⁻¹ ·d ⁻¹]	Total Removal	sCH ₄ rate [L·gVSS ⁻¹ ·d ⁻¹]	CH ₄ yield [LCH ₄ ·gCODr ⁻¹]
Phenol (3000) + Acetate (2 gCOD/L)+ NaCl (8gNa ⁺ /L)	0.115	100%	0.114	0.27
Phenol (6500) + Acetate-Butyrate (2:1) (2 gCOD/)+ NaCl (8gNa ⁺ /L)	0.200	100%	--	--

2.3.3.3 Effect of the addition of the acetate-butyrate on the specific phenol conversion rate

After the recovery of the biomass from phenol intoxication, R2 was fed with a 2:1 acetate-butyrate mixture at a concentration of 2 gCOD·L⁻¹ to determine the effect of the dosage of an additional CES that intrinsically generates H₂ during its conversion on the sPhCR and the phenol degraders and methanogens (Figure 2.6 A). During stage I, the sPhLR was kept at an average value of 17.1 ± 1.31 mgPh·gVSS⁻¹·d⁻¹, corresponding to an average phenol concentration in the influent of 0.5 g·L⁻¹. On day 10 after the dosage of butyrate, the sPhCR and the phenol removal efficiency decreased to 8.4 mgPh·gVSS⁻¹·d⁻¹ and 64%, respectively. Possibly, the increased butyrate concentration impacted the phenol conversion pathway. Nobu et al. (2017) indicated that phenol converting microorganisms such as *Syntrophorhabdus* sp., have an alternative phenol degradation pathway, which yields one molecule of butyrate and one of acetate. Therefore, the increased butyrate concentration in the AnMBR could have decreased phenol degradation by product inhibition (Figure 2.6 A).

During stage II, from day 32 to 90, a phenol removal efficiency of 100% was found up to a sPhLR (and sPhCR) of 200 mgPh·gVSS⁻¹·d⁻¹ (influent concentration 6.5 gPh·L⁻¹), being amongst the highest anaerobic sPhCRs' reported in the literature, and the highest value reported for suspended biomass under anaerobic and saline conditions (Table 2.3). When the sPhLR was increased to 260 mgPh·gVSS⁻¹·d⁻¹ (phenol concentration in the influent = 11.1 g·L⁻¹), at day 99, the sPhCR and the phenol removal efficiency started to decrease. However, the sPhCR and the removal efficiency had already decreased to 130 mgPh·gVSS⁻¹·d⁻¹ and 45%, respectively, meaning a reactor failure due to biomass intoxication.

$\text{gCH}_4\text{-COD}\cdot\text{gCODr}^{-1}$	HRT	Vol [L]	Reactor	Reference
68%	4 d	6	AnMBR	This study
--	4 d	6	AnMBR	This study

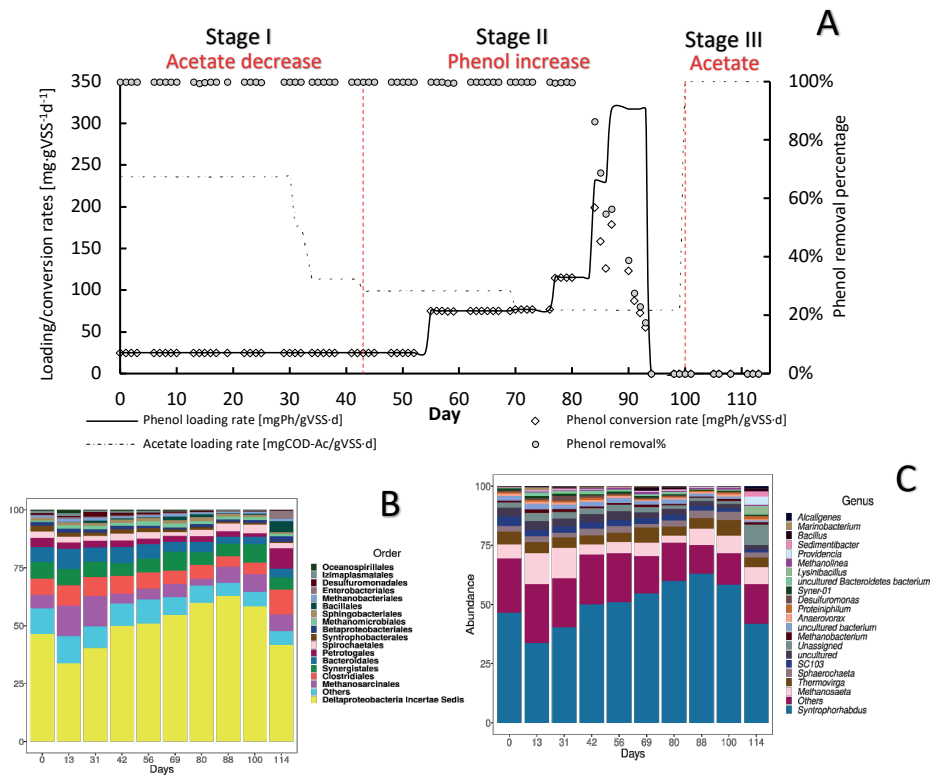


Figure 2.5. Operation (A) and microbial community dynamics (B) of the R2(b) with acetate [$2 \text{ gCOD}\cdot\text{L}^{-1}$] as an additional carbon and energy source. The graph in figure A shows the phenol loading and conversion rates, the acetate loading rate, and the phenol removal percentage during the AnMBR operation. Figures B and C show the microbial community dynamics, as the more abundant microbial orders (B) or genus (C) during the different operational days.

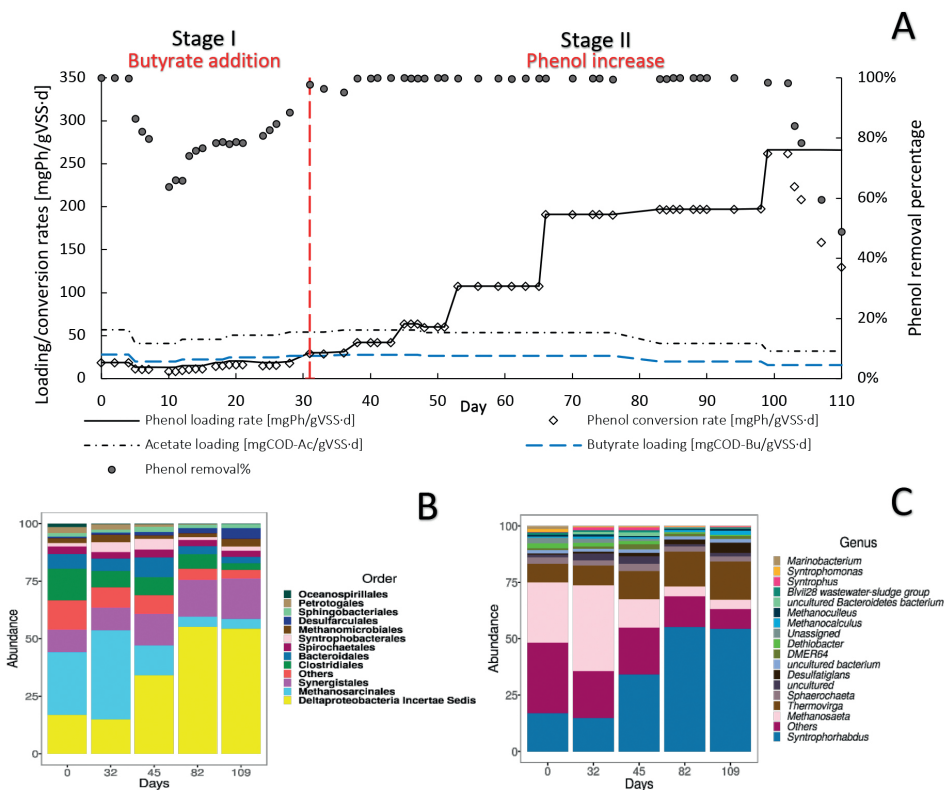


Figure 2.6. Operation (A) and microbial community dynamics (B) R2(b) with a 2 gCOD-L⁻¹, 2:1 acetate-butyrate mixture as an additional carbon and energy source. The graph in figure A shows the phenol loading and conversion rates, the acetate and butyrate loading rates, and the phenol removal percentage during the AnMBR operation. Figures B and C show the microbial community dynamics, as the more abundant microbial orders (B) or genus during the different operational days.

2.3.4 Analysis of the microbial community dynamics during the operation of the reactors

2.3.4.1 Microbial community dynamics in the AnMBR towards phenol as the main carbon and energy source

To get an insight into the microbial community structure in the AnMBR biomass during the reactor operation and to determine what was the effect of the sPhLRs on this structure, we analyzed the V3-V4 regions of the 16S rRNA gene of several biomass samples. The analysis showed that during the whole reactor operation, the more abundant microorganisms at genus level, were the Deltaproteobacteria *Syntrophorhabdus* sp. (Figure 2.4 B and C), which is a reported anaerobic syntrophic phenol degrader (Franchi et al., 2018; Nobu et al., 2015; Qiu et al., 2008), and the acetoclastic methanogenic *Methanosaeta* sp. Together, these microorganisms

represented 50% of the total microbial community; remarkably, no other genus had a relative abundance higher than 6% (Supplementary material). However, other microorganisms such as *Thermovirga* sp. ($5.8 \pm 2.1\%$), *Marinobacterium* ($2.1 \pm 1.8\%$), (Figure 2.4 C), and *Thauera* ($1.5 \pm 2.5\%$) were constantly present during the different stages. In this regard, *Thermovirga* sp., belonging to the order Clostridiales, has been reported in the microbial community of saline matrixes with either petrochemical (Dahle and Birkeland, 2006) or phenolic compounds (Wang et al., 2020). However, there are no studies suggesting phenol-degrading activity by this microorganism. *Marinobacterium* sp. has been reported as well as a community member of phenol-degrading reactors (Muñoz Sierra et al., 2019); although, most of the members of this genus are strictly aerobic, whereas *M. zhoushanense* is reported as facultative and halophilic microorganism (Han et al., 2016). *Thauera* sp. is a known phenol degrader, however it has been reported as nitrate reducer.

During stage I, at day 0, the relative percentage of *Syntrophorhabdus* sp. was 5.6%, which increased to a maximum of 46.3% in the last period of this first stage (day 59) and had an average relative abundance of $40.7 \pm 4.6\%$. For the methanogens, *Methanosaeta* sp. started at a relative abundance of 36.2%, and during the stage, it remained at an average of $8.4 \pm 1.7\%$.

In stage II, the relative abundance of *Syntrophorhabdus* sp. decreased to 41.2% (day 83) and 38.9% (day 100), which seemed to correlate with the decrease in the sPhCR (Section 2.3.3) and therefore, the removal percentage. The acetoclastic methanogen *Methanosaeta* sp. remained as the most abundant methanogenic microorganism, with an average relative abundance of 15% (days 83 and 100).

During stage III corresponding to the intoxication period (Section 2.3.3), the relative abundance of *Syntrophorhabdus* sp. kept decreasing with respect to the previous stage to a value of 19.7%, while the methanogen *Methanosaeta* sp. had a relative abundance of 14.3%. For this stage, the low abundance of *Syntrophorhabdus* sp. coincided with the observed toxic effect of phenol and the fact that no more phenol but only acetate was present in the influent.

2.3.4.2 Microbial community dynamics in the AnMBR with acetate as additional carbon and energy source

To determine the effect of the increase in the sPhLR and the dosage of acetate as additional CES on the microbial community structure, with a focus on the reported phenol degraders and the methanogens, we analyzed the microbial community structure of the R2(a) during different stages of its operation. We found, similar

to R1, that the most abundant bacteria and archaea were *Syntrophorhabdus* sp. and *Methanosaeta*, respectively (Figure 2.5 B & C). Same as in the operation of R1, no other genus had a relative abundance higher than 5%; although, *Thermovirga* sp. ($4.7 \pm 1.0\%$), was the next genus regarding relative abundance.

During stage I, the most abundant microorganism was the phenol degrader *Syntrophorhabdus* sp. with an average relative abundance of $40.2 \pm 6.4\%$. The methanogens were mainly represented by *Methanosaeta* with an average abundance of $10.6 \pm 4.1\%$. During stage II, after the sPhLR was increased, the relative abundance of *Syntrophorhabdus* sp. was increased, as well, to a maximum of 62.9% on day 88. However, on day 100, a decrease to 58.3% was observed, which correlated with the decrease in the phenol removal percentage (Section 2.3.3). For the methanogens, *Methanosaeta* sp. was the main microorganism during this stage with a maximum relative abundance of 7.5%.

During stage III, on day 114, a further decrease in the relative abundance of *Syntrophorhabdus* sp. to 41.8% was observed. However, the methanogen *Methanosaeta* sp. remained at a similar relative abundance as during stage II.

2.3.4.3 Microbial community dynamics in the AnMBR with the acetate-butyrate mixture

To determine the effect of the sPhLR and an hydrogen-generating additional CES on the microbial community structure, with a focus on the reported phenol degraders and the methanogens, we analyzed the microbial community structure of the R2(b) during different stages of its operation (Figure 2.6 B & C). For this reactor, the community was, again, mostly represented by the phenol degrader *Syntrophorhabdus* sp. and the acetoclastic *Methanosaeta* (>50%). As it was found in R1 and R2(a), there were no other genera with more than (5%) of relative abundance. However, in this reactor, the average relative abundance of *Thermovirga* sp. was $12.3 \pm 3.9\%$, which suggests that this microorganisms could potentially have a role in the phenol degradation process.

At the beginning of stage I, *Syntrophorhabdus* sp. and *Methanosaeta* sp. represented 17.0% and 32.5% of the microbial community, respectively. On day 32, after the start of the butyrate dosage, and the observed decrease in the phenol removal percentage, there was a slight decrease in *Syntrophorhabdus* sp. to 14.9%; that, as discussed in Section 2.3.5, it could possibly be related to an adverse effect of butyrate on the phenol degraders.

During stage II, on day 82, the relative abundance of *Syntrophorhabdus* sp. reached a maximum of 55.2%, which was 7% lower compared to the highest relative abundance

of this bacteria when the maximum sPhCR in the reactor operation with acetate was reached. Nonetheless, the sPhCR achieved with the acetate-butyrate mixture was 73% higher than that with only acetate (115 mgPh.gVSS⁻¹d⁻¹). For the methanogens, the acetoclastic *Methanosaeta* sp. remained as the main microorganism. On day 109, the relative abundance of *Syntrophorhabdus* sp. remained at 54%.

2.3.4.4 Canonical correspondence analysis

Canonical (or constrained) correspondence analyses (CCA) were performed to assess the changes in the microbial community structure during the operation of the reactors; and therefore, to correlate the effect of the increase in the sPhLR, and the dosage of acetate or the acetate-butyrate mixture with the different microbial communities in R1, R2(a) and R2(b) (Figure 2.7). CCA is an ordination technique that recovers the response of the community structure to different physical environmental variables, in this case the sPhLR and the sPhCR (Palmer, 1993).

The biplots for each reactor (Figure 2.7 A), in which the vectors indicate the importance of either sPhLR and sPhCR in the ordination process, showed a significant correlation ($p < 0.05$) between the community structures of the biomass of the reactors and the two variables. As it is seen in Figure 2.7 A & B, the community structures at different days (R1 = 13, 31, 51; R2(a) = 56, 69 and 80; R2(b) = 45, 82, 109), corresponding to the points at the right of the biplot, were correlated with a higher sPhLR and sPhCR capacity. In the comparison of the three reactors (Figure 2.7 B), it was noticed that the samples of R2(a) and R2(b) did not group together; however, because of the position of each sample respecting the vectors (sPhLR and sPhCR), it can be concluded that those community structures were more related to higher sPhLR and sPhCR. Regarding these two vectors explaining the environmental variables, it was decided to use both sPhLR and sPhCR, because even though sPhLR was the independent variable, sPhCR represented the biological activity of the biomass.

2.3.5 Discussion on the possible phenol-degrading-enhancing mechanisms

Regarding to the four discussed mechanisms which could enhance the sPhCR (Chapter 1, Section 1.2.8), co-metabolism (1) and/or (2) direct usage of acetate as a catabolic substrate by the phenol degraders seems the less likely. As it has been reported, the phenol degrader *Syntrophorhabdus* sp., excretes acetate through a cation-acetate symporter (Nobu et al., 2017). Furthermore, phenol degraders are a physiological population with defined substrates (Equation S6) (Qiu et al., 2008), being in this case, phenol and not acetate. However, the microbial community analyses results clearly indicate that with an increase in the sPhLR, the percentage of the biomass corresponding to the (reported) phenol degraders increased, reaching values over 50% of the total relative abundance, either at the order and genus levels (*Syntrophorhabdus*

sp.), of the biomass of R2(a) and R2(b) after the increase in the sPhLR (Figures 2.5 and 2.6, B & C). Note that the microbial community analyses were based on the study of the 16S rRNA gene, which may introduce inherent biases (Campanaro et al., 2018). As well, this analysis does not offer information about the metabolic state of the microorganisms, therefore, presence does not mean activity. Even though, with the addition of acetate or butyrate, the relative abundance of *Syntrophorhabdus* sp. reached values higher than 50%, which coincided with the highest sPhCRs achieved by the reactor. This correlation of the microbial community structure with the enhanced conversion was statistically confirmed by the CCA analysis (Section 2.3.4.4).

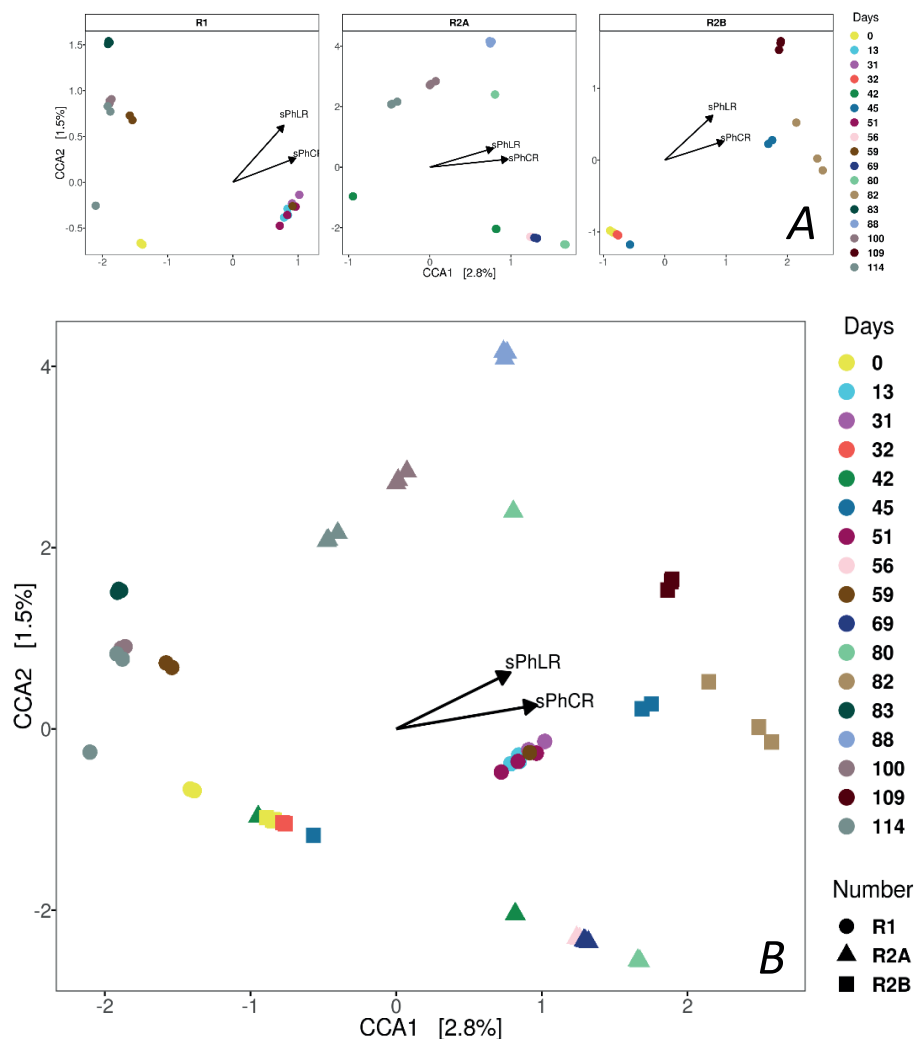


Figure 2.7. CCAs' for each of the reactors (A) and for all three (B). The samples that correspond to the reactors' operation with increased loading and conversion rates group to right of the biplots.

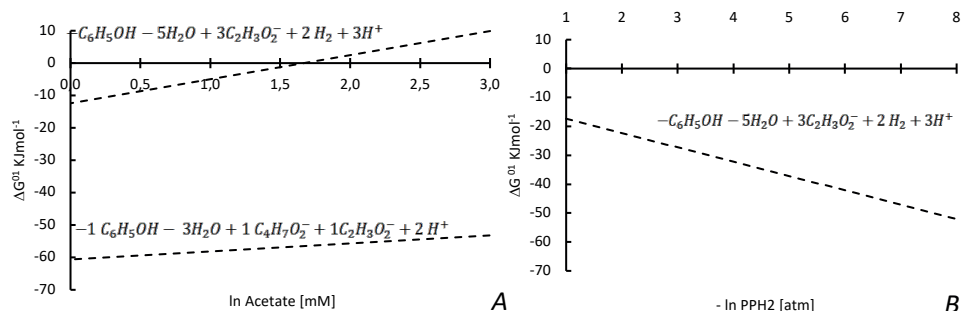


Figure 2.8. Effect of acetate (upper line) or butyrate (lower line) concentrations (A) or hydrogen partial pressure (B) on the ΔG° of the anaerobic phenol degradation reaction. The stoichiometry of each reaction is shown above the corresponding line. Note that the x axis on A is \ln while in B is $-\ln$; therefore, higher concentrations, but lower partial pressures are expected at the right of x axis.

On the other hand, our hypothesis is that the third identified mechanism, syntrophic association, could have played a role in the increase in sPhCR. Two different syntrophic associations with the methanogens are considered, either with the acetoclastics, which were the main methanogens (Section 2.3.4) and with the hydrogenotrophic. Considering the acetoclastic methanogens, Figure 2.8 shows the effect of the concentration of acetate on the Gibbs free energy change (ΔG° , standard conditions and pH = 7) of phenol degradation under anaerobic conditions (Appendix A.2, Section A.2.4), which shows that a low acetate concentration makes the reaction thermodynamically more favorable. Therefore, an abundant phenol-adapted acetoclastic methanogen population could offer advantages over phenol degradation. Nevertheless, R1 had similar values of the relative abundance of the acetoclastic methanogens (Supplementary material). Regarding reactor R2(b) and the second syntrophic process, it has been shown that anaerobic mineralisation of phenol requires the presence of balanced (syntrophic) associations that guarantee efficient interspecies electron transfer. In these associations, hydrogen-consuming microorganisms, such as the hydrogenotrophic methanogens, may act as the required electron sink (Qiu et al., 2008). For this reason, butyrate was added as additional CES in AnMBR experiment (R2(b)). However, the reactor fed with butyrate did not show a higher relative abundance of hydrogenotrophic archaea in comparison to the operation of the other reactors (Figure 2.9). Hydrogenotrophic microorganisms such as *Methanoculleus* sp. and *Methanocalculus* sp. were present at an average of $1.76 \pm 0.68\%$, whereas, when only acetate was dosed as additional CES, hydrogenotrophic methanogens such as *Methanobacterium* sp. and *Methanolinea* sp. were found in similar relative abundances ($1.42 \pm 0.42\%$). A similar percentage of $1.26 \pm 0.68\%$ was found for

the hydrogenotrophic *Methanobacterium* in the operation of R1, in which phenol as the sole CES was investigated.

Therefore, we hypothesize that the development of the (acetoclastic) methanogenic population could have enhanced the phenol conversion by keeping the degradation products, e.g. acetate, in a low concentration, allowing the constant conversion of phenol, and consequently promoting an increase of the abundance of the phenol-degrading microorganisms or possibly their specific conversion rate (Appendix 1, Eq. A.1.6).

Finally, regarding to the fourth mechanism considered (i.e., an increase in intermediate compounds involved in the conversion of phenolics), it could be possible that an increase in the HCO_3^- concentration, due to the fermentation of acetate, could have played a role in the enhancement of the sPhCR by promoting the carboxylation step needed for phenol degradation. It has been reported that in the absence of $\text{HCO}_3^-/\text{CO}_2$ phenol degradation under anaerobic conditions is hampered (Karlsson et al., 1999) and that the phenylphosphate carboxylase found in *Syntrophorhabdus* sp. is highly dependent on $\text{HCO}_3^-/\text{CO}_2$ (Karlsson et al., 1999; Nobu et al., 2015; Schühle and Fuchs, 2004). However, this hypothesis should be further tested.

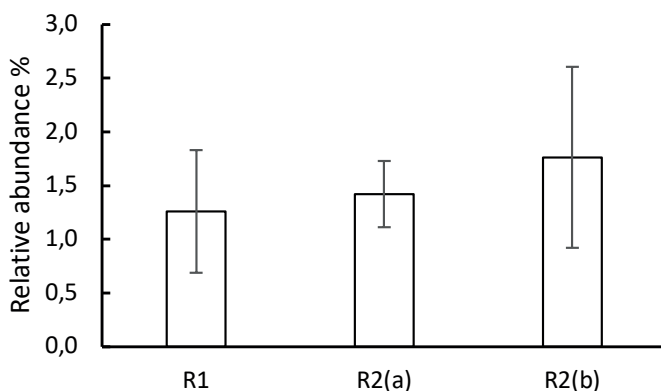


Figure 2.9. Average relative abundance percentage of the hydrogenotrophic methanogens in the operation of the three AnMBRs. n = 5 to 10, bars CI 95%.

2.4 Conclusions

The present study showed the feasibility of using AnMBR for the treatment of phenolic wastewater at high sodium concentrations. By performing batch tests with biomass previously acclimated to phenol and saline conditions, we got insights into phenol degradation kinetics as well as the inhibitory effect of phenol on the methanogenesis. By using two AnMBRs, with previously acclimated biomass as well, we assessed the feasibility of the degradation of phenol as the sole CES at $8 \text{ gNa}\cdot\text{L}^{-1}$ and determined the effect of the fed of two additional CES, acetate, and an acetate-butyrate mixture, on the sPhCR and the microbial population dynamics, thereby focusing on the phenol degraders and the methanogens.

The following conclusions can be derived:

- In batch reactors at $8 \text{ gNa}\cdot\text{L}^{-1}$, phenol at a concentration of $0.5 \text{ g}\cdot\text{L}^{-1}$ decreased the SMA with 27% in comparison to the control tests without phenol. A maximum sPhCR of $17.8 \pm 2.6 \text{ mgPh}\cdot\text{gVSS}^{-1}\cdot\text{d}^{-1}$ was determined for an initial phenol concentration of $500 \text{ mg}\cdot\text{L}^{-1}$.
- In the AnMBR, a stable sPhCR of $40 \text{ mgPh}\cdot\text{gVSS}^{-1}\cdot\text{L}^{-1}$ was measured when phenol contributed to 80% of the total COD. However, the sPhCR could not be maintained when phenol was the sole CES.
- In the AnMBR, when acetate was added as additional CES, a maximum sPhCR of $115 \text{ mgPh}\cdot\text{gVSS}^{-1}\cdot\text{L}^{-1}$ was determined.
- The highest sPhCR of $200 \text{ mgPh}\cdot\text{gVSS}^{-1}\cdot\text{L}^{-1}$ was found when a 2:1 acetate:butyrate mixture, based on COD, was fed to the AnMBR.
- During the operation of the reactors, the most abundant microorganisms were the phenol degrader *Syntrophorhabdus* sp. and the acetoclastic methanogen *Methanosaeta* sp., making more than 50% of the microbial community. Seemingly, there was a correlation ($p < 0.05$) between the increase in the sPhLR and the increase in the relative abundance of *Syntrophorhabdus* sp.

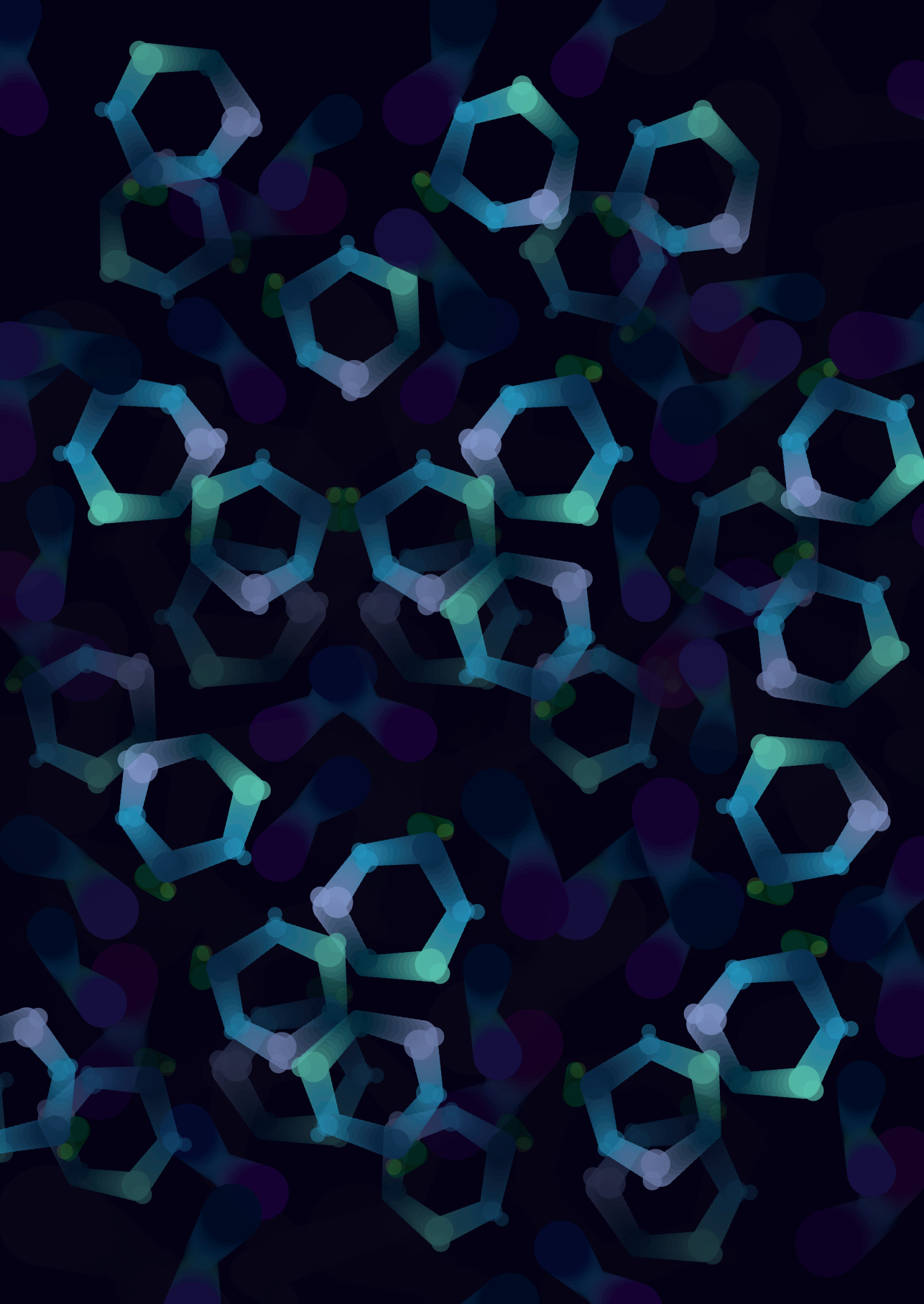
2.5 References

- Astals, S., Batstone, D.J., Tait, S., Jensen, P.D., 2015. Development and validation of a rapid test for anaerobic inhibition and toxicity. *Water Res.* 81, 208-215. <https://doi.org/https://doi.org/10.1016/j.watres.2015.05.063>.
- Blum, D.J.W., Hergenroeder, R., Parkin, G.F., Speece, R.E., 1986. Anaerobic Treatment of Coal Conversion Wastewater Constituents: Biodegradability and Toxicity. *Journal (Water Pollution Control Federation)* 58(2), 122-131.
- Bolyen, E., Rideout, J.R., Dillon, M.R., Bokulich, N.A., Abnet, C.C., Al-Ghalith, G.A., Alexander, H., Alm, E.J., Arumugam, M., Asnicar, F., Bai, Y., Bisanz, J.E., Bittinger, K., Brejnrod, A., Brislawn, C.J., Brown, C.T., Callahan, B.J., Caraballo-Rodriguez, A.M., Chase, J., Cope, E.K., Da Silva, R., Diener, C., Dorrestein, P.C., Douglas, G.M., Durall, D.M., Duvallet, C., Edwardson, C.F., Ernst, M., Estaki, M., Fouquier, J., Gauglitz, J.M., Gibbons, S.M., Gibson, D.L., Gonzalez, A., Gorlick, K., Guo, J., Hillmann, B., Holmes, S., Holste, H., Huttenhower, C., Huttley, G.A., Janssen, S., Jarmusch, A.K., Jiang, L., Kaehler, B.D., Kang, K.B., Keefe, C.R., Keim, P., Kelley, S.T., Knights, D., Koester, I., Kosciorek, T., Kreps, J., Langille, M.G.I., Lee, J., Ley, R., Liu, Y.X., Loftfield, E., Lozupone, C., Maher, M., Marotz, C., Martin, B.D., McDonald, D., McIver, L.J., Melnik, A.V., Metcalf, J.L., Morgan, S.C., Morton, J.T., Naimey, A.T., Navas-Molina, J.A., Nothias, L.F., Orchanian, S.B., Pearson, T., Peoples, S.L., Petras, D., Preuss, M.L., Priesse, E., Rasmussen, L.B., Rivers, A., Robeson, M.S., 2nd, Rosenthal, P., Segata, N., Shaffer, M., Shiffer, A., Sinha, R., Song, S.J., Spear, J.R., Swafford, A.D., Thompson, L.R., Torres, P.J., Trinh, P., Tripathi, A., Turnbaugh, P.J., Ul-Hasan, S., van der Hooft, J.J.J., Vargas, F., Vazquez-Baeza, Y., Vogtmann, E., von Hippel, M., Walters, W., Wan, Y., Wang, M., Warren, J., Weber, K.C., Williamson, C.H.D., Willis, A.D., Xu, Z.Z., Zaneveld, J.R., Zhang, Y., Zhu, Q., Knight, R., Caporaso, J.G., 2019. Reproducible, interactive, scalable and extensible microbiome data science using QIIME 2. *Nat. Biotechnol.* 37(8), 852-857. <https://doi.org/10.1038/s41587-019-0209-9>.
- Callahan, B.J., McMurdie, P.J., Rosen, M.J., Han, A.W., Johnson, A.J., Holmes, S.P., 2016. DADA2: High-resolution sample inference from Illumina amplicon data. *Nat Methods* 13(7), 581-583. <https://doi.org/10.1038/nmeth.3869>.
- Campanaro, S., Treu, L., Kougias, P.G., Zhu, X., Angelidaki, I., 2018. Taxonomy of anaerobic digestion microbiome reveals biases associated with the applied high throughput sequencing strategies. *Scientific Reports* 8(1), 1926. <https://doi.org/10.1038/s41598-018-20414-0>.
- Chen, Y., Cheng, J.J., Creamer, K.S., 2008. Inhibition of anaerobic digestion process: A review. *Bioresour. Technol.* 99(10), 4044-4064. <https://doi.org/http://dx.doi.org/10.1016/j.biortech.2007.01.057>.
- Collins, G., Foy, C., McHugh, S., Mahony, T., O'Flaherty, V., 2005. Anaerobic biological treatment of phenolic wastewater at 15–18°C. *Water Res.* 39(8), 1614-1620. <https://doi.org/https://doi.org/10.1016/j.watres.2005.01.017>.
- Dahle, H., Birkeland, N.-K., 2006. *Thermovirga lienii* gen. nov., sp. nov., a novel moderately thermophilic, anaerobic, amino-acid-degrading bacterium isolated from a North Sea oil well. *Int. J. Syst. Evol. Microbiol.* 56(7), 1539-1545. <https://doi.org/https://doi.org/10.1099/ijs.o.63894-0>.
- Dereli, R.K., Ersahin, M.E., Ozgun, H., Ozturk, I., Jeison, D., van der Zee, F., van Lier, J.B., 2012. Potentials of anaerobic membrane bioreactors to overcome treatment limitations induced by industrial wastewaters. *Bioresour. Technol.* 122, 160-170. <https://doi.org/10.1016/j.biortech.2012.05.139>.
- Fang, H.H., Liu, Y., Ke, S.Z., Zhang, T., 2004. Anaerobic degradation of phenol in wastewater at ambient temperature. *Water Sci. Technol.* 49(1), 95-102.
- Fang, H.H.P., Chan, O.-C., 1997. Toxicity of phenol towards anaerobic biogranules. *Water Res.* 31(9), 2229-2242. [https://doi.org/https://doi.org/10.1016/S0043-1354\(97\)00069-9](https://doi.org/https://doi.org/10.1016/S0043-1354(97)00069-9).

- Fang, H.H.P., Chen, T., Li, Y.-Y., Chui, H.-K., 1996. Degradation of phenol in wastewater in an upflow anaerobic sludge blanket reactor. *Water Res.* 30(6), 1353-1360. [https://doi.org/https://doi.org/10.1016/0043-1354\(95\)00309-6](https://doi.org/https://doi.org/10.1016/0043-1354(95)00309-6).
- Franchi, O., Rosenkranz, F., Chamy, R., 2018. Key microbial populations involved in anaerobic degradation of phenol and p-cresol using different inocula. *Electron. J. Biotechnol.* 35, 33-38. <https://doi.org/https://doi.org/10.1016/j.ejbt.2018.08.002>.
- Han, S.-B., Wang, R.-J., Yu, X.-Y., Su, Y., Sun, C., Fu, G.-Y., Zhang, C.-Y., Zhu, X.-F., Wu, M., 2016. *Marinobacterium zhoushanense* sp. nov., isolated from surface seawater. 66(9), 3437-3442. <https://doi.org/https://doi.org/10.1099/ijsem.0.001213>.
- He, H., Chen, Y., Li, X., Cheng, Y., Yang, C., Zeng, G., 2017. Influence of salinity on microorganisms in activated sludge processes: A review. *International Biodeterioration & Biodegradation* 119, 520-527. <https://doi.org/https://doi.org/10.1016/j.ibiod.2016.10.007>.
- Ji, Q., Tabassum, S., Hena, S., Silva, C.G., Yu, G., Zhang, Z., 2016. A review on the coal gasification wastewater treatment technologies: past, present and future outlook. *J. Clean. Prod.* 126, 38-55. <https://doi.org/https://doi.org/10.1016/j.jclepro.2016.02.147>.
- Karlsson, A., Ejlertsson, J., Nezirevic, D., Svensson, B.H., 1999. Degradation of phenol under meso- and thermophilic, anaerobic conditions. *Anaerobe* 5(1), 25-35. <https://doi.org/10.1006/anae.1998.0187>.
- Kennes, C., Mendez, R., Lema, J.M., 1997. Methanogenic degradation of p-cresol in batch and in continuous UASB reactors. *Water Res.* 31(7), 1549-1554. [https://doi.org/https://doi.org/10.1016/S0043-1354\(96\)00156-X](https://doi.org/https://doi.org/10.1016/S0043-1354(96)00156-X).
- Li, Y., Tabassum, S., Chu, C., Zhang, Z., 2017. Inhibitory effect of high phenol concentration in treating coal gasification wastewater in anaerobic biofilter. *J. Environ. Sci. (China)*. <https://doi.org/https://doi.org/10.1016/j.jes.2017.06.001>.
- Liang, D., Fang, H.H.P., 2010. Anaerobic Treatment of Phenolic Wastewaters, *Environmental Anaerobic Technology*. pp. 185-205. https://doi.org/10.1142/9781848165434_0009.
- Lin, H., Peng, W., Zhang, M., Chen, J., Hong, H., Zhang, Y., 2013. A review on anaerobic membrane bioreactors: Applications, membrane fouling and future perspectives. *Desalination* 314, 169-188. <https://doi.org/http://dx.doi.org/10.1016/j.desal.2013.01.019>.
- Maiti, D., Ansari, I., Rather, M.A., Deepa, A., 2019. Comprehensive review on wastewater discharged from the coal-related industries – characteristics and treatment strategies. *Water Sci. Technol.* 79(11), 2023-2035. <https://doi.org/10.2166/wst.2019.195> %J Water Science and Technology.
- McMurdie, P.J., Holmes, S., 2013. Phyloseq: an R package for reproducible interactive analysis and graphics of microbiome census data. *PLoS One* 8(4), e61217. <https://doi.org/10.1371/journal.pone.0061217>.
- Muñoz Sierra, J.D., Lafita, C., Gabaldón, C., Spanjers, H., van Lier, J.B., 2017. Trace metals supplementation in anaerobic membrane bioreactors treating highly saline phenolic wastewater. *Bioresour. Technol.* 234, 106-114. <https://doi.org/http://dx.doi.org/10.1016/j.biortech.2017.03.032>.
- Muñoz Sierra, J.D., Oosterkamp, M.J., Wang, W., Spanjers, H., van Lier, J.B., 2018. Impact of long-term salinity exposure in anaerobic membrane bioreactors treating phenolic wastewater: Performance robustness and endured microbial community. *Water Res.* 141, 172-184. <https://doi.org/https://doi.org/10.1016/j.watres.2018.05.006>.
- Muñoz Sierra, J.D., Oosterkamp, M.J., Wang, W., Spanjers, H., van Lier, J.B., 2019. Comparative performance of upflow anaerobic sludge blanket reactor and anaerobic membrane bioreactor treating phenolic wastewater: Overcoming high salinity. *Chem. Eng. J.* 366, 480-490. <https://doi.org/https://doi.org/10.1016/j.cej.2019.02.097>.

- Munoz Sierra, J.D., Wang, W., Cerqueda-Garcia, D., Oosterkamp, M.J., Spanjers, H., van Lier, J.B., 2018. Temperature susceptibility of a mesophilic anaerobic membrane bioreactor treating saline phenol-containing wastewater. *Chemosphere* 213, 92-102. <https://doi.org/10.1016/j.chemosphere.2018.09.023>.
- Nobu, M.K., Narihiro, T., Hideyuki, T., Qiu, Y.L., Sekiguchi, Y., Woyke, T., Goodwin, L., Davenport, K.W., Kamagata, Y., Liu, W.T., 2015. The genome of *Syntrophorhabdus aromaticivorans* strain UI provides new insights for syntrophic aromatic compound metabolism and electron flow. *Environ. Microbiol.* 17(12), 4861-4872. <https://doi.org/10.1111/1462-2920.12444>.
- Nobu, M.K., Narihiro, T., Liu, M., Kuroda, K., Mei, R., Liu, W.T., 2017. Thermodynamically diverse syntrophic aromatic compound catabolism. *Environ. Microbiol.* 19(11), 4576-4586. <https://doi.org/10.1111/1462-2920.13922>.
- Olguin-Lora, P., Puig-Grajales, L., Razo-Flores, E., 2003. Inhibition of the acetoclastic methanogenic activity by phenol and alkyl phenols. *Environ. Technol.* 24, 999-1006. <https://doi.org/10.1080/09593330309385638>.
- Palmer, M.W., 1993. Putting Things in Even Better Order: The Advantages of Canonical Correspondence Analysis. 74(8), 2215-2230. <https://doi.org/10.2307/1939575>.
- Qiu, Y.L., Hanada, S., Ohashi, A., Harada, H., Kamagata, Y., Sekiguchi, Y., 2008. *Syntrophorhabdus aromaticivorans* gen. nov., sp. nov., the first cultured anaerobe capable of degrading phenol to acetate in obligate syntrophic associations with a hydrogenotrophic methanogen. *Appl. Environ. Microbiol.* 74(7), 2051-2058. <https://doi.org/10.1128/aem.02378-07>.
- Quast, C., Pruesse, E., Yilmaz, P., Gerken, J., Schweer, T., Yarza, P., Peplies, J., Glockner, F.O., 2013. The SILVA ribosomal RNA gene database project: improved data processing and web-based tools. *Nucleic Acids Res.* 41(Database issue), D590-596. <https://doi.org/10.1093/nar/gks1219>.
- Ramakrishnan, A., Gupta, S.K., 2008. Effect of hydraulic retention time on the biodegradation of complex phenolic mixture from simulated coal wastewater in hybrid UASB reactors. *J. Hazard. Mater.* 153(1), 843-851. <https://doi.org/https://doi.org/10.1016/j.jhazmat.2007.09.034>.
- Razo-Flores, E.I.a., Iniestra-González, M., Field, J.A., Olguin-Lora, P., Puig-Grajales, L., 2003. Biodegradation of mixtures of phenolic compounds in an upward-flow anaerobic sludge blanket reactor. *J. Environ. Eng. (N. Y.)* 129(11), 999-1006.
- Rognes, T., Flouri, T., Nichols, B., Quince, C., Mahe, F., 2016. VSEARCH: a versatile open source tool for metagenomics. *PeerJ* 4, e2584. <https://doi.org/10.7717/peerj.2584>.
- Russell, J.B., Cook, G.M., 1995. Energetics of bacterial growth: balance of anabolic and catabolic reactions. *Microbiological reviews* 59(1), 48-62.
- Schühle, K., Fuchs, G., 2004. Phenylphosphate Carboxylase: a New C-C Lyase Involved in Anaerobic Phenol Metabolism in *Thauera aromatica*. 186(14), 4556-4567. <https://doi.org/10.1128/JB.186.14.4556-4567.2004> %J *Journal of Bacteriology*.
- Singer, P.C., Pfaender, F.K., Chinchilli, J., Maciorowski III, A.F., J.C.L, G., R., 1978. Assessment of Coal Conversion Wastewaters: Characterization and Preliminary Biotreatability. , in: EPA, E. (Ed.). U.S. Washington D.C.
- Tay, J.-H., He, Y.-X., Yan, Y.-G., 2000. Anaerobic biogranulation using phenol as the sole carbon source. *Water Environ. Res* 72(2), 189-194.
- Van Lier, J., Van der Zee, F., Frijters, C., Ersahin, M., 2015. Celebrating 40 years anaerobic sludge bed reactors for industrial wastewater treatment. *Rev. Environ. Sci. Bio.* 14(4), 681-702. <https://doi.org/https://doi.org/10.1007/s11157-015-9375-5>.
- Wang, J., Wu, B., Sierra, J.M., He, C., Hu, Z., Wang, W., 2020. Influence of particle size distribution on anaerobic degradation of phenol and analysis of methanogenic microbial community. *Environ. Sci. Pollut. Res.* 27(10), 10391-10403. <https://doi.org/10.1007/s11356-020-07665-z>.

- Wang, W., Wu, B., Pan, S., Yang, K., Hu, Z., Yuan, S., 2017. Performance robustness of the UASB reactors treating saline phenolic wastewater and analysis of microbial community structure. *J. Hazard. Mater.* 331, 21-27. <https://doi.org/https://doi.org/10.1016/j.jhazmat.2017.02.025>.
- Zhou, G.-M., Fang, H.H.P., 1997. Co-degradation of phenol and m-cresol in a UASB reactor. *Bioresour. Technol.* 61(1), 47-52. [https://doi.org/http://dx.doi.org/10.1016/S0960-8524\(97\)84698-6](https://doi.org/http://dx.doi.org/10.1016/S0960-8524(97)84698-6).



Chapter 3

Syntrophic acetate oxidation having a key role in thermophilic phenol conversion in anaerobic membrane bioreactor under saline conditions

This chapter is an adapted version of: Garcia Rea Víctor S., Muñoz Sierra Julian D., El-Kalliny Amer S., Cerqueda-Garcia Daniel, Lindeboom Ralph E.F., Spanjers Henri, van Lier Jules B. (2023). Syntrophic acetate oxidation having a key role in thermophilic phenol conversion in anaerobic membrane bioreactor under saline conditions, Chem. Eng. J., 455. DOI: <https://doi.org/10.1016/j.cej.2022.140305>.

Abstract

Phenol conversion under saline thermophilic anaerobic conditions requires the development and sustenance of a highly specialized microbial community. In the present research, an anaerobic membrane bioreactor (AnMBR) fed with an influent containing $0.5 \text{ g} \cdot \text{L}^{-1}$ phenol and $6.5 \text{ gNa}^+ \cdot \text{L}^{-1}$ was operated at 55°C for 300 days. Phenol degradation was limited when phenol was the sole substrate. However, phenol removal efficiency significantly ($p < 0.001$) increased to 80% corresponding to a conversion rate of $29 \text{ mgPhenol} \cdot \text{gVSS}^{-1} \cdot \text{d}^{-1}$ when acetate ($0.5 \text{ gCOD} \cdot \text{L}^{-1}$) was simultaneously provided. Isotopic analysis using ^{13}C labeled acetate and measuring $^{13}\text{CH}_4$ revealed that acetate was first oxidized to hydrogen and CO_2 , prior to methanogenesis, resulting in an increased abundance of hydrogenotrophic methanogens. It is hypothesized that the latter is of crucial importance for achieving effective anaerobic oxidation of phenol and its metabolites. Remarkably, the phenol conversion rate in the membrane-associated biomass was three times higher than in the suspended biomass. The observed difference in conversion rate could be explained by the presence of an increased abundance of hydrogenotrophic methanogens in the membrane-associated biomass confirmed by a microbial community analysis of Archaea. Benzoate was measured in the permeate, suggesting that phenol degradation occurred via the benzoyl-CoA pathway. Results of the current study, suggest that syntrophic acetate oxidation coupled with hydrogenotrophic methanogenesis, which results in the presence of an abundant electron sink, plays a key role in enhancing thermophilic phenol degradation. The obtained insights widen the application of anaerobic digestion to treat saline phenolic-rich wastewater at high temperatures.

3.1 Introduction

With the increasing focus on energy recovery from wastewater, thermophilic anaerobic digestion (AD) is of increasing industrial interest, because the avoidance of cooling before and re-heating after biological treatment could lead to large energy savings when closing industrial water loops is targeted (Duncan et al., 2017; van Lier et al., 2001). However, several constraints such as poor effluent quality and the carry-over of active biomass, which tends to destabilize the process, have narrowed the potential of thermophilic AD for industrial application so far (Dereli et al., 2012; van Lier, 1996). Besides, biomass retention or immobilization under thermophilic conditions is challenging to achieve, which may be aggravated by saline conditions (Muñoz Sierra et al., 2017; Muñoz Sierra et al., 2019).

Research on the anaerobic degradation of phenol under thermophilic conditions is only scarcely documented (Chen et al., 2008; Fang et al., 2006; Hoyos-Hernandez et al., 2014; Leven et al., 2012; Levén and Schnürer, 2005). Under mesophilic conditions, the benzoyl-CoA route has been described as the main degradation pathway in the anaerobic conversion of phenol into methane (Appendix A.3, Figure A.3.1 A) (Gibson and Harwood, 2002; Karlsson et al., 2000; Philipp and Schink, 2012). However, under thermophilic conditions, an alternative degradation pathway via caproate as the main intermediate was proposed (Appendix A.3, Figure A.3.1 B) (Fang et al., 2006; Karlsson et al., 1999).

The results presented in Chapter 2 showed that in AnMBRs under mesophilic and saline conditions, phenol degradation is enhanced by the dosage of additional carbon and energy sources such as acetate and butyrate by promoting the development of an enriched acetoclastic methanogenic population, attaining maximum specific phenol conversion rates of $200 \text{ mgPh} \cdot \text{gVSS}^{-1} \cdot \text{d}^{-1}$ (García Rea et al., 2020). However, under thermophilic conditions, this dependency on acetoclastic methanogenesis would be remarkable, since at high temperatures syntrophic acetate oxidation (SAO) is more pronounced [3, 4, 31]. SAO is carried out by syntrophic acetate-oxidizing bacteria (SAOB) that firstly oxidize acetate into HCO_3^- , H_2 , and H^+ (Eq. 3.1), followed by hydrogenotrophic methanogenesis (Eq. 3.2), (Westerholm et al., 2011). Under very extreme conditions, applying temperatures $> 75^\circ\text{C}$, SAO might even be the sole pathway in acetate conversion (van Lier, 1996).



In our present work, we investigated the simultaneous conversion of phenol and acetate under saline (6.5 g Na⁺L⁻¹) and thermophilic (55 °C) conditions using an AnMBR. By applying membrane filtration, complete biomass retention is achieved, promoting the development of the specialized microbial community needed for the process. The degradation pathway of acetate was determined by a ¹³C isotopic analysis and insight into the phenol degradation route was obtained by the measurement of different intermediates. The phenol removal efficiency and conversion rates of the suspended and membrane-associated biomass were determined. Analyses of the microbial community for getting insight into the role of acetate as an additional substrate were conducted and related to the bioconversion. Additionally, a thermodynamic and stoichiometric analysis of an anaerobic microorganism growing anaerobically on phenol was used to show and understand the syntrophic association for phenol degradation expected in the reactor's biomass and its effects on the thermodynamic feasibility of the degradation process.

3.2 Materials and methods

3.2.1 Anaerobic membrane bioreactor

The setup consisted of an AnMBR (7.0 L total volume, 6.5 L working volume) connected to a 130 mL external ultrafiltration module with a tubular inside-out PVDF membrane (X-Flow compact 33, Pentair, The Netherlands) as previously reported in Chapter 2. The membrane module was operated with a cross-flow velocity of $0.8 \pm 0.1 \text{ m} \cdot \text{s}^{-1}$ and a constant flux of 4.0 LMH ($Q = 1 \text{ L/d}$). The inoculum biomass was obtained from a full-scale UASB reactor treating petrochemical wastewater (Shell Moerdijk, The Netherlands), and it was acclimated and used in previous experiments (Muñoz Sierra et al., 2020). The reactor was mixed thoroughly by biomass recirculation at a rate of 200 d^{-1} . During reactor operation, the VSS concentration was kept at $1.90 \pm 0.28 \text{ gVSS} \cdot \text{L}^{-1}$, so the specific phenol loading rate was attained at a lower phenol concentration in the influent. Membrane filtration was operated with a cycle of 500 s of filtration, 20 s of backwashing (same flow as filtration), and 5 s idle.

3.2.2 Feeding solution during the different reactor operation stages

For the experiment, the reactor operation was divided into four main stages (Table 3.1). Micronutrients [$18 \text{ mL} \cdot \text{L}^{-1}$] & macronutrients [$9 \text{ mL} \cdot \text{L}^{-1}$] solutions, and phosphate buffer solutions A [$13.0 \text{ mL} \cdot \text{L}^{-1}$] and B [$19.9 \text{ mL} \cdot \text{L}^{-1}$], respectively, were added to the feeding solution. The composition of the solutions is reported in (García Rea et al., 2020). NaCl

in the feed was adjusted during the stages to maintain the sodium concentration in the reactor at $6.5 \text{ g}\cdot\text{L}^{-1}$.

Table 3.1. Feeding composition during the anaerobic membrane bioreactor operation.

Stages	Operation day	Yeast [$\text{g}\cdot\text{L}^{-1}$] extract	Phenol [$\text{g}\cdot\text{L}^{-1}/\text{gCOD}\cdot\text{L}^{-1}$]	Acetate [$\text{gCOD}\cdot\text{L}^{-1}$]
A	0 - 45	1.2	0.5 / 1.2	0
B	46 - 82	1.0, 0.5, 0.4	0.5 / 1.2	0
C	83 - 241	0.4	0.5 / 1.2	0.7
D	242 - 344	0.4	0.5 / 1.2	1.4

3.2.3 Chemical and physicochemical analysis

COD and phenol concentrations were determined as previously reported in Chapter 1. An extended-run-time protocol (23 min) was applied for the determination of VFA, ethanol, propanol, butanol, cyclohexanol, cyclohexanone, and benzoate as reported in (Garcia Rea et al., 2022).

3.2.4 Syntrophic acetate oxidation activity in the AnMBR biomass

For determining the SAO activity of the AnMBR biomass, a test was designed by modifying an existing protocol (Mulat et al., 2014). On day 304 of reactor operation, 1.6% (w/w) of the total acetate in the feed solution was dosed as ^{13}C -labeled sodium acetate ($^{12}\text{CH}_3^{13}\text{COO}^-$) (Merck, Germany). The acetate isotope was dosed for twenty days. During this period, biogas samples of approximately 24 mL from the reactor's gas line were collected and stored in 2 x 12 mL Labco exetainer vials (Labco, Germany). Samples were outsourced for analysis (Isolab, The Netherlands). The carbon isotope ratio of methane was analyzed with an Agilent 6890N GC (Agilent Technologies, Santa Clara, US) interfaced to a Finigan Delta S IRMS (Thermo Scientific, Bremen, Germany) using a Finigan GC-C II interface. The GC was equipped with a 12 m, 0.32 mm molsieve column (Agilent) and an injection valve. Samples were calibrated against a calibration standard. Results are reported in promille vs. Pee Dee Belemnite (PDB) (Hayes, 2004).

3.2.5 DNA extraction and microbial community dynamics study

Biomass from the reactor was sampled during the different operational stages. At the end of the reactor operation, the membrane module was sectioned and additional samples from the upper, middle, and lower parts of the membrane biofilm were taken. DNA extraction and storage were performed as previously reported (García Rea et al., 2020).

3.2.6 Targeted Amplicon libraries construction

Library construction and sequencing were performed at the Roy J. Carver Biotechnology Center, the University of Illinois at Urbana-Champaign. Approximately 1 ng of DNA was used for amplification with the bacterial 16S V3-F357-V4-R805 and archaeal 349F-806R primers in the Fluidigm Access Array. The barcoded amplicons generated from each sample were harvested, transferred to a 96 well plate, quantified on a Qubit fluorometer, and the average size of the amplicons was determined on a Fragment Analyzer (AATI, IA). All amplicons were pooled in equimolar concentration, size selected on a 2% agarose Ex-gel (ThermoFisher) to remove primer dimers and extracted from the isolated gel slice with a Qiagen gel extraction kit (Qiagen, Hilden, Germany). The cleaned size selected product was quantitated and run on a Fragment Analyzer again to confirm appropriate profile and for determination of average size. The pool was diluted to 5nM and further quantitated by qPCR on a CFX Connect Real-Time qPCR system (Biorad, Hercules, CA) for maximization of the number of clusters in the flow cell.

3.2.7 DNA sequencing

The pool was denatured and spiked with 20% non-indexed PhiX V3 control library provided by Illumina and loaded onto the MiSeq V2 flow cell at a concentration of 8 pM for cluster formation and sequencing. The libraries were sequenced from both ends of the molecules to a total read length of 250nt from each end. The run generated .bcl files which were converted into demultiplexed fastq files using bcl2fastq 2.20 (Illumina, CA).

3.2.8 Statistics and bioinformatics for the analysis of sequences

Statistical analyses (One way ANOVA, planned contrasts, Kruskal-Wallis test, and Wilcoxon robust ANOVA) were conducted in R (R Development Core Team, 2019).

The paired-end reads (2 × 250) were processed as detailed in (García Rea et al., 2020). An alignment was performed with the MAFFT algorithm. After masking positional conservations and gap filtering, a phylogeny was built with the FastTree algorithm. The feature table and phylogeny were exported to the R environment, and the statistical analyses were carried out with the phyloseq, ggplot2, and vegan packages (McMurdie and Holmes, 2013). A principal coordinate analysis (PCoA) was conducted with the weighted unfrac distance. The sequences were deposited in the SRA (NCBI) database under the accession number PRJNA671743.

3.2.9 *Stoichiometry and thermodynamics of anaerobic growth on phenol under thermophilic conditions*

The redox reactions used for the stoichiometric and thermodynamic analysis of anaerobic growth on phenol under thermophilic conditions were calculated according to Kleerebezem and van Loosdrecht (2010) (Kleerebezem and Van Loosdrecht, 2010). The Gibbs Free Energy Dissipation method was used for the calculation of the Gibbs free energy change of the reactions (ΔG_R) corrected for the expected products and reagents concentrations and process temperature ($\Delta G_R^{1,55^\circ\text{C}}$) (Kleerebezem and Van Loosdrecht, 2010). Through the coupling of catabolism and anabolism, the overall metabolic equations of anaerobic growth on phenol were derived and syntrophic relationships visualized. To perform the required calculations, the following foreseen concentrations and partial pressures expected in the AnMBR were used: phenol 0.53 mmol (50 mgPh·L⁻¹), acetate 0.017 mmol (1.0 mg·L⁻¹), carbon dioxide 0.4 atm, hydrogen 1×10⁻⁴ atm, ammonium 1 mmol (18 mg·L⁻¹), and H⁺ 1 × 10⁻⁷M.

3.3 Results and Discussion

3.3.1 *AnMBR operation for phenol degradation and its simultaneous conversion with acetate*

An AnMBR under saline thermophilic conditions was operated for 344 days to measure phenol degradation as the sole COD source or the simultaneous degradation of phenol with acetate in a reactor that ensures full biomass retention.

During stage A, phenol and yeast extract were the main COD sources. During the first 20 days, the phenol removal efficiency decreased to a minimum of 38.2% corresponding to a specific phenol conversion rate (sPhCR) of 11 mgPh·gVSS⁻¹d⁻¹ (day 19), and a phenol concentration in the permeate of 293 mgPh·L⁻¹ (Figure 3.1). However, phenol degradation was recovered on day 38. The average (\pm 95% confidence interval) phenol removal efficiency and sPhCR during stage A were 58.9 \pm 4.4% and 26.8 \pm 2.6 mgPh·gVSS⁻¹d⁻¹, respectively. Previous studies reported that yeast extract promotes the degradation of phenol (Karlsson et al., 2000) and phenolic compounds under anaerobic conditions (Chang et al., 2005; Yuan et al., 2011). Yeast extract is a source of COD, as well as macro- and micronutrients, vitamins, and amino acids, which are considered essential for anaerobic bacteria and archaea (Hendriks et al., 2018). However, the exact mechanism of how yeast extract may promote phenol degradation is completely unknown.

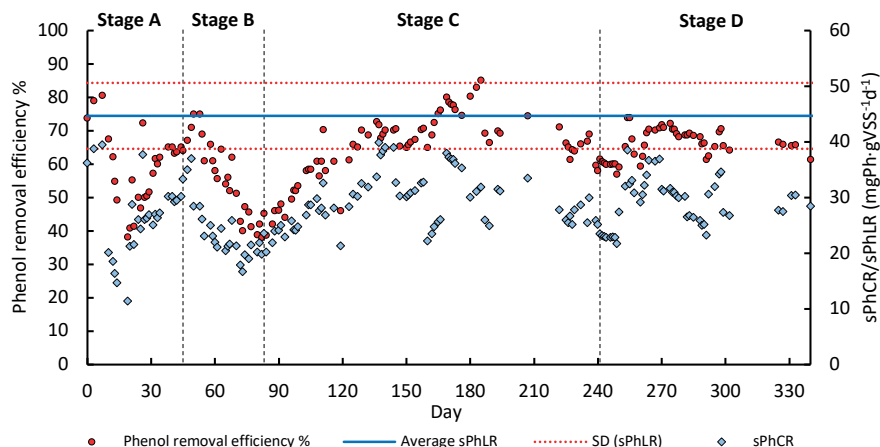


Figure 3.1. Phenol removal efficiency, specific phenol loading rate (sPhLR), and specific phenol conversion rate (sPhCR) of the AnMBR treating model phenolic and high salinity wastewater under thermophilic conditions. The red dotted lines show the interval for the standard deviation of the sPhLR.

At the start of stage B, the yeast extract concentration in the feeding solution was decreased from 1.2 to 0.4 gCOD/L, which resulted in a strong decrease in the phenol removal efficiency and sPhCR. Concomitantly, the phenol concentration in the permeate increased to a maximum concentration of 310 mgPh·L⁻¹ on day 82, corresponding to a removal efficiency of 38%. The average phenol removal efficiency and sPhCR during stage B were $55.2 \pm 4.8\%$ and 23.4 ± 2.0 mgPh·gVSS⁻¹·d⁻¹.

To study the simultaneous conversion of phenol and acetate, 30.4% of the influent COD [0.7 gCOD/L] was replaced by acetate on day 83 (beginning of stage C, Table 3.1), with phenol being 52.2% of the influent COD and yeast extract the remaining 17.4%. As a result, the phenol removal efficiency and sPhCR increased, reaching an average of $65.0 \pm 2.4\%$ and 29.2 ± 1.2 mgPh·gVSS⁻¹·d⁻¹, respectively. In the last stage (D), when phenol COD was 38.0% of the influent COD, the removal efficiency and sPhCR remained stable, with an average of $65.9 \pm 1.3\%$ and 29.2 ± 1.2 mgPh·gVSS⁻¹·d⁻¹, respectively. Based on a Kruskal-Wallis test, we determined that the phenol removal efficiency was significantly different when acetate was dosed ($H(3) = 21.9$, $p < 0.001$). Focused comparisons of the mean ranks showed that phenol removal efficiency was not significantly different ($p < 0.05$) between stages A and B (*difference* = 11), nor between stages C and D (*difference* = 0.5). Nonetheless, among the stages with (C & D) and without acetate (B), there were significant differences. A one-way ANOVA analysis showed that there was a significant effect of the dosage of acetate on the sPhCR as well, $F(3, 167) = 9.86$, $p < 0.001$, indicating that with the dosage of acetate the sPhCR was different. After the ANOVA, a comparison between the stages by planned contrasts

was made, and we determined that the sPhCR with acetate was significantly higher $t(167) = -4.9$, $p < 0.001$ (one-tailed) than the operation without acetate. The phenol loading rate [$\text{mgPhg} \cdot \text{VSS}^{-1} \cdot \text{d}^{-1}$] during the reactor operation was maintained at $44.7 \pm 0.9 \text{ mgPh gVSS}^{-1} \cdot \text{d}^{-1}$. A Wilcoxon robust ANOVA test showed that there was no significant difference in the mean sPhLR values across the four stages $F_t(52, 27) = 1.7$, $p = 0.17$.

The results obtained during the continuous operation suggested that the biomass of the AnMBR was not able to degrade phenol under saline thermophilic conditions when phenol was the sole COD source. Limited phenol degradation could be attributed to a reduced presence of a phenol-degrading microbial population or an inhibitory effect on such population. An inhibitory process due to phenol concentration will be very unlikely as it has been shown that inhibition is expected at higher concentrations ($> 600 \text{ mg} \cdot \text{L}^{-1}$) than those prevailing in the reactor (García Rea et al., 2020; Muñoz Sierra et al., 2020). Product accumulation or reduced product consumption may affect as well, for example in the case of the intermediates, acetate, and/or H_2 . Another possibility for limited phenol degradation is an impaired or decreased methanogenic population that is insufficiently capable of scavenging the reducing equivalents generated during phenol degradation steps, implying a cessation of the AD biochemical steps. Under the prevailing reactor conditions, SAO may be the major acetate degradation pathway, whereas hydrogenotrophic methanogenesis could be the main methane generation process. An impairment in the SAO activity might then lead to substrate shortage for the hydrogenotrophic methanogens. On the other hand, cessation of hydrogenotrophic methanogenesis will halt SAO and phenol degradation as the electrons generated in both processes will have no way to be disposed of. The addition of acetate [$0.7 \text{ gCOD} \cdot \text{L}^{-1}$ in the feed] significantly enhanced the sPhCR and phenol removal efficiency. Albeit, doubling the concentration of acetate [$1.4 \text{ gCOD} \cdot \text{L}^{-1}$ in the feed] did neither increase the removal efficiency nor the sPhCR.

Fang *et al.* (2006) reported thermophilic degradation of phenol as the sole COD source under thermophilic methanogenic conditions in a UASB reactor (2.8 L) with a volumetric phenol loading rate of $38 \text{ mgPh} \cdot \text{L}^{-1} \cdot \text{d}^{-1}$ (Fang et al., 2006); nonetheless, neither the specific conversion rate nor VSS concentration were reported. Sreekanth *et al.* 2009, reported the degradation of four different phenolic compounds in UASB reactors (7 L) under thermophilic conditions using glucose [$1.07 \text{ gCOD} \cdot \text{L}^{-1}$] in the feed as an additional COD source, but the mechanism by which glucose increased the degradation was not explained (Sreekanth et al., 2009). In previous studies, the effect of a temperature shift from 35°C to 55°C on phenol degradation in an AnMBR at $16 \text{ gNa}^+ \cdot \text{L}^{-1}$ was researched, using acetate [$19.5 \text{ gCOD} \cdot \text{L}^{-1}$] in the feed as an additional COD source, and an sPhCR of $1.7 \text{ mgPh} \cdot \text{gVSS}^{-1} \cdot \text{d}^{-1}$ was found (Munoz Sierra et al., 2018).

In addition, in a long-term study (338 days), we examined the phenol conversion at 55 °C and 18 gNa⁺L⁻¹ with acetate (10 – 20 g·L⁻¹) as an additional COD source, and found an sPhCR of 21 mgPh·gVSS⁻¹d⁻¹ (Muñoz Sierra et al., 2020), though neither the effect of acetate nor the mechanism in which it affected the process were elucidated. Remarkably, the sPhCR of 29.2 ± 1.2 mgPh·gVSS⁻¹d⁻¹ that we found in our present study is the highest reported under saline thermophilic conditions. It should be noted that in previous research, experiments were conducted at Na⁺ concentrations of 16-18 g·L⁻¹ (Muñoz Sierra et al., 2020; Munoz Sierra et al., 2018), which in combination with high temperature, and despite the presence of acetate, could have resulted in the observed low phenol conversion rates. However, the maximum sPhCR found in our present research is almost 7 times lower than the one reported for AnMBR biomass under saline (8.0 g Na⁺·L⁻¹) and mesophilic (35 °C) conditions (García Rea et al., 2020).

In Chapter 2, it was hypothesized that an abundant and active acetoclastic methanogenic sub-population is a prerequisite for effective anaerobic phenol degradation in an AnMBR under mesophilic and saline conditions. However, very likely, under thermophilic and saline conditions, the presence of SAO coupled to hydrogenotrophic methanogenesis will be more pronounced, while acetoclastic methanogenesis may play a less important role.

3.3.2 Syntrophic acetate oxidation determination by ¹³C isotope labeling in the continuous operation

To determine whether acetate was mainly converted via acetoclastic methanogenesis or SAO in the reactor, the $\delta^{13}\text{C}_{\text{PDB}}(\text{CH}_4)$ in the biogas of the AnMBR was assessed. The symbol δ expresses the abundance of isotope 13 of carbon in a sample, relative to the abundance of that same isotope in an arbitrarily designated reference material or isotopic standard (Hayes, 2004). The experiment resulted in an increase in the $\delta^{13}\text{C}_{\text{PDB}}(\text{CH}_4)$ in the reactor from 22, after 24 h of the feeding of the 1-¹³C-labeled acetate (day 304), to a maximum value of 368 (Figure 3.2) on day 319. On day 324, and after 24 h of removing the 1-¹³C-labeled acetate from the feed solution, the $\delta^{13}\text{C}_{\text{PDB}}(\text{CH}_4)$ decreased, reaching a value of -72 on day 342 corresponding to 40 days after the initial dosage of the 1-¹³C-labeled acetate. The observed peak in labeled ¹³CH₄, while feeding ¹³C labeled acetate (¹²CH₃¹³COO⁻) showed that acetate was indeed firstly anaerobically oxidized to HCO₃⁻ and then converted into methane by hydrogenotrophic methanogens (Eq. 3.1 and 3.2).

3.3.3 Phenol degradation intermediates

To assess whether phenol degradation occurred via the benzoyl-CoA or caproate pathways, the permeate was additionally analyzed for the presence of benzoate and

the expected different metabolites that may occur during the caproate degradation pathway (Section 3.2.3). Only benzoate was detected at a concentration up to $220 \text{ mg}\cdot\text{L}^{-1}$, which suggested that phenol degradation in the AnMBR under saline thermophilic conditions occurred via the benzoyl-CoA pathway (Fuchs et al., 2011). Fang *et al.* (2006) suggested that during thermophilic degradation of phenol, caproate, and cyclohexanone may occur as intermediate compounds (Fang et al., 2006). However, we were not able to detect caproate nor cyclohexanone during reactor operation, while benzoate was detected, in accordance with what has been reported by Hoyos-Hernandez et al. (2014) for thermophilic phenol degradation (Hoyos-Hernandez et al., 2014). The latter and our current results strongly indicate that phenol degradation under saline thermophilic anaerobic conditions followed the benzoyl-CoA pathway similar to under mesophilic conditions (Nobu et al., 2015). In this regard, some syntrophic aromatic compound degraders have been reported to excrete benzoate besides acetate (Nobu et al., 2017; Qiu et al., 2008). This process is reported to be conducted through benzoate thiolation (BamY) and transporter (BtrABCX) complexes to alleviate thermodynamic inhibition through decreased H_2 production (Nobu et al., 2017). However, such studies considered mesophilic microorganisms (e.g., *Syntrophorhabdus*) as a model; therefore, it is not clear whether the same process will be valid for phenol-degrading microorganisms under thermophilic conditions.

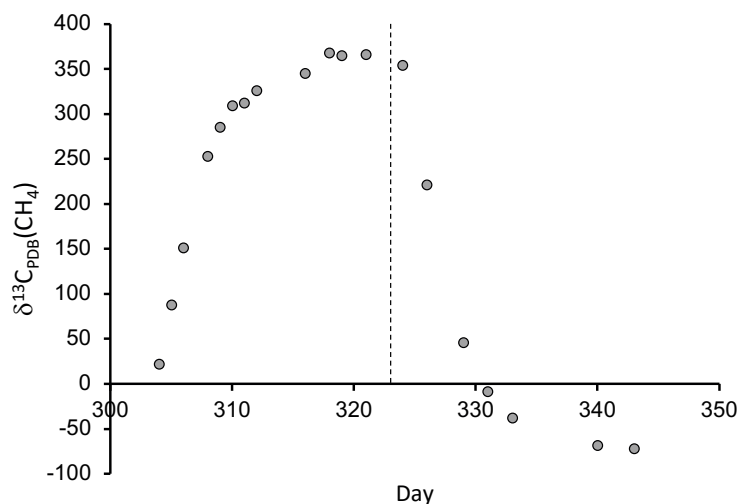


Figure 3.2. $\delta^{13}\text{C}_{\text{PDB}}(\text{CH}_4)$ in the methane of the AnMBR. After the dosage of ^{13}C -1 labeled acetate, there was an increase in the $\delta^{13}\text{C}_{\text{PDB}}(\text{CH}_4)$, which indicates that methane was enriched with the ^{13}C isotope. Such isotope enrichment suggests syntrophic acetate oxidation coupled to hydrogenotrophic activity. Once the dosage of the ^{13}C -1 labeled acetate stopped, the $\delta^{13}\text{C}_{\text{PDB}}(\text{CH}_4)$ decreased indicating, therefore, a decrease in the ^{13}C isotope content in methane.

Acetate was found during the first two stages when phenol was the main COD source. However, concentrations were low with an average of $29.3 \pm 29.1 \text{ mg}\cdot\text{L}^{-1}$ and $31.9 \pm 24.7 \text{ mg}\cdot\text{L}^{-1}$ and maximum values of $97 \text{ mg}\cdot\text{L}^{-1}$ and $73 \text{ mg}\cdot\text{L}^{-1}$ in Stages A and B, respectively. Acetate was not detected during the next operational periods. The accumulation of acetate during the first two stages might be related to a decrease in the SAO and/or hydrogenotrophic activity, which corroborates the decrease in phenol removal observed during both stages.

3.3.4 Contribution of the membrane-attached biomass to phenol conversion

To examine the contribution of the membrane-attached biomass to the observed phenol conversion, phenol, benzoate, and acetate in the reactor's bulk liquid and permeate were measured during stage D (Figure 3.3). For phenol, there was a significant reduction of 38 % in the permeate concentration in comparison to the reactor's bulk liquid concentration, $t(21) = -26.9$, $p < 0.001$. For acetate, the concentration in the reactor's bulk liquid was higher ($34.5 \text{ g}\cdot\text{L}^{-1}$) than in the permeate ($1.5 \text{ g}\cdot\text{L}^{-1}$). Whereas for benzoate, there was an increase in the permeate by a factor of 3.8, from $20.1 \text{ mg}\cdot\text{L}^{-1}$, in the reactor's bulk liquid to $75.5 \text{ mg}\cdot\text{L}^{-1}$. Results indicated that during the passage of the liquid through the membrane-attached biomass a further decrease in the phenol concentration occurred, meanwhile, an increase in the benzoate concentration was observed, while acetate was consumed by the membrane-attached biomass. Apparently, despite the low operational flux (4.0 LMH) and the used filtration cycle applying a short backwash time, a specialized microbial community developed on the membrane surface, which likely contributed to the general decrease in membrane permeability from $13.1 \pm 1.8 \text{ LMH}\cdot\text{bar}^{-1}$ in Stage A to 8.4 ± 1.2 in Stage D, having values of $6.5 \text{ LMH}\cdot\text{bar}^{-1}$ during the last days of operation (Appendix A.3, Section A.3.2). Besides, if phenol degradation indeed followed the benzoyl-CoA pathway, the increased benzoate concentration measured may indicate a thermodynamic constraint in the benzoyl-CoA degradation due to high H_2 concentration (Nobu et al., 2015).

It should be noted that the observed differences in concentrations of phenol, benzoate, and acetate over the membrane might be due to the relatively low bulk VSS concentration resulting in a relatively high contribution of the membrane-attached biomass to the overall conversion.

3.3.5 Membrane analysis

After determining the contribution of the membrane-attached biomass to phenol degradation and membrane permeability loss, the membrane was examined by environmental scanning electron microscopy (ESEM) and by optical microscopy to measure the dry and wet biomass layer thickness (Appendix A.3, Section A.3.3).

Based on the calculated average conversion rate of $29.1 \text{ mgPh}\cdot\text{gVSS}^{-1}\cdot\text{d}^{-1}$ in the reactor and assuming the density of the biomass in the biomass layer of the membrane as $1 \text{ g}\cdot\text{mL}^{-1}$, we calculated a required thickness of $337 \text{ }\mu\text{m}$ for achieving the observed conversion. The maximum measured thickness of the dried biofilm was $39.2 \text{ }\mu\text{m}$, while the wet layer was $106 \text{ }\mu\text{m}$. Apparently, the specific phenol conversion rate by the membrane-attached biomass was about 3.2 times higher than that observed for the bulk liquid biomass. Possibly, environmental conditions inside the biomass layer on the membrane were more advantageous for phenol conversion or, as previously hypothesized, (Section 3.3.4) a specialized phenol-degrading community developed in such membrane-attached biomass.

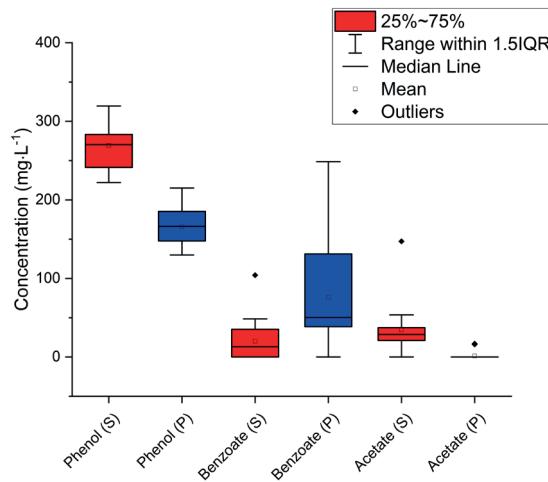


Figure 3.3. Phenol, benzoate, and acetate concentration in the reactor's bulk liquid and permeate of the AnMBR. The phenol and VFAs had a higher concentration inside the reactor when compared to the permeate. For benzoate, the concentration in the permeate was higher than the one in the reactor's bulk liquid. $n = 18$. (S) = supernatant and (P) = permeate.

3.3.6 Microbial community dynamics

To examine the microbial community dynamics along the different stages of reactor operation, and to determine whether there was a development of specialized microbial populations in the bulk liquid and the membrane-attached biomass (Figure 3.4), the relative abundances of bacteria and archaea at different time instants were analyzed.

For Bacteria, the results showed a high relative abundance of microorganisms from the class Gammaproteobacteria (22.6% A, 36.0% B, 27.3% C, 22.7% D, and 0.9 in the membrane), with *Morganella* sp., *Providencia* sp. and *Tepidiphilus* sp. being the most abundant genera. However, none of these microorganisms have been reported as

phenol degraders or have been found in phenol-degrading reactors under thermophilic conditions. The class Thermotogae showed high relative abundance during the first two stages (25.9% A, 24.3% B, 8.4% C, 6.6% D, and 0.4 in the membrane) and consisted mainly of *Petrotoga* sp., *Mesotoga* sp. and *Defluviitoga*. The microorganisms of this class have been reported in reactors treating phenolic wastewater under mesophilic (Franchi et al., 2018), thermophilic (Chen et al., 2008), and saline thermophilic conditions (Muñoz Sierra et al., 2020). Moreover, some of these microorganisms are thermophiles, halophiles, and hydrogen-producing (Conners et al., 2006). Class Synergistia (9.3 – 18.3%) had high relative abundances as well (Figure 3.4 A & B), mainly represented by *Acetomicrobium* sp., an acetate-forming microorganism reported in thermophilic digesters (Dykstra et al., 2020), found during all four stages with relative abundances of 8.5% (A), 17.0% (B), 8.9% (C), 7.4% (D) and 3.5% in the membrane-attached biomass. The class Clostridia increased from 2.9% in stage B to 7.9 and 17.2% in stages C and D respectively, and was present in the membrane-attached biomass as well (29.2%). Members of this class have been reported as SAOB such as *Syntrophaceticus* sp. (Dykstra et al., 2020; Westerholm et al., 2011) with relative abundances of 2.4% (A), 0.2% (B), 2.6% (C), 4.8% (D) and 24.4% in the membrane-attached biomass. *Syntrophaceticus* sp. was the most abundant genus during the last two stages, where acetate was fed as an additional COD source.

Regarding possible phenol degraders, we mainly found microorganisms from the class Clostridia that are commonly reported in anaerobic reactors degrading phenol, and have been suggested to have phenol degradation activity (Chen et al., 2008; Franchi et al., 2020; Na et al., 2016; Zhang et al., 2005) such as *Clostridium sensu stricto* and *Pelotomaculum* sp. (Chen et al., 2008). However, their relative abundance during the stages was low (6.0 %) which could explain the relatively low phenol removal efficiency. Overall, and opposite to what has been reported for phenol degradation in AnMBRs and batch reactors under mesophilic conditions, at 55 °C we did not find a high abundance of known specific phenol degraders, such as *Syntrophorhabdus* sp. (Franchi et al., 2018; García Rea et al., 2022; García Rea et al., 2020). Possibly, thermophilic phenol degraders are not described yet, but results may also explain the observed lower phenol removal efficiencies and sPhCR in comparison to AnMBRs under mesophilic conditions.

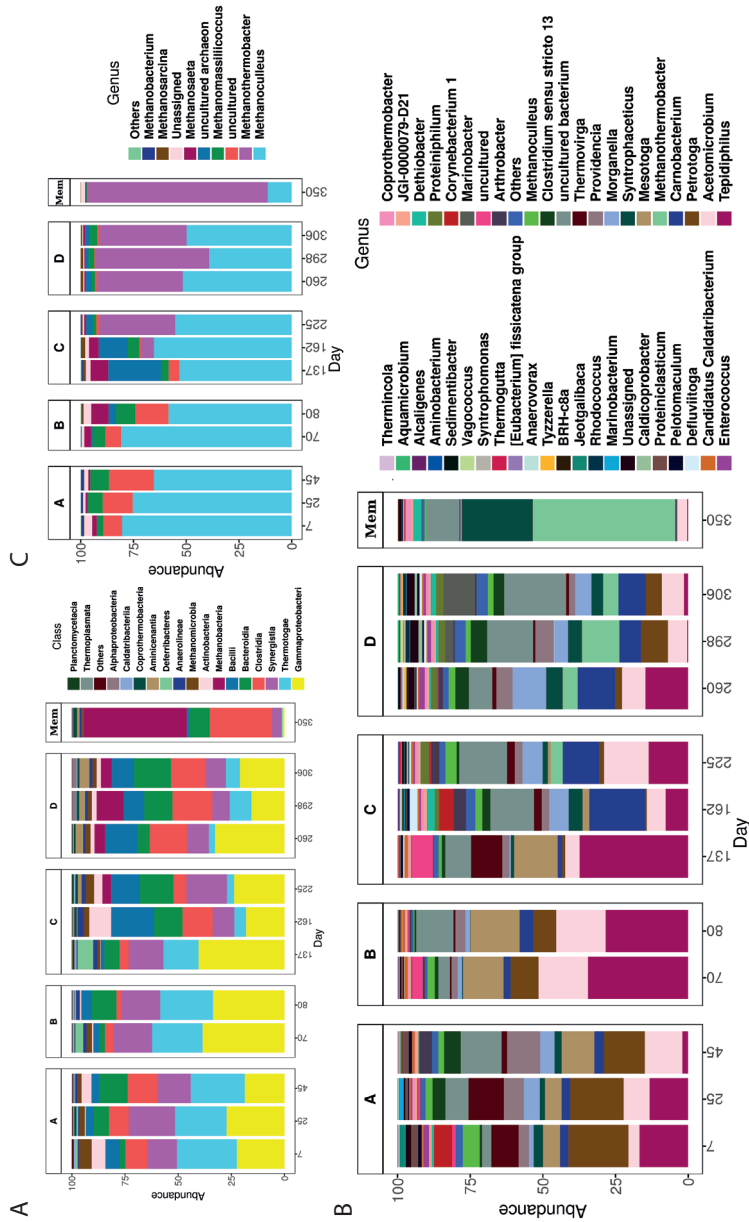


Figure 3-4. Relative abundance of Bacteria (A and B) and Archaea (C) in the AnMBR biomass during the different reactor operation stages (A-D) and in the membrane-attached biomass (Mem). For Bacteria, the class and genus taxonomic ranks are shown whereas for Archaea just genus. In A, it is noticeable the increase in the clostridia class for the stages C and D, with genus as *Syntrophaceticus* and *Clostridia sensu stricto* reported as SAOB and phenol degrader bacterium, respectively. *Archaea* microorganisms were mainly hydrogenotrophic and represented most of the community in the membrane (Mem).

For Archaea, the microbial community analysis showed that the predominant microorganisms were hydrogenotrophic methanogens. Their relative abundance in stage A was 3.4% which previously decreased to 1.4% in stage B. After the addition of acetate, an increase in the abundance was observed to 3.9% in stage C, and 9.7% in stage D. Remarkably, the hydrogenotrophic methanogens represented 49.6% of the microorganisms in the membrane-attached biomass (Figure 3.4 A & C). A detailed analysis in the Archaea domain showed that the microbial community profile had a marked presence in the reactor's biomass of *Methanoculleus* sp., (73.7% in A, 69.6% in B, 57.9% in C, 46.8% in D and 22.7% in the membrane-attached biomass) from the class Methanomicrobia, and *Methanothermobacter* sp. (class Methanobacteria) during the stage D and in the membrane-attached biomass (end of the experiment), with relative abundances of 45.2% and 73.5%, respectively. The distinct presence of hydrogenotrophic methanogens over acetoclastic ones suggests the predominant presence of HM. Hydrogenotrophic methanogens played a crucial role in the ultimate COD conversion to CH₄, which was confirmed by the results of the 1-¹³C labeled acetate experiment. After dosing the 1-¹³C labeled acetate to the AnMBR, the $\delta^{13}\text{C}_{\text{PDB}}(\text{CH}_4)$ increased during days 304 -321, indicating an increased content of ¹³C in the methane (Section 3.3.2). This is in accordance with the high relative abundance of the hydrogenotrophic methanogens *Methanoculleus* sp. (49.7%) and *Methanothermobacter* sp. (41.3%) and the presence of bacteria such as *Syntrophaceticus* sp. (3.9%), described as SAOB (Westerholm et al., 2010). It should be realized that anaerobic biomass under thermophilic conditions have relatively high growth and decay rates meaning that unfed periods or periods with low loading rates may result in relatively high decay of the hydrogenotrophic methanogenic sub-population. For the same reason, feeding a reactor with solely phenol is very difficult to operate under high temperatures and saline conditions.

The prevalence of hydrogenotrophic microorganisms was consistent with our hypothesis that acetate degradation was related to a high SAO activity, explaining the $\delta^{13}\text{C}_{\text{PDB}}(\text{CH}_4)$ observations after the dosage of the labeled acetate.

Figure 3.5 shows the PCoA of the microbial communities during the different stages of the reactor operation, and the community that developed in the membrane-attached biomass. Although between stages B and C there is an overlap (days 70 (B), 80 (B), and 137(C)), there is a difference between the microbial communities in stages A and D. Remarkably, the community developed on the membrane was clearly different from the community in the AnMBR bulk biomass.

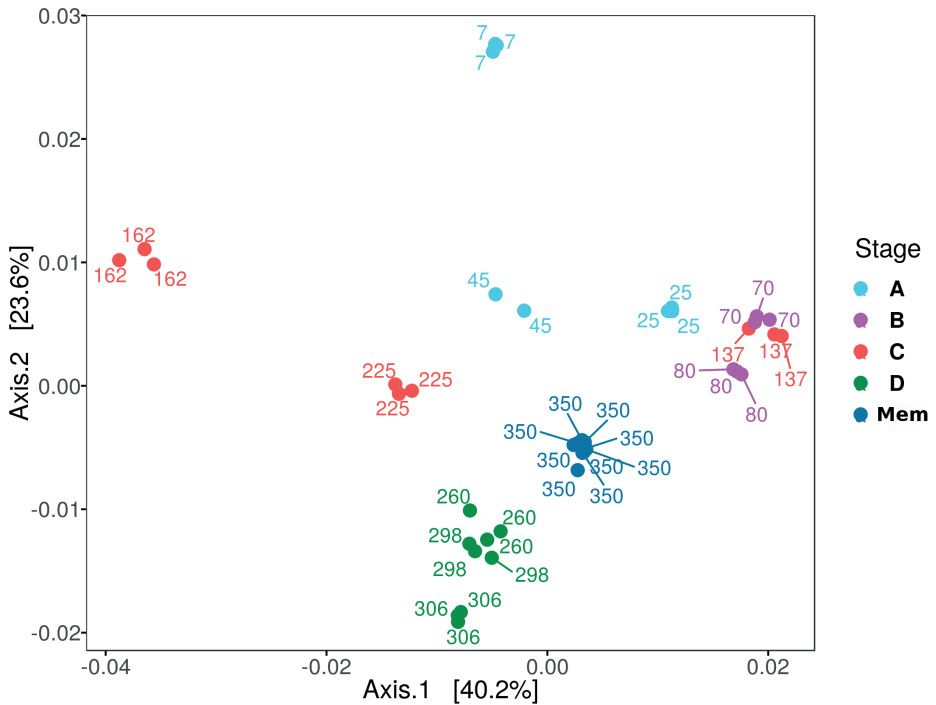


Figure 3.5. Principal coordinate analysis of the microbial communities during the different reactor operation stages (A-D) and in the membrane (Mem).

3.3.7 *Stoichiometry and thermodynamics of anaerobic growth on phenol under thermophilic conditions: effects of hydrogen partial pressure and syntrophic relationships*

A thermodynamic state analysis of environmental systems is a tool that provides a better insight into the microbial processes and related metabolism (Kleerebezem and Van Loosdrecht, 2010). It allows the identification of the stoichiometry of the overall redox reaction in the system, the (sub)reactions occurring, and the effects of physicochemical variables (such as temperature) or microbial syntrophic interactions on the thermodynamic feasibility of these reactions (Kleerebezem and Van Loosdrecht, 2010).

The stoichiometry of the catabolic (Eq. 3.5), anabolic (Eq. 3.8), and metabolic reactions (Eq. 3.9) of anaerobic growth on phenol are presented in Table 3.2. The reactions consider a microorganism capable of complete oxidation of phenol into acetate (Qiu et al., 2008).

At 55°C the increase in the hydrogen partial pressure (P_{H_2}) has a strong effect on the thermodynamics of both catabolic and metabolic reactions increasing the $\Delta G_{R, 55^\circ C}$ mainly due to the presence of H_2 as a reaction product (Eq. 3.5 and Eq. 3.9) (Figure 3.6 A). Thus, the decrease in the $\Delta G_{R, 55^\circ C}$ will increase the thermodynamic feasibility of both, catabolic and metabolic phenol conversion reactions implying the requirement of a syntrophic relationship between the phenol degraders with hydrogen consumers, e.g., hydrogenotrophic methanogens (Figure 3.6 B).

Table 3.2. Stoichiometry of anaerobic growth on phenol. The catabolic (Eq. 3.5), anabolic (Eq. 3.8), and metabolic (Eq. 3.9) reactions are shown.

	Reaction	Stoichiometry	Eq. No
Catabolism	Oxidation: phenol to acetate	$-C_6H_5OH - 5H_2O + 3C_2H_3O_2^- + 7H^+ + 4e^-$	Eq. 3.3
	Reduction: H^+ respiration	$-e^- - H^+ + 0.5 H_2$	Eq. 3.4
	Overall catabolic reaction	$-C_6H_5OH - 5H_2O + 3C_2H_3O_2^- + 2H_2 + 3H^+$	Eq. 3.5
Anabolism	Oxidation: phenol to biomass	$-0.17 C_6H_5OH - 0.33H_2O - 0.2NH_4^+ + CH_{1.8}O_{0.5}N_{0.2} + 0.67 H^+ + 0.47 e^-$	Eq. 3.6
	Reduction: H^+ respiration	$-e^- - H^+ + 0.5 H_2$	Eq. 3.7
	Overall anabolic reaction	$-0.17 C_6H_5OH - 0.33H_2O - 0.2NH_4^+ + CH_{1.8}O_{0.5}N_{0.2} + 0.24 H_2 + 0.2 H^+$	Eq. 3.8
Metabolism of anaerobic growth on phenol		$-2.31C_6H_5OH - 11.07H_2O - 0.20NH_4^+ + CH_{1.8}O_{0.5}N_{0.2} + 6.44C_2H_3O_2^- + 4.53H_2 + 6.64H^+$	Eq. 3.9

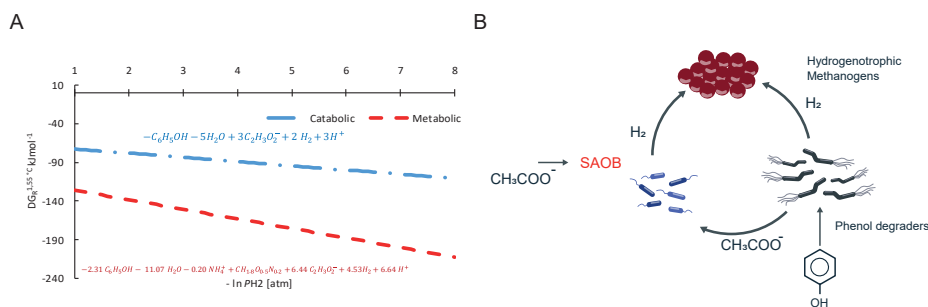


Figure 3.6. Effect of the changes in the hydrogen partial pressure (PH_2) on the $\Delta G_{1,55^\circ C}$ (correction for temperature and reagents concentration) of the catabolic (blue) and metabolic reactions (red) of phenol degradation under thermophilic anaerobic conditions. The metabolic equation considers a microorganism capable of the anaerobic degradation of phenol to acetate and hydrogen (A). Scheme for the proposed syntrophic association for phenol degradation under thermophilic anaerobic conditions between phenol degraders, syntrophic acetate oxidizing bacteria (SAOB) and hydrogenotrophic methanogens.

In agreement with previous work (García Rea et al., 2020), it was initially proposed that a robust and active acetoclastic methanogenic population could enhance phenol degradation by maintaining the concentration of acetate low. Our current results show that under thermophilic conditions we should modify this hypothesis to the need of a robust and active hydrogenotrophic methanogenic population acting as an effective scavenger of reducing equivalents (electron sink). The presence of such hydrogenotrophic population mainly depends on an active SAOB population able to maintain a low acetate concentration while ensuring hydrogen production (Figure 3.6 B).

Some authors have proposed that supplementation with hydrogen may enhance phenol degradation by increasing the conversion of phenol to (4-hydroxy)benzoate (Karlsson et al., 1999; Wu et al., 2019). However, it is unlikely that hydrogen is used during this oxidative step, as the mechanism for converting phenol into benzoylCoA requires a carboxylation, thiolation, and finally a dehydroxylation (Nobu et al., 2015). Dependence on hydrogen for such a process will be unlikely unless the 4hydroxybenzoyl-CoA reductase, which catalyzes the reductive dehydroxylation from 4hydroxybenzoyl-CoA to benzoylCoA could obtain its reducing equivalents (H) from H_2 . Similar mechanisms may be speculated for the downstream reductive steps, e.g., ring splitting by the action of the benzoyl-CoA reductase to yield cyclohex1,5dienecarbonylCoA, a process that has been suggested to be mediated by the electron donor ferredoxin (Nobu et al., 2015). Nevertheless, genomic analyses performed in a mesophilic phenol degrading community have shown that for energy conservation and electron flow, such microorganism has an electron-confurcating system which is used to produce H_2 while regenerating NAD^+ and oxidized ferredoxin (Fd_{ox}) (Nobu et al., 2015). More research is needed to determine the effect of hydrogen supplementation on the phenol degradation process and its biochemical implications.

3.4 Conclusions

It was shown that during the operation of an AnMBR under saline thermophilic anaerobic conditions, the addition of acetate as an extra COD source, significantly increased ($p < 0.001$) the phenol removal efficiency and the specific phenol conversion rate up to 65% and $29 \text{ mgPh} \cdot \text{gVSS}^{-1} \cdot \text{d}^{-1}$, respectively.

For the degradation of the organic compounds, syntrophic acetate oxidation coupled to hydrogenotrophic methanogenesis seemed to be the main pathway for acetate conversion and methane production, whereas benzoate measurement in the reactor's bulk liquid and permeate suggests that phenol degradation in the AnMBR under saline thermophilic anaerobic conditions follows the benzoyl-CoA pathway. The membrane-attached biomass exhibited an sPhCR of approx. three times higher than the reactor's bulk biomass.

The microbial community dynamics showed a high relative abundance of hydrogenotrophic methanogens in the suspended and the membrane-attached biomass; furthermore, the microbial community corresponding to the membrane-attached biomass had a high abundance of SAOB.

Finally, the stoichiometric and thermodynamic analyses support our hypothesis for the need of an abundant and active hydrogenotrophic methanogenic sub-population in the AnMBR acting as an electron sink and therefore increasing the sPhCR by avoiding (bio)energetical constraints.

3.5 Outlook, recommendations, and further applications

The present study showed that the treatment of thermophilic saline phenolic wastewater is possible provided a complete and robust methanogenic ecosystem is ensured. The main problems faced by anaerobic sludge-bed reactors when treating these types of effluents are related to biomass degranulation and subsequent washout. However, these problems are mitigated by coupling the bioreactor with a membrane filtration unit, which guarantees the retention of all specialized microbial populations needed for the degradation of phenol, namely phenol degraders and methanogens. However, under saline thermophilic conditions, and as highlighted by the isotopic $^{13}\text{CH}_4$ analysis, the methanogenic population, will mainly comprise hydrogenotrophic instead of acetoclastic archaea. Therefore, providing the hydrogenotrophic population with reducing equivalents from an easily degradable COD source, for example, hydrogen coming from SAO, will support their development. In this regard, other specific microbial populations, such as SAOB, will then play a more pronounced role in the conversion process. Results from the AnMBR operation, explained by the decrease in thermodynamic constraints, indeed showed higher phenol removal efficiency when simultaneously degraded with acetate. The development of a biofilm layer on the reactor's membrane, enriched with SAOB and hydrogenotrophic methanogens in addition to phenol degraders, supported our hypothesis on the required presence of syntrophic consortia for achieving enhanced phenol degradation.

Future research is needed to address the limitations of the present study and expand the knowledge regarding the degradation of toxic & inhibitory compounds under saline and thermophilic conditions. In our present work, we limited the simultaneous degradation to a compound that might be expected in chemical wastewater. However, other COD sources, such as carbohydrates (mono-, di-, and complex saccharides) may have as well an enhancing positive effect on the degradation of phenolic or other aromatic molecules, either when targeting the degradation of one compound or even in compound mixtures. The effect of hydrogen and CO_2 supplementation in the phenol

conversion process under thermophilic conditions is another possibility. Recently, experiments on anaerobic biochemical conversions using high-pressure reactors have been conducted (Ceron-Chafla et al., 2020) allowing the application of different H_2 partial pressures. High-pressure reactors can be used to investigate whether an increased pH_2 would lead to accelerated conversion rates, for example, by enhancing the reductive aromatic ring splitting, e.g., converting benzoate to alkyl products. Although our present results indicate that the degradation pathway of phenol under thermophilic conditions is similar to that under mesophilic conditions and follows the benzoyl-CoA route, more insight into the molecular, biochemical, and microbiological aspects is indispensable for fully understanding the conversion process. In this regard, it remains uncertain why the molecular biology analyses did not reveal the presence of a sound phenol-degrading microorganism such as *Syntrophorhabdus* sp. Thus far, no detailed studies were performed in which the thermophilic phenol degradation pathway is completely described as it has been done for mesophilic conditions (Nobu et al., 2015). Moreover, cake layer results indicate that conversion rates might be improved by the development of additional biofilm layers inside the reactor, for example by adding carrier materials such as those used in moving bed bioreactors. Finally, the presence of high salinity (and changes herein) adds another constraint to the conversion process and microbial consortia that needs to be fully understood. For instance, higher salinities will imply higher energy requirements for maintenance leading to additional stress when treating phenolic compounds.

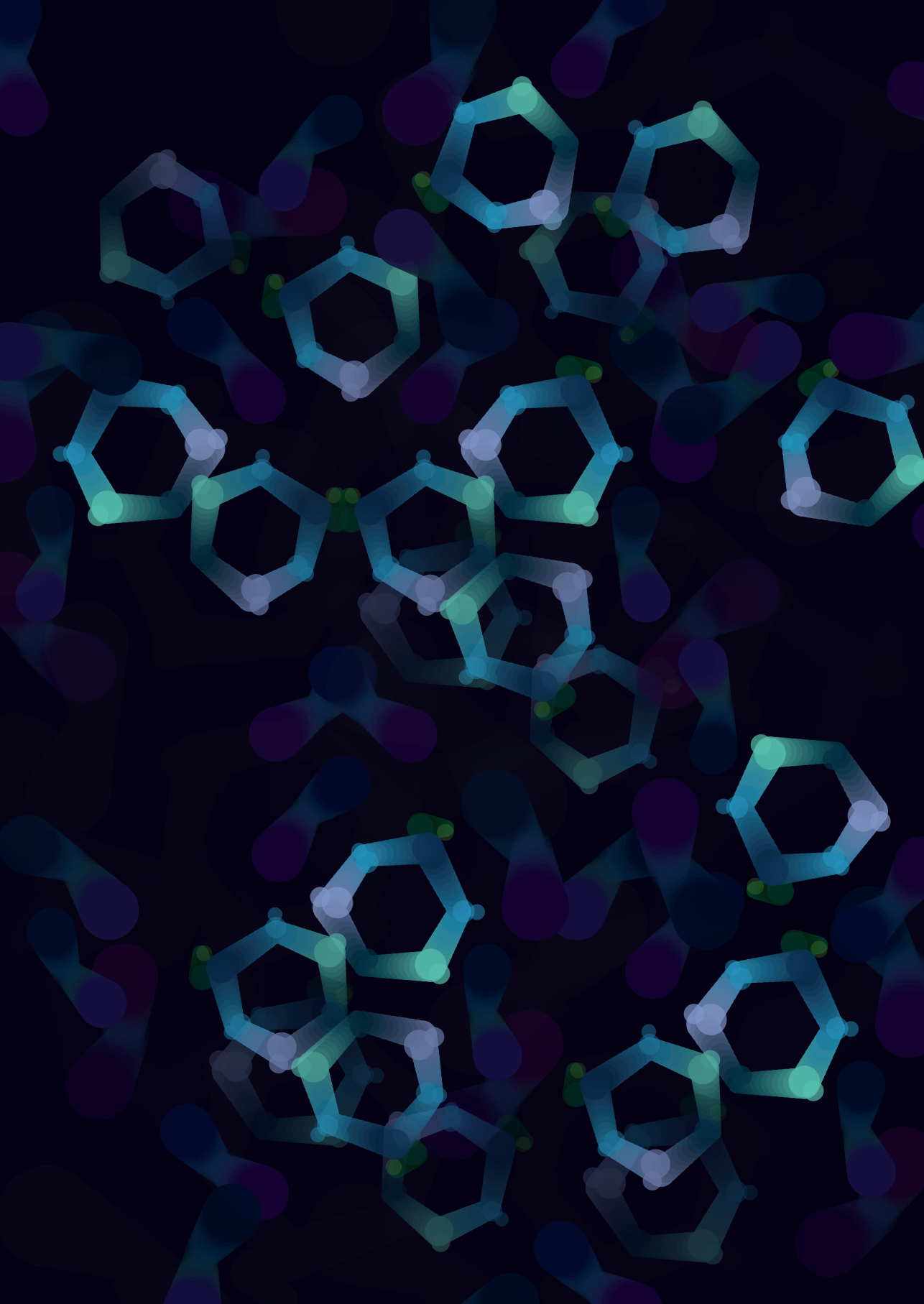
In the current situation and considering a near future in which energy is becoming more expensive, the gained knowledge offers useful applications. In our present work, we used acetate as an additional COD source, which will be questionable at full-scale due to the involved costs. Though, the codegradation of phenolic streams under thermophilic conditions with acetate-rich waste streams may be a possibility. In many chemical wastewater streams, acetate is commonly found, such as rubber vulcanization wastewater, having temperatures exceeding 40 °C (Yeoh et al., 2002). In addition, acetate is the central intermediate, or precursor, for methanogenesis, meaning that any additional COD will generate acetate. The potential for simultaneous digestion of industrial streams will be highest at industrial parks, where wastewater streams are generally cooled to the mesophilic temperature range. Nevertheless, particularly for phenol conversion, and possibly other toxic and inhibitory compounds, higher efficiencies and (specific) loading & conversion rates are expected under mesophilic conditions. However, when recovery of hot process water is anticipated, the thermophilic digestion route might be considered as most beneficial.

3.6 References

- Ceron-Chafla, P., Kleerebezem, R., Rabaey, K., van Lier, J.B., Lindeboom, R.E.F., 2020. Direct and Indirect Effects of Increased CO₂ Partial Pressure on the Bioenergetics of Syntrophic Propionate and Butyrate Conversion. *Environ. Sci. Technol.* 54(19), 12583-12592. <https://doi.org/10.1021/acs.est.0c02022>.
- Chang, B.V., Chiang, F., Yuan, S.Y., 2005. Anaerobic degradation of nonylphenol in sludge. *Chemosphere* 59(10), 1415-1420. <https://doi.org/10.1016/j.chemosphere.2004.12.055>.
- Chen, C.-L., Wu, J.-H., Liu, W.-T., 2008. Identification of important microbial populations in the mesophilic and thermophilic phenol-degrading methanogenic consortia. *Water Res.* 42(8-9), 1963-1976. <https://doi.org/http://dx.doi.org/10.1016/j.watres.2007.11.037>.
- Connors, S.B., Mongodin, E.F., Johnson, M.R., Montero, C.I., Nelson, K.E., Kelly, R.M., 2006. Microbial biochemistry, physiology, and biotechnology of hyperthermophilic *Thermotoga* species. *FEMS Microbiol. Rev.* 30(6), 872-905. <https://doi.org/10.1111/j.1574-6976.2006.00039.x> %J FEMS Microbiology Reviews.
- Dereli, R.K., Ersahin, M.E., Ozgun, H., Ozturk, I., Jeison, D., van der Zee, F., van Lier, J.B., 2012. Potentials of anaerobic membrane bioreactors to overcome treatment limitations induced by industrial wastewaters. *Bioresour. Technol.* 122, 160-170. <https://doi.org/10.1016/j.biortech.2012.05.139>.
- Duncan, J., Bokhary, A., Fatehi, P., Kong, F., Lin, H., Liao, B., 2017. Thermophilic membrane bioreactors: A review. *Bioresour. Technol.* 243, 1180-1193. <https://doi.org/https://doi.org/10.1016/j.biortech.2017.07.059>.
- Dykstra, S., Jansen, L., Gallert, C., 2020. Syntrophic acetate oxidation replaces acetoclastic methanogenesis during thermophilic digestion of biowaste. *Microbiome* 8(1), 105. <https://doi.org/10.1186/s40168-020-00862-5>.
- Fang, H., Liang, D., Zhang, T., Liu, Y., 2006. Anaerobic treatment of phenol in wastewater under thermophilic condition. *Water Res.* 40(3), 427-434. <https://doi.org/10.1016/j.watres.2005.11.025>.
- Franchi, O., Cabrol, L., Chamy, R., Rosenkranz, F., 2020. Correlations between microbial population dynamics, bamA gene abundance and performance of anaerobic sequencing batch reactor (ASBR) treating increasing concentrations of phenol. *J. Biotechnol.* 310, 40-48. <https://doi.org/https://doi.org/10.1016/j.jbiotec.2020.01.010>.
- Franchi, O., Rosenkranz, F., Chamy, R., 2018. Key microbial populations involved in anaerobic degradation of phenol and p-cresol using different inocula. *Electron. J. Biotechnol.* 35, 33-38. <https://doi.org/https://doi.org/10.1016/j.ejbt.2018.08.002>.
- Fuchs, G., Boll, M., Heider, J., 2011. Microbial degradation of aromatic compounds - from one strategy to four. *Nat. Rev. Microbiol.* 9(11), 803-816. <https://doi.org/10.1038/nrmicro2652>.
- Garcia Rea, V.S., Egerland Bueno, B., Cerqueda-García, D., Muñoz Sierra, J.D., Spanjers, H., van Lier, J.B., 2022. Degradation of p-cresol, resorcinol, and phenol in anaerobic membrane bioreactors under saline conditions. *Chem. Eng. J.* 430, 132672. <https://doi.org/https://doi.org/10.1016/j.cej.2021.132672>.
- García Rea, V.S., Muñoz Sierra, J.D., Fonseca Aponte, L.M., Cerqueda-García, D., Quchani, K.M., Spanjers, H., van Lier, J.B., 2020. Enhancing Phenol Conversion Rates in Saline Anaerobic Membrane Bioreactor Using Acetate and Butyrate as Additional Carbon and Energy Sources. *Front. Microbiol.* 11(2958). <https://doi.org/10.3389/fmicb.2020.604173>.
- Gibson, J., Harwood, C.S., 2002. Metabolic Diversity in Aromatic Compound Utilization by Anaerobic Microbes. *Annu. Rev. Microbiol.* 56(1), 345-369. <https://doi.org/10.1146/annurev.micro.56.012302.160749>.
- Hayes, J.M., 2004. An introduction to isotopic calculations

- Hendriks, A.T.W.M., van Lier, J.B., de Kreuk, M.K., 2018. Growth media in anaerobic fermentative processes: The underestimated potential of thermophilic fermentation and anaerobic digestion. *Biotechnol. Adv.* 36(1), 1-13. <https://doi.org/https://doi.org/10.1016/j.biotechadv.2017.08.004>.
- Hoyos-Hernandez, C., Hoffmann, M., Guenne, A., Mazeas, L., 2014. Elucidation of the thermophilic phenol biodegradation pathway via benzoate during the anaerobic digestion of municipal solid waste. *Chemosphere* 97, 115-119. <https://doi.org/10.1016/j.chemosphere.2013.10.045>.
- Karlsson, A., Ejlertsson, J., Nezirevic, D., Svensson, B.H., 1999. Degradation of phenol under meso- and thermophilic, anaerobic conditions. *Anaerobe* 5(1), 25-35. <https://doi.org/10.1006/anae.1998.0187>.
- Karlsson, A., Ejlertsson, J., Svensson, B.H., 2000. CO₂-dependent fermentation of phenol to acetate, butyrate and benzoate by an anaerobic, pasteurised culture. *Arch. Microbiol.* 173(5-6), 398-402. <https://doi.org/10.1007/s002030000160>.
- Kleerebezem, R., Van Loosdrecht, M.C.M., 2010. A Generalized Method for Thermodynamic State Analysis of Environmental Systems. *Crit. Rev. Environ. Sci. Technol.* 40(1), 1-54. <https://doi.org/10.1080/10643380802000974>.
- Leven, L., Nyberg, K., Schnurer, A., 2012. Conversion of phenols during anaerobic digestion of organic solid waste--a review of important microorganisms and impact of temperature. *J. Environ. Manage.* 95 Suppl, S99-103. <https://doi.org/10.1016/j.jenvman.2010.10.021>.
- Levé, L., Schnürer, A., 2005. Effects of temperature on biological degradation of phenols, benzoates and phthalates under methanogenic conditions. *Int. Biodeterior. Biodegrad.* 55(2), 153-160. <https://doi.org/http://dx.doi.org/10.1016/j.ibiod.2004.09.004>.
- McMurdie, P.J., Holmes, S., 2013. Phyloseq: an R package for reproducible interactive analysis and graphics of microbiome census data. *PLoS One* 8(4), e61217. <https://doi.org/10.1371/journal.pone.0061217>.
- Mulat, D.G., Ward, A.J., Adamsen, A.P.S., Voigt, N.V., Nielsen, J.L., Feilberg, A., 2014. Quantifying Contribution of Syntrophic Acetate Oxidation to Methane Production in Thermophilic Anaerobic Reactors by Membrane Inlet Mass Spectrometry. *Environ. Sci. Technol.* 48(4), 2505-2511. <https://doi.org/10.1021/es403144e>.
- Muñoz Sierra, J.D., García Rea, V.S., Cerqueda-García, D., Spanjers, H., van Lier, J.B., 2020. Anaerobic Conversion of Saline Phenol-Containing Wastewater Under Thermophilic Conditions in a Membrane Bioreactor. *Front. Bioeng. Biotechnol.* 8(1125). <https://doi.org/10.3389/fbioe.2020.565311>.
- Muñoz Sierra, J.D., Lafita, C., Gabaldón, C., Spanjers, H., van Lier, J.B., 2017. Trace metals supplementation in anaerobic membrane bioreactors treating highly saline phenolic wastewater. *Bioresour. Technol.* 234, 106-114. <https://doi.org/http://dx.doi.org/10.1016/j.biortech.2017.03.032>.
- Muñoz Sierra, J.D., Oosterkamp, M.J., Wang, W., Spanjers, H., van Lier, J.B., 2019. Comparative performance of upflow anaerobic sludge blanket reactor and anaerobic membrane bioreactor treating phenolic wastewater: Overcoming high salinity. *Chem. Eng. J.* 366, 480-490. <https://doi.org/https://doi.org/10.1016/j.cej.2019.02.097>.
- Munoz Sierra, J.D., Wang, W., Cerqueda-Garcia, D., Oosterkamp, M.J., Spanjers, H., van Lier, J.B., 2018. Temperature susceptibility of a mesophilic anaerobic membrane bioreactor treating saline phenol-containing wastewater. *Chemosphere* 213, 92-102. <https://doi.org/10.1016/j.chemosphere.2018.09.023>.
- Na, J.-G., Lee, M.-K., Yun, Y.-M., Moon, C., Kim, M.-S., Kim, D.-H., 2016. Microbial community analysis of anaerobic granules in phenol-degrading UASB by next generation sequencing. *Biochem. Eng. J.* 112, 241-248. <https://doi.org/https://doi.org/10.1016/j.bej.2016.04.030>.

- Nobu, M.K., Narihiro, T., Hideyuki, T., Qiu, Y.L., Sekiguchi, Y., Woyke, T., Goodwin, L., Davenport, K.W., Kamagata, Y., Liu, W.T., 2015. The genome of *Syntrophorhabdus aromaticivorans* strain UI provides new insights for syntrophic aromatic compound metabolism and electron flow. *Environ. Microbiol.* 17(12), 4861-4872. <https://doi.org/10.1111/1462-2920.12444>.
- Nobu, M.K., Narihiro, T., Liu, M., Kuroda, K., Mei, R., Liu, W.T., 2017. Thermodynamically diverse syntrophic aromatic compound catabolism. *Environ. Microbiol.* 19(11), 4576-4586. <https://doi.org/10.1111/1462-2920.13922>.
- Philipp, B., Schink, B., 2012. Different strategies in anaerobic biodegradation of aromatic compounds: nitrate reducers versus strict anaerobes. *Environ. Microbiol. Rep.* 4(5), 469-478. <https://doi.org/10.1111/j.1758-2229.2011.00304.x>.
- Qiu, Y.-L., Hanada, S., Ohashi, A., Harada, H., Kamagata, Y., Sekiguchi, Y., 2008. Anaerobe Capable of Degrading Phenol to Acetate in Obligate Syntrophic Associations with a Hydrogenotrophic Methanogen. *Appl. Environ. Microbiol.* 74, 2051-2058. <https://doi.org/10.1128/AEM.02378-07>.
- R Development Core Team, 2019. R: A language and environment for statistical computing R Foundation for Statistical Computing. <https://www.r-project.org/>.
- Sreekanth, D., Sivaramakrishna, D., Himabindu, V., Anjaneyulu, Y., 2009. Thermophilic degradation of phenolic compounds in lab scale hybrid up flow anaerobic sludge blanket reactors. *J. Hazard. Mater.* 164(2-3), 1532-1539. <https://doi.org/http://dx.doi.org/10.1016/j.jhazmat.2008.09.070>.
- van Lier, J.B., 1996. Limitations of thermophilic anaerobic wastewater treatment and the consequences for process design. *Antonie van Leeuwenhoek* 69(1), 1-14. <https://doi.org/10.1007/bf00641606>.
- van Lier, J.B., Tilche, A., Ahring, B.K., Macarie, H., Moletta, R., Dohanyos, M., Pol, L.W., Lens, P., Verstraete, W., 2001. New perspectives in anaerobic digestion. *Water Sci. Technol.* 43(1), 1-18. <https://doi.org/https://doi.org/10.2166/wst.2001.0001>.
- Westerholm, M., Dolfing, J., Sherry, A., Gray, N.D., Head, I.M., Schnürer, A., 2011. Quantification of syntrophic acetate-oxidizing microbial communities in biogas processes. *Environ. Microbiol. Rep.* 3(4), 500-505. <https://doi.org/10.1111/j.1758-2229.2011.00249.x>.
- Westerholm, M., Roos, S., Schnürer, A., 2010. *Syntrophaceticus schinkii* gen. nov., sp. nov., an anaerobic, syntrophic acetate-oxidizing bacterium isolated from a mesophilic anaerobic filter. *FEMS Microbiol. Lett.* 309(1), 100-104. <https://doi.org/10.1111/j.1574-6968.2010.02023.x>.
- Wu, B., He, C., Yuan, S., Hu, Z., Wang, W., 2019. Hydrogen enrichment as a bioaugmentation tool to alleviate ammonia inhibition on anaerobic digestion of phenol-containing wastewater. *Bioresour. Technol.* 276, 97-102. <https://doi.org/10.1016/j.biortech.2018.12.099>.
- Yeoh, B.E.E., Morimura, S., Ikbai, Shigematsu, T., Razreena, A.R., Kida, K., 2002. Simultaneous Removal of TOC Compounds and NO₃⁻ in a Combined System of Chemical and Biological Processes for the Treatment of Wastewater from Rubber Thread Manufacturing. *Jpn. J. Water Treat. Biol.* 38, 57-67. <https://doi.org/10.2521/jswtb.38.57>.
- Yuan, S.Y., Chen, S.J., Chang, B.V., 2011. Anaerobic degradation of tetrachlorobisphenol-A in river sediment. *Int. Biodeterior. Biodegrad.* 65(1), 185-190. <https://doi.org/https://doi.org/10.1016/j.ibiod.2010.11.001>.
- Zhang, T., Ke, S.Z., Liu, Y., Fang, H.P., 2005. Microbial characteristics of a methanogenic phenol-degrading sludge. *Water Sci. Technol.* 52(1-2), 73-78. <https://doi.org/10.2166/wst.2005.0500> %J Water Science and Technology.



Chapter 4

Degradation of *p*-cresol, resorcinol, and phenol in anaerobic membrane bioreactors under saline conditions

This chapter is an adapted version of: Garcia Rea Víctor S., Egerland Bueno B., Cerqueda-Garcia Daniel, Muñoz Sierra Julian D., Spanjers Henri, van Lier Jules B. (2022). Degradation of *p*-cresol, resorcinol, and phenol in anaerobic membrane bioreactors under saline conditions. Chem. Eng. J., 430. DOI: <https://doi.org/10.1016/j.cej.2021.132672>.

Abstract

Treating petrochemical wastewater is a challenge for conventional anaerobic reactors. One example is coal gasification wastewater that, besides its salinity, is rich in toxic and inhibitory aromatics, such as phenol, cresols, and resorcinol. Studies have shown that phenol and *p*-cresol share the same degradation intermediates, whereas resorcinol is degraded via another route. This study investigates the simultaneous degradation of *p*-cresol or resorcinol with phenol under anaerobic saline conditions. Batch experiments with anaerobic phenol-degrading biomass were conducted to assess the feasibility of the degradation of *p*-cresol and resorcinol. Volumetric uptake values of $11.4 \pm 2.4 \text{ mg}_{\text{p-cresol}} \cdot \text{L}^{-1} \cdot \text{d}^{-1}$ and $4.2 \pm 1.9 \text{ mg}_{\text{resorcinol}} \cdot \text{L}^{-1} \cdot \text{d}^{-1}$ were determined. The effect of *p*-cresol and resorcinol on the specific methanogenic activity and the cell viability in phenol-degrading and non-adapted biomass was assessed. Half maximal inhibitory concentration (IC_{50}) values of $0.73 \text{ g}_{\text{p-cresol}} \cdot \text{L}^{-1}$ and $3.00 \text{ g}_{\text{resorcinol}} \cdot \text{L}^{-1}$ were estimated for phenol-degrading biomass, whereas IC_{50} values of $0.60 \text{ g}_{\text{p-cresol}} \cdot \text{L}^{-1}$ and $0.25 \text{ g}_{\text{resorcinol}} \cdot \text{L}^{-1}$ were estimated for the non-adapted biomass. *p*-Cresol caused a higher decrease in the non-damaged cell counts in comparison to resorcinol. Two anaerobic membrane bioreactors under saline conditions [$8 \text{ g Na}^+ \cdot \text{L}^{-1}$] were fed with mixtures of either phenol-*p*-cresol or phenol-resorcinol. At an influent phenol concentration of $2 \text{ g} \cdot \text{L}^{-1}$, maximum conversion rates of $130 \text{ mg}_{\text{p-cresol}} \cdot \text{L}^{-1} \cdot \text{d}^{-1}$ and $180 \text{ mg}_{\text{resorcinol}} \cdot \text{L}^{-1} \cdot \text{d}^{-1}$ were found. In both AnMBRs, *Syntrophorhabdus* sp. and *Methanosaeta* sp. were the most abundant bacteria and methanogen, respectively. The feasibility of simultaneous conversion of phenolic compounds under saline conditions in AnMBRs opens novel perspectives for the high-rate anaerobic treatment of chemical wastewater.

4.1 Introduction

Several studies have reported the treatment of phenolic compounds mixtures by using up-flow anaerobic sludge blanket (UASB) reactors (Veeresh et al., 2005). According to (Fang and Zhou, 2000), the UASB reactor effectively removes phenol and *p*-cresol from wastewater at a combined concentration of over $1.0 \text{ g}\cdot\text{L}^{-1}$, corresponding to $2.6 \text{ g COD}\cdot\text{L}^{-1}$ (72% phenol, 28% *p*-cresol). Results indicate that phenol has a better biodegradability than *p*-cresol (Fang and Zhou, 2000). Also, using UASB technology to study the biodegradation of phenol and *p*-cresol mixtures (Razo-Flores et al., 2003) reported 90% of COD removal at a volumetric organic loading rate (vOLR) of $7 \text{ kg COD}\cdot\text{m}^3\cdot\text{d}^{-1}$. It was concluded that cresols concentration should not exceed $6.0 \text{ g}\cdot\text{L}^{-1}$ ($1500 \text{ mg COD}\cdot\text{L}^{-1}$). (Wu et al., 2020) obtained high COD removal efficiencies (80-100%) and complete removal of phenolic compounds operating a UASB reactor treating a synthetic CGWW composed of phenol, catechol, resorcinol hydroquinone, acetate, yeast extract, and micro- and macro-nutrients at a vORL of $2.6 \text{ g COD}\cdot\text{L}^{-1}\cdot\text{d}^{-1}$. The influent concentration of phenolic compounds was $1.0 \text{ g}\cdot\text{L}^{-1}$, corresponding to $1.5 \text{ g COD}\cdot\text{L}^{-1}$ of phenol and $0.7 \text{ g COD}\cdot\text{L}^{-1}$ of the dihydrophenol isomers (Wu et al., 2020).

High concentrations of phenol and other phenolic compounds such as *p*-cresol and resorcinol can hamper the proper performance of the treatment process (Li et al., 2017). Furthermore, the high concentration of dissolved salts makes this wastewater a challenge for conventional anaerobic treatment, mainly because the granulation process can be affected, leading to biomass wash-out (Hemmelmann et al., 2013; Jeison et al., 2008; Muñoz Sierra et al., 2019).

The presence of phenol may affect different microorganisms, such as phenol degraders (acetogens) or methanogens (Chen et al., 2014), where inhibitory or toxic effects on the methanogens would impede the entire degradation process. Inhibition is defined as a biostatic effect resulting in the impairment of the biomass function or activity, whereas toxicity is defined as biocidal effect on microorganisms being mainly irreversible (Astals et al., 2015). Compared with hydrogenotrophic methanogens, the acetoclastic ones may be affected more severely by toxic or inhibitory compounds (Astals et al., 2015; Chen et al., 2014). Therefore, accumulating phenol concentrations might affect mesophilic phenol-degrading reactors since acetoclastic methanogens were previously observed as the predominant methanogenic subpopulation in phenol-degrading AnMBRs under saline conditions (García Rea et al., 2020; Muñoz Sierra et al., 2019).

Even when the degradation pathways of phenol, *p*-cresol, and resorcinol under anoxic (nitrate-reducing conditions) or sulfate-reducing conditions and by defined

cultures have been widely reported (Fuchs et al., 2011; Gibson and Harwood, 2002; Philipp and Schink, 2012), the degradation of these compounds under strict anaerobic (methanogenic) conditions by mixed cultures is not fully understood. It has been shown that *Syntrophorhabdus*, a phenol degrader, has the capability of *p*-cresol degradation under strictly anaerobic conditions as well (Franchi et al., 2018b; Qiu, Y.L. et al., 2008). However, thus far, it has not been identified which are the microorganisms responsible for resorcinol degradation under anaerobic conditions. In addition, it is not known whether phenol and *p*-cresol degraders also have the capacity to convert resorcinol synergistically.

To further elucidate the anaerobic conversion potential of phenolic-rich wastewaters by suspended (and non-granular) biomass in a full-biomass-retention system (AnMBR), in which a more specific microbial consortium is expected to be cultivated, the maximum conversion rates of *p*-cresol and resorcinol when simultaneously degraded with phenol in a matrix with a sodium concentration of 8 g·L⁻¹ were determined. Also, the inhibitory effect of *p*-cresol and resorcinol on the acetotrophic methanogenic activity and the toxic effect, as cellular membrane damage, of both phenolic compounds on the phenol degrading biomass were assessed. By analyzing the thermodynamics of the anaerobic degradation of *p*-cresol and resorcinol, a theoretical backup to the results observed during the reactor operation was provided. Microbial community analyses revealed which microorganisms may be responsible for the degradation of phenol, *p*-cresol, and resorcinol in mixed culture systems under anaerobic conditions such as those of the AnMBRs. Furthermore, these molecular analysis will allow to compare the phylogenetic similarity between microbial communities of the AnMBRs degrading either phenol-*p*-cresol or phenol-resorcinol under saline conditions. The results obtained in this research may be of considerable practical importance, because granular-sludge reactors are prone to suffer from biomass degranulation and wash out when treating this type of biologically extreme wastewater.

4.2 Materials and Methods

4.2.1 Analytical techniques

4.2.1.1 Phenol, *p*-cresol, and resorcinol concentrations measurement

Phenol and *p*-cresol concentrations were measured by gas chromatography (GC) using an Agilent 7890A (Agilent Technologies, USA) chromatographer as reported in (García Rea et al., 2020). The runtime was 15 min with a flow of 67 mL·min⁻¹. The sample injection volume was 1 µL.

Sample preparation was done as previously reported (García Rea et al., 2020). Phenol concentration was double-checked by spectrophotometry using a Hach DR 3900

spectrophotometer (Colorado, USA), using Hach phenol detection cells LCK346 (Colorado, USA) following the manufacturers' instructions.

Resorcinol was measured by high-performance liquid chromatography (HPLC). The column used was a C18 Kinetex Core-Shell (Phenomenex, USA). The column temperature was 40 °C. As eluent, a mixture of ultrapure water (60%) and acetonitrile (40%) was used, with a flow of 0.6 mL·min⁻¹. A UV detector was used, with wavelengths of 270 nm for channel 1 and 280 nm for channel 2.

4.2.1.2 COD, volatile fatty acids, and biogas composition determination

COD was measured by spectrophotometry using a Hach DR3900 (Hach, Germany) spectrophotometer. Depending on the COD concentration, LCK314 or LCK514 COD cuvette tests were used, following the manufacturers' instructions. To prepare the sample, 1 mL of permeate was filtered through a 0.45 µm filter (Chromafil Xtra PES-45/25). Proper dilutions were made to keep the COD concentration in the measurable range and to avoid interference due to Cl⁻.

Volatile fatty acids (VFAs) were measured by GC-FID using the same sample preparation and chromatography protocols as described in Chapter 2, Section 2.1.1.

Biogas composition was determined by GC. The chromatograph was an Agilent 7890 (Agilent Technologies, USA) coupled to a thermal conductivity detector (TCD) and a column HP-PLOT Molesieve (19095P-MS6) with dimensions of 60 m x 530 µm x 20 µm. Helium was used as a carrier gas with a flow rate of 10 mL·min⁻¹ and a split ratio of 1:1. The oven temperature was 40 °C for 6 min and then increased by 25°C·min⁻¹ to 100 °C, the total run time was 10 min. The temperature of the TCD was 200 °C. For the samples, 5 to 10 mL of biogas were taken and injected into the GC-TCD.

4.2.2 Batch tests

4.2.2.2 Anaerobic biodegradability tests for *p*-cresol and resorcinol by phenol-degrading biomass

A series of batch tests with initial concentrations of 50, 100, 250, or 500 mg·L⁻¹ with either *p*-cresol or resorcinol as sole carbon and energy source (CES) were carried out. The tests were performed in triplicates in 250 mL Schott glass reactors (working volume 200 mL), using a substrate-biomass ratio of 2 g COD·gVSS⁻¹. The biomass was taken from a phenol-degrading AnMBR. To ensure anaerobic conditions, the glass reactors were flushed with N₂ for one minute. Per gram of substrate COD, 0.75 mL of micronutrient solution, 1.53 mL of macronutrient solution, and 50 mg of yeast extract (Sigma Aldrich) were added (Hendriks et al., 2018). Per each mL of medium,

30.5 mL of phosphate solution A and 19.5 mL of phosphate solution B were added. The composition of the different solutions is reported in our previous work (García Rea et al., 2020).

The bottles were incubated at 35 °C in a temperature-controlled shaker (New Brunswick Innova, Germany) at 130 rpm. Samples (0.5 to 1.0 mL) were periodically taken from the medium and filtered through a 0.45 µm filter (Chromafil Xtra PES-45/25). *p*-Cresol, resorcinol, VFAs, and COD were determined in the filtrate as specified in Chapter 2, Section 2.1.

4.2.2.3 Specific methanogenic activity inhibition and cellular membrane damage

For assessing the specific methanogenic activity (SMA), the protocol proposed by Spanjers and Vanrolleghem was used, except for the micronutrient dosage which was 0.6 mL·L⁻¹ instead of 6 mL·L⁻¹ (Spanjers and Vanrolleghem, 2016). Tests were carried out in triplicates in 250 mL Schott glass bottles at 35° C, 130 rpm, and anaerobic conditions. Sodium acetate-trihydrate (Sigma Aldrich, USA) was used as the substrate at a concentration of 2.0 gCOD_{acetate}·L⁻¹. The biomass was taken from a phenol-degrading AnMBR (García Rea et al., 2020). The batch reactors kept a substrate-inoculum ratio of 2 (gCOD·gVSS⁻¹). Macro and micro-nutrient solutions were added as described in Chapter 2, Section 2.2.

Accumulated biogas production was recorded by an AMPTS II system (Bioprocess Control, Sweden). Initial and final COD and acetate concentrations and pH values were measured as described in Chapter 2, Section 2.1. Different *p*cresol and resorcinol concentrations were used.

Membrane cell damage was assessed by flow cytometry (FCM). Samples of the biomass were taken before starting the SMA tests and once the tests were finished. For sample preparation, 5 mL of biomass were taken and diluted with 0.22 µm-filtered phosphate-buffered saline 1:500 (Falcioni et al., 2006). The mixture was sonicated three times for 45s at 4 °C and 100 W. To determine the total cell count, 495 µL of the sonicated mixture were stained with 5 µL of SYBR Green I dilution (S7563, Thermo Fisher, Massachusetts, USA). For the damaged-wall-cells measurement, the cells in the sonicated mixture were stained with 5 µL of SYBR Green I and propidium iodide (P4170, Merk, Germany) [30 mM] solutions. After the staining addition, the samples were gently vortexed and incubated in the dark at 37 °C for 10 min. The FCM was done in a BD Accuri C6 flow cytometer (Becton Dickinson, New Jersey, USA). The concentration of the samples was adjusted to have less than 2000 events ·µL⁻¹. The results are reported as the percentage of non-damaged cells in comparison to a control bottle.

Once the assays with the AnMBR biomass were completed, the SMA inhibition and membrane cell damage tests for *p*-cresol and resorcinol were repeated using anaerobically digested sewage sludge coming from a municipal wastewater treatment plant (Harsnashpolder, The Netherlands).

4.2.3 *Simultaneous degradation of phenol with p-cresol or resorcinol*

4.2.3.1 Anaerobic membrane bioreactors operation

Two reactors (6.5 L working volume, 7.0 total volume) equipped with a membrane module (approximately 130 cm³), with a 64 cm length and 5.5 mm diameter, inside-out ultrafiltration (30 nm nominal pore size) tubular PVDF membrane (Pentair, The Netherlands), were used for the continuous experiment for the simultaneous degradation of phenol with either *p*-cresol or resorcinol. Both reactors shared the same configuration (Figure 4.1). R1 was used for the degradation of phenol-*p*-cresol and R2 for phenol-resorcinol.

Each setup was fully automated and was equipped with influent and effluent pumps (Watson Marlow 120 U) and a recirculation pump (Watson Marlow 160 U). To determine the TMP, two pressure sensors (AE Sensors, The Netherlands) with a range from -800 to 600 mbar measured the pressure of the bulk sludge at the entrance and the exit of the membrane, and a third sensor of the same characteristics measured the pressure at the permeate side. The reactor volume was kept constant using two pressure sensors (AE Sensors, The Netherlands), ranging from 0 to 100 mbar, located at the top and the bottom of the reactor. Temperature and pH were measured online using pH/temperature sensors (Endress & Hauser, Memosens and Mettler Toledo). To keep temperature constant (35 °C), a water bath (Tamson Instruments, The Netherlands) was used to recirculate water through the reactor's jacketed double wall.

The biomass was mixed by internal recirculation at a rate of approx. 300 d⁻¹ with a flow of approx. 1830 L·d⁻¹. Therefore, the membrane was operated with a cross-flow velocity of 1.0 m·s⁻¹.

The reactors were fed with synthetic wastewater containing phenol [2 g·L⁻¹], acetate [2 g COD·L⁻¹], and either *p*-cresol (R1) or resorcinol (R2) at different concentrations (Table 4.1). Micro- and macronutrient solutions, phosphate buffers, and yeast extract were added to the feeding medium as specified in Chapter 2 Section 2.2.1. Sodium chloride was added to keep the Na⁺ concentration at 8 g·L⁻¹.

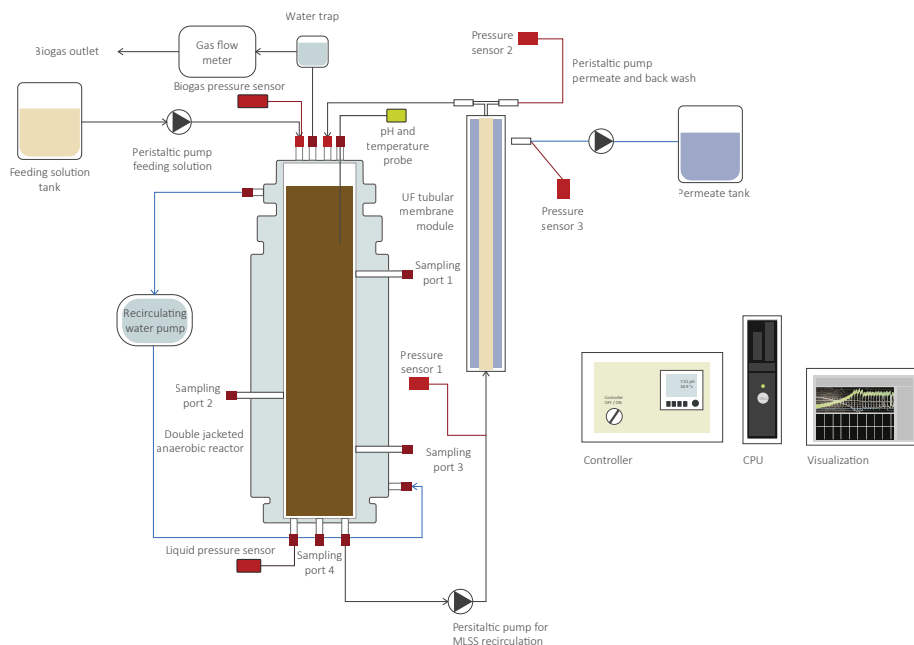


Figure 4.1. Scheme of the AnMBR set-up.

4.2.3.2 DNA extraction for microbial community composition analysis

Samples from the reactors were taken at specified days of reactor operation. A total volume of 1.5 – 2.0 mL of biomass were transferred to microcentrifuge tubes (Eppendorf, Germany). The tubes were centrifuged for 5 min at 10.000 g. The supernatant was discarded and the biomass pellet was frozen at -80 °C. For the extraction, the cell pellets were melted and DNA was recovered using a DNA extraction kit (DNeasy UltraClean Microbial Kit, Qiagen, Germany) following the instructions provided by the manufacturer.

4.2.3.3 16S rRNA gene amplification, sequencing, and data processing

DNA (16S rRNA gene) amplification was done using Illumina Novaseq 6000 platform by Novogene. The hypervariable regions V3-V4 were amplified using the primer set 341F [(5'- 3') CCTAYGGGRBGCASCAG] and 806R [(5'- 3') GGACTACNNGGTATCTAAT]. The PCR reactions were carried out with Phusion® High- Fidelity PCR Master Mix (New England Biolabs). The DNA sequencing data was processed as described in Garcia Rea et. al 2020 (García Rea et al., 2020). The sequences were deposited in the SRA (NCBI) database under the accession number PRJNA739995.

Table 4.1. Influent concentration and resulting volumetric loading rate of phenolic compounds during the operation of R1 and R2.

R1				R2			
Phase	Operation days	<i>p</i> -Cresol [mg·L ⁻¹]	<i>p</i> -Cresol vOLR [mg·L ⁻¹ ·d ⁻¹]	Phase	Operation days	Resorcinol [mg·L ⁻¹]	Resorcinol vOLR [mg·L ⁻¹ ·d ⁻¹]
I	0 - 8	25	4	I	0-15	50	8
II	9 - 21	50	8	II	16 - 25	100	17
III	22 - 33	100	17	III	26 - 31	200	30
IV	34 - 47	200	30	IV	32 - 43	400	65
V	48 - 58	300	50	V	44 - 53	600	100
VI	59 - 67	400	65	VI	54 - 63	800	130
VII	68 - 94	800	130	VII	64 - 77	1200	200
VIII	95 - 101	1200	200	-	-	-	-
IX	102 - 112	1600	267	-	-	-	-

4.2.4 Thermodynamic state analysis

For the thermodynamic analysis of the *p*-cresol and resorcinol degradation, the Gibbs Energy Dissipation method (Kleerebezem and Van Loosdrecht, 2010) was used. Through the coupling of catabolism and anabolism, the overall metabolic equations of anaerobic growth on *p*-cresol and resorcinol were derived. To perform the required calculations, the following foreseen concentrations and partial pressures expected in the AnMBR were used: *p*-cresol and resorcinol 0.1 mmol (10 mg·L⁻¹), acetate 0.02 mmol (1.2 mg·L⁻¹), carbon dioxide 0.4 atm, hydrogen 1 × 10⁻⁴ atm, ammonium 5 × 10⁻⁸ mmol, and H⁺ 1 × 10⁻⁷ M.

4.3 Results

4.3.1 Anaerobic biodegradability of *p*-cresol and resorcinol by phenol-degrading biomass

To assess whether *p*-cresol and resorcinol could be anaerobically converted by using biomass from a phenol degrading AnMBR under saline conditions, and if so, to have an insight into the degradation kinetics, either *p*-cresol or resorcinol were fed as sole CES to the biomass and the concentration of the compounds was continuously measured. The anaerobic conversion at different initial concentrations of *p*-cresol and resorcinol is presented in Figure 4.2 A and B, respectively. A zero-order kinetic model was fitted to the data to estimate the volumetric- ($r_{s,v}$) and the specific ($r_{s,s}$) substrate conversion rates (Table 4.2).

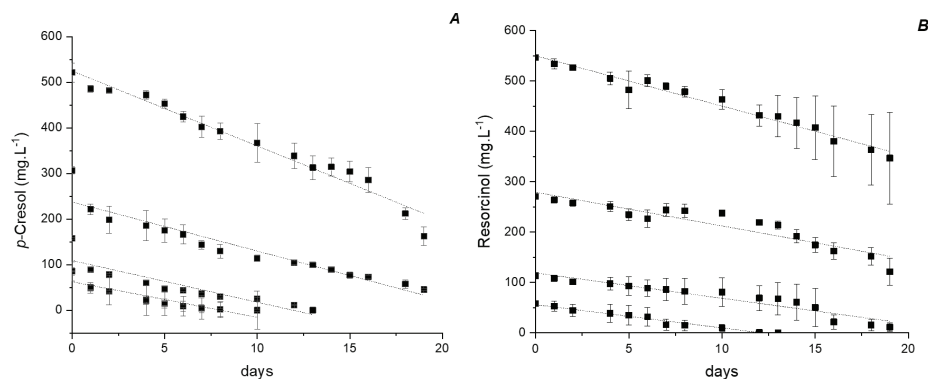


Figure 4.2. Zero order-kinetic model fitting to the batch test data for *p*-cresol (A) and resorcinol (B).

Figure 4.2 shows that, even without previous exposure to the compounds, both phenolic compounds were degraded by the biomass. The degradation in the batch reactors seemed to follow a linear relationship, with conversion of *p*-cresol (ave $r_{s,v} = 11 \pm 3.3 \text{ mg} \cdot \text{L}^{-1} \cdot \text{d}^{-1}$) faster than resorcinol (ave $r_{s,v} = 6.6 \pm 2.1 \text{ mg} \cdot \text{L}^{-1} \cdot \text{d}^{-1}$). However, and even when the volumetric conversion rates were similar between the different initial concentrations, the biomass specific conversion rates for both compounds showed a decrease with higher (initial) concentrations (Table 4.2).

Table 4.2. Volumetric ($r_{s,v}$) and specific ($r_{s,s}$) substrate uptake rates for *p*-cresol and resorcinol in batch tests.

Initial concentration [mg·L ⁻¹]	<i>p</i> -Cresol			Resorcinol		
	$r_{s,v}$ [mg·L ⁻¹ ·d ⁻¹]	R ²	$r_{s,s}$ [mg·gVSS ⁻¹ ·d ⁻¹]	$r_{s,v}$ [mg·L ⁻¹ ·d ⁻¹]	R ²	$r_{s,s}$ [mg·gVSS ⁻¹ ·d ⁻¹]
50	7.8 ± 1.3	0.84	44.0 ± 7.8	4.6 ± 0.3	0.97	26.6 ± 6.4
100	9.1 ± 1.45	0.81	19.3 ± 0.6	5 ± 0.4	0.91	8.8 ± 1.5
250	10.8 ± 0.9	0.89	8.5 ± 1.2	6.7 ± 0.7	0.87	5 ± 0.8
500	16.4 ± 0.8	0.96	6.5 ± 1.7	10 ± 0.4	0.97	3.5 ± 1.6

4.3.2 Specific methanogenic activity inhibition and cell viability

To determine if *p*-cresol and resorcinol inhibited the acetoclastic methanogenesis, the SMA inhibition of the phenol-degrading AnMBR biomass in the presence of both phenolic compounds (Figure 4.3 A & B) was assessed. In addition, to determine whether *p*-cresol and resorcinol had a toxic effect on the AnMBR biomass, the cell membrane integrity by the livedeath cell staining protocol (Nescerecka et al., 2016) was analyzed (Figure 4.3 C & D) once the SMA was finished. Finally, to assess and compare the inhibitory and toxic effects of *p*-cresol and resorcinol on nonadapted biomass, the

tests were repeated with biomass coming from a municipal anaerobic sludge digester (Figure 4.4 A-D).

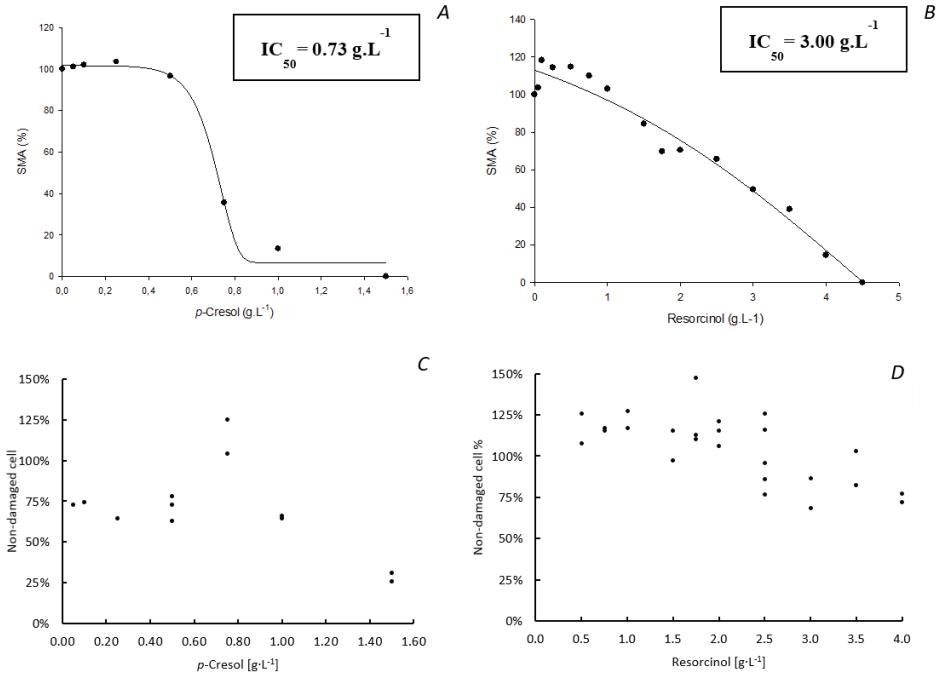


Figure 4.3. Acetoclastic SMA inhibition percentage in the phenol-degrading sludge in the presence of *p*-cresol (A) and resorcinol (B). Percentage of non-damaged cells, in respect of the control, in the anaerobic biomass after the SMA inhibition tests with *p*-cresol (C) and resorcinol (D).

By fitting a four parameter logistic model (Lee and Hwang, 2019), the half maximal inhibitory concentrations (IC₅₀) for both compounds in the phenol-degrading biomass were estimated as IC_{50-*p*-cresol} = 0.73 g L⁻¹, and IC_{50-resorcinol} = 3.00 g L⁻¹ which implies that *p*-cresol has a higher inhibitory effect on the acetotrophic methanogens in comparison to resorcinol. Figure 4.3 (C & D) shows the results of the FCM performed once the SMA inhibition tests were finished. It can be observed that at *p*-cresol concentrations of up to 1.0 g L⁻¹ there is not a marked decrease in undamaged cells. At 0.75 g *p*-cresol L⁻¹, an over-estimation of non-damaged cells was observed, which is further considered as an outlier. However, at a concentration of 1.5 g L⁻¹, almost 75% of the cells were damaged; nevertheless, the variability of the data should be considered. This implies that at concentrations below 1.0 g L⁻¹ the inhibition was mainly biostatic, whereas at 1.5 g L⁻¹, in addition to the biostatic inhibition, there was a higher percentage of cell-membrane-damaged cells which may be associated with a biocidal (inhibitory) effect or toxicity (Astals et al., 2015). With respect to resorcinol, results show that even at the

higher concentrations the percentages of non-damaged cells hardly decreased. At a concentration of $4 \text{ g}_{\text{resorcinol}} \cdot \text{L}^{-1}$ there was an increase of 25% in damaged cells in comparison with the control. Implying that resorcinol had mainly biostatic and not toxic (biocidal) effects on the biomass.

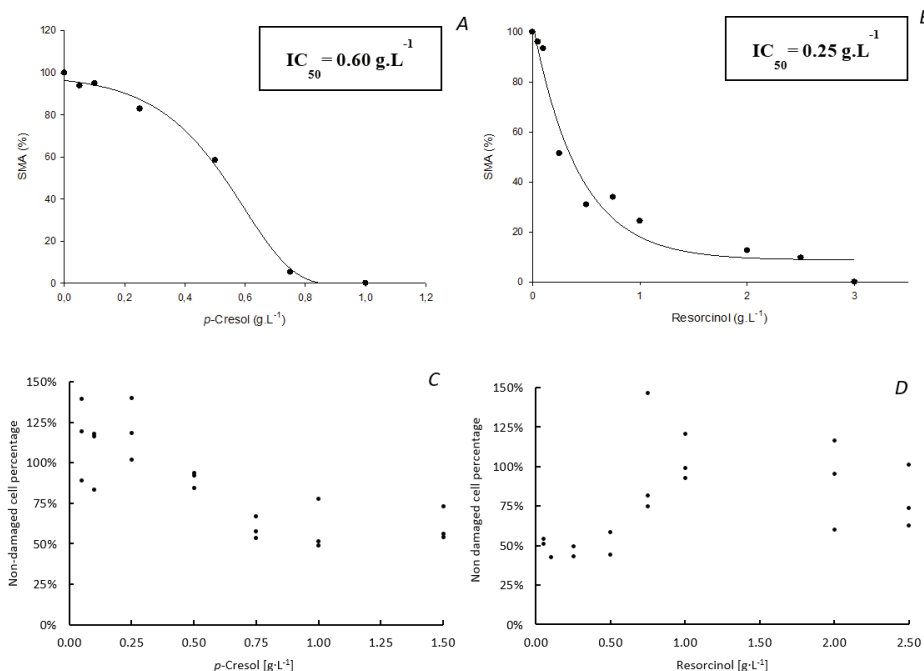


Figure 4.4. Acetoclastic SMA inhibition percentage in the MWWTP sludge in the presence of *p*-cresol (A) and resorcinol (B). Percentage of non-damaged cells, in respect of the control, in the anaerobic biomass after the SMA inhibition tests with *p*-cresol (C) and resorcinol (D).

Regarding the non-adapted biomass, the estimated IC_{50} values were 18% ($\text{IC}_{50\text{-p-cresol}} = 0.60 \text{ g} \cdot \text{L}^{-1}$) and 92% ($\text{IC}_{50\text{-resorcinol}} = 0.25 \text{ g} \cdot \text{L}^{-1}$) lower than the ones for the phenol-degrading AnMBR biomass. Opposite to what was observed for the phenol-degrading AnMBR biomass, *p*-cresol at concentrations of 1.0 and $1.5 \text{ g}_{\text{pcresol}} \cdot \text{L}^{-1}$ caused a decrease of approx. 50% of the non-damaged cells, which was lower in comparison with what was observed with the AnMBR-adapted biomass. However, even at the concentration of $0.75 \text{ g}_{\text{pcresol}} \cdot \text{L}^{-1}$ the methanogenic activity was almost completely inhibited, giving an activity of only 5.2% of the control. On the other hand, the IC_{50} value for resorcinol in the non-adapted biomass was 92% lower than the obtained IC_{50} value for the phenol-degrading biomass. The FCM, showed that there was not an increase in the membrane-damaged cells even at concentrations that caused high inhibition of methanogenesis. However, and opposite to what was observed with the phenol degrading AnMBR sludge,

there was no negative trend in the non-damaged cell percentage with increasing concentration of resorcinol.

Half maximum inhibitory concentration (IC_{50}) values for methanogenesis with regard to phenol, *p*-cresol, and resorcinol have been reported by other researchers (Olguin-Lora et al., 2003; Sierra-Alvarez and Lettinga, 1991) (Table 4.3). However, most of the values were obtained using anaerobic granular sludge as inoculum, mainly coming from UASB reactors. On the other hand, although *p*-cresol and resorcinol are toxic compounds, to the best of the author's knowledge, no studies are reported on the effect of these compounds on the cell viability.

Two AnMBRs with phenol-degrading and salt-adapted biomass were operated to assess the maximum conversion rates of *p*-cresol or resorcinol, together with phenol, under continuous-flow reactor conditions with low to moderate bulk concentrations of the phenolic compounds. Periodically, sludge samples were taken to study the dynamics of the microbial communities. Reactor 1 (R1) was fed with a mixture of *p*-cresol and phenol, and Reactor 2 (R2) with a mixture of resorcinol and phenol (Table 4.1).

Table 4.3. IC_{50} values reported for *p*-Cresol and resorcinol

References	Compound	IC_{50}	Biomass
Olguin-Lora et al. 2003	<i>p</i> -Cresol	0.39 g·L ⁻¹	Non-acclimated granular sludge
Olguin-Lora et al. 2003	<i>p</i> -Cresol	1.03 g·L ⁻¹	Phenol-acclimated granular sludge
Sierra-Alvarez and Lettinga, 1991	<i>p</i> -Cresol	0.62 g·L ⁻¹	Granular sludge from a full-scale UASB treating distillery wastewater
Sierra-Alvarez and Lettinga, 1991	Resorcinol	1.81 g·L ⁻¹	Granular sludge from a full-scale UASB treating distillery wastewater
This study	<i>p</i> -Cresol	0.73 g·L ⁻¹	Suspended biomass from a phenol-degrading AnMBR (8 gNa·L ⁻¹)
This study	<i>p</i> -Cresol	0.60 g·L ⁻¹	Anaerobically digested biomass from an MWWTP
This study	Resorcinol	3.00 g·L ⁻¹	Suspended biomass from a phenol-degrading AnMBR (8 gNa·L ⁻¹)
This study	Resorcinol	0.25 g·L ⁻¹	Anaerobically digested biomass from an MWWTP

Nine different volumetric *p*-cresol loading rates ($v_{p\text{-cresol}}\text{LR}$) were applied (Table 4.1). Up to a load of $130 \text{ mg}_{p\text{-cresol}} \cdot \text{L}^{-1} \cdot \text{d}^{-1}$, 100% removal of phenol and *p*-cresol was achieved, corresponding to a specific *p*-cresol conversion rate ($s_{p\text{-cresol}}\text{CR}$) of $22 \text{ mg}_{p\text{-cresol}} \cdot \text{gVSS}^{-1} \cdot \text{d}^{-1}$ and a specific phenol conversion rate of ($s_{\text{phenol}}\text{CR}$) of $56 \text{ mg}_{\text{ph}} \cdot \text{gVSS}^{-1} \cdot \text{d}^{-1}$. However, on day 102, when the $v_{p\text{-cresol}}\text{LR}$ reached $200 \text{ mg}_{p\text{-cresol}} \cdot \text{L}^{-1} \cdot \text{d}^{-1}$, the removal efficiencies of both phenol and *p*-cresol decreased practically at the same time, most likely implying an intoxication of the reactor biomass caused by accumulating *p*-cresol (Figure 4.5 A).

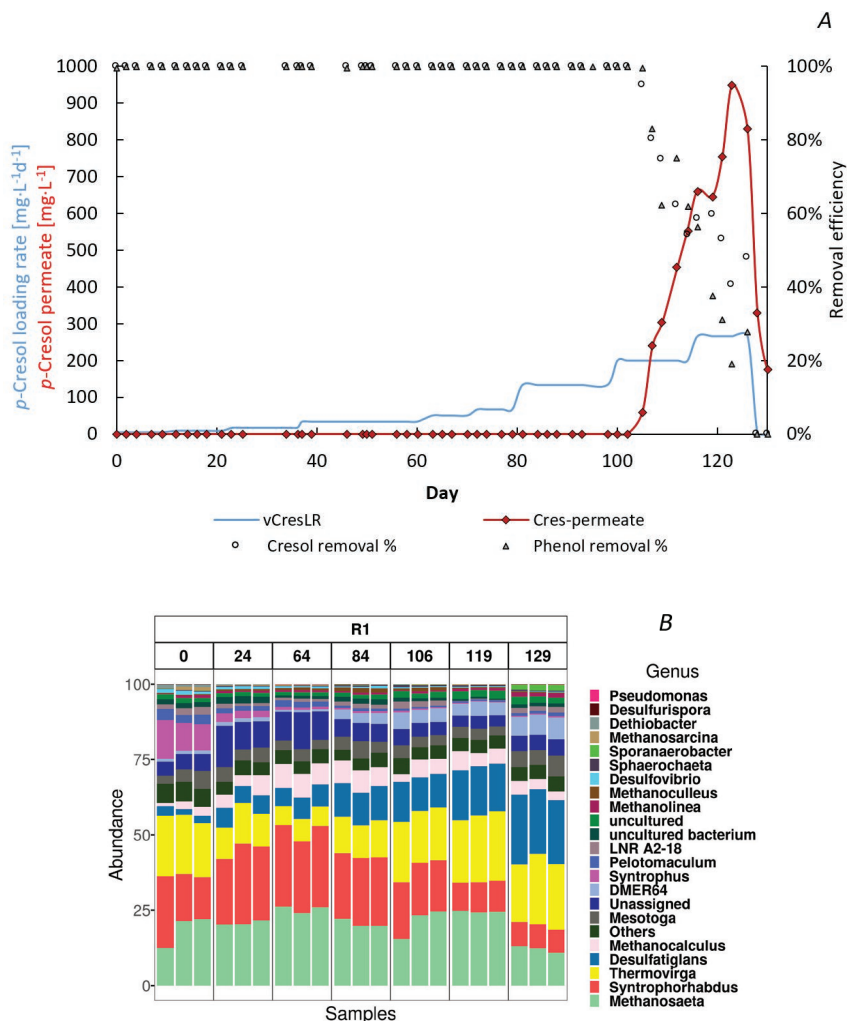


Figure 4.5. Operation of R1 for the simultaneous degradation of *p*-cresol and phenol (A), and relative abundance of microorganisms (genus) during different operation days (B). In (A), the left y axis represents either the *p*-cresol volumetric loading rate [$\text{mg}_{p\text{-cresol}} \cdot \text{gVSS}^{-1} \cdot \text{d}^{-1}$] or the concentration of *p*-cresol in the permeate [$\text{mg}_{p\text{-cresol}} \cdot \text{L}^{-1}$].

Concerning the microbial community structure (Figure 4.5 B), the 4 most abundant microorganisms comprising $62.2 \pm 4.7\%$ of the entire community during the whole reactor operation included the strict acetoclastic methanogen *Methanosaeta* sp. ($20.4 \pm 4.8\%$), *Syntrophorhabdus* sp. ($18.0 \pm 6.9\%$) a reported phenol and *p*-cresol degrader, *Thermovirga* sp. ($15.8 \pm 5.6\%$), and *Desulfatiglans* sp. ($11.0 \pm 6.3\%$). After the increase in the $v_{p\text{-cresol}}$ LR and therefore in the *p*-cresol concentration in the bulk of the reactor, there was a decrease in the relative abundance of *Syntrophorhabdus* sp from $17.8 \pm 1.0\%$ (day 106), corresponding to a 100% removal efficiency of *p*-cresol and phenol, to $9.9 \pm 0.5\%$ on day 119, and then to $7.9 \pm 0.3\%$ on day 129. *Methanosaeta* had a decrease in its relative abundance as well, from $24.5 \pm 0.3\%$ on day 119 to $12.1 \pm 1.1\%$ on day 129. The other two most abundant genera did not show a clear decrease in their relative abundances.

4.3.2.1 Simultaneous degradation of phenol and resorcinol

Seven volumetric resorcinol loading rates ($v_{\text{resorcinol}}$ LR) were applied to R2. Though, each time the $v_{\text{resorcinol}}$ LR was increased, there was a decrease in the removal efficiency of resorcinol (Figure 4.6 A). The phenol removal efficiency was affected when the resorcinol concentration started to increase, e.g., days 29 - 48. However, even when resorcinol concentrations were higher than $200 \text{ mg} \cdot \text{L}^{-1}$ (day 43 and 69, Figure 4.6 A), the conversion rates, and therefore, the removal efficiencies of phenol and resorcinol recovered. On day 59, at a $v_{\text{resorcinol}}$ LR of $100 \text{ mg}_{\text{resorcinol}} \cdot \text{L}^{-1} \cdot \text{d}^{-1}$, removal efficiencies of 98% and 100% were found for resorcinol and phenol respectively, corresponding to specific conversion rates ($s_{\text{resorcinol}}$ CR) of $16 \text{ mg}_{\text{resorcinol}} \cdot \text{gVSS}^{-1} \cdot \text{d}^{-1}$ and $54 \text{ mg}_{\text{phenol}} \cdot \text{gVSS}^{-1} \cdot \text{d}^{-1}$. However, on day 66, there was a decrease to 52% and 73% in the resorcinol and phenol removal efficiencies, respectively. On day 69, when the $v_{\text{resorcinol}}$ LR was increased to $130 \text{ mg}_{\text{res}} \cdot \text{L}^{-1} \cdot \text{d}^{-1}$, the resorcinol concentration in the permeate started to increase, resulting in a reduced resorcinol removal efficiency of 52% and 66% for phenol. Nonetheless, on day 73, and with a $v_{\text{resorcinol}}$ LR = $200 \text{ mg}_{\text{res}} \cdot \text{L}^{-1} \cdot \text{d}^{-1}$, a recovery in the removal efficiency was observed, reaching 90% and 99% for resorcinol and phenol, respectively. The subsequent increase in the $v_{\text{resorcinol}}$ LR to $250 \text{ mg}_{\text{Res}} \cdot \text{L}^{-1} \cdot \text{d}^{-1}$ on day 87 caused the resorcinol and phenol conversion failure. In contrast to what was observed in R1, the phenol removal efficiency decreased after two days (day 87) of the last drop in the resorcinol removal efficiency.

For the microbial structure (Figure 4.6 B), three main microorganisms comprised $66.5 \pm 7.9\%$ of the entire community during the whole reactor operation. These microorganisms were the phenol degrader *Syntrophorhabdus* sp. ($24.2 \pm 5.6\%$), *Thermovirga* sp. ($21.8 \pm 4.3\%$), and the acetoclastic methanogen *Methanosaeta* sp. ($20.6 \pm 5.0\%$). Opposite to what was observed in R1, the *Methanosaeta* sp. was not the most abundant microorganism. In contrast, *Syntrophorhabdus* sp. dominated the community,

which suggested that *Syntrophorhabdus* sp. could have contributed to the degradation, not just of phenol but of resorcinol as well. Another observed difference with respect to R1 is that even in the periods when the removal efficiency of resorcinol decreased, there was no noticeable impact on the main groups of microorganisms, especially *Syntrophorhabdus* sp. and *Methanosaeta* sp. As well, *Thermovirga* sp. remained constant during all the stages and, similar to what was observed for the operation with *p*-cresol, *Desulfatiglans* sp. was the fourth most abundant microorganism; though, on average, its relative abundance was $3.9 \pm 1.5\%$ in comparison to the $11.0 \pm 6.3\%$ found for R1.

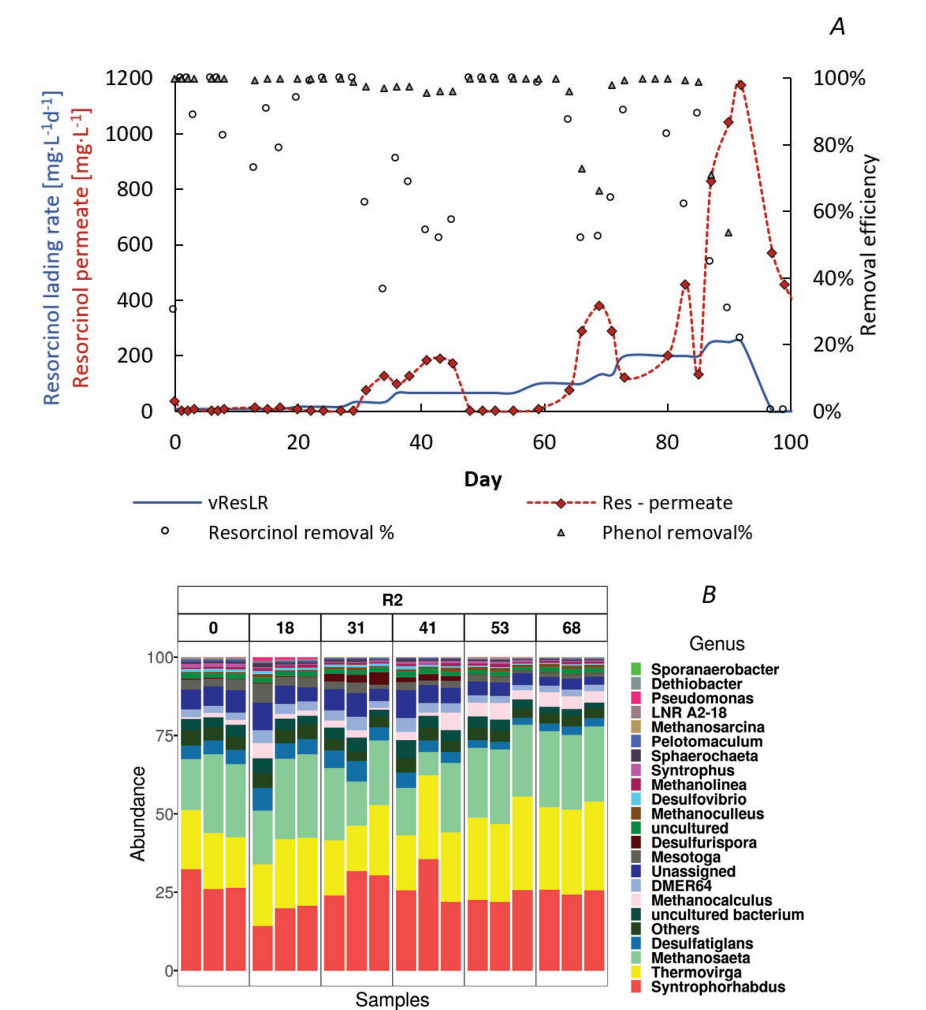


Figure 4.6. Operation of R2 for the simultaneous degradation of resorcinol and phenol (A), and relative abundance of microorganisms (genus) during different operation days (B). In (A), the left y axis represents either the resorcinol volumetric loading rate [mg_{resorcinol}·gVSS⁻¹·d⁻¹] or the concentration of resorcinol [mg_{resorcinol}·L⁻¹] in the permeate.

To compare the similarities between the microbial communities of the two reactors, a principal coordinate analysis (PCoA) was performed (Figure 4.7 A). By comparing the microbial communities of both reactors, it is possible to conclude that there was no statistical ($p < 0.05$) difference between the communities as there is no clear separation, neither any clustering between the samples (Figure 4.7 B). This suggests that the microbial communities were phylogenetically similar, and the mixture of phenol, *p*-cresol, and resorcinol can be degraded either by the same microorganism or by phylogenetically closely related microorganisms.

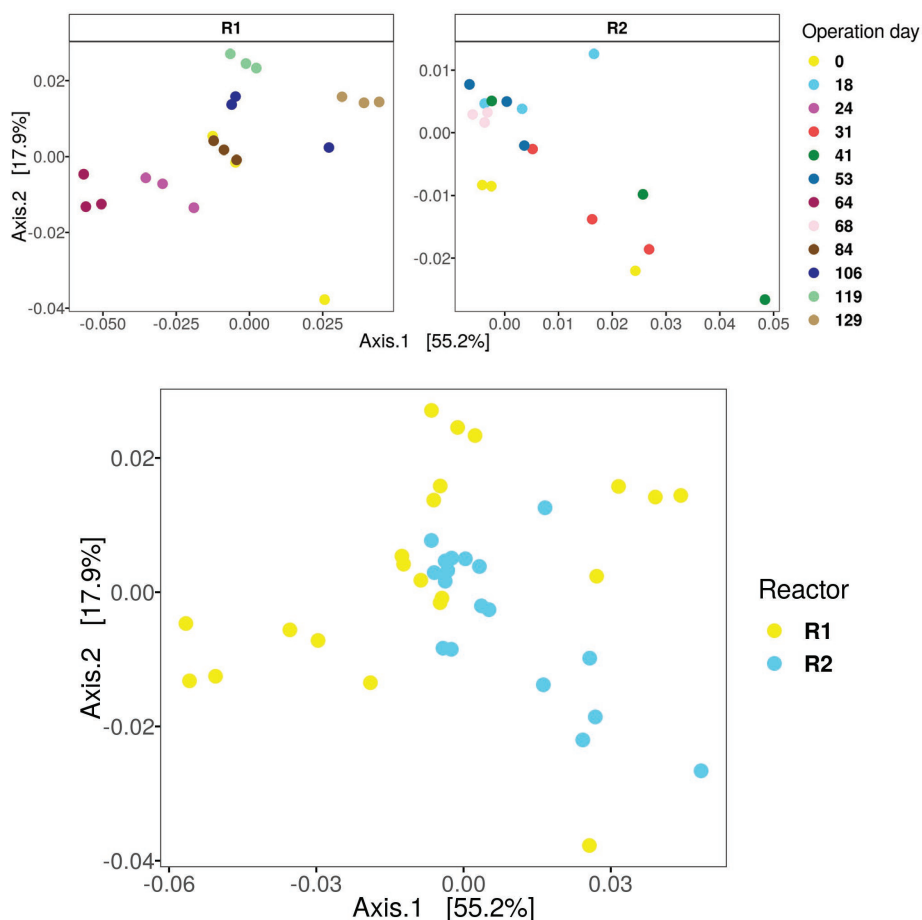


Figure 7. PCoA of the microbial communities from R1 and R2 during the reactor operation (A). PCoA of the combined samples of the reactors (B). Each dot represents a different sample, and community structure, in a specific moment of the operation of R1 (yellow) or R2 (blue).

4.3.3 Thermodynamic state analysis

To theoretically support the observed results obtained during the batch and continuous experiments and to better understand the (bio)chemical reactions of the anaerobic growth on *p*-cresol and resorcinol, a thermodynamic analysis was performed.

4.3.3.1 *p*-Cresol

Degradation of *p*-cresol under strict anaerobic (methanogenic) conditions has been reported elsewhere (Franchi et al., 2018b). Specifically, one microorganism species, *Syntrophorhabdus (aromaticivorans)* has been identified to convert *p*-cresol into acetate in a syntrophic association with a hydrogenotrophic methanogen (Nobu et al., 2015; Qiu, Y.L. et al., 2008). For the anaerobic growth on *p*-cresol, the complete oxidation of *p*-cresol into acetate was considered for the catabolic reaction of (Table 4.4, Eq. 4.1A). For the reduction reaction, the proton (H^+) respiration was considered (Table 4.4 Eq. 4.2B), as this is a common electron acceptor under methanogenic conditions (Kleerebezem and Van Loosdrecht, 2010). For the anabolism, the oxidation reaction was considered to be the conversion of *p*-cresol (degree of reduction $\gamma = 4.86$) into biomass ($C_1 N_{0.2} O_{0.5} H_{1.8}; \gamma = 4.20$) (Kleerebezem and Van Loosdrecht, 2010), whereas the reduction reaction was considered the same as in the catabolism. Table 4.4 presents the values for standard Gibbs free energy change (ΔG_R°) of the reactions and the values corrected for the expected concentrations and temperature ($\Delta G_R^{1,T}$) in the reactor.

4.3.3.2 Resorcinol

For the catabolism, the complete conversion of resorcinol into acetate was considered as the oxidation reaction (Table 4.5, Eq. 4.1B). As the process will occur under methanogenic conditions, H^+ respiration was considered for the reduction reaction (Table 4.5, Eq. 4.2B). For the anabolism, the conversion of resorcinol ($\gamma = 4.33$) into biomass ($\gamma = 4.2$) (Heijnen and Kleerebezem, 2010) was considered as the oxidation reaction, and H^+ respiration as the reduction reaction. Table 4.4 shows the values of ΔG_R° , and $\Delta G_R^{1,T}$ (corrections for reactor conditions).

As can be observed in Tables 4.3 and 4.4, both catabolic oxidation reactions (Eq. 4.1A & 4.1B) are thermodynamically non-favorable under standard conditions ($T = 298\text{ K}$, $P = 1\text{ atm}$, concentrations = 1 M). However, under physiological conditions, correction for temperature, and (expected) concentrations and partial pressures, the $\Delta G_R^{(01,T)}$ becomes more negative.

4.4 Discussion

Our present results clearly show that the degradation of *p*-cresol and resorcinol started without any lag phase using AnMBR phenol-fed biomass that was never

exposed to these compounds (Figure 4.2 A & B). The estimated $r_{s,s}$ showed a high variability in results with maximum values of $44.0 \pm 7.8 \text{ mg}_{\text{p-cresol}} \cdot \text{gVSS}^{-1} \cdot \text{d}^{-1}$ and $26.6 \pm 6.4 \text{ mg}_{\text{resorcinol}} \cdot \text{gVSS}^{-1} \cdot \text{d}^{-1}$ ($\text{ave}_{\text{p-cresol}} = 11.3 \pm 15.8 \text{ mg} \cdot \text{gVSS}^{-1} \cdot \text{d}^{-1}$; $\text{ave}_{\text{resorcinol}} = 8.2 \pm 7.5 \text{ mg} \cdot \text{gVSS}^{-1} \cdot \text{d}^{-1}$) (Table 4.2), in which increasing initial concentrations of the phenolic compounds yield lower $r_{s,s}$ values. Results indicate that substrate inhibition is limiting the conversion rates. For *p*-cresol, the calculated $r_{s,v}$ are higher than those reported in a recent study ($3.7 - 7.8 \text{ mg} \cdot \text{L}^{-1} \cdot \text{d}^{-1}$, $\text{VSS} = 4.0 \text{ g} \cdot \text{L}^{-1}$) (Franchi et al., 2018b). The immediate start of *p*-cresol conversion might be attributed to the fact that phenol and *p*-cresol share the same degradation route via 4-hydroxybenzoyl-CoA (Carmona et al., 2009; Fuchs et al., 2011; Philipp and Schink, 2012), and at least one of the identified species of microorganisms, *Syntrophorhabdus* sp., has been reported to have the capability to degrade both compounds under methanogenic conditions (Qiu, Y.L. et al., 2008). Under anoxic (nitrate-reducing) conditions or sulfate-reducing conditions, phenol is carboxylated in the para-position yielding 4-hydroxybenzoate, whereas *p*-cresol is hydroxylated at the methyl group by an oxygen-independent reaction; in both cases, the benzoyl-CoA is the intermediate from which the subsequent steps in the degradation pathway are shared (Fuchs, 2008; Fuchs et al., 2011).

On the other hand, resorcinol follows a 4-hydroxybenzoyl-CoA independent pathway (Carmona et al., 2009; Fuchs et al., 2011). Resorcinol can be anaerobically degraded either oxidatively or reductively by conversion routes that do not involve benzoyl-CoA (Gibson and Harwood, 2002; Philipp and Schink, 2012). The reduction of resorcinol was found in fermenting *Clostridium* sp., which possesses resorcinol reductase, catalyzing the reduction of resorcinol to 1,3-cyclohexadione. The reduced intermediate is then hydrolytically cleaved to 5-oxocaproic acid that is broken down into acetate and butyrate. The second possible pathway, which is energetically favorable, but thus far only identified for denitrifying bacteria, is an oxidative reaction releasing hydroxyhydroquinone (Carmona et al., 2009; Fuchs et al., 2011). Therefore, its conversion by anaerobic phenol-degrading biomass was not anticipated, implying that the biomass had a wider catabolic diversity than expected. However, and in comparison with phenol and *p*-cresol, resorcinol can be reduced more easily because it carries hydroxyl groups in meta position, which allows tautomerization to the enol form generating an isolated double bond that can act as electron acceptor (Schink et al., 2000).

The anaerobic biomass coming from the phenol-degrading AnMBR under saline conditions showed a higher inhibition on the SMA due to *p*-cresol compared with resorcinol addition (Figure 4.3 A & B). The results obtained during the inhibition tests agree with the observations of Liang and Fang (2010), who attributed the increased

inhibitory effect of *p*-cresol to the higher hydrophobicity of the molecule compared to resorcinol (Liang and Fang, 2010).

The phenol-degrading AnMBR biomass had a 29% lower IC_{50} value for *p*-cresol than the one reported for phenol-adapted granular biomass, but 18% higher than the one from a distillery wastewater (Table 4.3). In the case of resorcinol, the IC_{50} value was 66% higher than the reported value for the granular biomass from the distillery wastewater. However, opposite to the reported studies, the AnMBR biomass used in the present study was not granular but suspended, so more susceptible to toxicants. Besides, the tests were performed under saline conditions, which might add additional stress to the biomass (Wang et al., 2017).

Cell membrane damage related to toxicity can be considered as biocidal inhibition (Batstone et al., 2002). Therefore, the percentage of membrane-damaged cells after the SMA tests was related to whether the decrease in the methanogenic activity was due to toxicity (biocidal inhibition) or to an impairment of the methanogenic function (biostatic inhibition). Our results support the hypothesis that the effect of *p*-cresol on the methanogens is mainly biostatic at low concentrations and toxic, or biocidal, at high concentrations. In contrast, the inhibition by resorcinol is mainly owing to a biostatic inhibition. As well, combining the results from the SMA, FCM, and inhibition tests, it may be possible to conclude that the activity of the *p*-cresol and resorcinol degraders was affected before the methanogenic activity.

The results from R1 showed a rapid adaptation of the biomass to the degradation of the new substrate *p*-cresol, which might be attributed to the shared microbial metabolic pathway during phenol *p*-cresol conversion. On the other hand, full biomass retention likely led to in-situ bio-augmentation of the proper bacteria (Lebiocka et al., 2018). As previously reported, an adapted, abundant, and active methanogenic population is required for the proper degradation of phenol (García Rea et al., 2020), which appeared to be the case for the combined degradation of phenol along with *p*-cresol (R1) (or resorcinol (R2)). The thermodynamic analysis showed that the catabolic conversion of *p*-cresol has a positive ΔG_R° (standard conditions), but becomes negative under the prevailing reactor conditions, mainly because of the neutral pH and the decrease in the concentration of produced intermediates, i.e., hydrogen and acetate. The anabolic metabolism of one mol of *p*-cresol produces 7.13 moles of hydrogen; therefore, and similar to the degradation of phenol, *p*-cresol requires a syntrophic association, meaning that there should be a continuous removal of the (produced) hydrogen by, e.g., hydrogenotrophic methanogens, so both anabolic and catabolic reactions can proceed (Eq. 4.3A & 4.7A). In a recent study, the enhancement of anaerobic phenol

Table 4.4. Stoichiometry and thermodynamic values for the degradation of *p*-cresol under methanogenic conditions. Units of all ΔG_R are in kJ·mol⁻¹

	Reaction	Stoichiometry	ΔG_R°	$\Delta G_R^{1,T}$	Eq. No
<i>p</i> -Cresol Catabolism	Oxidation: <i>p</i> -cresol to acetate	$-C_7H_8O_1-6H_2O+3.5C_2H_3O_2^-+9.5H^++6e^-$	163.1	-275.5	Eq. 4.1A
	Reduction: H ⁺ respiration	$-e^-H^++0.5H_2$	0	27.7	Eq. 4.2A
	Overall catabolic reaction	$-C_7H_8O_1-6H_2O+3.5C_2H_3O_2^-+3H_2+3.5H^+$	163.1	-108.9	Eq. 4.3A
<i>p</i> -Cresol Anabolism	Oxidation: <i>p</i> -cresol to biomass	$-0.14C_7H_8O_1-0.36H_2O-0.2NH_4^++C_1N_{0.2}O_{0.5}H_{1.8}+0.86H^++0.66e^-$	39.0	12.0	Eq. 4.4A
	Reduction: H ⁺ respiration	$-e^-H^++0.5H_2$	0	27.7	Eq. 4.5A
	Overall anabolic reaction	$-0.14C_7H_8O_1-0.36H_2O-0.2NH_4^+-0.08CO_2+C_1N_{0.2}O_{0.5}H_{1.8}+0.33H_2+0.2H^+$	39.0	30.32	Eq. 4.6A
	Metabolism of anaerobic growth on <i>p</i>-cresol	$-2.41C_7H_8O_1-13.96H_2O-0.2NH_4^+-0.08CO_2+C_1N_{0.2}O_{0.5}H_{1.8}+7.94C_2H_3O_2^-+7.13H_2+8.14H^+$	408.7	-216.6	Eq. 4.7A

Table 4.5. Stoichiometry and thermodynamic values for the degradation of resorcinol under methanogenic conditions. Units of all ΔG_R are kJ·mol⁻¹.

	Reaction	Stoichiometry	ΔG_R°	$\Delta G_R^{1,T}$	Eq. No
Resorcinol Catabolism	Oxidation: resorcinol to acetate	$-C_6H_6O_2-4H_2O+3C_2H_3O_2^-+5H^++2e^-$	66.5	-186.4	Eq. 4.1B
	Reduction: H ⁺ respiration	$-e^-H^++0.5H_2$	0	27.7	Eq. 4.2B
	Overall catabolic reaction	$-C_6H_6O_2-4H_2O+3C_2H_3O_2^-+1H_2+3H^+$	66.5	-130.9	Eq. 4.3B
Resorcinol Anabolism	Oxidation: resorcinol to biomass	$-0.17C_6H_6O_2-0.17H_2O-0.2NH_4^++C_1N_{0.2}O_{0.5}H_{1.8}+0.34H^++0.14e^-$	26.9	24.1	Eq. 4.4B
	Reduction: H ⁺ respiration	$-e^-H^++0.5H_2$	0	27.7	Eq. 4.5B
	Overall anabolic reaction	$-0.17C_6H_6O_2-0.17H_2O-0.2NH_4^++C_1N_{0.2}O_{0.5}H_{1.8}+0.07H_2+0.2H^+$	26.9	24.1	Eq. 4.6B
	Metabolism of anaerobic growth on resorcinol	$-1.98C_6H_6O_2-7.43H_2O-0.2NH_4^++C_1N_{0.2}O_{0.5}H_{1.8}+5.45C_2H_3O_2^-+1.89H_2+5.65H^+$	147.7	-199.3	Eq. 4.7B

degradation during the simultaneous conversion with acetate, which correlated with the presence of an abundant acetoclastic methanogenic population was reported by our research group (García Rea et al., 2020). For the combined degradation of phenol and *p*-cresol, the same effect could be expected as 3.3 moles of acetate per mol of *p*-cresol are produced during its anaerobic conversion (Eq. 4.7A). The inhibition of the reactor biomass, and thus the simultaneous decrease in the conversion of the phenolic compounds, confirmed that the same microorganism or microbial group might perform phenol and *p*-cresol degradation.

About R2 and in agreement with the batch tests, it was demonstrated that anaerobic resorcinol degradation occurred without any lag phase, which confirmed the hypothesis of the suspected broader metabolic capacity of the biomass. Even at the beginning of reactor operation, and with a $v_{p\text{-cresol}}$ LR of 30 mg·L⁻¹·d⁻¹, the resorcinol removal efficiency remained about 100%. As previously discussed, this result was not expected; in fact, resorcinol was chosen because of its abundance in GCWW and because it's a substrate with a different degradation pathway than phenol.

Opposite to what was observed for R1, the degradation of resorcinol was not as stable in comparison to *p*-cresol, as the removal efficiency decreased each time a higher $v_{\text{resorcinol}}$ LR was implemented. Nevertheless, even when the resorcinol concentration was as high as 450 mg·L⁻¹ (day 83, Figure 4.6 B), the biomass recovered the resorcinol (and phenol) degradation activity. This is in line with the data gathered in the toxicity analysis (Figure 4.3 D), that showed no lethal (toxic) effects of resorcinol on the biomass, especially at concentrations prevailing in the reactor; therefore, in a case of an acute inhibition by resorcinol, as what happened in R2 operation, it could be expected a rapid recovery of the removal efficiency, mainly because all the biomass is retained inside of the reactor due to the membrane filtration process.

Similar to *p*-cresol degradation, the anaerobic conversion of resorcinol produces hydrogen and acetate. Under standard conditions, the catabolic ($\Delta G_R^\circ = 66.5 \text{ kJ}\cdot\text{mol}^{-1}$) and the metabolic reactions ($\Delta G_R^\circ = 147.0 \text{ kJ}\cdot\text{mol}^{-1}$) are non-spontaneous; however, under the prevailing reactor conditions, the reactions become thermodynamically favorable. Parallel to *p*-cresol conversion, this might be attributed to the effective consumption of intermediate products by (syntrophic) microbial associations of acetoclastic and hydrogenotrophic methanogens (Qiu, Y.-L. et al., 2008; Qiu, Y.L. et al., 2008). Although, it has been reported that resorcinol can be fermented into acetate and malate (Carmona et al., 2009), or butyrate and acetate (Tschech and Schink, 1985), the complete oxidation to acetate in syntrophic cooperation with a hydrogen scavenger in a mixed culture was reported as well (Tschech and Schink, 1985). In this respect, Tschech and Schink,

1985, mentioned that the complete oxidation in acetate and hydrogen might offer energetic advantages. Even though resorcinol fermentation into butyrate and acetate is thermodynamically more advantageous than the complete oxidation into acetate and H_2 , the acetate-producers would be able to participate in the interspecies hydrogen transfer, which would benefit them over the butyrate-forming resorcinol-degraders if the reducing equivalents are indeed effectively transferred (Tschech and Schink, 1985).

Most of the studies on the anaerobic degradation of *p*-cresol and resorcinol were based on granular sludge bed technology, mainly UASB (Table 4.6). In some of these studies, the authors did not report the VSS concentrations in the reactors; therefore, it is not feasible to compare the biomass performance based on the vOLRs. As well, just a couple of studies were performed under saline conditions (Wang et al., 2017; Wu et al., 2020). Wang et al. 2017, working with UASB reactors at a $[Na^+]$ of $10g \cdot L^{-1}$, reported sCR of approx. $16 \text{ mg}_{\text{phenol}} \cdot gVSS^{-1} \cdot d^{-1}$, $15 \text{ mg}_{\text{catechol}} \cdot gVSS^{-1} \cdot d^{-1}$, $8 \text{ mg}_{\text{resorcinol}} \cdot gVSS^{-1} \cdot d^{-1}$, and $7 \text{ mg}_{\text{hydroquinone}} \cdot gVSS^{-1} \cdot d^{-1}$, whereas average values of $54.69.7 \text{ mg}_{\text{phenol}} \cdot gVSS^{-1} \cdot d^{-1}$ for R1 and $95.410.4 \text{ mg}_{\text{phenol}} \cdot gVSS^{-1} \cdot d^{-1}$ for R2, and maximum sCRs of $21 \text{ mg}_{\text{p-cresol}} \cdot gVSS^{-1} \cdot d^{-1}$ and $16 \text{ mg}_{\text{resorcinol}} \cdot gVSS^{-1} \cdot d^{-1}$ were found in the here presented study. Thus, to the best of the authors' knowledge, the results presented in this article are the only results reported for AnMBRs, filled with suspended biomass.

For the microbial community study, the combined results from the reactor performance and the molecular analysis suggested, as reported in the literature, that the degradation of both phenol and *p*-cresol was performed by *Syntrophorhabdus* sp. (Qiu, Y.-L. et al., 2008; Qiu, Y.L. et al., 2008). However, this hypothesis should be further tested because studies based on the 16S rRNA gene give information regarding the presence and not the (metabolic) activities of the microorganisms. Nonetheless, it was clear that *Syntrophorhabdus* sp. was the second and the first most abundant microorganism during the operation of R1 and R2, respectively. For R1, the conversion capacities of phenol and *p*-cresol were lost simultaneously with the increase in organic load to 200 and $260 \text{ mg}_{\text{p-cresol}} \cdot L^{-1} \cdot d^{-1}$, which corresponded with the decrease in the relative abundance of *Syntrophorhabdus* sp. Even though some microorganisms, such as *Syntrophorhabdus* sp., have been identified as phenol degraders (Qiu, Y.-L. et al., 2008; Qiu, Y.L. et al., 2008), the key microorganisms that perform the anaerobic degradation of other phenolic compounds are still uncertain, and the results found in the literature are diverse. *Syntrophus*, and other genera belonging to *Anaerolineaceae*, were the main bacteria found in an upflow anaerobic sludge blanket reactor treating synthetic CGGW containing phenol, catechol, and resorcinol (Wu et al., 2020). Based on their results, the authors indicated that those microorganisms were mainly responsible for the degradation of the phenolic compounds. In other studies, *Syntrophorhabdus*

and *Bacillus* appeared as the responsible microorganism for the hydrolysis of phenol and *p*-cresol in a UASB reactor (Franchi et al., 2018a). Franchi et al. 2018, found that *Syntrophorhabdus*, together with hydrogenotrophic archaea, increased their relative abundance after the degradation of phenol and *p*-cresol, indicating the important role of these microorganisms during the degradation of the mentioned aromatics, which agrees with the here obtained results (Franchi et al., 2018b).

Regarding the third most abundant genera, *Thermovirga* sp. has been reported in UASB reactors (Wang et al., 2017; Wu et al., 2020) and AnMBRs degrading phenol under saline conditions (García Rea et al., 2020; Munoz Sierra et al., 2018). *Thermovirga* sp. is a halotolerant microorganism; however, no phenol degrading activity has been associated with this microorganism yet; instead, it was related to protein and aminoacids fermentation (Dahle and Birkeland, 2006).

Desulfatiglans sp. was the fourth most abundant microorganism during R1 operation. It was found in R2 as well, though in lower abundance. This is a mesophilic and strictly anaerobic microorganism reported to (mainly) use sulfate and other inorganic sulfur compounds as electron acceptors (Rabus et al., 2006; Suzuki et al., 2014). Phenol and

Table 4.6. Reactors treating phenolic compound mixtures

References	Reactor	Temp (°C)	HRT	OLR(gCOD·L ⁻¹ ·d ⁻¹)	Operation time (d)
Latkar and Chakrabarti, 1994	UASB	RT	-	9.51	10
Kennes et al. 1997	UASB	35	0.67 d	<6*	50
Fang and Zhou, 2000	UASB	37	2-24 h	2.2 – 7.4	440
Razo-Flores et al. 2003	UASB	30	0.5–0.6 d	7.0	200
Wang et al. 2017	UASB	35	48 h	2.7	250
Wu et al. 2020	UASB	35	48 h	≈ 2.5-4.1	162
This study	AnMBR	35	6 d	1.63	112
This study	AnMBR	36	6 d	1.44	77

benzoate serve as preferable electron donors (Suzuki et al., 2014). However, according to Jochum et al., *Desulfatiglans* related populations have a versatile metabolic potential (Jochum et al., 2018). They can be sulfate-reducers or conserve energy by acetogenesis or fermentation. Such microorganisms can access a wide range of carbon substrates, including aromatic compounds which are preferred over fatty acids (Jochum et al., 2018). The best growth occurs with benzoate (Suzuki et al., 2014), which is the intermediate product from phenol and *p*-cresol anaerobic degradation, explaining its high relative abundance in R1 and R2.

Because of the additional acetate that was fed in the reactor influent, the high abundance of acetate consuming methanogens, such as *Methanosaeta* sp. was expected. In addition, hydrogenotrophic methanogens, such as *Methanobacterium* sp., *Methanolinea* sp., (reported as halotolerant) (Sakai et al., 2012), and *Methanocalculus* were present; however, they represented only 3 % and 2 % of the all identified methanogens.

For R2, as well as for R1, the results suggest that *Syntrophorhabdus* sp. may also have resorcinol fermentative capacities. This broader substrate diversity would explain the results observed in the batch tests for the degradation of resorcinol (Section 4.3.1). At

Substrate	Influent Concentration	Removal percentage	Additional carbon/ energy source
Resorcinol + catechol + hydroquinone	$50 \text{ mg}_{\text{resorcinol}} \cdot \text{L}^{-1} + 200 \text{ mg}_{\text{catechol}} \cdot \text{L}^{-1} / 50 \text{ mg}_{\text{resorcinol}} \cdot \text{L}^{-1} + 200 \text{ mg}_{\text{hydroquinone}} \cdot \text{L}^{-1}$	95%	
<i>p</i> -Cresol	$650 \text{ mg} \cdot \text{L}^{-1}$	80%	VFA
Phenol + <i>p</i> -cresol	$800 \text{ mg}_{\text{phenol}} \cdot \text{L}^{-1}$ and $300 \text{ mg}_{\text{p-cresol}} \cdot \text{L}^{-1}$	Up to 95% phenol, up to 65% <i>p</i> -cresol, COD 22–98%	Sucrose for startup/No
Phenol + <i>p</i> -cresol + <i>o</i> -cresol	$550 \text{ mg}_{\text{phenol}} \cdot \text{L}^{-1}$, $132 \text{ mg}_{\text{p-cresol}} \cdot \text{L}^{-1}$ and $132 \text{ mg}_{\text{o-cresol}} \cdot \text{L}^{-1}$	> 90 %	Acetate for startup
Phenol, catechol, resorcinol, hydroquinone	$1000 \text{ mg} \cdot \text{L}^{-1}$	80–100%	Acetate
Phenol, catechol, resorcinol, hydroquinone	$1000 \text{ mg} \cdot \text{L}^{-1}$	80–96%	Acetate
<i>p</i>-Cresol and phenol	$1200 \text{ mg}_{\text{p-cresol}} \cdot \text{L}^{-1}$ and $2000 \text{ mg}_{\text{phenol}} \cdot \text{L}^{-1}$	Up to 100%	Acetate
Resorcinol and phenol	$800 \text{ mg}_{\text{resorcinol}} \cdot \text{L}^{-1}$ and $2000 \text{ mg}_{\text{phenol}} \cdot \text{L}^{-1}$	Up to 100%	Acetate

the start of the incubation, degradation was not expected because 1) the biomass was previously not in contact with resorcinol, 2) *Syntrophorhabdus* sp. was not reported as a resorcinol degrader, and 3) phenol and resorcinol are reported to have different conversion pathways when anaerobically degraded (Carmona et al., 2009; Fuchs et al., 2011; Philipp and Schink, 2012). However, it is still unclear why phenol conversion was not affected when the $v_{\text{resorcinol}}$ LR was increased, while resorcinol conversion was (days 85 – 87). As previously mentioned, metabolic hypotheses cannot be verified using solely ribosomal gene analysis, which implies that a functional or metabolic study using an enriched culture should be performed to conclude the hypothesis's validity. As well, and based on the fact that phenol conversion continued after resorcinol degradation was stopped, it may be that resorcinol was converted by another microorganism or group of microorganisms, which were overloaded at the increased $v_{\text{resorcinol}}$ LR. Nevertheless, *Syntrophorhabdus* sp. was the most abundant microorganism during all the stages of reactor operation, and *Thermovirga* sp. has not been reported as a resorcinol degrading microorganism; though, it has been commonly found in AnMBRs degrading phenolic compounds (García Rea et al., 2020). Finally, the PCoA analysis of R1 and R2 (Figure 4.7 B) showed no changes in the microbial community that could be related to a specialization of the biomass towards *p*-cresol or resorcinol degradation. Furthermore, there were no statistical ($p < 0.05$) differences in the comparison of the communities of R2 with the communities of R1, supporting the hypothesis that *Syntrophorhabdus* sp. could play a role as well in the resorcinol degradation.

4.5 Conclusions

Based on the results of this research, the following is concluded:

- The degradation of both *p*-cresol and resorcinol in batch tests was described with a zero-order kinetic model. The maximum values for the specific conversion rates were $44 \pm 8 \text{ mg}_{\text{p-cresol}} \cdot \text{gVSS}^{-1} \cdot \text{d}^{-1}$ and $26 \pm 6.4 \text{ mg}_{\text{resorcinol}} \cdot \text{gVSS}^{-1} \cdot \text{d}^{-1}$. However, increasing bulk concentrations of these phenolic compounds caused a decrease in the conversion rates.
- IC_{50} values for the acetoclastic SMA of $0.73 \text{ g} \cdot \text{L}^{-1}$ for *p*-cresol and $3.00 \text{ g} \cdot \text{L}^{-1}$ for resorcinol were estimated for phenol-degrading biomass and $0.60 \text{ g} \cdot \text{L}^{-1}$ for *p*-cresol and $0.25 \text{ g} \cdot \text{L}^{-1}$ for resorcinol for non-adapted biomass.
- For both phenol-degrading and non-adapted biomass, *p*-cresol caused a higher decrease in the viable cells count than resorcinol.
- For R1, 100% removal efficiency at a $v_{\text{p-cresol}}$ LR of $130 \text{ mg}_{\text{p-cresol}} \cdot \text{L}^{-1} \cdot \text{d}^{-1}$ and an influent concentration of $800 \text{ mg} \cdot \text{L}^{-1}$ was found, corresponding to a $s_{\text{p-cresol}} \text{CR}$ of $22 \text{ mg}_{\text{p-cresol}} \cdot \text{gVSS}^{-1} \cdot \text{d}^{-1}$. For R2, 90% removal efficiency at a $v_{\text{resorcinol}}$ LR of $200 \text{ mg}_{\text{Res}} \cdot \text{L}^{-1} \cdot \text{d}^{-1}$

and an influent concentration of $1200 \text{ mg}_{\text{resorcinol}} \cdot \text{L}^{-1}$ was found, corresponding to a $s_{\text{resorcinol}}$ CR of $16 \text{ mg}_{\text{resorcinol}} \cdot \text{gVSS}^{-1} \text{d}^{-1}$.

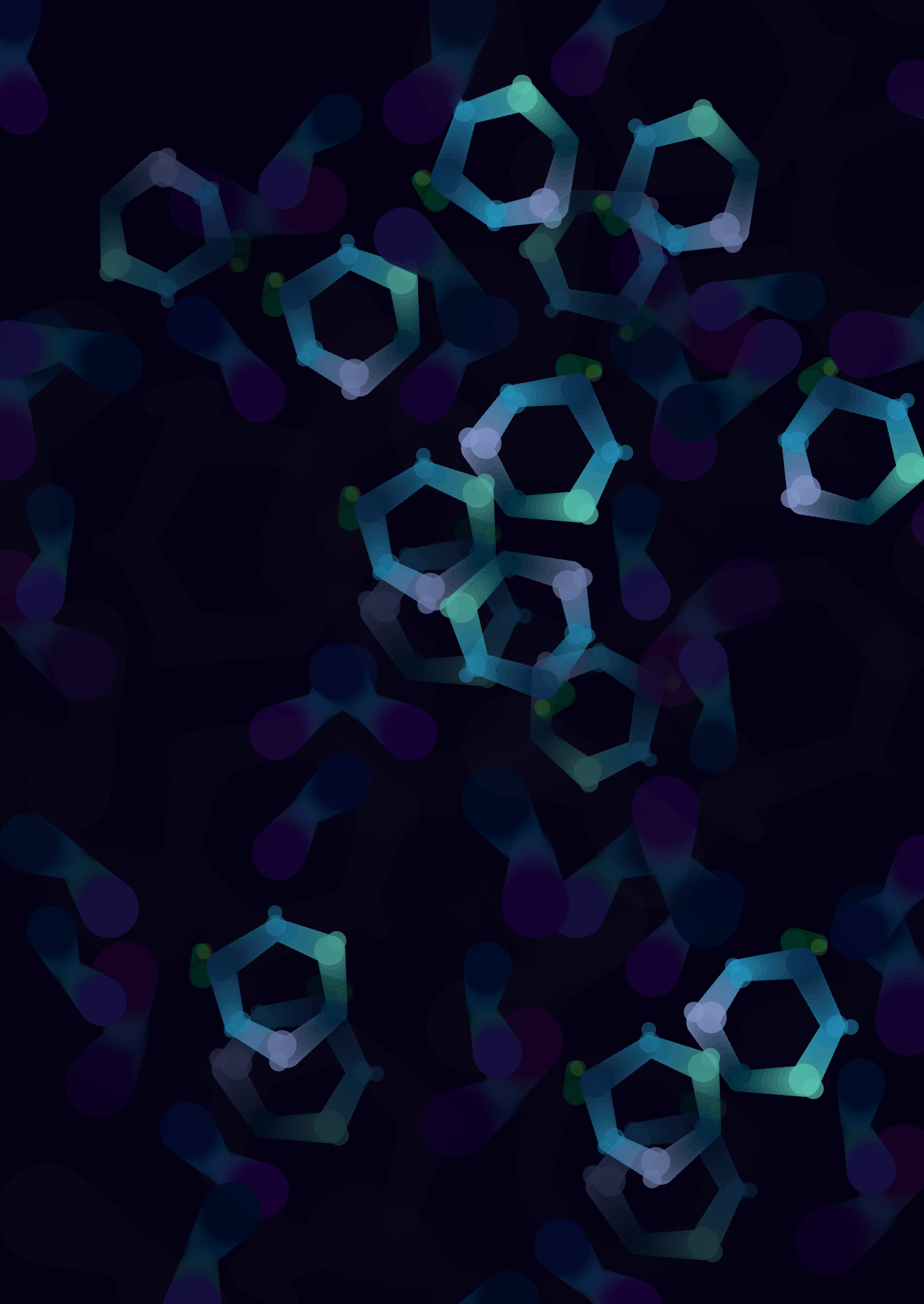
- In both AnMBRs, *Methanosaeta* sp. was the most abundant methanogen, while *Syntrophorhabdus* sp. was the most abundant bacteria, suggesting that *Syntrophorhabdus* sp. was the responsible microorganisms for the degradation of phenol and *p*-cresol. As well, *Syntrophorhabdus* sp. may have a role in resorcinol degradation.
- PCoA analyses showed that the microbial community structures found during the operation of the two reactors had a high phylogenetic similarity.

4.6 References

- Astals, S., Batstone, D.J., Tait, S., Jensen, P.D., 2015. Development and validation of a rapid test for anaerobic inhibition and toxicity. *Water Res.* 81, 208-215. <https://doi.org/https://doi.org/10.1016/j.watres.2015.05.063>.
- Batstone, D.J., Keller, J., Angelidaki, I., Kalyuzhnyi, S.V., Pavlostathis, S.G., Rozzi, A., Sanders, W.T.M., Siegrist, H., Vavilin, V.A., 2002. The IWA Anaerobic Digestion Model No 1 (ADM1). *Water Sci. Technol.* 45(10), 65-73. <https://doi.org/10.2166/wst.2002.0292> %J Water Science and Technology.
- Carmona, M., Zamarro, M.T., Blázquez, B., Durante-Rodríguez, G., Juárez, J.F., Valderrama, J.A., Barragán, M.J., García, J.L., Díaz, E., 2009. Anaerobic catabolism of aromatic compounds: a genetic and genomic view. *Microbiol Mol Biol Rev* 73(1), 71-133. <https://doi.org/10.1128/mmbr.00021-08>.
- Chen, J.L., Ortiz, R., Steele, T.W.J., Stuckey, D.C., 2014. Toxicants inhibiting anaerobic digestion: A review. *Biotechnol. Adv.* 32(8), 1523-1534. <https://doi.org/http://dx.doi.org/10.1016/j.biotechadv.2014.10.005>.
- Dahle, H., Birkeland, N.-K., 2006. *Thermovirga lienii* gen. nov., sp. nov., a novel moderately thermophilic, anaerobic, amino-acid-degrading bacterium isolated from a North Sea oil well. *Int. J. Syst. Evol. Microbiol.* 56(7), 1539-1545. <https://doi.org/https://doi.org/10.1099/ijs.0.63894-0>.
- Falcioni, T., Manti, A., Boi, P., Canonico, B., Balsamo, M., Papa, S., 2006. Comparison of disruption procedures for enumeration of activated sludge floc bacteria by flow cytometry. *Cytom. Part B-Clin. Cytom.* 70(3), 149-153. <https://doi.org/10.1002/cyto.b.20097>.
- Fang, H.H., Zhou, G.-M., 2000. Degradation of phenol and p-cresol in reactors. *Water Sci. Technol.* 42(5-6), 237-244.
- Franchi, O., Bovio, P., Ortega-Martínez, E., Rosenkranz, F., Chamy, R., 2018a. Active and total microbial community dynamics and the role of functional genes *bamA* and *mcrA* during anaerobic digestion of phenol and p-cresol. *Bioresour. Technol.* 264, 290-297. <https://doi.org/https://doi.org/10.1016/j.biortech.2018.05.060>.
- Franchi, O., Rosenkranz, F., Chamy, R., 2018b. Key microbial populations involved in anaerobic degradation of phenol and p-cresol using different inocula. *Electron. J. Biotechnol.* 35, 33-38. <https://doi.org/https://doi.org/10.1016/j.ejbt.2018.08.002>.
- Fuchs, G., 2008. Anaerobic metabolism of aromatic compounds. *Ann. N.Y. Acad. Sci.* 1125(1), 82-99.
- Fuchs, G., Boll, M., Heider, J., 2011. Microbial degradation of aromatic compounds - from one strategy to four. *Nat. Rev. Microbiol.* 9(11), 803-816. <https://doi.org/10.1038/nrmicro2652>.
- García Rea, V.S., Muñoz Sierra, J.D., Fonseca Aponte, L.M., Cerqueda-García, D., Quchani, K.M., Spanjers, H., van Lier, J.B., 2020. Enhancing Phenol Conversion Rates in Saline Anaerobic Membrane Bioreactor Using Acetate and Butyrate as Additional Carbon and Energy Sources. *Front. Microbiol.* 11(2958). <https://doi.org/10.3389/fmicb.2020.604173>.
- Gibson, J., Harwood, C.S., 2002. Metabolic Diversity in Aromatic Compound Utilization by Anaerobic Microbes. *Annu. Rev. Microbiol.* 56(1), 345-369. <https://doi.org/10.1146/annurev.micro.56.012302.160749>.
- Heijnen, J.J., Kleerebezem, R., 2010. Bioenergetics of Microbial Growth, *Encyclopedia of Industrial Biotechnology*. pp. 1-66. <https://doi.org/10.1002/9780470054581.eib084>.
- Hemmelmann, A., Torres, A., Vergara, C., Azocar, L., Jeison, D., 2013. Application of anaerobic membrane bioreactors for the treatment of protein-containing wastewaters under saline conditions. *J. Chem. Technol. Biotechnol.* 88(4), 658-663.
- Hendriks, A.T.W.M., van Lier, J.B., de Kreuk, M.K., 2018. Growth media in anaerobic fermentative processes: The underestimated potential of thermophilic fermentation and anaerobic digestion. *Biotechnol. Adv.* 36(1), 1-13. <https://doi.org/https://doi.org/10.1016/j.biotechadv.2017.08.004>.

- Jeison, D., Kremer, B., van Lier, J.B., 2008. Application of membrane enhanced biomass retention to the anaerobic treatment of acidified wastewaters under extreme saline conditions. *Sep. Purif. Technol.* 64(2), 198-205. <https://doi.org/http://dx.doi.org/10.1016/j.seppur.2008.10.009>.
- Jochum, L.M., Schreiber, L., Marshall, I.P.G., Jørgensen, B.B., Schramm, A., Kjeldsen, K.U., 2018. Single-Cell Genomics Reveals a Diverse Metabolic Potential of Uncultivated Desulfatiglans-Related Deltaproteobacteria Widely Distributed in Marine Sediment. *Front. Microbiol.* 9(2038). <https://doi.org/10.3389/fmicb.2018.02038>.
- Kleerebezem, R., Van Loosdrecht, M.C.M., 2010. A Generalized Method for Thermodynamic State Analysis of Environmental Systems. *Crit. Rev. Environ. Sci. Technol.* 40(1), 1-54. <https://doi.org/10.1080/10643380802000974>.
- Lebiocka, M., Montusiewicz, A., Cydzik-Kwiatkowska, A., 2018. Effect of Bioaugmentation on Biogas Yields and Kinetics in Anaerobic Digestion of Sewage Sludge. *Int J Environ Res Public Health* 15(8). <https://doi.org/10.3390/ijerph15081717>.
- Lee, J., Hwang, S., 2019. Single and combined inhibition of Methanosaeta concilii by ammonia, sodium ion and hydrogen sulfide. *Bioresour. Technol.* 281, 401-411. <https://doi.org/https://doi.org/10.1016/j.biortech.2019.02.106>.
- Li, Y., Tabassum, S., Chu, C., Zhang, Z., 2017. Inhibitory effect of high phenol concentration in treating coal gasification wastewater in anaerobic biofilter. *J. Environ. Sci. (China)*. <https://doi.org/https://doi.org/10.1016/j.jes.2017.06.001>.
- Liang, D., Fang, H.H.P., 2010. Anaerobic Treatment of Phenolic Wastewaters, *Environmental Anaerobic Technology*. pp. 185-205. https://doi.org/10.1142/9781848165434_0009.
- Muñoz Sierra, J.D., Oosterkamp, M.J., Wang, W., Spanjers, H., van Lier, J.B., 2019. Comparative performance of upflow anaerobic sludge blanket reactor and anaerobic membrane bioreactor treating phenolic wastewater: Overcoming high salinity. *Chem. Eng. J.* 366, 480-490. <https://doi.org/https://doi.org/10.1016/j.cej.2019.02.097>.
- Munoz Sierra, J.D., Wang, W., Cerqueda-Garcia, D., Oosterkamp, M.J., Spanjers, H., van Lier, J.B., 2018. Temperature susceptibility of a mesophilic anaerobic membrane bioreactor treating saline phenol-containing wastewater. *Chemosphere* 213, 92-102. <https://doi.org/10.1016/j.chemosphere.2018.09.023>.
- Nescerecka, A., Hammes, F., Juhna, T., 2016. A pipeline for developing and testing staining protocols for flow cytometry, demonstrated with SYBR Green I and propidium iodide viability staining. *Journal of microbiological methods* 131, 172-180. <https://doi.org/10.1016/j.mimet.2016.10.022>.
- Nobu, M.K., Narihiro, T., Hideyuki, T., Qiu, Y.L., Sekiguchi, Y., Woyke, T., Goodwin, L., Davenport, K.W., Kamagata, Y., Liu, W.T., 2015. The genome of Syntrophorhabdus aromaticivorans strain UI provides new insights for syntrophic aromatic compound metabolism and electron flow. *Environ. Microbiol.* 17(12), 4861-4872. <https://doi.org/10.1111/1462-2920.12444>.
- Olguin-Lora, P., Puig-Grajales, L., Razo-Flores, E., 2003. Inhibition of the acetoclastic methanogenic activity by phenol and alkyl phenols. *Environ. Technol.* 24, 999-1006. <https://doi.org/10.1080/09593330309385638>.
- Philipp, B., Schink, B., 2012. Different strategies in anaerobic biodegradation of aromatic compounds: nitrate reducers versus strict anaerobes. *Environ. Microbiol. Rep.* 4(5), 469-478. <https://doi.org/10.1111/j.1758-2229.2011.00304.x>.
- Qiu, Y.-L., Hanada, S., Ohashi, A., Harada, H., Kamagata, Y., Sekiguchi, Y., 2008. Anaerobe Capable of Degrading Phenol to Acetate in Obligate Syntrophic Associations with a Hydrogenotrophic Methanogen. *Appl. Environ. Microbiol.* 74, 2051-2058. <https://doi.org/10.1128/AEM.02378-07>.

- Qiu, Y.L., Hanada, S., Ohashi, A., Harada, H., Kamagata, Y., Sekiguchi, Y., 2008. *Syntrophorhabdus aromaticivorans* gen. nov., sp. nov., the first cultured anaerobe capable of degrading phenol to acetate in obligate syntrophic associations with a hydrogenotrophic methanogen. *Appl. Environ. Microbiol.* 74(7), 2051-2058. <https://doi.org/10.1128/aem.02378-07>.
- Rabus, R., Hansen, T.A., Widdel, F., 2006. Dissimilatory Sulfate- and Sulfur-Reducing Prokaryotes, in: Dworkin, M., Falkow, S., Rosenberg, E., Schleifer, K.-H., Stackebrandt, E. (Eds.), *The Prokaryotes: Volume 2: Ecophysiology and Biochemistry*. Springer New York, New York, NY, pp. 659-768. https://doi.org/10.1007/O-387-30742-7_22.
- Razo-Flores, E.I.a., Iniestra-González, M., Field, J.A., Olguín-Lora, P., Puig-Grajales, L., 2003. Biodegradation of mixtures of phenolic compounds in an upward-flow anaerobic sludge blanket reactor. *J. Environ. Eng. (N. Y.)* 129(11), 999-1006.
- Sakai, S., Ehara, M., Tseng, I.C., Yamaguchi, T., Bräuer, S.L., Cadillo-Quiroz, H., Zinder, S.H., Imachi, H., 2012. *Methanolinea mesophila* sp. nov., a hydrogenotrophic methanogen isolated from rice field soil, and proposal of the archaeal family *Methanoregulaceae* fam. nov. within the order *Methanomicrobiales*. *International journal of systematic and evolutionary microbiology* 62(Pt 6), 1389-1395. <https://doi.org/10.1099/ijs.o.035048-0>.
- Schink, B., Philipp, B., Muller, J., 2000. Anaerobic degradation of phenolic compounds. *Naturwissenschaften* 87(1), 12-23. <https://doi.org/https://doi.org/10.1007/s001140050002>.
- Sierra-Alvarez, R., Lettinga, G., 1991. The effect of aromatic structure on the inhibition of acetoclastic methanogenesis in granular sludge. *Appl. Microbiol. Biotechnol.* 34(4), 544-550. <https://doi.org/10.1007/BF00180586>.
- Spanjers, H., Vanrolleghem, P.A., 2016. Respirometry, in: Brdjanovic, D., Nielsen, P.H., López-Vazquez, C.M., van Loosdrecht, M.C.M. (Eds.), *Experimental Methods in Wastewater Treatment*. IWA Publishing. <https://doi.org/https://doi.org/10.2166/9781780404752>.
- Suzuki, D., Li, Z., Cui, X., Zhang, C., Katayama, A., 2014. Reclassification of *Desulfobacterium anilini* as *Desulfatiglans anilini* comb. nov. within *Desulfatiglans* gen. nov., and description of a 4-chlorophenol-degrading sulfate-reducing bacterium, *Desulfatiglans parachlorophenolica* sp. nov. *Int. J. Syst. Evol. Microbiol.* 64(Pt_9), 3081-3086. <https://doi.org/https://doi.org/10.1099/ijs.o.064360-0>.
- Tschech, A., Schink, B., 1985. Fermentative degradation of resorcinol and resorcylic acids. *Arch. Microbiol.* 143(1), 52-59.
- Veeresh, G.S., Kumar, P., Mehrotra, I., 2005. Treatment of phenol and cresols in upflow anaerobic sludge blanket (UASB) process: a review. *Water Res.* 39(1), 154-170. <https://doi.org/http://dx.doi.org/10.1016/j.watres.2004.07.028>.
- Wang, W., Wu, B., Pan, S., Yang, K., Hu, Z., Yuan, S., 2017. Performance robustness of the UASB reactors treating saline phenolic wastewater and analysis of microbial community structure. *J. Hazard. Mater.* 331, 21-27. <https://doi.org/https://doi.org/10.1016/j.jhazmat.2017.02.025>.
- Wu, B., Wang, J., Hu, Z., Yuan, S., Wang, W., 2020. Anaerobic biotransformation and potential impact of quinoline in an anaerobic methanogenic reactor treating synthetic coal gasification wastewater and response of microbial community. *J. Hazard. Mater.* 384, 121404. <https://doi.org/10.1016/j.jhazmat.2019.121404>



Chapter 5

Chemical characterization and anaerobic treatment of bitumen fume condensate using a membrane bioreactor

This chapter is an adapted version of: Garcia Rea Victor S., Egerland Bueno B., Muñoz Sierra Julian D., Nair Athira, Lopez Prieto Israel J., Cerqueda-Garcia Daniel, van Lier Jules B., Spanjers Henri. (2023). Chemical characterization and anaerobic treatment of bitumen fume condensate using a membrane bioreactor. J. Hazard. Mater., 477. DOI: <https://doi.org/10.1016/j.jhazmat.2022.130709>

Abstract

Bitumen fume condensate (BFC) is a hazardous wastewater generated at asphalt reclamation and production sites. BFC contains a wide variety of potentially toxic organic pollutants that negatively affect anaerobic processes. In this study, we chemically characterized BFC produced at an industrial site and evaluated its degradation under anaerobic conditions. Analyses identified about 900 compounds including acetate, polycyclic aromatic hydrocarbons, phenolic compounds, and metal ions. We estimated the half maximal inhibitory concentrations (IC_{50}) of methanogenesis of 120, 224, and 990 mgCOD·L⁻¹ for three types of anaerobic biomass, which indicated the enrichment and adaptation potentials of methanogenic biomass to the wastewater constituents. We operated an AnMBR (7.0 L, 35 °C) for 188 days with a mixture of BFC, phenol, acetate, and nutrients. The reactor showed a maximum average COD removal efficiency of 87.7 ± 7.0 %, that corresponded to an organic conversion rate of 286 ± 71 mgCOD⁻¹·L⁻¹·d⁻¹. The microbial characterization of the reactor's biomass showed the acetoclastic methanogen *Methanosaeta* as the most abundant microorganism (43 %), whereas the aromatic and phenol degrader *Syntrophorhabdus* was continuously present with abundances up to 11.5%. The obtained results offer the possibility for the application of AnMBRs for the treatment of BFC or other petrochemical wastewater.

5.1 Introduction

The application of AD for the treatment of (petro)chemical wastewater has gradually expanded since the installation of the first high-rate AD plant for the depuration of wastewater containing purified terephthalic acid (PTA) in 1989 (Macarie, 2000). Further research is nevertheless required to broaden the AD application potentials as a result of the current increase in production and discharge of (petro)chemical wastewater (Ji et al., 2016; Tian et al., 2020).

Phenol and phenolics, benzoate, and PTA, are aromatic compounds considered common petrochemical pollutants that are treated under anaerobic conditions (Garcia Rea et al., 2022; Kleerebezem et al., 2005; Macarie, 2000). The treatment of more complex wastewater has, however, received limited scholarly attention (Bhattacharyya et al., 2013). Few studies have applied AD for the degradation of non-synthetic industrial petrochemical wastewater (Garcia-Mancha et al., 2012; Jafarzadeh et al., 2012; Noyola et al., 2000; Stergar et al., 2003). This is especially apparent in the case of petrochemical wastewater from the asphalt and road industry, for example, during the production of reclaimed asphalt pavement (RAP).

The RAP is generated when old asphalt layers or pavement materials are removed, milled, and reused to produce new pavement. In this process, the old asphalt is heated and mixed with new materials such as stones, sand, and bitumen. Such a process releases fumes mainly originated from the bitumen (Binet et al., 2002; Roy et al., 2007). Once the fumes are condensed, the condensate is rich in paraffinic, naphthenic, aromatic (phenol and other phenolics), polycyclic aromatic hydrocarbons (PAH) (Binet et al., 2002; Roy et al., 2007), and volatile organic compounds (VOC) (Boczkaj et al., 2017).

Several compounds that could be toxic or inhibitory to anaerobic microorganisms have been reported in the bitumen fume condensates (BFC). Among them, the major pollutants reported are naphthalene, acenaphthene, fluorene, phenanthrene, pyrene, benzo[a]pyrene, and anthracene (Table 1) (Binet et al., 2002; Boczkaj et al., 2017; Roy et al., 2007). Remarkably, some of these compounds have been biodegraded under anaerobic conditions (Carmona et al., 2009).

The anaerobic conversion of BTEX (benzene, toluene, ethylbenzene, and xylene), naphthalene, methylnaphthalene, and phenanthrene has been reported (Carmona et al., 2009). No biodegradation studies have, however, been conducted for most of the compounds present in the BFC. Similarly, their toxic and inhibitory effects on anaerobic biomass are unknown. Hence, it is uncertain whether the treatment of this type of wastewater is feasible under anaerobic conditions, or if the BFC wastewater

constituents could negatively affect the operation of anaerobic reactors, for example, by the display of toxic or inhibitory effects on the methanogenic biomass.

This study characterized the BFC produced from RAP, assessed its negative effects on methanogenic biomass, and determined its biodegradation potential when an AnMBR was used. We analyzed the BFC through targeted and non-targeted screening techniques such as gas chromatography and mass spectrometry. Similarly, we determined the BFC's potential inhibitory or toxic effects on three types of anaerobic biomass sources. We operated and evaluated the performance of an AnMBR which treated BFC wastewater amended with phenol, acetate, and nutrients. Lastly, we studied the microbial community dynamics in the AnMBR's biomass during the different operational stages.

5.2 Materials and Methods

5.2.1 *Chemical oxygen demand and volatile suspended solids*

The COD was measured using COD determination kits (Lange Hach COD cuvette test LCK314 and LCK514) and was assessed spectrophotometrically using a Lange Hach DR3900 spectrophotometer. Volatile suspended solids (VSS) concentration was measured following Standard Methods (Rand et al., 1976).

Ethanol, propanol, butanol, cyclohexanol, cyclohexanone, phenol, *p*-cresol, volatile fatty acids (VFA) (acetic, propionic, isobutyric, butyric, isovaleric, valeric, isocaproic, and hexanoic acids), and benzoate concentrations were measured in a gas chromatographer coupled to a flame ionization detector (GC-FID). The machine used was a GC Agilent 7890A chromatograph (Agilent, USA) equipped with an Agilent 19091F-112 column of 25 m x 320 μm x 0.5 μm . Helium was used as carrier gas with a flow rate of 2.46 mL $\cdot\text{min}^{-1}$. The GC oven temperature was programmed to be 80 °C for 1 min; then it was increased to 120 °C and finally to 180 °C in 4.5 min. The run time was set to 25 min. The temperature of the detector was set at 240 °C. The phenol concentration was double-checked spectrophotometrically (DR 3900 Hach) using Merck – Spectroquant® Phenol cell tests (Merck, Germany).

5.2.2 *Characterization of the organic compounds in the BFC*

BFC from a road and asphalt industry (Royal BAM, The Netherlands) was continuously withdrawn from an industrial plant (Bergen op Zoom, The Netherlands) for 180 days. A short description of the bitumen fume condensate generation method is provided in Appendix A.4, Section A.4.1. Analytical techniques were applied to characterize the composition of the BFC. These included gas chromatography-tandem mass spectrometry (GC-MS/MS), gas chromatography-mass spectrometry quadrupole time

of flight (GC/MS-QTOF), and inductively coupled plasma mass spectrometry (ICP-MS). A volatilization test was performed to verify the possible volatilization of the compounds present in the BFC (Appendix A.4, Section A.4.2).


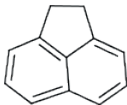

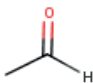

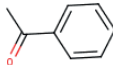

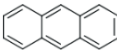
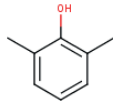
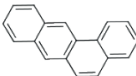
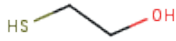
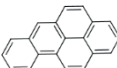
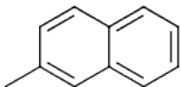
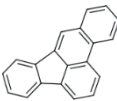
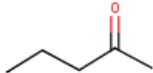
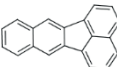
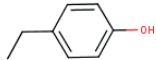
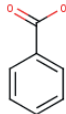
5.2.2.1 Targeted analysis: gas chromatography-tandem mass spectrometry

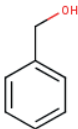
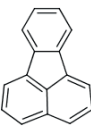
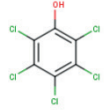
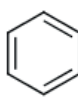
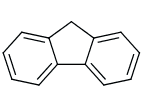
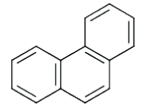
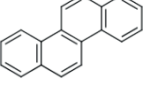
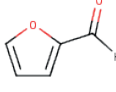
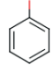
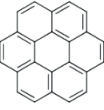
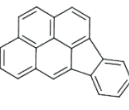
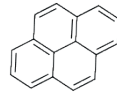
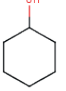
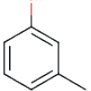
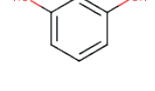

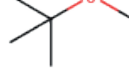
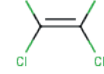
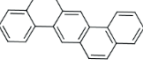
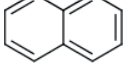
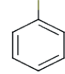
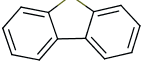
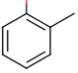
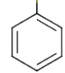
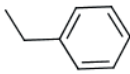
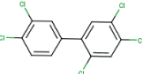
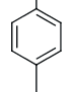
A targeted (68 compounds) GC-MS/MS analysis was performed by Het Waterlaboratorium (Haarlem, The Netherlands) using a Thermo Scientific TSQ 8000 triple quadrupole GC-MS/MS equipment with a high-volume programmable temperature vaporizing injector (Thermo Scientific, Massachusetts, USA). The column used was a Rxi-5-Sil-MS (fused silica) capillary column (Restek, Pennsylvania, USA) with a size of 25 m x 0.32 mm. Samples were prepared by filtering 10 mL of the BFC [1.12 gCOD·L⁻¹] through a 0.45 µm filter (Spartan, Whatman). The organic components of the BFC were then extracted using an in-vial extraction with pentane as the organic phase. For the injection, the inlet had a temperature of 40 °C and had a split flow of 40 mL·min⁻¹. The program method utilized a carrier flow of 2.0 mL·min⁻¹. The oven temperature program was as follows: initial temperature 60 °C held for 5 min, then ramped with a rate of 10 °C·min⁻¹ to 150 °C. Afterward, a second ramp was performed with a rate of 15 °C·min⁻¹ until a temperature of 300 °C was reached and subsequently held for 14 min. The quantification of the different compounds was performed in the single reaction monitoring mode and identified according to the Dutch standard NTA 8379:2014 en: Water quality – Guidelines for the identification of target compounds by gas and liquid chromatography and mass spectrometry.

5.2.2.2 Non-targeted analysis: gas chromatography-mass spectrometry quadrupole time of flight

A full scan analysis in electronic impact and positive chemical ionization mode was conducted using a GC/MS-QTOF on an Agilent 7200 Accurate mass GC/MS-QTOF. The column used was a DB-5 30 m x 0.25 mm x 0.25 µm (capillary column). The program method utilized a column flow of 1.2 mL·min⁻¹ with an oven temperature program as follows: initial temperature 40 °C held for 5 min, then ramped with 10 °C·min⁻¹ to 300 °C and held for 5 min. The inlet temperature was 250 °C and the transfer line temperature was 280 °C. Liquid-liquid extraction was used to extract volatile organic compounds. The procedure was as follows: 100 mL of BFC sample were added into a 125 mL separation funnel. Then 5 mL of methylene chloride were added and shaken for about 3 minutes. Methylene chloride was collected into conical extraction vials. This procedure was repeated twice to obtain approximately 15 mL of the organic phase. Extractions were dried through 1 g of sodium sulfate set on glass Pasteur pipets. After that, extractions were re-concentrated through nitrogen evaporation at a flow rate of

Table 1. Major pollutants reported in BFC condensate.

1-Butanol		Acenaphthene		Benzyl alcohol
1-Decanethiol		Acetaldehyde		Benzene
1-Heptanol		Acetophenone		Chrysene
1-Hexanol		Anthracene		Coronene
2,6-Dimethylphenol		Benzo[a]anthracene		Cyclohexanol
2-Mercaptoethanol		Benzo[a]pyrene		Cyclohexanone
2-Methylnaphthalene		Benzo[b]fluoranthene		Dibenz[a,h]-anthracene
2-Pentanone		Benzo[k]fluoranthene		Dibenzothiophene
4-Ethylphenol		Benzoate		Ethylbenzene

	Fluoranthene		Phenanthrene	
	Fluorene		Phenanthrene	
	Furfural		Phenol	
	Indenol[1,2,3-c,d] Pyrene		Pyrene	
	m-Cresol		Resorcinol	
	MTBE		Tetrachloro-ethylene	
	Naphthalene		Thioanisole	
	o-Cresol		Thiophenol	
	Pentachloro-biphenyl		Para-xylene	

0.8 mL·min⁻¹. The final volume was approximately 2 mL. Before injection, extractions were stored for 24 h at -20°C in 2 mL amber glass vials.

Mass Hunter unknown analysis version B.08.00 was used for identifying unknown compounds. The mass spectral similarity search was performed by using NIST MS search 2.0 (NIST/EPA/NIH Mass Spectral Library, NIST 08, National Institute of Standards and Technology, 2008, Gaithersburg, MD).

5.2.3 *Elemental analysis by inductively coupled plasma mass spectrometry*

Various elements and their concentrations were analyzed in six samples of BFC, two of feeding solution, and two of AnMBR permeate using ICP-MS. Before the analysis was performed, the samples were acidified (1% v/v) with HNO₃ (69%). Proper dilutions were prepared to keep the concentration of the analytes below 5 mg·L⁻¹. An ICP-MS model PlasmaQuant MS (Analytik Jena, Germany) was used for the analysis. 10 mL samples were injected into the equipment. Argon flow was 0.9 L·min⁻¹ and nebulizer flow was 1.1 L·min⁻¹.

5.2.4 *Precipitation of the metals in the BFC*

Per each L of BFC (pH = 3) 30.5 mL of phosphate solution A and 19.5 mL of phosphate solution B were added (pH = 7.4). The composition of the solutions is reported in (García Rea et al., 2020). The precipitate was separated from the solution by centrifugation (14 min, 10000 g) and the supernatant was filtered through a glass-fiber filter of 0.7 µm. Metals were measured in the BFC, in the filtrate, and reactor's permeate as specified in Section 5.2.4.

5.2.5 *Effect of the BFC on the specific methanogenic activity and cell membrane integrity of anaerobic biomass*

5.2.5.1 *Specific methanogenic activity inhibition*

Batch tests with various BFC concentrations (Table 2) were performed in 250 mL Schott (Schott Germany) glass bottles using three distinct inocula: a) phenol-degrading AnMBR-cultivated suspended biomass (García Rea et al., 2020), b) granular biomass from a UASB treating petrochemical wastewater (Shell Moerdijk, The Netherlands), and c) anaerobic suspended biomass coming from a municipal wastewater treatment plant (MWWTP) (Harnaspolder, The Netherlands). Enough biomass inoculum was taken to have a final reactor volume of 200 mL, the VSS concentration in the reactor was 4 g·L⁻¹. Acetate at a concentration of 2 gCOD·L⁻¹ was used as substrate. Per each gram of COD, 0.3 mL of micronutrients and 3 mL of macronutrients solution were added (Hendriks et al., 2018). The composition of the solutions is reported in (García Rea et al., 2020).

The reactors were incubated at 130 rpm under mesophilic conditions (35 °C) in a temperature-controlled rotary shaker (New Brunswick Scientific, Innova 44). Methane production was measured online using an AMPTS II system (Bioprocess Control, Sweden). Each experimental condition was performed in triplicates. The specific methanogenic activity (SMA) value was calculated according to (Spanjers and Vanrolleghem, 2016). For the estimation of the half-maximum inhibitory concentration (IC_{50}) of the BFC on the SMA, a four-parameter logistic model was fit to the data using Sigma Plot software 12 (Lee and Hwang, 2019).

Table 2. BFC concentration used for the SMA/cell membrane integrity batch tests.

Inoculum	Bitumen fume condensate concentration [mgCOD·L ⁻¹]
Municipal WTPP	0, 75, 135, 250.
Petrochemical WTPP	0, 75, 125, 250, 500, 750, 1000.
AnMBR-cultivated	0, 75, 125, 250, 500, 750, 1000.

5.2.5.2 Cell membrane integrity determination

The cell membrane integrity of the anaerobic biomass used for the SMA assays was measured by flow cytometry (FCM) before and after the exposure to the various concentrations of BFC (Section 5.2.6.1). Approximately, 1 mL sample of inoculum and medium were taken before the start of the SMA test and after the experiments were finished. The samples were diluted with PBS 1:500 (0.22 µm-filtered) (Falcioni et al., 2006) and prepared and measured as reported by (Garcia Rea et al., 2022).

5.2.6 AnMBR operation

5.2.6.1 AnMBR setup

An AnMBR was operated for 188 days. The setup comprised a fully-automatized 7 L AnMBR with a working volume of 5 L (Figure 5.1). The reactor was coupled to an ultrafiltration PVDF membrane (Pentair, The Netherlands) with a nominal pore size of 30 nm. The reactor volume was controlled using two pressure sensors (AE Sensors, The Netherlands). The sensor located at the bottom of the reactor, measured the hydrostatic and gas pressures and had a range of 0-70 mbar. The sensor located at the top was used for the gas pressure measurement and measured a range of 0-20 mbar. The temperature was kept constant at 35 °C with a water bath (Tamson Instruments, The Netherlands) that recirculated water through the reactor double-jacketed wall. To improve the mixing in the reactor, the biogas produced was recirculated in the reactor using a gas pump (KNF, The Netherlands). Total biogas production was measured by a gas meter (Ritter, Germany).

Anaerobic granular biomass from a UASB reactor treating petrochemical wastewater (Shell Moerdijk, The Netherlands) was used as seed biomass. The initial VSS concentration was $6 \text{ g}\cdot\text{L}^{-1}$.

5.2.6.2 AnMBR feeding medium and operational conditions

Table 3 shows the composition of the feeding medium of the AnMBR within the different stages of the reactor operation. Micro- & macronutrient and phosphate buffer solutions were added to the feeding medium as stated in Section 5.2.6.1. Based on (Hendriks et al., 2018) and (Garcia Rea et al., 2022), 50 mg of yeast extract were added per gram of COD in the feeding medium. The corresponding organic loading rates (OLR) and hydraulic retention time (HRT) are also shown.

5.2.7 Microbial community dynamics

5.2.7.1 Biomass sampling, DNA extraction, 16S rRNA gene amplification, and DNA data processing

Approximately, 1 mL samples were taken from each of the three biomass sources used for the batch assays before the tests were started (Section 5.2.6.1). Similarly, 0.5 to 1.0 mL of biomass samples were taken from the reactor during several days of reactor operation. All the samples were processed and stored as reported in (García Rea et al., 2020). The DNA was extracted with DNeasy UltraClean Microbial Kit (Qiagen, Germany). The DNA quantity and quality were checked using the Qubit 3.0 DNA detection system (Qubit dsDNA HS assay kit, Life Technologies, United States). The amplification of the V3-V4 hypervariable regions of the 16S rRNA gene was conducted by Novogene as reported in (García Rea et al., 2020). The sequences were deposited in the SRA (NCBI) database under the accession number PRJNA748451.

Table 3. AnMBR feeding medium composition and operational conditions

Stage	Day	BFC [gCOD·L ⁻¹]	Acetate [gCOD·L ⁻¹]	Phenol [gCOD·L ⁻¹]	OLR* [gCOD·L ⁻¹ ·d ⁻¹]	HRT [d]
A	0-30	1.2	0.5	1.2	0.82 ± 0.19	2.9 ± 0.7
B	31-57	$1.2 - 0.4$	0.5	1.2	0.59 ± 0.23	3.7 ± 1.2
C	58-165	$0.4 - 0.2$	0.5	0.5	0.33 ± 0.09	4.1 ± 1.0
D	166-172	0.3	0.5	0.2	0.29 ± 0.07	3.7 ± 0.4
E	173-188	0.3	0.25	0	0.31 ± 0.06	2.1 ± 0.7

*The OLR and the HRT are reported with \pm standard deviation (SD).

The bioinformatics for the analysis of the 16S rRNA gene sequences was performed as reported in (García Rea et al., 2020). The QIIME2 pipeline (Bolyen et al., 2019) and the R environment with the phyloseq library were employed to perform the statistical

analysis. A principal coordinate analysis (PCoA) for the three biomass sources used for the batch assays (Section 5.2.6) was conducted using R and applying the weighted UniFrac distance matrix. An association analysis with the MaAsLin2 (Microbiome Multivariable Associations with Linear Models) approach was performed in R using the MaAsLin 2 package (Mallick et al., 2021). The relative abundance of genus over 1% and 25% in relative abundance and prevalence, respectively, were correlated with the COD removal efficiency of the reactor during the different reactor operation stages. The associations with a corrected p-value < 0.05 were considered significant.

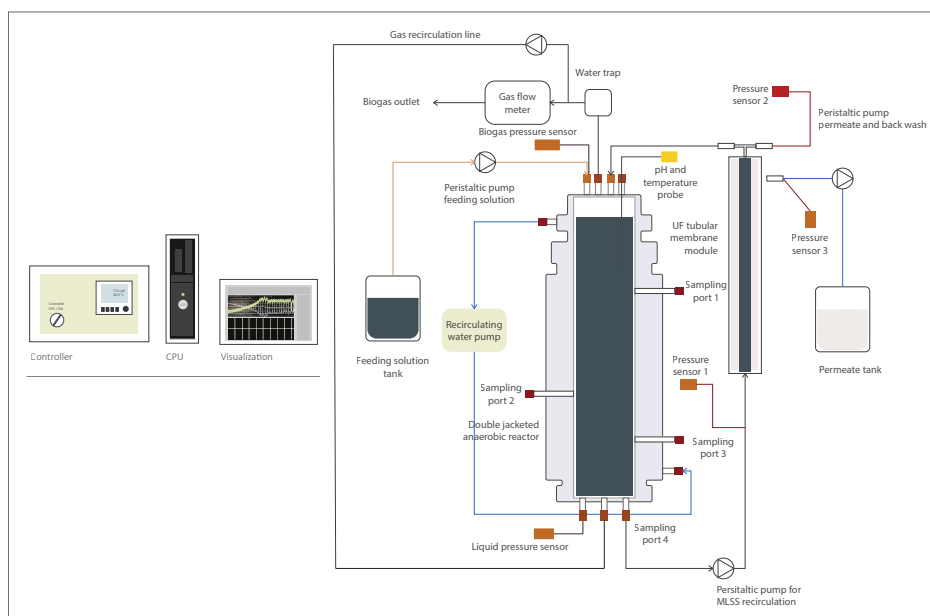


Figure 5.1. Scheme of the AnMBR setup used during the continuous experiment.

5.3 Results and Discussion

5.3.1 Bitumen fume condensate characterization

5.3.1.1 COD

The COD in the different samples was measured for an initial characterization of BFC. The COD showed a range from 0.24 to 1.20 gCOD·L⁻¹ (average: 0.58 gCOD·L⁻¹ ± 0.39, n = 33), most likely because the BFC collection method at the industrial site was not standardized (Appendix A.4, Section A.4.1). (Boczkaj et al., 2017) reported COD concentrations between 18 and 22 g·L⁻¹ in post oxidative effluents from a bitumen production plant; however, to the best of the authors' knowledge, there are no reports on COD values of BFC. The COD-BFC could cause toxic or inhibitory effects on the anaerobic biomass because of the nature of its pollutants, even when such COD

concentration is low in comparison to other industrial effluents (e.g. food industry) (Macarie, 2000; Mutamim et al., 2013).

5.3.1.2 Phenol and volatile fatty acids

Based on the GC-FID analysis, acetic acid at a concentration of $13 \text{ mg}\cdot\text{L}^{-1}$ ($13.9 \text{ mgCOD}\cdot\text{L}^{-1}$) and phenol at a concentration of $8.3 \text{ mg}\cdot\text{L}^{-1}$ ($19.7 \text{ mgCOD}\cdot\text{L}^{-1}$) were found in a BFC sample of $500 \text{ mgCOD}\cdot\text{L}^{-1}$. Phenol and VFA can be found as pollutants in petrochemical wastewater (Ji et al., 2016; Singer et al., 1978) and can be used as carbon and energy sources by anaerobic microorganisms. Other VFAs were not detected by the GC-FID; nor were compounds such as ethanol, propanol, butanol, cyclohexanol, cyclohexanone, *p*-cresol, or benzoate.

5.3.1.3 Organic compounds targeted analysis: GC-MS/MS

The GC-MS/MS targeted analysis showed different concentrations of aromatic hydrocarbon compounds such as naphthalene [$0.70 \text{ }\mu\text{g}\cdot\text{L}^{-1}$], acenaphthylene [$0.27 \text{ }\mu\text{g}\cdot\text{L}^{-1}$], propyzamide [$0.18 \text{ }\mu\text{g}\cdot\text{L}^{-1}$], *p,p*-DDT [$0.07 \text{ }\mu\text{g}\cdot\text{L}^{-1}$], fluorene [$0.04 \text{ }\mu\text{g}\cdot\text{L}^{-1}$], phenanthrene [$0.04 \text{ }\mu\text{g}\cdot\text{L}^{-1}$], acenaphthene [$0.03 \text{ }\mu\text{g}\cdot\text{L}^{-1}$], and fluoranthene [$0.02 \text{ }\mu\text{g}\cdot\text{L}^{-1}$]. Table A.4.1 (Appendix A.4, Section A.4.3) shows the list of the 67 analyzed commonly reported organic compounds in BFC and their concentrations. The aromatic compounds and PAH determined in the analysis agree with what is reported in the literature (Binet et al., 2002; Boczkaj et al., 2017; Roy et al., 2007).

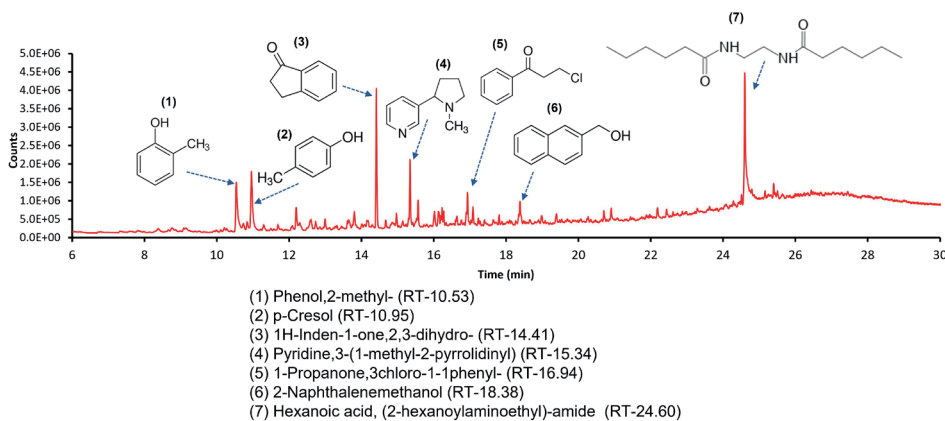


Figure 5.2. GC-MS/QTOF chromatogram of the bitumen fume condensate with the proposed molecular structures and names corresponding to the major peaks found. The most common names for the next compounds are provided in brackets: phenol, 2-methyl (*o*-cresol), 1H-inden-1-one, 2,3-dihydro (1-indanone), pyridine, 3-(1-methyl-2-pyrrolidinyl) (nicotine), and 1-propanone, 3-chloro-1-phenyl (β -chloropropiophenone).

5.3.1.4 Organic compound non-targeted analysis: GC-MS QTOF

The GC-MS QTOF analysis detected several peaks corresponding to compounds such as p-cresol, o-cresol (phenol, 2-methyl), and 2-naphthalene methanol when the unknown organic compounds in BFC were analyzed. Similarly, the compounds 1-indanone (1H-inden-1-one, 2,3-dihydro) and hexanoic acid (2-hexanoylaminoethyl)-amide exhibited high peak areas. We proposed the structures of these compounds based on their accurate mass obtained from the matching NIST data library. Figure 5.2 shows the chromatogram of the BFC where the compounds with larger peak areas are depicted. A full scan detected 933 compounds, but only 430 matched the NIST's database. Compounds shown in Table A.4.2 (Appendix A.4, Section A.4.4) are tentative compounds that corresponded to an 80% of chemical structure match with those found in the library. Surrogate organic parameters analyses (Appendix A.4, Section A.4.5) confirmed the high content of aromatic compounds.

5.3.1.5 Elemental analysis by inductively coupled plasma mass spectrometry

Our results showed the presence of 20 elements (metals and several non-metals) in the BFC, the reactor's feeding, and permeate (Figure 5.3 A & B). The highest concentrations corresponded to iron [$310.9 \pm 129.8 \text{ mg}\cdot\text{L}^{-1}$], sulfur [$299.0 \pm 135.3 \text{ mg}\cdot\text{L}^{-1}$], silicon [$153.2 \pm 2.6 \text{ mg}\cdot\text{L}^{-1}$], calcium [$85.9 \pm 27.2 \text{ mg}\cdot\text{L}^{-1}$], and sodium [$69.8 \pm 1.4 \text{ mg}\cdot\text{L}^{-1}$]. Due to the nature of the BFC, the presence of metals was not expected. However, the presence of the ions may be related to the leaching of these metals from the chimney and piping systems as the BFC was acidic ($\text{pH} = 3$). A precipitation was performed by increasing the pH of the BFC. The precipitate was then separated by filtration over a $0.45 \mu\text{m}$ membrane filter. The precipitation and filtration steps were conducted prior to the biochemical tests or to the reactor feeding to avoid a possible inhibition of the methanogenic biomass due to metal concentration, for example, iron, or an increase in the clogging and fouling of the membrane (Abdelrahman et al., 2020; Baek et al., 2019). The iron concentration was decreased from 310 ± 130 in the BFC to $70 \text{ mg}\cdot\text{L}^{-1}$ in the feeding solution. Iodine and bromine ions were detected in low concentrations (Appendix A.4, Section A.4.6).

5.3.2 Biochemical tests

5.3.2.1 Specific methanogenic activity inhibition

The results showed a completely inhibited biogas production at an initial BFC concentration of $250 \text{ mgCOD}\cdot\text{BFC}\cdot\text{L}^{-1}$ for the MWWTP's anaerobic suspended biomass (Figure 5.4 A). We estimated an IC_{50} value of $120 \text{ mgCOD}\cdot\text{BFC}\cdot\text{L}^{-1}$ (Figure 5.4B) by applying the four-parameter model equation (Lee and Hwang, 2019). A decrease in the SMA values was observed when the COD-BFC's concentrations were increased (Figure 5.4 B). Such a decrease corresponded to 22.1 9.4% and 54.4 12.5% less methane

production rate than the control (acetate $2 \text{ gCOD}\cdot\text{L}^{-1}$) for the concentrations of 75 and $125 \text{ mgCOD-BFC}\cdot\text{L}^{-1}$, respectively.

The granular biomass coming from the UASB treating petrochemical wastewater was less sensitive to BFC. No complete SMA inhibition was observed (Figure 5.5 A), even at the highest BFC-COD concentration ($1000 \text{ mgCOD}\cdot\text{L}^{-1}$). An IC_{50} value of $224 \text{ mgCOD}\cdot\text{L}^{-1}$ was estimated for this biomass (Figure 5.5 B). Although a considerable lag phase was observed for BFC concentrations higher than $250 \text{ mgCOD}\cdot\text{L}^{-1}$, all COD was ultimately converted to methane.

The inhibitory effect of the BFC-COD on the SMA of the phenol-degrading AnMBR-cultivated suspended biomass (Figure 5.6 A) was even lower than on the other two biomass sources, having an estimated IC_{50} value of $930 \text{ mgCOD}\cdot\text{L}^{-1}$ (Figure 5.6 B). The extent of the methane production was not affected even at the highest BFC-COD concentrations (Figure 5.6 A), which is similar to the results observed for the granular biomass treating petrochemical wastewater. The lag phase was only present for concentrations higher than $500 \text{ mgCOD}\cdot\text{L}^{-1}$, and it was shorter in comparison to the lag phases found for the petrochemical biomass.

The AD process can be inhibited by most of the organic compounds present in BFC such as PAH, (alkyl-) benzenes, phenolics, alkanes, etc. (Chen et al., 2014; Chen et al., 2008). (Olguin-Lora et al., 2003) reported IC_{50} values of 0.43 and $0.58 \text{ g}\cdot\text{L}^{-1}$ for *o*-cresol and 0.39 and $1.03 \text{ g}\cdot\text{L}^{-1}$ for *p*-cresol on non-adapted and adapted anaerobic granular biomass, respectively.

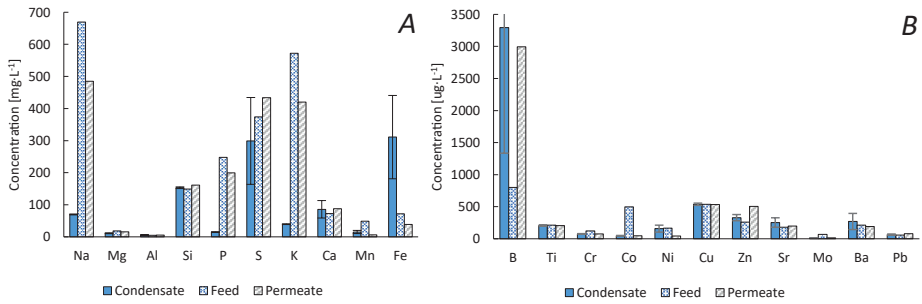


Figure 5.3. Concentrations of the major (A) and minor (B) elements found in the bitumen fume condensate and the reactor's feed & permeate. Error bars = SD, $n = 6$ for BFC and 2 for feeding solution and permeate.

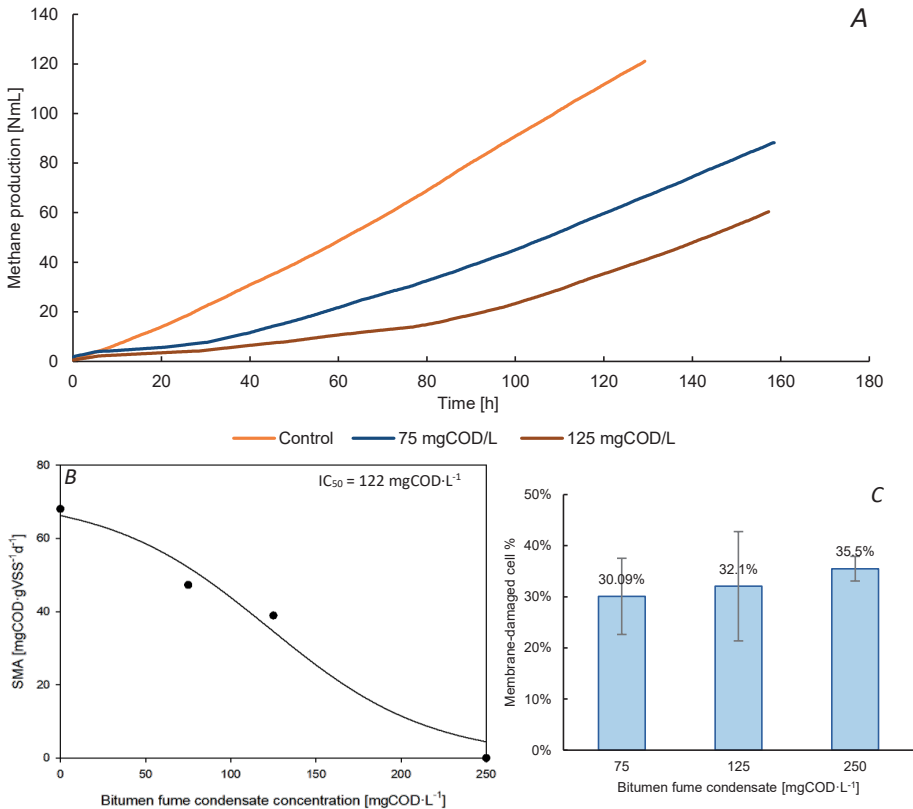


Figure 5.4. Accumulated methane production for the different BFC concentrations used. The assays were performed in triplicates, the most representative curves are shown (A). In the assay corresponding to 250 mg BFC-COD $\cdot\text{L}^{-1}$ there was a total inhibition of the methanogenic activity, meaning no biogas production (A). SMA inhibition in anaerobic municipal sludge due to the dosage of BFC, each point represents the average of three assays (B). Membrane-damaged-cell percentage after finalizing the SMA test (C), $n = 3$, bars = SD.

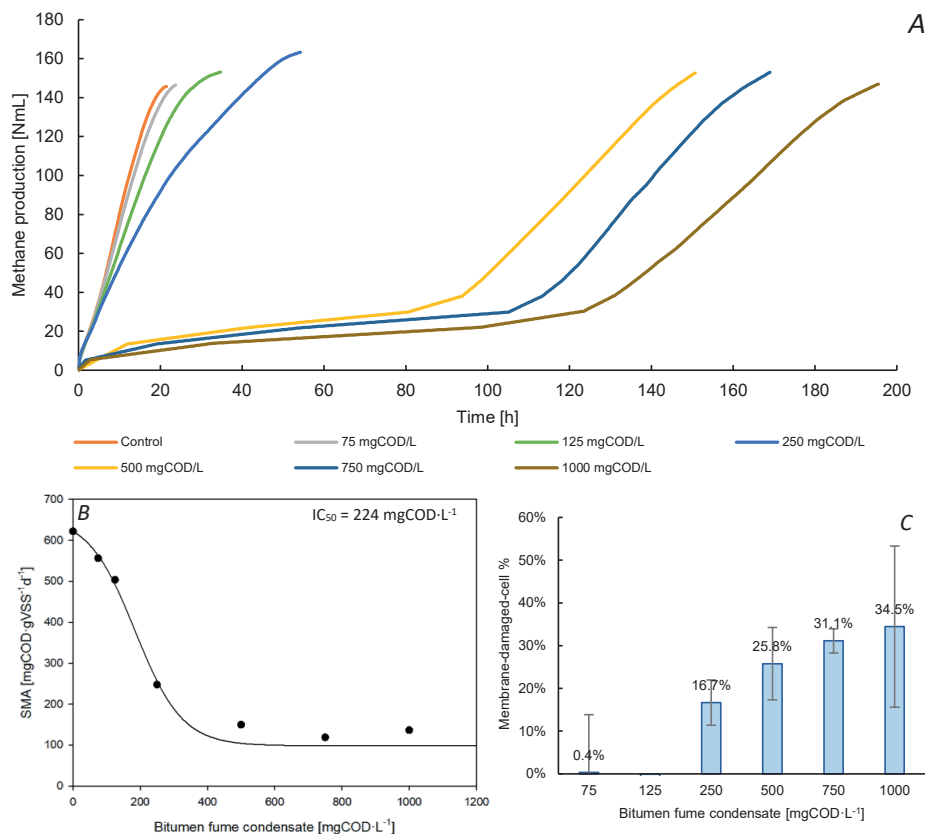


Figure 5.5. Accumulated methane production for the different BFC concentrations used. The assays were performed in triplicates, the most representative curves are shown (A). SMA inhibition in anaerobic sludge from a petrochemical WWTP due to the dosage of BFC, each point represents the average of three assays (B). Membrane-damaged-cell percentage after finalizing the SMA test (C), $n = 3$, bars = SD.

The suspended biomass from the phenol-degrading AnMBR was the most active and resistant to the inhibitory effects of the BFC in comparison to the other two biomass sources. (Garcia Rea et al., 2022) showed that anaerobic biomass from a phenol-degrading AnMBR is less inhibited by other phenolic compounds, such as *p*-cresol and resorcinol, compared to anaerobic suspended biomass harvested from an MWWTP. The lower inhibition was attributed to the (full) biomass retention offered by the membrane. (Garcia Rea et al., 2022) states that the resulting methanogenic consortia was more resistant to phenolics, likely due to the continuous exposure to phenol that combined with the membrane filtration ensured that all the exposed biomass was retained inside the reactor. Our present results subscribe to this hypothesis, as we saw that the phenol-degrading AnMBR biomass was less prone to inhibition by

the aromatic compounds-rich BFC (Figure 5.6 A & B) and had the most abundant methanogenic population (Section 3.2.3).

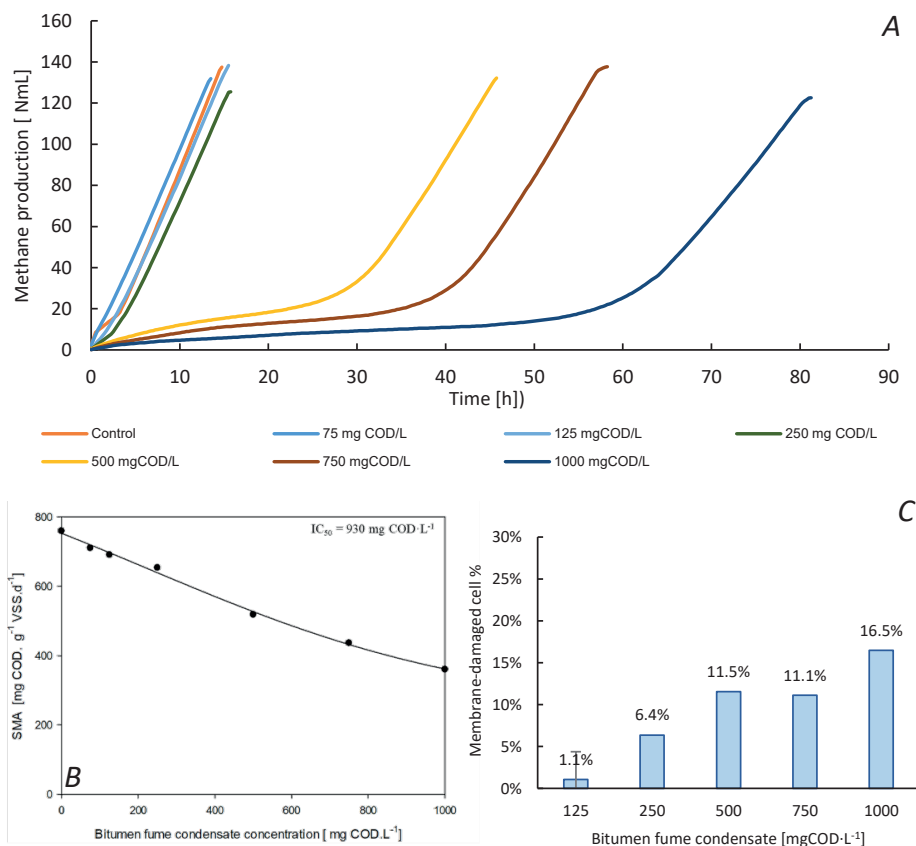


Figure 5.6. Accumulated methane production for the different BFC concentrations used. The assays were performed in triplicates, the most representative curves are shown (A). SMA inhibition in an AnMBR-cultivated phenol-degrading anaerobic sludge due to the dosage of BFC, each point represents the average of three assays (B). Membrane-damaged-cell percentage after finalizing the SMA test (C), $n = 3$ for [125 mg COD · L⁻¹] and $n = 2$ for [250 - 1000 mg COD · L⁻¹], bars = SD.

5.3.2.2 Cell membrane integrity determination

To determine whether the inhibitory effect of BFC on the different biomass sources was biostatic or biocidal (Batstone et al., 2002), we analyzed the cell membrane integrity by the live-dead cell protocol (Falcioni et al., 2006) once the SMA inhibition tests were concluded. For the suspended biomass from the MWWTP, we observed a maximum of 35% increase in damaged cells with the highest BFC concentration of 250 mg COD · L⁻¹ in comparison to the control assays (Figure 5.4 C). For the granular biomass

that treated petrochemical wastewater, we observed a maximum of 34.5 % increase in damaged cells at a concentration of 1000 mgCOD·L⁻¹ (Figure 5.5 C). In contrast, for the suspended AnMBR-cultivated biomass there was a 16.5% increase in damaged cells with a BFC concentration of 1000 mgCOD·L⁻¹ (Figure 5.6 C).

The SMA inhibition in the anaerobic suspended biomass from the MWWTP (Section 5.3.2.1) could have also been related to an increase in biomass decay. The granular biomass from the UASB reactor had higher percentages of membrane-damaged cells for the three highest COD-BFC concentrations in comparison to the AnMBR-cultivated biomass, but suffered less damage than the municipal biomass. The kinetic and morphologic performance of the UASB granular biomass might be attributed to: 1) the granular biomass was acclimatized to (petrochemical) aromatic compounds, mainly benzoate and other hydrocarbons, and 2) the granular morphology provided extra protection to the core anaerobic microorganisms due to a) the possible degradation of toxic organic compounds at the outer layers of the granules, and b) steric and/or electrostatic hindrance of the more hydrophobic aromatic compounds which may have access to the inner parts of the granules. The latter reasons might result in a lower exposure of the methanogens to inhibitory or toxic concentrations of specific pollutants. Although the analysis was targeted to all the prokaryotes in the biomass, and not solely to the methanogenic population, it could be possible that the methanogens were most affected, as (acetoclastic) methanogens are reported as one of the most commonly affected groups in the AD process (Astals et al., 2015; Chen et al., 2008).

From the obtained results, it can be concluded that biomass grown in an AnMBR with a previous (chronic) exposure to phenol was less prone to biocidal inhibition caused by the BFC in comparison to the other two biomass sources.

5.3.2.3 Microbial community structure of the three biomass sources

The molecular analysis performed in the three different biomass sources used in the batch tests showed that the biomass coming from the phenol-degrading AnMBR had the highest relative abundance of the acetoclastic methanogenic microorganism *Methanosaeta* sp. ($36.7 \pm 8.9\%$), namely 7.0 and 20.6 times higher in comparison to the granular ($5.3 \pm 1.3\%$) and suspended municipal anaerobic biomass ($1.8 \pm 0.3\%$), respectively (Figure 5.7). It should be noticed, however, that this reactor was fed with an acetate-phenol mixture (García Rea et al., 2020), which explains the high abundance of the (acetoclastic) methanogens. *Thermovirga* sp. was found in high abundance as well ($14.6 \pm 1.7\%$). This microorganism has been reported in phenol-degrading AnMBRs and UASB reactors (García Rea et al., 2020; Muñoz Sierra et al., 2020; Wang et al., 2020); although, its role is still unknown. *Syntrophus* sp. had a relative abundance of $4.0 \pm 1.1\%$.

This microorganism is a reported syntrophic anaerobic degrader of aromatic compounds such as benzoate (McInerney et al., 2007), and has been reported as a possible degrader of aromatic compounds present in various (petro)chemical wastewater (Porter and Young, 2014; Ruan et al., 2016). *Syntrophorhabdus* sp., a reported phenol degrader (Nobu et al., 2015) presented a relative abundance of $2.5 \pm 0.8\%$.

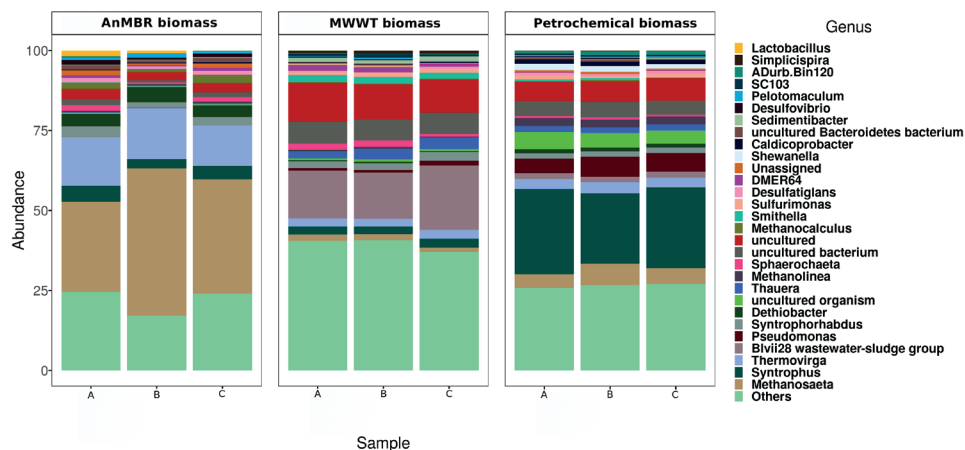


Figure 5.7. Microbial community structure at genus level of the different sludge sources. A, B, and C represent each of the triplicates of the samples.

The granular biomass from the UASB reactor had a higher abundance of *Syntrophus* sp. ($24.7 \pm 2.4\%$), a microorganism that is related to the degradation of aromatic compounds, especially benzoate (McInerney et al., 2007), which may explain the decrease in the inhibitory effects caused by the BFC. Other abundant bacteria included *Pseudomonas* sp. ($5.6 \pm 0.8\%$), *Thermovirga* sp. ($3.2 \pm 0.3\%$), and *Syntrophorhabdus* sp. ($1.6 \pm 0.1\%$). The archaeal population was mainly represented by *Methanosaeta* sp. ($5.3 \pm 1.3\%$) and the hydrogenotrophic methanogen *Methanolinea* sp. ($5.3 \pm 0.1\%$).

The anaerobic biomass from the municipal wastewater treatment plant had a low relative abundance of methanogens, e.g., *Methanosaeta* sp. ($1.8 \pm 0.3\%$), and syntrophic aromatic degraders such as *Syntrophus* sp. ($2.6 \pm 0.2\%$) and *Syntrophorhabdus* sp. ($2.3 \pm 0.3\%$). The highest abundance (39.4 ± 2.1) corresponded to non-identified microorganisms.

A principal coordinate analysis performed on the three biomass sources showed that the communities were significantly different ($p < 0.05$) (Appendix A.4, Section A.4.7, Figure A.4.4). In summary, the results observed in the microbial community analysis

confirmed that the AnMBR-cultivated biomass had an abundant, highly active, and robust methanogenic population.

The continuous exposure of (anaerobic) biomass to a certain type of stress, for example a toxic substrate or wastewater, will likely result in adaptation of the biomass to the new conditions. Most commonly, adaptation entails a shift of the microbial community towards a more resistant, and in principle, less diverse community (Knapp and Bromley-Challoner, 2003). The new community will comprise microorganisms that are capable of withstanding the stressful conditions to which the biomass has been exposed. Regarding the phenol-degrading AnMBR biomass, a microbial community with a large fraction of phenol degraders was expected. Similarly, the petrochemical granular biomass was continuously exposed to benzoate, which would result in enrichment of benzoate degraders. Therefore, and very likely, a low percentage of membrane-damaged microorganisms was observed in the sludge adapted to aromatics after exposure to BFC, compared to the non-adapted biomass. A second adaptation mechanism could have been the induction, activation or up-regulation of gene expression which results in the production of enzymes (Knapp and Bromley-Challoner, 2003). Newly or highly expressed enzymes may provide a higher resistance to the microorganisms after the exposure to the BFC. A third and last mechanism considered will be the development or acquisition of mutations that will offer the microorganisms higher resistance to the stress conditions.

5.3.3 *BFC biodegradation in AnMBR*

The AnMBR was seeded with biomass from the UASB reactor treating petrochemical wastewater, characterized by a diverse microbial community and rich in aromatic-degrading microorganisms. The BFC influent was enriched with phenol and acetate to enhance the phenol-degrading and methanogenic activity of the biomass (García Rea et al., 2020; Wang et al., 2010). After the reactor's start-up, the phenol addition was gradually reduced and eliminated from the feeding solution (Table 3).

5.3.3.1 *Conversion rates and COD & phenol removal efficiencies*

Stages A and B (Figure 5.8 A) were distinguished by a relatively high OLRs (Table 3). The corresponding average organic conversion rates (OCR) were $330 \pm 110 \text{ mgCOD} \cdot \text{L}^{-1} \cdot \text{d}^{-1}$ and $254 \pm 103 \text{ mgCOD} \cdot \text{L}^{-1} \cdot \text{d}^{-1}$, respectively. Average sludge conversion rates (SCR) of $45 \pm 15 \text{ mgCOD} \cdot \text{gVSS}^{-1} \cdot \text{d}^{-1}$ and $45 \pm 14 \text{ mgCOD} \cdot \text{gVSS}^{-1} \cdot \text{d}^{-1}$ were determined for stages A and B, respectively, after the consideration of the VSS concentration.

The corresponding average OCRs remained at a similar level in the next three stages, i.e., $274 \pm 116 \text{ mgCOD} \cdot \text{L}^{-1} \cdot \text{d}^{-1}$, $269 \pm 65 \text{ mgCOD} \cdot \text{L}^{-1} \cdot \text{d}^{-1}$, and $257 \pm 59 \text{ mgCOD} \cdot \text{L}^{-1} \cdot \text{d}^{-1}$,

respectively. However, the average SCR increased to $77 \pm 41 \text{ mgCOD} \cdot \text{gVSS}^{-1} \cdot \text{d}^{-1}$ (Stage C), $120 \pm 39 \text{ mgCOD} \cdot \text{gVSS}^{-1} \cdot \text{d}^{-1}$ (Stage D), and $97 \pm 29 \text{ mgCOD} \cdot \text{gVSS}^{-1} \cdot \text{d}^{-1}$ (Stage E) because of a decreased VSS concentration.

Applied volumetric loading and conversion rates were relatively low, mainly attributable to the low COD-BFC concentration (Table 3 and Figure A.4.5, Appendix A.4, Section A.4.8). Unfortunately, we did not have access to higher volumes of BFC to increase the loading rate. Therefore, the biomass concentration in the reactor was kept below the average AnMBR reported values to allow us to observe faster responses in the sludge loading rate (SLR) when the influent COD was varied (Dereli et al., 2012; Dvořák et al., 2015). Hence, employing higher biomass concentrations can easily increase the AnMBR removal efficiency.

Figure 5.8 B shows the COD concentration in the permeate, the COD which corresponded to the residual phenol in the permeate, and the COD removal efficiency during the reactor operation. There was a significant difference $t(82) = 24.27, p < 0.001$ for the COD concentration in the feeding of the reactor and the permeate during the whole reactor operation, similarly during each of the different stages (Data not shown). In the first 30 days of operation (stage A), the COD removal efficiency was $37.9 \pm 3.9\%$, mostly related to the fact that phenol was not biodegraded (average removal = $5.1 \pm 4.8\%$); however, all the acetate was converted. The HRT was increased to 4 days on day 31 (stage B) with a concomitant increase to $43.0 \pm 3.2\%$ in the COD removal efficiency; nonetheless, phenol degradation remained low (average = $13.1 \pm 2.4\%$). The phenol concentration in the influent was reduced from 1.2 to 0.5 $\text{gCOD}_{\text{Phenol}} \cdot \text{L}^{-1}$ (stage C) after 57 days of the exposure of the biomass to the phenol which caused an increase in the COD removal efficiency. The removal efficiency decreased due to a technical failure in the pumping system of the reactor on day 73. The minimum removal efficiency of 22% was reached on day 87. Nevertheless, the COD removal efficiency was recovered (84%) on day 94. The average COD and phenol removal efficiencies in stage C were $80.2 \pm 20.7\%$ and $87.0 \pm 22.4\%$, respectively. In stage D, the phenol concentration was further decreased from 0.50 to 0.25 $\text{gCOD}_{\text{Phenol}} \cdot \text{L}^{-1}$ on day 166, the COD removal efficiency was $91.6 \pm 0.9\%$. For stage E, an average COD removal efficiency of $82.1 \pm 6.2\%$ was found. Therefore, considering the last 100 days of operation, the reactor had an average COD removal efficiency of $87.7 \pm 7.0\%$ corresponding to an OLR of $286 \pm 71 \text{ mgCOD} \cdot \text{L}^{-1} \cdot \text{d}^{-1}$ and an SCR of $97 \pm 33 \text{ mgCOD} \cdot \text{gVSS}^{-1} \cdot \text{d}^{-1}$. It is suggested that the dosage of acetate to an AnMBR enhances the phenol conversion due to an increase in the (acetoclastic) methanogenic population that allowed higher acetate consumption, likely because of the improvement in the conversion of phenol to acetate (García Rea et al., 2020). (Wang et al., 2010) suggested that the dosage of phenol as an additional carbon and energy

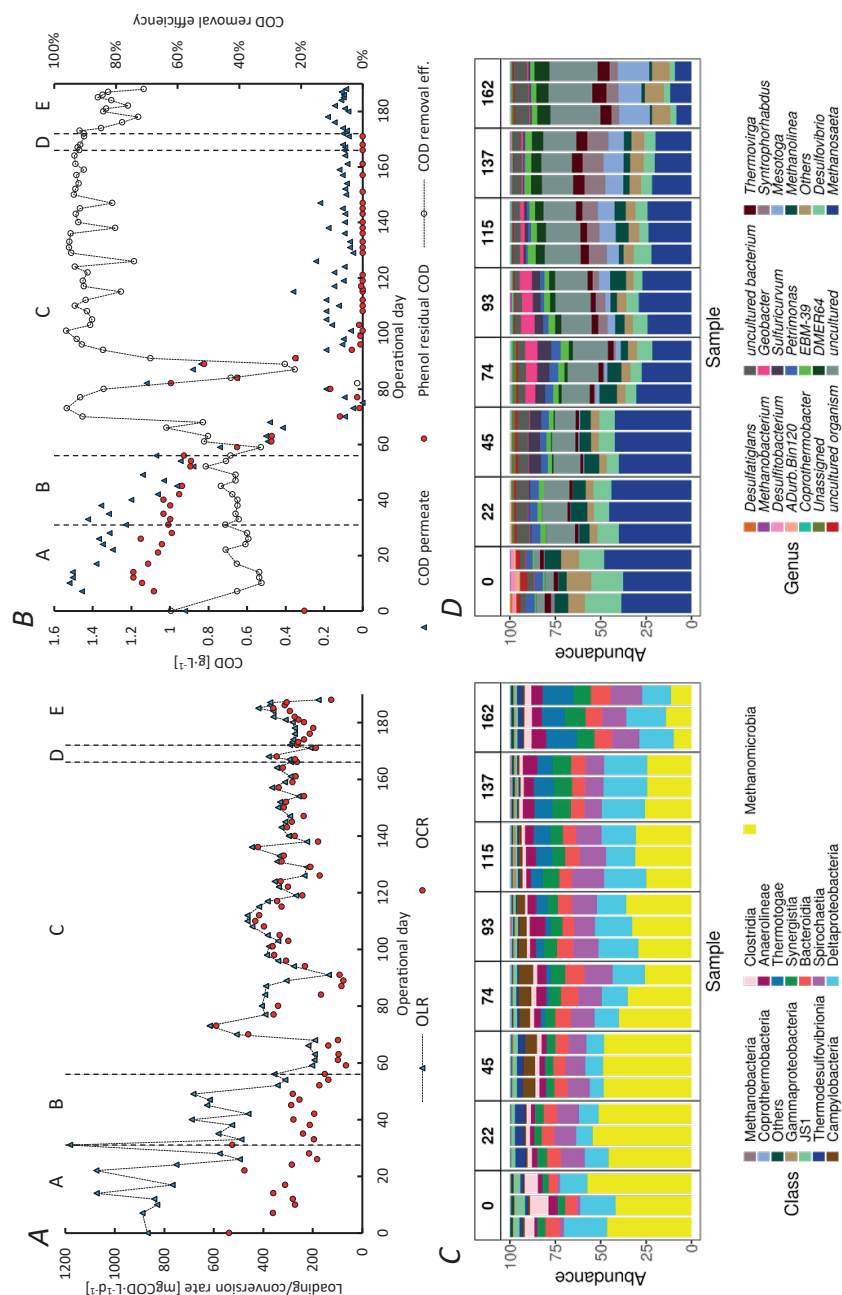


Figure 5.8. Volumetric organic loading and conversion rates in the AnMMBR (A) and total COD & phenol COD in the influent, and COD removal efficiency (B). Microbial community profile during the reactor operation in Class (C) or Genus (D), the triplicates of each of the samples are shown.

source may enhance the degradation of toxic and refractory compounds, such as those present in coal gasification wastewater (CGWW). Finally, the phenol was completely removed from the feeding on day 172 (Stage E), which resulted only in a slight decrease in the COD removal efficiency to 82.1 ± 6.2 %.

We estimated the removed COD that corresponded to the BFC by performing a COD balance based on the known COD concentrations of phenol and VFAs in the feeding solution and the reactor's permeate. Figure A.4.5 (Appendix A.4, Section A.4.8) shows the COD-BFC concentration in the influent and the calculated COD-BFC removal efficiency.

The initial anaerobic conversion of aromatic hydrocarbons, such as phenolics and PAHs, is started by an enzymatic process known as activation (Foght, 2008). For this process, five main reactions are suggested: a) fumarate addition, b) methylation of unsubstituted aromatics, c) hydroxylation via dehydrogenases, d) direct carboxylation, and e) phosphorylation (Foght, 2008; Ladino-Orjuela et al., 2016). After the activation, the molecules can be directed via pathways yielding central metabolites such as the benzoyl-CoA, which can be then further metabolized via ring saturation and ring cleavage and β -oxidation in the so-called central or lower pathways (Carmona et al., 2009; Ladino-Orjuela et al., 2016).

Various compounds found in the BFC analysis are known to be biodegradable under anaerobic conditions (Carmona et al., 2009; Kraiselburd et al., 2019; Ladino-Orjuela et al., 2016). (Carmona et al., 2009) and (Nobu et al., 2015) reported the detailed anaerobic degradation pathway for compounds such as phenol, *p*-cresol, and *o*-cresol. Also for fluoranthene, its methanogenic degradation has been reported (Fuchedzhieva et al., 2008), but the degradation pathway is unknown. For compounds such as naphthalene, fluorene, acenaphthene, anthracene, and phenanthrene the degradation route by mixed cultures under strict anaerobic conditions is either reported (Chang et al., 2003) or strongly suggested (Dhar et al., 2020) but has not yet been described (Foght, 2008). Nevertheless, insights into the degradation routes have been obtained under sulfate and/or nitrate reducing conditions (Figure 5.9), for example, for naphthalene and methylnaphthalene (Meckenstock and Mouttaki, 2011), phenanthrene (Kraiselburd et al., 2019), acenaphthene (Meckenstock et al., 2004), fluorene (Tsai et al., 2009). Nonetheless, the detailed degradation routes for the majority of the compounds contained in the BFC are unknown. Figure 5.9 shows a summary scheme of the reported degradation routes for the major organic compounds found in the BFC.

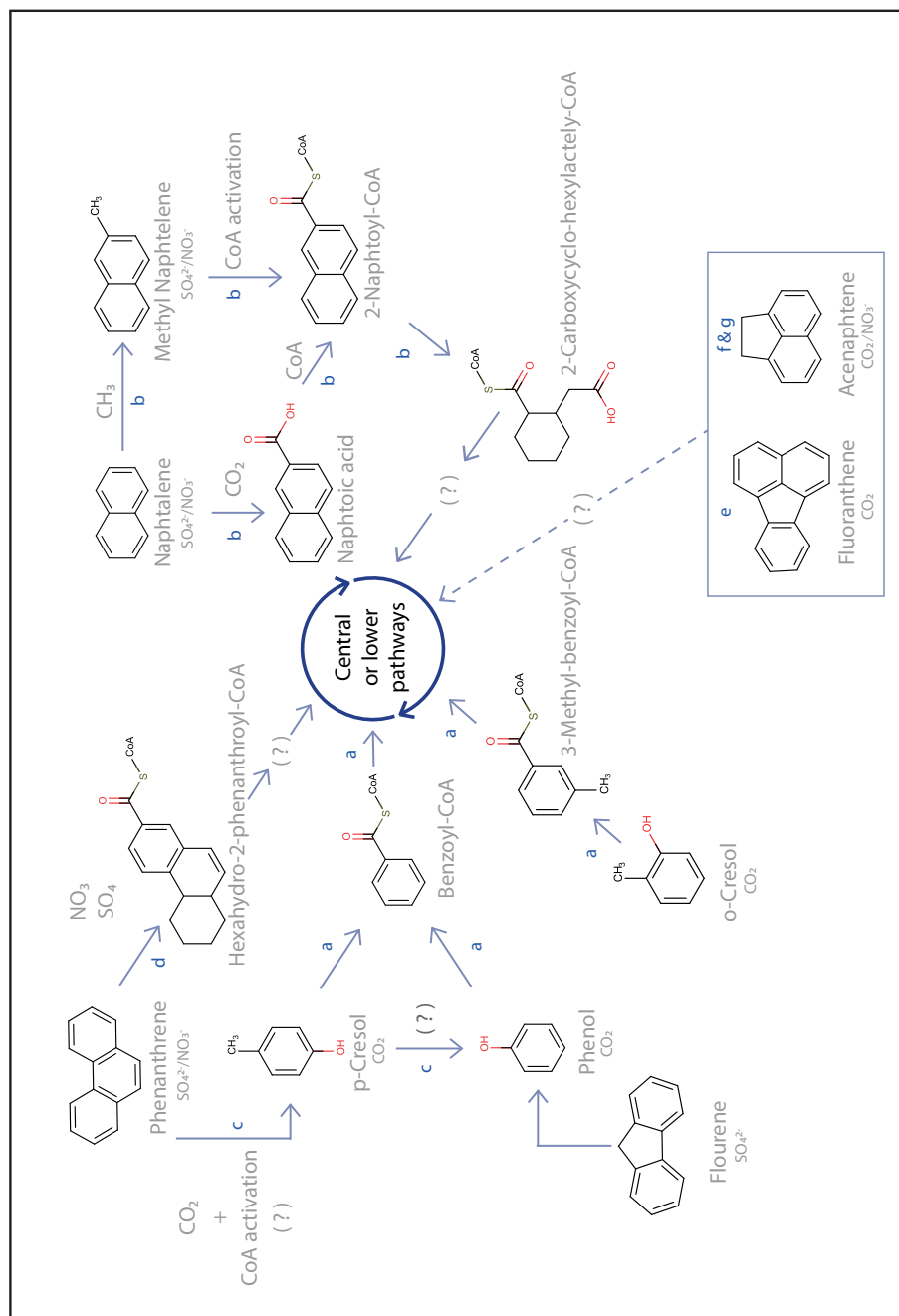


Figure 5.9. Summary scheme of the reported degradation pathways of the major organic compounds found in the BFC. The redox conditions for which the routes have been elucidated or proposed are indicated. References: a (Carmona et al., 2009), b (Meckenstock and Mouttaki, 2011), c (Tsai et al., 2009), d (Kraiselburg et al., 2019), e (Fuehdezhiava et al., 2008), f (Meckenstock et al., 2004), and g (Chang et al., 2003).

Previous research studies conducted in the past decades investigated the anaerobic treatment of (petro)chemical wastewater (Chapter 1, Section 1.2.2, Table 1.1), but most of them focused on the degradation of specific compounds such as purified terephthalic acid (PTA) (Guyot et al., 1990; Kleerebezem et al., 2005; Noyola et al., 2000), and benzene, toluene, ethylbenzene, and xylenes (BTEX) (Ribeiro et al., 2013). AD showed to be a feasible option for the treatment of those types of wastewater, with reactors that achieved COD removal efficiencies exceeding 80%. However, poor reactor performance with low COD removal efficiency (45%) was also reported (Guyot et al., 1990).

Fewer studies have dealt with more complex and non-synthetic petrochemical wastewater (Chapter 1, Section 1.2.2, Table 1.1). Coal gasification wastewater (CGWW) is a typical toxic/inhibitory matrix with similar compounds as those reported in BFC, such as phenolics and PAH. (Wang et al., 2010) reported the application of AD to treat this wastewater, either with the dosage of methanol ($500 \text{ mg} \cdot \text{L}^{-1}$) as an additional carbon and energy source or by using a step-feed strategy (Wang et al., 2011). These studies reported enhanced COD and phenol removal efficiencies between 55 and 75%, applying an OLR of $3.5 \text{ kgCOD} \cdot \text{m}^{-3} \cdot \text{d}^{-1}$ for the former study (Wang et al., 2010), and influent concentrations of $2,500 \text{ mgCOD} \cdot \text{L}^{-1}$ and $500 \text{ mgPhenol} \cdot \text{L}^{-1}$ for the latter (Wang et al., 2011). (Gasim et al., 2012) reported the degradation of petroleum refinery wastewater using UASB reactors, under six OLRs between 0.6 and $4.1 \text{ kgCOD} \cdot \text{m}^{-3} \cdot \text{d}^{-1}$. The conclusion of their study was that AD in UASB reactors is suitable to treat the petroleum refinery wastewater. The UASB reactor achieved a COD removal efficiency of 83% (effluent COD = $350 \text{ mg} \cdot \text{L}^{-1}$) at an OLR of $1.2 \text{ kgCOD} \cdot \text{m}^{-3} \cdot \text{d}^{-1}$. (Jafarzadeh et al., 2012) reported the treatment of petrochemical wastewaters with pollutants such as ethylene, propylene, benzene, among others. The hybrid reactor (UASB/Filter) treated OLRs between 0.5 and $24 \text{ kg}_{\text{total}} \text{COD} \cdot \text{m}^{-3} \cdot \text{d}^{-1}$, with an HRT of 4-48 h and removal efficiencies between 42-86%.

Most of the studies conducted for the anaerobic treatment of petrochemical wastewater have reported the usage of sludge bed reactors, such as UASB and EGSB reactors, even when petrochemical wastewater may hamper the anaerobic granulation process (Chapter 1, Section 1.2.2, Table 1.1). Only a few studies were conducted with AnMBRs. (Wang et al., 2013) reported the treatment of bamboo industry wastewater, rich in alkenes, benzenes, esters, and phenolics, using AnMBR. Different OLRs from 2.2 to $11.0 \text{ kgCOD} \cdot \text{m}^{-3} \cdot \text{d}^{-1}$ were applied with HRTs of 2-10 d. The COD removal efficiency reported was 91%, higher than that of an EGSB under the same conditions. (Bhattacharyya et al., 2013) used a 25 L submerged AnMBR for the treatment of high-COD ($85 \text{ gCOD} \cdot \text{L}^{-1}$) synthetic petrochemical wastewater containing formaldehyde besides acrylic and

acetic acids the main pollutants. At an OLR of $3.4 \text{ kgCOD} \cdot \text{m}^{-3} \cdot \text{d}^{-1}$, the COD and acrylic acid removal efficiencies were higher than 99%.

5.3.3.2 Microbial community dynamics in the AnMBR

The molecular analysis of the reactor's biomass showed a dynamic microbial community during the different stages. Figure 5.8 (C & D) shows the relative abundance of microorganisms in the biomass either at class (A) or genus (B) level. During the start of reactor operation (day 0) and the first two stages (day 22, Stage A; day 45, Stage B), the highest relative abundance corresponded to the (acetoclastic) methanogen *Methanosaeta* sp. with $42.3 \pm 4.2\%$ and $41.5 \pm 1.3\%$ respectively. This was in part expected as the BFC wastewater was amended with acetate. Furthermore, acetotrophic methanogenesis occurs mainly via the acetoclastic pathway (García Rea et al., 2020) when phenolic wastewater is degraded under mesophilic conditions. The samples of the stage C and beginning the stage D (days 74, 93, 115, 137, and 162), showed a decrease in the relative abundance of methanogens, which may be related to the decrease in the influent acetate concentration. However, this decline did not affect the COD conversion rates and removal efficiencies.

The mesophilic hydrogenotrophic archaea *Methanolinea* sp. was the second most abundant methanogen during the AnMBR operation. According to (Narihiro et al., 2015), the *Methanolinea* genus was found in microbial communities enriched with substrates that require syntrophic conversion. Likewise, *Methanolinea* preferentially partner in syntrophic consortia that scavenges the reducing equivalents. *Desulfovibrio* sp. was identified during the entire AnMBR operation, and its relative abundance decreased together with the methanogenic microorganisms. The *Desulfovibrio* genus includes sulfate-reducing bacteria that contributes in the metabolism of fermentative systems (Wegmann et al., 2017). For example, it is reported that sulfate reducers can obtain energy via fermentative pathways at low (or none) sulfate concentrations. Under these conditions, sulfate reducers act as syntrophic partners through H_2 production, but they switch to sulfate respiration once SO_4^{2-} is available (Rabus et al., 2006). *Desulfovibrio* sp. can degrade nitroaromatic compounds (Zhang and Bennett, 2005) and hydroxyhydroquinone (Philipp and Schink, 2012). This microorganism has also been found in a UASB reactor that treated saline phenolic wastewater (Wang et al., 2017), horizontal anaerobic immobilized biomass reactors for BTEX treatment (de Nardi et al., 2002), and in the anaerobic degradation of CGWW (Li et al., 2018).

In stage C, we found a noticeable presence of the phenol (and other aromatic compounds) degrader *Syntrophorhabdus* sp. (Qiu et al., 2008). *Syntrophorhabdus* sp. can convert some aromatic compounds into easily biodegradable substrates, such as

acetate, which could eventually be used by other microorganisms as a carbon source. At this stage (C), *Syntrophorhabdus*' relative abundance increased from $0.9 \pm 0.3\%$ on day 74 to 11.6 ± 0.1 on day 137. However, on day 162 there was a decrease to $5.3 \pm 0.2\%$ which coincided with the decrease in the COD removal efficiency (Figure 5.8).

Although 16S rRNA analysis does not allow to conclude about the activity of microorganisms, it might be possible that *Syntrophorhabdus* sp. was a key microorganism in the degradation of aromatic compounds present in the IBC due to its metabolic capabilities (García Rea et al., 2020; Nobu et al., 2015; Qiu et al., 2008).

Geobacter genus was found with an abundance of up to $6.8 \pm 0.7\%$ in stage C (day 93). This microorganism is reported to be capable of metabolizing aromatics via the Benzoyl-CoA pathway with the help of iron reducers (Foght, 2008; Philipp and Schink, 2012). In addition, it also has been identified in anaerobic biomass which treated coal gasification wastewater (Zhu et al., 2018) and wastewater containing phenanthrene (Lin et al., 2019).

The genera *Mesotoga* and *Thermovirga* were identified in increasing abundance from day 74 to 162. The genus *Mesotoga* includes bacteria with a potential role in the degradation of halogenated aromatic compounds. For example, *Mesotoga* has been reported in the anaerobic degradation of phenanthrene (Lin et al., 2019), a compound found in the BFC. *Thermovirga* sp. is a fermentative bacteria genus with a strong hydrolysis ability and it has been reported in phenol-degrading (García Rea et al., 2020; Muñoz Sierra et al., 2018) and in a UASB reactor which treated CGWW. Its role in the degradation of phenol, however, has not yet been identified.

The results from the MaAsLin 2 approach showed the significant correlation ($p < 0.05$) of the twelve most important genera found in the reactor's biomass and the COD removal efficiency during the different reactor operation stages (Figure 5.10). For microorganisms such as *Desulfovibrio*, *Methanolinea*, or *Methanosaeta*, there was a negative correlation. Increased COD removal efficiencies were measured when the relative abundances of the aforementioned microorganisms decreased. Nevertheless, *Syntrophorhabdus* (a reported phenol and aromatic compound degrader), *Thermovirga*, and other microorganisms such as DMER64, EBM-39, and a fraction of uncultured bacteria, had an increase in their relative abundance. It must be noted that genomic analysis based on the 16S rRNA gene cannot be directly linked to microbial activity. These results allow us, however, to have a better understanding of the process(es) that might be occurring in the reactor biomass. Based on our results, we hypothesized that the increase in the COD removal efficiency observed during the reactor operation

was related to the increase in the mentioned genera instead of to the decrease of microorganisms such as the methanogens. Methanogenesis can be considered the key step in the AD process. Thus, a decrease or impairment in the methanogenic subpopulations (acetoclastic or hydrogenotrophic) will likely result in the a decrease or the complete cessation of the AD biochemical processes.

The BFC was characterized by an average of 0.58 ± 0.39 mgCOD·L⁻¹ (n = 33), and a maximum value of 1.20 gCOD·L⁻¹. From the 993 compounds detected in the GC-QTOF analysis, only 72 compounds corresponded with an 80% match in relation to the compounds described in the reference library.

The major organic compounds identified were acetate, phenol, naphthalene, acenaphthylene, propylamide, fluorene, phenanthrene, acenaphthene, and fluoranthene. The BFC content of iron, sulfur, silicon, and calcium was high (85 – 310 mg/L). After the precipitation step, iron concentration was decreased by 76.9% in the feeding of the AnMBR. BFC concentrations of 120 mgCOD·L⁻¹ for anaerobic biomass from an MWWTP, 224 mgCOD·L⁻¹ for granular biomass from a petrochemical WWTP, and 900 mgCOD·L⁻¹ for the biomass from a saline phenol-degrading AnMBR decreased the methanogenic activity to half of the maximum value and were regarded as the 50% inhibition concentration (IC₅₀). Accordingly, when exposed to BFC [1000 mgCOD·L⁻¹], the biomass coming from the saline phenol-degrading AnMBR had less damaged (membrane) cells in comparison to the other two biomass sources. Furthermore, the biomass from the phenol degrading AnMBR had the most abundant acetoclastic methanogenic population (*Methanosaeta* sp.), but the granular biomass treating petrochemical wastewater showed a higher relative abundance of syntrophic degraders of aromatic compounds (*Syntrophus* sp.).

We operated for 188 days an AnMBR fed with a mixture of BFC, phenol, acetate, and nutrients. During the last 100 days, the reactor had an average COD removal efficiency of 87.7 ± 7.0 % which corresponded to an OLR of 286 ± 71 mgCOD·L⁻¹·d⁻¹ and an SCR of 97 ± 33 mgCOD·gVSS⁻¹·d⁻¹. The microbial community dynamics in the reactor's biomass indicated that the most abundant microorganisms were the methanogens. The syntrophic degrader of aromatic compounds, *Syntrophorhabdus* sp., remained relatively constant during the reactor operation.

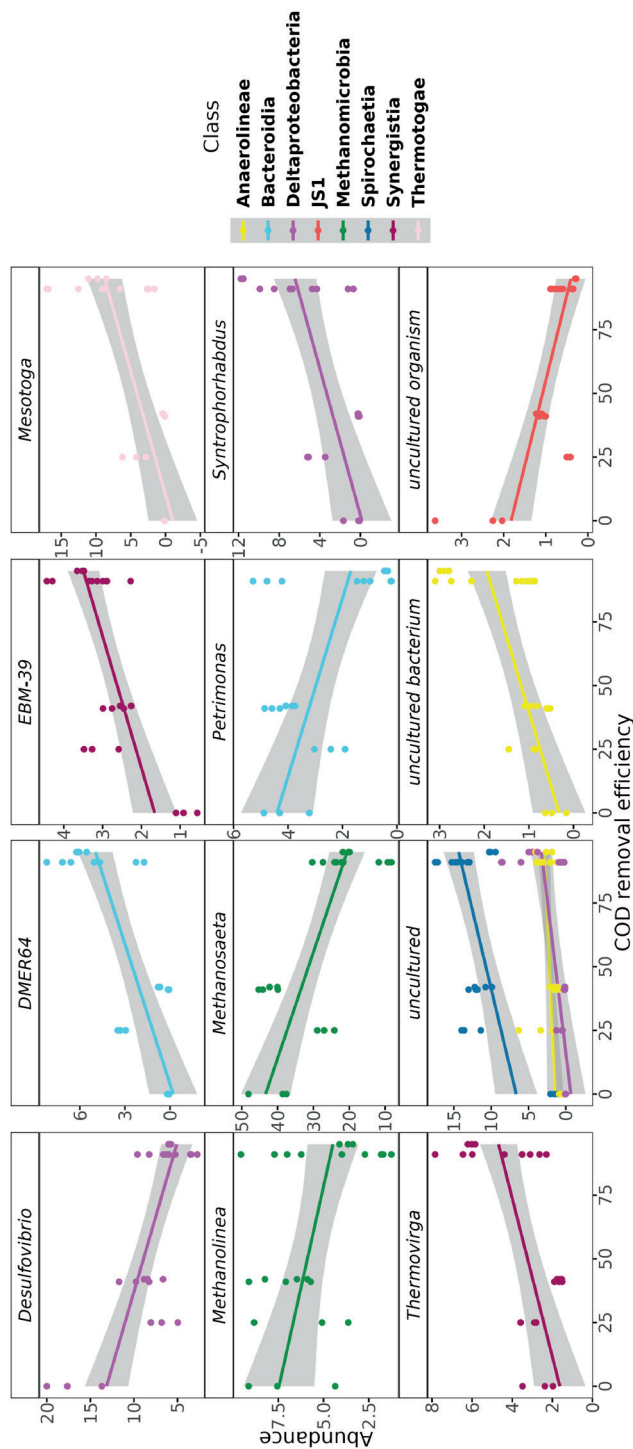


Figure 5.10. MaAsLin 2 analysis performed for the twelve most abundant genus in the reactor's biomass and the COD removal efficiency during the different reactor operation stages.

5.4 References

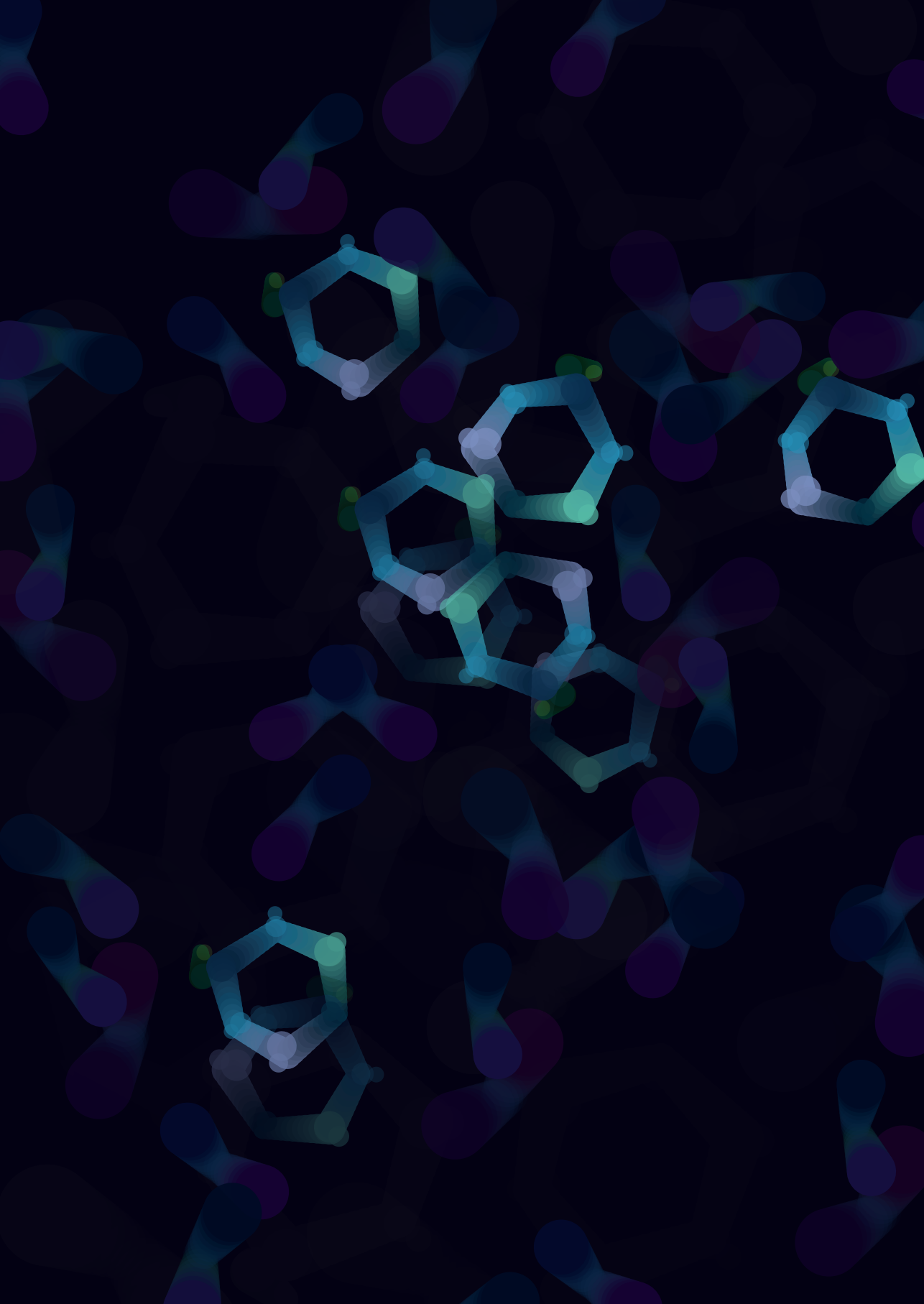
- Abdelrahman, A.M., Ozgun, H., Dereli, R.K., Isik, O., Ozcan, O.Y., van Lier, J.B., Ozturk, I., Ersahin, M.E., 2020. Anaerobic membrane bioreactors for sludge digestion: Current status and future perspectives. *Crit. Rev. Environ. Sci. Technol.*, 1-39. <https://doi.org/10.1080/10643389.2020.1780879>.
- Astals, S., Batstone, D.J., Tait, S., Jensen, P.D., 2015. Development and validation of a rapid test for anaerobic inhibition and toxicity. *Water Res.* 81, 208-215. <https://doi.org/https://doi.org/10.1016/j.watres.2015.05.063>.
- Baek, G., Kim, J., Lee, C., 2019. A review of the effects of iron compounds on methanogenesis in anaerobic environments. *Renew. Sust. Energ. Rev.* 113, 109282. <https://doi.org/https://doi.org/10.1016/j.rser.2019.109282>.
- Batstone, D.J., Keller, J., Angelidaki, I., Kalyuzhnyi, S.V., Pavlostathis, S.G., Rozzi, A., Sanders, W.T.M., Siegrist, H., Vavilin, V.A., 2002. The IWA Anaerobic Digestion Model No 1 (ADM1). *Water Sci. Technol.* 45(10), 65-73. <https://doi.org/10.2166/wst.2002.0292> %J Water Science and Technology.
- Bhattacharyya, D., Allison, M.J., Webb, J.R., Zanatta, G.M., Singh, K.S., Grant, S.R., 2013. Treatment of an Industrial Wastewater Containing Acrylic Acid and Formaldehyde in an Anaerobic Membrane Bioreactor. *J. Hazard. Toxic Radioact. Waste* 17(1), 74-79. [https://doi.org/doi:10.1061/\(ASCE\)HZ.2153-5515.0000148](https://doi.org/doi:10.1061/(ASCE)HZ.2153-5515.0000148).
- Binet, S., Pfohl-Leszkowicz, A., Brandt, H., Lafontaine, M., Castegnaro, M., 2002. Bitumen fumes: review of work on the potential risk to workers and the present knowledge on its origin. *Sci. Total Environ.* 300(1), 37-49. [https://doi.org/https://doi.org/10.1016/S0048-9697\(02\)00279-6](https://doi.org/https://doi.org/10.1016/S0048-9697(02)00279-6).
- Boczka, G., Fernandes, A., Makoš, P., 2017. Study of Different Advanced Oxidation Processes for Wastewater Treatment from Petroleum Bitumen Production at Basic pH. *Ind. Eng. Chem. Res.* 56, 8806-8814. <https://doi.org/10.1021/acs.iecr.7b01507>.
- Bolyen, E., Rideout, J.R., Dillon, M.R., Bokulich, N.A., Abnet, C.C., Al-Ghalith, G.A., Alexander, H., Alm, E.J., Arumugam, M., Asnicar, F., Bai, Y., Bisanz, J.E., Bittinger, K., Brejnrod, A., Brislawn, C.J., Brown, C.T., Callahan, B.J., Caraballo-Rodriguez, A.M., Chase, J., Cope, E.K., Da Silva, R., Diener, C., Dorrestein, P.C., Douglas, G.M., Durall, D.M., Duvallet, C., Edwardson, C.F., Ernst, M., Estaki, M., Fouquier, J., Gauglitz, J.M., Gibbons, S.M., Gibson, D.L., Gonzalez, A., Gorlick, K., Guo, J., Hillmann, B., Holmes, S., Holste, H., Huttenhower, C., Huttley, G.A., Janssen, S., Jarmusch, A.K., Jiang, L., Kaehler, B.D., Kang, K.B., Keefe, C.R., Keim, P., Kelley, S.T., Knights, D., Koester, I., Kosciulek, T., Kreps, J., Langille, M.G.I., Lee, J., Ley, R., Liu, Y.X., Loftfield, E., Lozupone, C., Maher, M., Marotz, C., Martin, B.D., McDonald, D., McIver, L.J., Melnik, A.V., Metcalf, J.L., Morgan, S.C., Morton, J.T., Naimey, A.T., Navas-Molina, J.A., Nothias, L.F., Orchanian, S.B., Pearson, T., Peoples, S.L., Petras, D., Preuss, M.L., Priesse, E., Rasmussen, L.B., Rivers, A., Robeson, M.S., 2nd, Rosenthal, P., Segata, N., Shaffer, M., Shiffer, A., Sinha, R., Song, S.J., Spear, J.R., Swafford, A.D., Thompson, L.R., Torres, P.J., Trinh, P., Tripathi, A., Turnbaugh, P.J., Ul-Hasan, S., van der Hooft, J.J.J., Vargas, F., Vazquez-Baeza, Y., Vogtmann, E., von Hippel, M., Walters, W., Wan, Y., Wang, M., Warren, J., Weber, K.C., Williamson, C.H.D., Willis, A.D., Xu, Z.Z., Zaneveld, J.R., Zhang, Y., Zhu, Q., Knight, R., Caporaso, J.G., 2019. Reproducible, interactive, scalable and extensible microbiome data science using QIIME 2. *Nat. Biotechnol.* 37(8), 852-857. <https://doi.org/10.1038/s41587-019-0209-9>.
- Carmona, M., Zamarró, M.T., Blázquez, B., Durante-Rodríguez, G., Juárez, J.F., Valderrama, J.A., Barragán, M.J., García, J.L., Díaz, E., 2009. Anaerobic catabolism of aromatic compounds: a genetic and genomic view. *Microbiol Mol Biol Rev* 73(1), 71-133. <https://doi.org/10.1128/mmbr.00021-08>.
- Chang, B.V., Chang, S.W., Yuan, S.Y., 2003. Anaerobic degradation of polycyclic aromatic hydrocarbons in sludge. *Advances in Environmental Research* 7(3), 623-628. [https://doi.org/https://doi.org/10.1016/S1093-0191\(02\)00047-3](https://doi.org/https://doi.org/10.1016/S1093-0191(02)00047-3).

- Chen, J.L., Ortiz, R., Steele, T.W.J., Stuckey, D.C., 2014. Toxicants inhibiting anaerobic digestion: A review. *Biotechnol. Adv.* 32(8), 1523-1534. <https://doi.org/http://dx.doi.org/10.1016/j.biotechadv.2014.10.005>.
- Chen, Y., Cheng, J.J., Creamer, K.S., 2008. Inhibition of anaerobic digestion process: A review. *Bioresour. Technol.* 99(10), 4044-4064. <https://doi.org/http://dx.doi.org/10.1016/j.biortech.2007.01.057>.
- de Nardi, I.R., Varesche, M.B.A., Zaiat, M., Foresti, E., 2002. Anaerobic degradation of BTEX in a packed-bed reactor. *Water Sci. Technol.* 45(10), 175-180. <https://doi.org/10.2166/wst.2002.0323> %J Water Science and Technology.
- Dereli, R.K., Ersahin, M.E., Ozgun, H., Ozturk, I., Jeison, D., van der Zee, F., van Lier, J.B., 2012. Potentials of anaerobic membrane bioreactors to overcome treatment limitations induced by industrial wastewaters. *Bioresour. Technol.* 122, 160-170. <https://doi.org/10.1016/j.biortech.2012.05.139>.
- Dhar, K., Subashchandrabose, S.R., Venkateswarlu, K., Krishnan, K., Megharaj, M., 2020. Anaerobic Microbial Degradation of Polycyclic Aromatic Hydrocarbons: A Comprehensive Review, in: de Voogt, P. (Ed.) *Reviews of Environmental Contamination and Toxicology Volume 251*. Springer International Publishing, Cham, pp. 25-108. https://doi.org/10.1007/398_2019_29.
- Dvořák, L., Gómez, M., Dolina, J., Černín, A., 2015. Anaerobic membrane bioreactors—a mini review with emphasis on industrial wastewater treatment: applications, limitations and perspectives. *Desalination Water Treat.*, 1-15. <https://doi.org/https://doi.org/10.1080/19443994.2015.1100879>.
- Falcioni, T., Manti, A., Boi, P., Canonico, B., Balsamo, M., Papa, S., 2006. Comparison of disruption procedures for enumeration of activated sludge floc bacteria by flow cytometry. *Cytometry B Clin Cytom* 70(3), 149-153. <https://doi.org/10.1002/cyto.b.20097>.
- Foght, J., 2008. Anaerobic biodegradation of aromatic hydrocarbons: pathways and prospects. *J. Mol. Microbiol. Biotechnol.* 15(2-3), 93-120. <https://doi.org/10.1159/000121324>.
- Fuchedzhieva, N., Karakashev, D., Angelidaki, I., 2008. Anaerobic biodegradation of fluoranthene under methanogenic conditions in presence of surface-active compounds. *J. Hazard. Mater.* 153(1), 123-127. <https://doi.org/https://doi.org/10.1016/j.jhazmat.2007.08.027>.
- García-Mancha, N., Puyol, D., Monsalvo, V.M., Rajhi, H., Mohedano, A.F., Rodriguez, J.J., 2012. Anaerobic treatment of wastewater from used industrial oil recovery. *J. Chem. Technol. Biotechnol.* 87(9), 1320-1328. <https://doi.org/10.1002/jctb.3753>.
- García Rea, V.S., Egerland Bueno, B., Cerqueda-García, D., Muñoz Sierra, J.D., Spanjers, H., van Lier, J.B., 2022. Degradation of p-cresol, resorcinol, and phenol in anaerobic membrane bioreactors under saline conditions. *Chem. Eng. J.* 430, 132672. <https://doi.org/https://doi.org/10.1016/j.cej.2021.132672>.
- García Rea, V.S., Muñoz Sierra, J.D., Fonseca Aponte, L.M., Cerqueda-García, D., Quchani, K.M., Spanjers, H., van Lier, J.B., 2020. Enhancing Phenol Conversion Rates in Saline Anaerobic Membrane Bioreactor Using Acetate and Butyrate as Additional Carbon and Energy Sources. *Front. Microbiol.* 11(2958). <https://doi.org/10.3389/fmicb.2020.604173>.
- Gasim, H., Kutty, S., Isa, M.H., 2012. Anaerobic treatment of petroleum refinery wastewater. *Int. J. Chem. Mol. Eng.* 6(8), 512-515.
- Guyot, J.P., Macarie, H., Noyola, A., 1990. Anaerobic digestion Of a Petrochemical Wastewater using the UASB process. *Appl. Biochem. Biotechnol.* 24(1), 579-589. <https://doi.org/10.1007/BF02920280>.
- Hendriks, A.T.W.M., van Lier, J.B., de Kreuk, M.K., 2018. Growth media in anaerobic fermentative processes: The underestimated potential of thermophilic fermentation and anaerobic digestion. *Biotechnol. Adv.* 36(1), 1-13. <https://doi.org/https://doi.org/10.1016/j.biotechadv.2017.08.004>.

- Jafarzadeh, M.T., Mehrdadi, N., Hashemian, S.J., 2012. Application of an anaerobic hybrid reactor for petrochemical effluent treatment. *Water Sci. Technol.* 65(12), 2098-2105. <https://doi.org/10.2166/wst.2012.088>.
- Ji, Q., Tabassum, S., Hena, S., Silva, C.G., Yu, G., Zhang, Z., 2016. A review on the coal gasification wastewater treatment technologies: past, present and future outlook. *J. Clean. Prod.* 126, 38-55. <https://doi.org/https://doi.org/10.1016/j.jclepro.2016.02.147>.
- Kleerebezem, R., Beckers, J., Hulshoff Pol, L.W., Lettinga, G., 2005. High rate treatment of terephthalic acid production wastewater in a two-stage anaerobic bioreactor. *Biotechnol. Bioeng.* 91(2), 169-179. <https://doi.org/10.1002/bit.20502>.
- Knapp, J.S., Bromley-Challoner, K.C.A., 2003. 34 - Recalcitrant organic compounds, in: Mara, D., Horan, N. (Eds.), *Handbook of Water and Wastewater Microbiology*. Academic Press, London, pp. 559-595. <https://doi.org/https://doi.org/10.1016/B978-012470100-7/50035-2>.
- Kraiselburd, I., Bröls, T., Heilmann, G., Kaschani, F., Kaiser, M., Meckenstock, R.U., 2019. Metabolic reconstruction of the genome of candidate *Desulfatiglans TRIP_1* and identification of key candidate enzymes for anaerobic phenanthrene degradation. *Environ. Microbiol.* 21(4), 1267-1286. <https://doi.org/https://doi.org/10.1111/1462-2920.14527>.
- Ladino-Orjuela, G., Gomes, E., da Silva, R., Salt, C., Parsons, J.R., 2016. Metabolic Pathways for Degradation of Aromatic Hydrocarbons by Bacteria, *Reviews of Environmental Contamination and Toxicology* Volume 237. Springer, pp. 105-121. https://doi.org/https://doi.org/10.1007/978-3-319-23573-8_5.
- Lee, J., Hwang, S., 2019. Single and combined inhibition of *Methanosaeta concilii* by ammonia, sodium ion and hydrogen sulfide. *Bioresour. Technol.* 281, 401-411. <https://doi.org/https://doi.org/10.1016/j.biortech.2019.02.106>.
- Li, Y., Tabassum, S., Chu, C., Zhang, Z., 2018. Inhibitory effect of high phenol concentration in treating coal gasification wastewater in anaerobic biofilter. *J. Environ. Sci.* 64, 207-215. <https://doi.org/https://doi.org/10.1016/j.jes.2017.06.001>.
- Lin, C., Wu, P., Liu, Y., Wong, J.W.C., Yong, X., Wu, X., Xie, X., Jia, H., Zhou, J., 2019. Enhanced biogas production and biodegradation of phenanthrene in wastewater sludge treated anaerobic digestion reactors fitted with a bioelectrode system. *Chem. Eng. J.* 365, 1-9. <https://doi.org/https://doi.org/10.1016/j.cej.2019.02.027>.
- Macarie, H., 2000. Overview of the application of anaerobic treatment to chemical and petrochemical wastewaters. *Water Sci. Technol.* 42(5-6), 201-214. <https://doi.org/https://doi.org/10.2166/wst.2000.0515>.
- Mallick, H., Rahnavard, A., McIver, L.J., Ma, S., Zhang, Y., Nguyen, L.H., Tickle, T.L., Weingart, G., Ren, B., Schwager, E.H., Chatterjee, S., Thompson, K.N., Wilkinson, J.E., Subramanian, A., Lu, Y., Waldron, L., Paulson, J.N., Franzosa, E.A., Bravo, H.C., Huttenhower, C., 2021. Multivariable association discovery in population-scale meta-omics studies. *PLOS Computational Biology* 17(11), e1009442. <https://doi.org/10.1371/journal.pcbi.1009442>.
- McInerney, M.J., Rohlin, L., Mouttaki, H., Kim, U., Krupp, R.S., Rios-Hernandez, L., Sieber, J., Struchtemeyer, C.G., Bhattacharyya, A., Campbell, J.W., Gunsalus, R.P., 2007. The genome of *Syntrophus aciditrophicus*: life at the thermodynamic limit of microbial growth. *Proc. Natl. Acad. Sci. U.S.A.* 104(18), 7600-7605. <https://doi.org/10.1073/pnas.0610456104>.
- Meckenstock, R.U., Mouttaki, H., 2011. Anaerobic degradation of non-substituted aromatic hydrocarbons. *Curr. Opin. Biotechnol.* 22(3), 406-414. <https://doi.org/10.1016/j.copbio.2011.02.009>.
- Meckenstock, R.U., Safinowski, M., Griebler, C., 2004. Anaerobic degradation of polycyclic aromatic hydrocarbons. *FEMS Microbiol. Ecol.* 49(1), 27-36. <https://doi.org/10.1016/j.femsec.2004.02.019>.

- Muñoz Sierra, J.D., García Rea, V.S., Cerqueda-García, D., Spanjers, H., van Lier, J.B., 2020. Anaerobic Conversion of Saline Phenol-Containing Wastewater Under Thermophilic Conditions in a Membrane Bioreactor. *Front. Bioeng. Biotechnol.* 8(1125). <https://doi.org/10.3389/fbioe.2020.565311>.
- Muñoz Sierra, J.D., Oosterkamp, M.J., Wang, W., Spanjers, H., van Lier, J.B., 2018. Impact of long-term salinity exposure in anaerobic membrane bioreactors treating phenolic wastewater: Performance robustness and endured microbial community. *Water Res.* 141, 172-184. <https://doi.org/https://doi.org/10.1016/j.watres.2018.05.006>.
- Mutamim, N.S.A., Noor, Z.Z., Hassan, M.A.A., Yuniarto, A., Olsson, G., 2013. Membrane bioreactor: Applications and limitations in treating high strength industrial wastewater. *Chem. Eng. J.* 225, 109-119. <https://doi.org/http://dx.doi.org/10.1016/j.cej.2013.02.131>.
- Narihiro, T., Nobu, M.K., Kim, N.K., Kamagata, Y., Liu, W.T., 2015. The nexus of syntrophy-associated microbiota in anaerobic digestion revealed by long-term enrichment and community survey. *Environ. Microbiol.* 17(5), 1707-1720. <https://doi.org/10.1111/1462-2920.12616>.
- Nobu, M.K., Narihiro, T., Hideyuki, T., Qiu, Y.L., Sekiguchi, Y., Woyke, T., Goodwin, L., Davenport, K.W., Kamagata, Y., Liu, W.T., 2015. The genome of *Syntrophorhabdus aromaticivorans* strain UI provides new insights for syntrophic aromatic compound metabolism and electron flow. *Environ. Microbiol.* 17(12), 4861-4872. <https://doi.org/10.1111/1462-2920.12444>.
- Noyola, A., Macarie, H., Varela, F., Landrieu, S., Marcelo, R., Rosas, M.A., 2000. Upgrade of a petrochemical wastewater treatment plant by an upflow anaerobic pond. *Water Sci. Technol.* 42(5-6), 269-276. <https://doi.org/10.2166/wst.2000.0523> %J Water Science and Technology.
- Olguin-Lora, P., Puig-Grajales, L., Razo-Flores, E., 2003. Inhibition of the acetoclastic methanogenic activity by phenol and alkyl phenols. *Environ. Technol.* 24, 999-1006. <https://doi.org/10.1080/09593330309385638>.
- Philipp, B., Schink, B., 2012. Different strategies in anaerobic biodegradation of aromatic compounds: nitrate reducers versus strict anaerobes. *Environ. Microbiol. Rep.* 4(5), 469-478. <https://doi.org/10.1111/j.1758-2229.2011.00304.x>.
- Porter, A.W., Young, L.Y., 2014. Chapter Five - Benzoyl-CoA, a Universal Biomarker for Anaerobic Degradation of Aromatic Compounds, in: Sariaslani, S., Gadd, G.M. (Eds.), *Adv. Appl. Microbiol.* Academic Press, pp. 167-203. <https://doi.org/https://doi.org/10.1016/B978-0-12-800260-5.00005-X>.
- Qiu, Y.L., Hanada, S., Ohashi, A., Harada, H., Kamagata, Y., Sekiguchi, Y., 2008. *Syntrophorhabdus aromaticivorans* gen. nov., sp. nov., the first cultured anaerobe capable of degrading phenol to acetate in obligate syntrophic associations with a hydrogenotrophic methanogen. *Appl. Environ. Microbiol.* 74(7), 2051-2058. <https://doi.org/10.1128/aem.02378-07>.
- Rabus, R., Hansen, T.A., Widdel, F., 2006. Dissimilatory Sulfate- and Sulfur-Reducing Prokaryotes, in: Dworkin, M., Falkow, S., Rosenberg, E., Schleifer, K.-H., Stackebrandt, E. (Eds.), *The Prokaryotes: Volume 2: Ecophysiology and Biochemistry*. Springer New York, New York, NY, pp. 659-768. https://doi.org/10.1007/0-387-30742-7_22.
- Rand, M.C., Greenberg, A.E., Taras, M.J., 1976. Standard methods for the examination of water and wastewater. 14th edition. Prepared and published jointly by American Public Health Association, American Water Works Association, and Water Pollution Control Federation.
- Ribeiro, R., de Nardi, I.R., Fernandes, B.S., Foresti, E., Zaiat, M., 2013. BTEX removal in a horizontal-flow anaerobic immobilized biomass reactor under denitrifying conditions. *Biodegradation* 24(2), 269-278. <https://doi.org/10.1007/s10532-012-9585-2>.
- Roy, T.A., Kriech, A.J., Mackerer, C.R., 2007. Percutaneous Absorption of Polycyclic Aromatic Compounds from Bitumen Fume Condensate. *J. Occup. Environ. Hyg.* 4(sup1), 137-143. <https://doi.org/10.1080/15459620701334814>.

- Ruan, M.-Y., Liang, B., Mbadinga, S.M., Zhou, L., Wang, L.-Y., Liu, J.-F., Gu, J.-D., Mu, B.-Z., 2016. Molecular diversity of bacterial *bamA* gene involved in anaerobic degradation of aromatic hydrocarbons in mesophilic petroleum reservoirs. *Int. Biodeterior. Biodegrad.* 114, 122-128. <https://doi.org/https://doi.org/10.1016/j.ibiod.2016.06.005>.
- Singer, P.C., Pfaender, F.K., Chinchilli, J., Maciorowski III, A.F., J.C.L, G., R., 1978. Assessment of Coal Conversion Wastewaters: Characterization and Preliminary Biotreatability. , in: EPA, E. (Ed.). U.S. Washington D.C.
- Spanjers, H., Vanrolleghem, P.A., 2016. Respirometry, in: Brdjanovic, D., Nielsen, P.H., López-Vazquez, C.M., van Loosdrecht, M.C.M. (Eds.), *Experimental Methods in Wastewater Treatment*. IWA Publishing. <https://doi.org/https://doi.org/10.2166/9781780404752>.
- Stergar, V., Zagorc-Koncan, J., Zgajnar-Gotvanj, A., 2003. Laboratory scale and pilot plant study on treatment of toxic wastewater from the petrochemical industry by UASB reactors. *Water Sci. Technol.* 48(8), 97-102. <https://doi.org/https://doi.org/10.2166/wst.2003.0457>.
- Tian, X., Song, Y., Shen, Z., Zhou, Y., Wang, K., Jin, X., Han, Z., Liu, T., 2020. A comprehensive review on toxic petrochemical wastewater pretreatment and advanced treatment. *J. Clean. Prod.* 245, 118692. <https://doi.org/https://doi.org/10.1016/j.jclepro.2019.118692>.
- Tsai, J.-C., Kumar, M., Lin, J.-G., 2009. Anaerobic biotransformation of fluorene and phenanthrene by sulfate-reducing bacteria and identification of biotransformation pathway. *J. Hazard. Mater.* 164(2), 847-855. <https://doi.org/https://doi.org/10.1016/j.jhazmat.2008.08.101>.
- Wang, J., Wu, B., Sierra, J.M., He, C., Hu, Z., Wang, W., 2020. Influence of particle size distribution on anaerobic degradation of phenol and analysis of methanogenic microbial community. *Environ. Sci. Pollut. Res.* 27(10), 10391-10403. <https://doi.org/10.1007/s11356-020-07665-z>.
- Wang, W., Han, H., Yuan, M., Li, H., 2010. Enhanced anaerobic biodegradability of real coal gasification wastewater with methanol addition. *J. Environ. Sci. (China)* 22(12), 1868-1874. [https://doi.org/https://doi.org/10.1016/S1001-0742\(09\)60327-2](https://doi.org/https://doi.org/10.1016/S1001-0742(09)60327-2).
- Wang, W., Han, H., Yuan, M., Li, H., Fang, F., Wang, K., 2011. Treatment of coal gasification wastewater by a two-continuous UASB system with step-feed for COD and phenols removal. *Bioresour. Technol.* 102(9), 5454-5460. <https://doi.org/https://doi.org/10.1016/j.biortech.2010.10.019>.
- Wang, W., Wu, B., Pan, S., Yang, K., Hu, Z., Yuan, S., 2017. Performance robustness of the UASB reactors treating saline phenolic wastewater and analysis of microbial community structure. *J. Hazard. Mater.* 331, 21-27. <https://doi.org/https://doi.org/10.1016/j.jhazmat.2017.02.025>.
- Wang, W., Yang, Q., Zheng, S., Wu, D., 2013. Anaerobic membrane bioreactor (AnMBR) for bamboo industry wastewater treatment. *Bioresour. Technol.* 149, 292-300. <https://doi.org/10.1016/j.biortech.2013.09.068>.
- Wegmann, U., Nueno Palop, C., Mayer, M.J., Crost, E., Narbad, A., 2017. Complete Genome Sequence of *Desulfovibrio piger* FI11049. *Genome Announc* 5(7). <https://doi.org/10.1128/genomeA.01528-16>.
- Zhang, C., Bennett, G.N., 2005. Biodegradation of xenobiotics by anaerobic bacteria. *Appl. Microbiol. Biotechnol.* 67(5), 600-618. <https://doi.org/10.1007/s00253-004-1864-3>.
- Zhu, H., Han, Y., Ma, W., Han, H., Ma, W., Xu, C., 2018. New insights into enhanced anaerobic degradation of coal gasification wastewater (CGW) with the assistance of graphene. *Bioresour. Technol.* 262, 302-309. <https://doi.org/https://doi.org/10.1016/j.biortech.2018.04.080>.



Chapter 6

Conclusions, outlook,
and recommendations

6.1 Conclusions

The objective of this thesis was to investigate the anaerobic degradation of selected aromatic compounds, including phenol, *p*-cresol, and resorcinol, as well as petrochemical wastewater, by utilizing membrane bioreactors. Phenol degradation was researched at two different temperatures corresponding to the mesophilic (35 °C) and the thermophilic (55 °C) operation ranges. The simultaneous degradation of *p*-cresol and resorcinol with phenol was studied, and the toxic and inhibitory effects of *p*-cresol and resorcinol on phenol-degrading biomass were assessed. Thermodynamic analyses of the bioconversion of aromatic compounds and microbial community analyses were conducted to understand and explain the results obtained during the reactor operation. Finally, the AnMBR was employed for the treatment of bitumen fume condensate (BFC), a petrochemical wastewater produced at a Dutch asphalt industry. In summary, the following conclusions were drawn:

1. Under saline anaerobic conditions, the specific conversion rate of the toxic and inhibitory compound, phenol, was enhanced through the dosage of easily biodegradable carbon and energy sources, namely, acetate and butyrate. Acetate and an acetate-butyrate mixture increased the specific phenol conversion rate (sPhCR) in comparison to the control reactor in which phenol was the sole carbon and energy source. Specific phenol conversion rates of 115 and 210 mgPh·gVSS⁻¹·d⁻¹ were observed for the reactors simultaneously fed with phenol and acetate [2 gCOD·L⁻¹] and with phenol and the 2:1 acetate butyrate mixture [2 gCOD·L⁻¹], respectively (Chapter 2).

2. Efficient and effective degradation of phenol required the presence of an active, abundant, and robust methanogenic population in the reactor's biomass. The development of an abundant methanogenic population in the reactor's biomass was considered crucial to enhance the sPhCR, when phenol was simultaneously degraded with acetate or an acetate:butyrate mixture. It was hypothesized that acetoclastic and hydrogenotrophic methanogens act as either acetate-consumers or ubiquitous electron sink, respectively, in the syntrophic conversion of intermediates from phenol conversion, ensuring stable phenol degradation rates. Depending on the temperature conditions of the reactor during its operation, either acetoclastic (mesophilic) or hydrogenotrophic (thermophilic) methanogenesis will be essential for maintaining the optimal thermodynamic conditions for phenol degradation (Chapter 2 and 3).

3. The specific phenol conversion rate and phenol removal efficiency of an AnMBR operated under saline thermophilic conditions was lower than those of an AnMBR operated under saline mesophilic conditions. The maximum sPhCR calculated for the thermophilic reactor was 29 mgPh·gVSS⁻¹·d⁻¹. This value was considerably lower than

the sPhCR calculated for the mesophilic reactor, with a maximum of 115 mgPh·gVSS⁻¹·d⁻¹ (Chapter 2). The result agrees with the inability of specific phenol degraders, such as *Syntrophorhabdus* to grow under saline thermophilic conditions (Chapter 3).

4. The methanogenic activity in an AnMBR operated under saline thermophilic conditions was mainly hydrogenotrophic and not acetoclastic, whereas acetate degradation occurred mainly via syntrophic acetate oxidation. The ¹³C carbon originating from the labelled acetate (¹²CH₃¹³COO⁻) was detected in the methane produced within the reactor. Furthermore, the microbial community and the archaeal population analyses showed an abundant presence of hydrogenotrophic methanogens and syntrophic acetate oxidizers. Under thermophilic conditions, it was observed that the hydrogenotrophic methanogens were primarily responsible for maintaining favorable thermodynamics for the involved biochemical reactions, thereby enhancing syntrophic conversions (Chapter 3).

5. Presented results strongly indicated that phenol degradation followed the benzoyl-CoA and not the caproate pathway in an AnMBR under saline thermophilic conditions. The analysis performed in the permeate of the AnMBR operated at 55 °C showed the presence of benzoate, whereas no caproate was detected during the experiment (Chapter 3).

6. The salt-adapted phenol-degrading biomass had a broader catabolic activity than expected as it was able to degrade compounds to which the biomass was not previously exposed, namely *p*-cresol and resorcinol. The degradation of *p*-cresol by the salt-adapted phenol degrading biomass originating from the AnMBR was anticipated because *p*-cresol shares the same metabolic pathway as phenol, namely, the benzoyl-CoA pathway. However, resorcinol is a compound that is characterized by a different degradation pathway. In addition, the AnMBR's biomass was capable of degrading resorcinol without a lag time in both batch tests and continuous flow tests. Microbial community analysis and PCoA corroborated the phylogenetic similarity of the phenol-*p*-cresol and the phenol-resorcinol microbial communities (Chapter 4 and 5).

7. The salt-adapted phenol-degrading biomass exhibited higher specific *p*-cresol conversion rates in comparison to the specific resorcinol conversion rates. Maximum specific in-situ conversion rates of 22 mg_{*p*-cresol}·gVSS⁻¹·d⁻¹ and 16 mg_{resorcinol}·gVSS⁻¹·d⁻¹ were calculated from the data obtained during the operation of AnMBRs degrading mixtures of *p*-cresol-phenol and resorcinol-phenol, respectively, under saline conditions (Chapter 4). Amplicon sequencing analysis (16S rRNA gene) showed no phylogenetic differences between the microbial communities in both reactors. Likely, the same

microorganisms might have been responsible for the phenol, *p*-cresol, and resorcinol degradation (Chapter 4).

8. A previous exposure of the anaerobic biomass to phenol resulted in increased tolerance to other inhibitory and toxic petrochemical compounds, including those in a complex matrix such as the bitumen fume condensate wastewater. The phenol-degrading AnMBR biomass showed higher resilience, lower degree of membrane damage, and lower inhibition of its acetoclastic methanogenic activity in comparison to non-adapted granular or suspended degrading biomass (Chapter 4 and 5), when the biomass was exposed to other toxic and inhibitory aromatic compounds, namely *p*-cresol (Chapter 4), resorcinol (Chapter 4), or the mixture of (non-)aromatic compounds in the BFC (Chapter 2).

9. The inhibition exerted by *p*-cresol on anaerobic biomass was related to a biocidal effect, whereas the inhibition exerted by resorcinol was related to a biostatic effect. The salt-adapted phenol-degrading anaerobic biomass harvested from an AnMBR showed IC_{50} values of $0.73 \text{ g}_{\text{p-cresol}} \cdot \text{L}^{-1}$ and $3.00 \text{ g}_{\text{resorcinol}} \cdot \text{L}^{-1}$, whereas the anaerobic biomass obtained from a municipal sewage sludge digester showed IC_{50} values of $0.60 \text{ g}_{\text{p-cresol}} \cdot \text{L}^{-1}$ and $0.25 \text{ g}_{\text{resorcinol}} \cdot \text{L}^{-1}$. Increasing *p*-cresol concentrations decreased the percentage of non-damaged cells in both biomass types, whereas resorcinol had a minor effect on the percentage of non-damaged cells (Chapter 4).

10. BFC is a highly complex petrochemical wastewater matrix with more than 900 organic and inorganic compounds. The targeted and non-targeted analyses of the BFC revealed a high diversity of pollutants with organic compounds, such as aromatics and PAHs, being the most prevalent. The ICP-MS analyses also showed the presence of iron, sulfur, and silicon (Chapter 5).

11. The AnMBR showed to be a robust system for the treatment of BFC. The AnMBR exhibited high COD removal efficiencies during the 188 days of continuous operation with BFC as the substrate (Chapter 5). During the operational period of the AnMBR, a sludge loading rate of $97 \text{ mgCOD} \cdot \text{gVSS}^{-1} \cdot \text{d}^{-1}$ was applied leading to an COD removal efficiency of 88%.

6.2 Outlook and research recommendations

Anaerobic digestion is increasingly being applied in the treatment of industrial wastewaters that were previously deemed unsuitable for (anaerobic) biological systems, because of their high content of toxic and inhibitory compounds, and their frequent high salinity and temperature. In high-rate anaerobic treatment, sludge

bed or expanded bed bioreactors are commonly preferred. However, when biomass retention cannot be guaranteed and biofilm formation, either in the form of granules or grown on a carrier material, is non-viable or highly compromised, membrane bioreactors offer a more appropriate solution. Furthermore, AnMBRs are considered the most suitable option when aiming for high conversion rates of biodegradable toxic or inhibitory compounds. By applying completely mixed conditions, toxicant concentrations in the AnMBR sludge are at very low and non-inhibitory levels. Moreover, with toxic or inhibitory wastewaters the bioconversion process is generally of greater concern than the membrane filtration process. As discussed in this thesis, (petro)chemical wastewater is often discharged with extreme characteristics for biological treatment. Therefore, based on the present work, it is concluded that the AnMBR technology can be regarded as the best option for the treatment of such wastewater. It is foreseen, that AnMBR application on (petro)chemical wastewater will expand the current limits of anaerobic digestion.

6.2.1 Safety recommendations for working with toxic compounds

6.2.1.1 Safety at work

Anyone working in a lab environment, at pilot reactor facilities, or in the surrounding area must follow the local health and safety regulations. General considerations must be considered, for example, 1) no allowance for eating and/or drinking in these testing facilities; 2) keep the working space tidy and ordered, 3) keep walking pathways free of obstacles, 4) keep personal hygiene, 5) use personal protection equipment when needed, 6) take into account warning signs and safety instructions, 7) wear a portable gas detector when no active ventilation and no fixed gas detectors are available in the working space, 8) avoid the use of jewelry, for example, rings when working in the laboratory, 9) keep long hair tied back and do not wear any headwear, 11) wear jeans and fully closed shoes, 10) do not use any type of headsets during the work in the laboratory.

6.2.1.2 Chemicals

Several toxic compounds, for example, phenol, p-cresol, resorcinol, and BFC, were handled during the experiments conducted for this PhD research. Safety measurements and regulations should always be followed to avoid any unsafe situation. Before starting to work with any of the mentioned compounds read the corresponding material safety and data sheets.

Phenol: <https://www.sigmaaldrich.com/NL/en/sds/sial/p5566/>.

p-Cresol: <https://www.sigmaaldrich.com/NL/en/sds/sigald/c85751>.

Resorcinol: <https://www.sigmaaldrich.com/NL/en/sds/sial/307521>.

In case of any chemical spills on the skin or eyes, the affected part(s) should be immediately rinsed with tap water for at least 15 minutes. Therefore, the availability of safety equipment should be confirmed before starting the work with toxic compounds. Showers and eye washers should be easily reachable at the working place or close to the place where the chemicals are used and/or stored.

The use of personal protective equipment (PPE) is mandatory while working with the toxic compounds. For example, gloves (preferable nitrile), protection glasses, and a lab coat should always be used in the working place.

Dangerous gases and vapors may be released during the handling procedures of the chemicals, in the off-gases of the reactor, or during sampling. The use of a filter mask respirator with organic vapor cartridges is recommended when working with concentrated chemicals, for example, during the preparation of the feeding medium. Do not touch the filter mask respirator with the used gloves to avoid any possible contamination.

6.2.1.3 Guidelines in case of chemical spill

Alert people in the immediate area in case of a chemical spill. Use PPE as gloves, protection glasses, lab coat, and filter mask respirator to perform any cleaning activity. Confine the spill to the smallest area possible. Use appropriate equipment to absorb the spillage. Collect the residual and place it in the correct container to be disposed as chemical waste. Dispose of all the contaminated material, for example, gloves. Wash your hands properly. Wash your clothes as soon as possible.

6.2.2 Guidance for practical application: results implication

Currently, there is an increased interest of chemical companies to apply anaerobic digestion for the treatment of their wastewater. However, the full-scale application of AD for the treatment of (petro)chemical industrial wastewater may be hindered due to factors such as low biodegradability together with low conversion rates of certain toxic or inhibitory organic compounds and decrease in the biomass activity due to the wastewater characteristics. The enhancement of the degradation of toxic and inhibitory compounds is, therefore, an important topic to widen the application potential of full-scale anaerobic technology for the treatment of industrial (petro) chemical wastewater.

The development of a robust methanogenic population is needed for an enhanced degradation of (a model) toxic and inhibitory compound such as phenol. The dosage of additional CES in the form of acetate and butyrate showed an improvement in

the specific phenol conversion rate in comparison to the degradation of phenol as the sole CES. The obtained results are of high interest for practice as they allowed us to have a better understanding of the effect of easily biodegradable CES on the phenol conversion efficacy and on the microbial community associated to it. Nevertheless, for full-scale installations, there might be a reluctance towards the addition of extra reagents that will bring more operational costs. However, in many chemical wastewaters, acetate (which was also used in this thesis research) is present in concentrations of interest. In case the toxic stream does not contain any easily biodegradable CES, a clear possibility arises in the simultaneous degradation of streams that contain toxic and inhibitory compounds and streams comprising easily biodegradable CES. These process schemes may be considered in industrial parks in which different waste streams containing a variety of pollutants are produced by the companies located at the park. The overall objective of simultaneous digestion of toxic or recalcitrant compounds with easily biodegradable CES is the development of an abundant, active, and robust methanogenic population. With a properly functioning methanogenic population, and thus methanogenic biochemical conversion step, it is ensured that the syntrophic relationships needed to achieve the degradation of the toxic compounds will be present in the reactor.

Results clearly showed that the treatment of thermophilic saline phenolic wastewater is possible provided a robust methanogenic ecosystem is ensured. Under saline thermophilic conditions, the methanogenic population will mainly comprise hydrogenotrophic instead of acetoclastic archaea. Very likely, the hydrogenotrophic population will be provided with the required reducing equivalents from an easily degradable COD source, for example acetate, which is syntrophically oxidized via H_2/CO_2 . Hence, other specific microbial populations, such as SAOB, will then play a more pronounced role in the conversion process.

In the current situation and considering a near future in which energy becomes more expensive, the gained knowledge in this thesis offers useful applications. As previously suggested, the simultaneous degradation of phenolic streams under thermophilic conditions with acetate-rich waste streams may be a possibility. As mentioned, in many chemical wastewater streams, acetate is commonly found, such as rubber vulcanization wastewater, having temperatures exceeding 40 °C (Yeoh et al., 2002). In addition, acetate is the central intermediate, or precursor, for methanogenesis, which means that practically, any additional COD will generate acetate. Particularly for phenol conversion, and possibly other toxic and inhibitory compounds, higher efficiencies and (specific) loading & conversion rates are expected under mesophilic

conditions. However, when recovery of hot process wastewater is anticipated, the thermophilic digestion route might be considered as most beneficial.

Commonly, the wastewater coming from (petro)chemical industries will comprise a wide variety of pollutants. Therefore, the degradation of a broader number of compounds (COD) present in the wastewater will imply a more successful application of the proposed treatment method. Pollutants with similar structures may share degradation pathways; however, due to the diversity of the chemical compounds in such wastewater, many of them may follow different degradation routes. The development of a microbial community that can be used as starting (seeding) material for the degradation of several toxic or inhibitory compounds may therefore provide advantages for the proposed treatment process.

The degradation of resorcinol by phenol-degrading biomass opens the possibilities to grow biomass using model toxic and inhibitory compounds and further use it for the degradation of a broader range of pollutants/substrates in different wastewater types. Of similar importance is that the previous acclimation to phenol conferred the methanogens a higher resistance to the inhibitory effects of the two other compounds, *p*-cresol and resorcinol, to which the microorganisms were not previously exposed. Similarly, the phenol-degrading biomass showed a higher resistance to the toxic effects of the BFC.

The BFC wastewater comprises a complex matrix of diverse organic and inorganic pollutants. Although, the main compounds were found to be organics, which, as shown by detailed analytical work, were principally aromatics. The treatment of such a complex waste stream will most likely represent a challenge to granular sludge bed reactors due to the wastewater components and the toxic and inhibitory effects that they can be exerted onto the biomass. Besides low biomass growth rate and yield, biomass degranulation and washout, and therefore poor reactor performance are expected if granular sludge bed-reactors are used for the treatment of wastewater such as the BFC. In full-scale operation, therefore, a continuous reseedling of granular sludge should be foreseen. Consequently, more time will be needed to adapt the newly seeded biomass to the prevalent conditions and more expenses will be needed for the acquisition of new sludge. To prevent a sudden lack of biomass, a biomass buffer tank should be considered in full-scale projects, implying higher CaPex. In the proposed AnMBR technology, all biomass will be effectively retained and the aforementioned problems will be less apparent.

6.2.3 *Guidance for practical application: full-scale implementation*

The design of full-scale AnMBRs will be based on the same principle as granular sludge bed technology. Namely, by delimiting a design sludge loading rate (SLR) that might be in the range of $0.2 - 0.5 \text{ kgCOD} \cdot \text{kgVSS}^{-1} \cdot \text{d}^{-1}$, approximately, based on the average specific methanogenic activity of anaerobic granular sludge (van Lier et al., 2020). The organic loading rate (OLR) ($\text{kgCOD} \cdot \text{m}^{-3} \cdot \text{d}^{-1}$) will depend on the nature of pollutants, the biomass quantity (concentration) and specific methanogenic activity. In addition, a design membrane flux should be defined that might range between the $10 - 20 \text{ LMH}$ (van Lier et al., 2019). Based on the design flux and wastewater flow, then, the required membrane area can be calculated. It should be noted that the SLR is likely lower during the treatment of (petro)chemical wastewater in which the conversion of COD, consisting of the toxic and/or inhibitory pollutants in the wastewater, will have a higher importance than achieving the highest OLR of the reactor.

Depending on the wastewater characteristics, an equalization/conditioning tank might be considered, in which part of the COD is simultaneously converted into VFA prior to the reactor feeding. However, that part of the COD could also act as additional CES, stimulating the anaerobic degradation of substrates, such as phenol and phenolics. Therefore, the size of such equalization tank should be as low as possible.

In the operation of the full-scale AnMBR installation, it is recommended to continuously monitor the process parameters such as COD removal efficiency, VFA and alkalinity, and (macro)nutrients concentrations in the effluent, particularly when complex wastewater matrices are treated. Furthermore, any additional information obtained in ex-situ batch tests, such as the IC_{50} values, can be used to assess the maximum allowable in-reactor concentrations for certain pollutants. Following the results of these batch tests, the SLR should be kept in a value in which no build-up of inhibitory or toxic compounds will be observed, or in which the concentrations will be maintained below inhibitory or toxic levels. Similarly, membrane fluxes and TMP as indicators for membrane fouling and clogging should be continuously monitored. The latter parameters will give insight in the applicable membrane operational cycles and required chemical cleaning cycles to maintain the maximum allowable membrane fluxes.

The application of AnMBRs at full-scale is still in development. Currently, the main constraints for the application of AnMBRs in full-scale are related to the CaPex and OpEx, inherently coupled to membrane filtration systems. Advances in material sciences may possibly decrease operational problems related to membrane fouling and allow the AnMBRs to reach and sustain high operational fluxes. Thus far, the

application of AnMBRs is restricted to a specific niche of complex wastewaters that, because of its characteristics, hampers, disrupts, or inhibits the biomass granulation process in conventional sludge bed reactors.

6.2.4 Research recommendations

The following topics are suggested for further investigation, following up on the conclusions of the research conducted in this project:

Other COD sources such as carbohydrates (mono-, di-, and complex saccharides) may be tested to determine their effect on the degradation of phenol or other aromatic compounds, either when targeting the degradation of one compound, or in mixtures. However, it should be noted that this recommendation is based on scientific curiosity rather than industrial application. In full-scale, the addition of carbohydrates as additional carbon and energy source is less likely to be implemented, or will even be avoided to reduce capex and opex of the installation.

The effect of CO_2 or hydrogen supplementation may be tested for the enhancement of the degradation of phenol or other phenolic compounds under mesophilic and thermophilic conditions. It has previously been reported that CO_2 is needed for phenol carboxylation (Fuchs, 2008) and that phenol degradation depends on CO_2 (Karlsson et al., 2000). Similarly, it has been suggested that hydrogen supplementation may have an enhancing effect on phenol degradation (Karlsson et al., 1999). High-pressure reactors (Ceron-Chafla et al., 2020) can be used to investigate whether increased CO_2 or H_2 partial pressures would lead to accelerated conversion rates, for example, by increasing phenol carboxylation rate or reductive aromatic ring splitting. It should be noted that both carboxylation and the reductive ring splitting are intracellular processes.

Phosphates were used as a pH buffer during the experiments reported in this thesis. However, carboxylation is a key step during the anaerobic degradation of aromatic compounds, and it has been suggested that CO_2 , HCO_3^- , or CO_3^{2-} might have a positive effect in the phenol degradation process (Karlsson et al., 2000). Therefore, the use of carbonate buffer is recommended for future experiments.

The use of ^{13}C -labeled isotopic molecules such as acetate or phenol is recommended for the study of the metabolism of the molecules by the use of stable isotope probing (SIP) (Wang and Yao, 2021; Deng et al., 2023). For example, ^{13}C -labeled acetate can be used to determine if under mesophilic conditions the methanogenic archaea is the only trophic group capable of consuming acetate, or if other populations, namely the phenol degraders, can also use acetate as CES. Furthermore, by using labeled phenol,

SIP will enable the identification of the microorganisms that degrade phenol. In the experiments conducted in this thesis, it was not fully clear which of the microorganisms are responsible for phenol degradation under saline thermophilic conditions.

The molecular, biochemical, and microbiological aspects of phenol degradation under (saline) thermophilic conditions should be better understood. To date, no comprehensive studies have been performed to elucidate the thermophilic phenol degradation pathway, unlike the studies conducted under mesophilic conditions (Nobu et al., 2015). Our results indicate that the phenol degradation pathway under thermophilic conditions is similar to the pathway under mesophilic conditions and follows the benzoyl-CoA route. Nevertheless, it remains unclear why metagenomic analyses did not reveal the presence of a sound phenol-degrading microorganism such as *Syntrophorhabdus* sp.

Results did not sufficiently reveal the understanding of the inhibitory processes considering the sub-cell mechanisms that are affected in the biomass. Experimentation with single, toxic or inhibitory, compounds may shed light on the effects (changes in IC_{50} or LC_{50}) of such compounds on different types of microorganisms besides the methanogens. It will be impossible to discern the exact mechanism(s) affecting the biomass activity when a complex matrix such as BFC is used. In addition, the molecular basis of microbial adaptation to toxic or inhibitory compounds is not completely understood.

The degradation routes for most of the compounds present in the BFC are completely unknown under anaerobic conditions. The study of the individual degradation routes of organic compounds is challenging, and likely not possible because of all the requirements to perform proper research under anaerobic conditions. However, the results obtained in this thesis suggest the possibility of a broader spectrum of organic molecules that can be anaerobically degraded when the proper microbial populations are developed and retained inside the reactor.

More extensive research is required on the treatment of complex (petro-)chemical wastewater such as BFC. However, for conducting such experiments, higher amounts, and higher concentrations of BFC are required, which can be attained by implementing a better fume collection method. Unlimited availability of BFC will allow the increase in the COD load of the reactor and the extension of the operation time of the AnMBR with BFC as the sole substrate. In addition, simultaneous operation of an AnMBR and a granular sludge bed reactor for BFC treatment will allow comparing the reactors' performance and stability in terms of COD removal efficiency, sludge loading and

conversion rates, and toxic effects on the biomass. Energy consumption and costs estimates of AnMBR operation in comparison to a granular sludge bed reactor will yield valuable information for any upscaling of the technology.

The experiments reported in this thesis were conducted at an approximately infinite SRT to promote the development of slow-growing populations needed for the degradation of phenol, *p*-cresol, resorcinol, or the BFC. However, extremely long SRTs will imply a practically zero growth rate, due to the inverse relationship of the biomass growth rate with the SRT. Therefore, different SRTs may be studied to determine the optimal SRT for the development of the required biomass and the degradation of the compounds (COD).

AnMBRs can be used for the treatment of toxic, inhibitory, or presumably anaerobically-recalcitrant substrates to determine whether degradation under anaerobic conditions can be achieved when full biomass retention is ensured. In principle, the AnMBR represents the optimal reactor concept to promote the growth and development of toxicant degraders because of the full biomass retention offered by the reactor.

Finally, the use of DIET to enhance the degradation of toxic and inhibitory compounds may be further studied (Xu et al., 2019; Zhu et al., 2018). Experiments using compounds such as magnetite may show an increase in the degradation of aromatic compounds which need strong syntrophic relationships to channel the electrons produced during the biochemical degradation.

6.3 References

- Ceron-Chafla, P., Kleerebezem, R., Rabaey, K., van Lier, J.B., Lindeboom, R.E.F., 2020. Direct and Indirect Effects of Increased CO₂ Partial Pressure on the Bioenergetics of Syntrophic Propionate and Butyrate Conversion. *Environ. Sci. Technol.* 54(19), 12583-12592. <https://doi.org/10.1021/acs.est.0c02022>.
- Deng, Z., Poulsen, J. S., Nielsen, J., Weissbrodt, D., Spanjers, H., van Lier, Jules. (2023). Identification of protein-degraders in an anaerobic digester by protein stable isotope probing combined with metagenomics. *10.21203/rs.3.rs-3067754/v1*.
- Fuchs, G., 2008. Anaerobic metabolism of aromatic compounds. *Ann. N.Y. Acad. Sci.* 1125(1), 82-99.
- Karlsson, A., Ejlertsson, J., Nezirevic, D., Svensson, B.H., 1999. Degradation of phenol under meso- and thermophilic, anaerobic conditions. *Anaerobe* 5(1), 25-35. <https://doi.org/10.1006/anae.1998.0187>.
- Karlsson, A., Ejlertsson, J., Svensson, B.H., 2000. CO₂-dependent fermentation of phenol to acetate, butyrate and benzoate by an anaerobic, pasteurised culture. *Arch. Microbiol.* 173(5-6), 398-402. <https://doi.org/10.1007/s002030000160>.
- Nobu, M.K., Narihiro, T., Hideyuki, T., Qiu, Y.L., Sekiguchi, Y., Woyke, T., Goodwin, L., Davenport, K.W., Kamagata, Y., Liu, W.T., 2015. The genome of *Syntrophorhabdus aromaticivorans* strain UI provides new insights for syntrophic aromatic compound metabolism and electron flow. *Environ. Microbiol.* 17(12), 4861-4872. <https://doi.org/10.1111/1462-2920.12444>.
- van Lier, J.B., A. Seco, B. Jefferson, M.E. Ersahin and A. Robles (2019). Upgrading anaerobic sewage treatment applying membranes: AnMBR and UF post filtration. In: C.A. Chernicharo & T. Bressani-Ribeiro (eds). *Anaerobic Reactors for Sewage Treatment: Design, Construction, and Operation*, Chapter 11. IWA Publishing, doi: 10.2166/9781780409238_0349
- Van Lier, J.B., Mahmoud, N., Zeeman, G., 2020. Anaerobic wastewater treatment, in: Chen, G., van Loosdrecht, M.C.M., Ekama, G.A.B., D. (Eds.), *Biological wastewater treatment: principles, modelling and design*. IWA Publishing, pp. 701 - 756.
- Wang, J., Yao, H., 2021. Chapter 7 - Applications of DNA/RNA-stable isotope probing (SIP) in environmental microbiology, in: Gurtler, V. (Ed.) *Methods in Microbiology*. Academic Press, pp. 227-267. <https://doi.org/https://doi.org/10.1016/bs.mim.2020.11.004>.
- Xu, H., Chang, J., Wang, H., Liu, Y., Zhang, X., Liang, P., Huang, X., 2019. Enhancing direct interspecies electron transfer in syntrophic-methanogenic associations with (semi)conductive iron oxides: Effects and mechanisms. *Sci. Total Environ.* 695, 133876. <https://doi.org/https://doi.org/10.1016/j.scitotenv.2019.133876>.
- Yeoh, B.E.E., Morimura, S., Ikbal, Shigematsu, T., Razreena, A.R., Kida, K., 2002. Simultaneous Removal of TOC Compounds and NO₃⁻ in a Combined System of Chemical and Biological Processes for the Treatment of Wastewater from Rubber Thread Manufacturing. *Jpn. J. Water Treat. Biol.* 38, 57-67. <https://doi.org/10.2521/jswtb.38.57>.
- Zhu, H., Han, Y., Ma, W., Han, H., Ma, W., Xu, C., 2018. New insights into enhanced anaerobic degradation of coal gasification wastewater (CGW) with the assistance of graphene. *Bioresour. Technol.* 262, 302-309. <https://doi.org/https://doi.org/10.1016/j.biortech.2018.04.080>.

Appendix A1

Supplementary material Chapter 1

A.1 Appendix: Introduction

A.1.1 ADM1-based equations for phenol degradation

Based on the anaerobic digestion model No. 1 (ADM1) (Batstone et al., 2002) the following set of equations can be proposed to define the growth of phenol degraders and the consumption of phenol:

$$\frac{dX_{Ph}}{dt} = \mu_{Ph} \cdot X_{Ph} - k_{dPh} \cdot X_{Ph} \quad \text{Equation A.1.1}$$

$$\frac{dS_{Ph}}{dt} = -\frac{dX_{Ph}}{dt} \cdot \frac{1}{Y_{Ph}} \quad \text{Equation A.1.2}$$

Where:

X_{Ph} = Concentration of the active phenol degrader population [gCOD_{vss}·L⁻¹].

μ_{Ph} = Growth rate of the phenol degrader population [h⁻¹].

k_{dPh} = Decay rate of the phenol degrader population [h⁻¹].

S_{Ph} = Phenol concentration [gCOD_{phenol}·L⁻¹].

Y_{Ph} = Yield of phenol degraders on phenol [gCOD_{vss}/gCOD_{phenol}].

The growth rate of the phenol degraders is considered to follow a Haldane kinetic (Suidan et al., 1988) defined by:

$$\mu_{Ph} = \mu_{maxPh} \cdot \frac{S_{Ph}}{S_{Ph} + k_{sPh} + \frac{S_{Ph}^2}{k_{iPh}}} \quad \text{Equation A.1.3}$$

Where:

μ_{maxPh} = Maximum growth rate of the phenol degrader population [h⁻¹].

k_{sPh} = Half saturation coefficient [gCOD_{phenol}·L⁻¹].

k_{iPh} = Haldane inhibition constant [gCOD_{phenol}·L⁻¹].

And considering that m_{max} could be defined as:

$$\mu_{maxPh} = k_{maxPh} \cdot Y_{Ph} \quad \text{Equation A.1.4.}$$

Where:

k_{maxPh} = Maximum specific uptake rate of the active phenol degrader population [gCOD_{phenol}·gCOD_{vss}⁻¹·d⁻¹].

We can substitute in Eq. A.1.4 in Eq. A.1.3

$$\mu_{Ph} = k_{maxPh} \cdot Y_{Ph} \cdot \frac{S_{Ph}}{S_{Ph} + k_{sPh} + \frac{S_{Ph}^2}{k_{iPh}}} \quad \text{Equation A.1.5}$$

Substituting Eq. A.1.5 in equation A.1.1.

$$\frac{dX_{Ph}}{dt} = k_{maxPh} \cdot Y_{Ph} \cdot \frac{S_{Ph}}{S_{Ph} + k_{sPh} + \frac{S^2}{K_{iPh}}} \cdot X_{Ph} - k_{dphenol} \quad \text{Equation A.1.6}$$

Substituting Eq. A.1.6 in Eq. A.1.2 and taking into consideration that k_d does not imply phenol consumption

$$\frac{dS_{Ph}}{dt} = -k_{maxPh} \cdot \frac{S_{Ph}}{S_{Ph} + k_{sPh} + \frac{S^2}{K_{iPh}}} \cdot X_{Ph} \quad \text{Equation A.1.7}$$

According to equation A.1.6 and A.1.7, the active phenol-degrader population [X_{ph}] is capable of only use phenol [S_{ph}] as CES, while other physiological microbial populations use the other CES (Batstone et al., 2002) for example, the acetate degraders [X_{Ac}].

According to equation A.1.7, a higher phenol degradation rate could be promoted by the increase of the active concentration of the phenol degraders [X_{ph}], an increase in the specific uptake rate [k_{maxPh}] or by the increase in both.

A.1.2 References

Batstone, D.J., Keller, J., Angelidaki, I., Kalyuzhnyi, S.V., Pavlostathis, S.G., Rozzi, A., Sanders, W.T.M., Siegrist, H., Vavilin, V.A., 2002. The IWA Anaerobic Digestion Model No 1 (ADM1). Water Sci. Technol. 45(10), 65-73. <https://doi.org/10.2166/wst.2002.0292> [Water Science and Technology.



Appendix A2

Supplementary material Chapter 2



A.2 Appendix: Enhancing Phenol Conversion Rates in Saline Anaerobic Membrane Bioreactor Using Acetate and Butyrate as Additional Carbon and Energy Sources

A2.1 SMA inhibition data

Table A.2.1. Data from the SMA inhibition tests performed in the AnMBR biomass.

Experiment	Phenol [mg·L ⁻¹]	Control SMA*	Condition SMA* values			Average SMA*	SMA factor relative to control
1	50	0.25	0.25	0.27		0.26	1.03
2	200	0.19	0.26	0.22	0.22	0.23	1.27
3	200	0.49	0.38	0.44	0.41	0.41	0.82
4	500	0.40	0.26	0.33	0.32	0.30	0.75
5	500	0.40	0.230	0.26	0.28	0.28	0.71

*All SMA values are presented as $\text{gCOD-CH}_4\cdot\text{gVSS}^{-1}\cdot\text{d}^{-1}$

A.2.2 Inhibition of the acetoclastic SMA of the AnMBR sludge by acetate and butyrate degradation activity

The effect of high concentration of acetate on the specific methanogenic activity (SMA) of the sludge was determined with a series of batch test. Even though the maximum acetate COD concentration in the influent of the AnMBRs was set on $2.0 \text{ g}\cdot\text{L}^{-1}$, we wanted to confirm that the biomass would not be inhibited by the acetate.

To perform the experiments, 250 mL Scott glass reactors were used. Biomass from the AnMBR was taken to have a final VSS concentration in the batch reactors of $4 \text{ g}\cdot\text{L}^{-1}$ ($I/S = 2$ for the control with $2.0 \text{ gAc}\cdot\text{COD}\cdot\text{L}^{-1}$). Macro- and micronutrient solutions, phosphate solution A and phosphate solution B, and Na^+ as NaCl were dosed as in the same concentration as detailed for the AnMBRs (Section 2.3). A shaker (New Brunswick™, Eppendorf, Germany) at 130 rpm and at 35°C was used for the incubation. Methane production was continuously measured by an AMPTS system (Bioprocess Control, Sweden) following manufacturer's instruction.

To assess the biomass capacity for butyrate degradation, the batch experiments were repeated using sodium butyrate at 0.5, 2.0, and $3.0 \text{ gCOD}\cdot\text{L}^{-1}$ as the only carbon and energy source.

A.2.2.1 Results and discussion

The batch tests assays, showed that with an initial COD concentration of $10 \text{ g}\cdot\text{L}^{-1}$, the biomass had a similar SMA ($0.31 \pm 0.03 \text{ gCODCH}_4\cdot\text{gVSS}^{-1}\text{d}^{-1}$) value when compared to an initial acetate concentration of $2 \text{ gCOD}\cdot\text{L}^{-1}$ ($0.28 \pm 0.14 \text{ gCODCH}_4\cdot\text{gVSS}^{-1}\text{d}^{-1}$) meaning that the acetoclastic methanogenic population in the AnMBR biomass was active and not inhibited even at high acetate concentrations. Although acetate degradation under anaerobic conditions is commonly described following a Monod degradation kinetics (Batstone et al., 2002), it has also been reported to follow a Haldane kinetic, in which there is an inhibition at high substrate concentrations (Kus and Wiesmann, 1995; Vavilin and Lokshina, 1996).

Both SMA values are in the range for acetoclastic methanogenesis of phenol-degrader suspended biomass in a saline matrix (Muñoz Sierra et al., 2017). However, the values are lower to those reported for phenol-degrading granular biomass such as 0.64 (Fang et al., 1996), 1.10 (Zhou and Fang, 1997), 0.72 (Tay et al., 2000), 1.02 (Fang and Zhou, 2000), 0.75 and 0.72 (Tay et al., 2001) $\text{gCODCH}_4\cdot\text{gVSS}^{-1}\text{d}^{-1}$. Also, our values are lower in comparison to the reported SMA values for phenol-degrading granular biomass in saline matrix going from 1.0 to $3.1 \text{ gCODCH}_4\cdot\text{gVSS}^{-1}\text{d}^{-1}$ (Wang et al., 2017).

For butyrate, and despite a lag phase of 2.5 days, an average SMA value of $0.18 \text{ gCODCH}_4\cdot\text{gVSS}^{-1}\text{d}^{-1}$ was found (data not shown). Only one reported value in the literature of $0.89 \text{ gCODCH}_4\cdot\text{gVSS}^{-1}\text{d}^{-1}$ for phenol-degrading biomass (Fang and Zhou, 2000) was found. Which was higher than the value that we obtained ($0.18 \pm 0.01 \text{ gCODCH}_4\cdot\text{gVSS}^{-1}\text{d}^{-1}$). However, since butyrate was fully converted into CH_4 it indicated that the sludge had butyrate oxidizer microorganisms confirming that butyrate could be used by the sludge as a CES.

A.2.3 Second experiment for the reactor operation towards the usage of phenol as main carbon and energy source and the related microbial community

To double check whether phenol degradation was feasible with phenol as the main/unique carbon and energy source, a second continuous experiment with the AnMBR 1 (R1(S1)) was carried out following a different strategy.

The experiment began after the recovery the biomass following the intoxication by phenol [$0.9 \text{ gPh}\cdot\text{L}^{-1}$]. The same composition and concentrations of micro- and macronutrient solution, buffer solution, and yeast extract were used for the feeding solution. To carry out the experiment, R1 was operated during 100 days, and the operation was divided into three stages (Figure A.2.1). During stage 1, acetate [0.9



and $0.7 \text{ gCOD}\cdot\text{L}^{-1}$) and phenol at different concentrations [0.1 , 0.2 , 0.4 , 0.5 , and $0.65 \text{ gPh}\cdot\text{L}^{-1}$]. At day 53 the second stage started, and the acetate concentration in the influent was decreased to $0.07 \text{ gCOD}\cdot\text{L}^{-1}$. At day 85 the phenol concentration was decreased 0.65 to $0.56 \text{ g}\cdot\text{L}^{-1}$. In the third stage, at day 89, acetate concentration in the influent was increased to $0.6 \text{ gCOD}\cdot\text{L}^{-1}$ and at day 92 phenol was decreased to from 0.56 to $0.50 \text{ g}\cdot\text{L}^{-1}$. After the dosage of acetate, the sPhCR was regained.

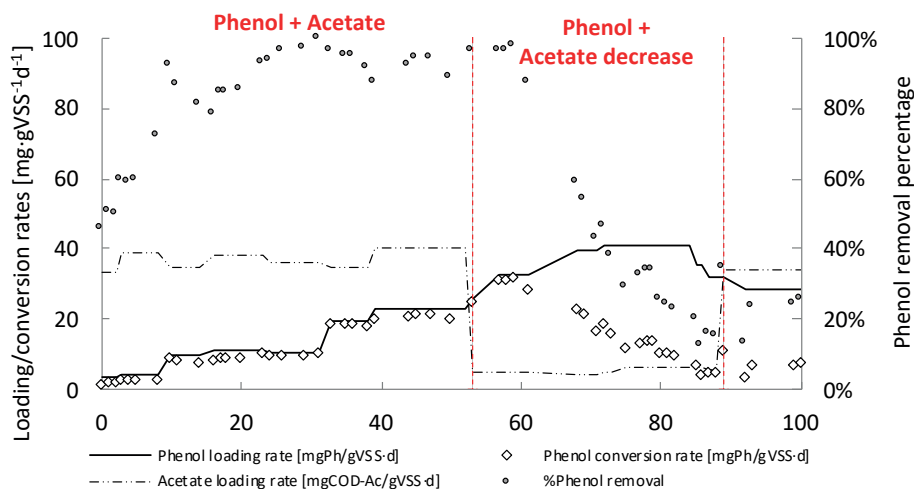


Figure A.2.1. Second operation of the AnMBR towards the usage of phenol as the main carbon and energy source (CaES).

A.2.4 Thermodynamic data for the calculation of ΔG°

Table A.2.2. Thermodynamic data for the different molecules in the phenol degradation reaction

Compound name	Chemical formula	MW (g/mol)	G° (KJ/mol)	Reference
Phenol	$\text{C}_6\text{H}_5\text{OH}$	94.11	-29.7	Hanselmann <i>et al.</i> 1991
Acetate	$\text{C}_2\text{H}_3\text{O}_2^-$	59.04	-369.4	Heijnen & Kleerebezem 2010
Butyrate	$\text{C}_4\text{H}_7\text{O}_2^-$	87.09	-352.6	Heijnen & Kleerebezem 2010
Water	H_2O	18.01	-237.18	Heijnen & Kleerebezem 2010
Hydrogen	H_2	2.02	0	Heijnen & Kleerebezem 2010
Proton	H^+	1.01	0	Hanselmann <i>et al.</i> 1991
Electron	e^-	0.00	0	Heijnen & Kleerebezem 2010

A.2.5 Biogas composition and production rate for the AnMBRs operation

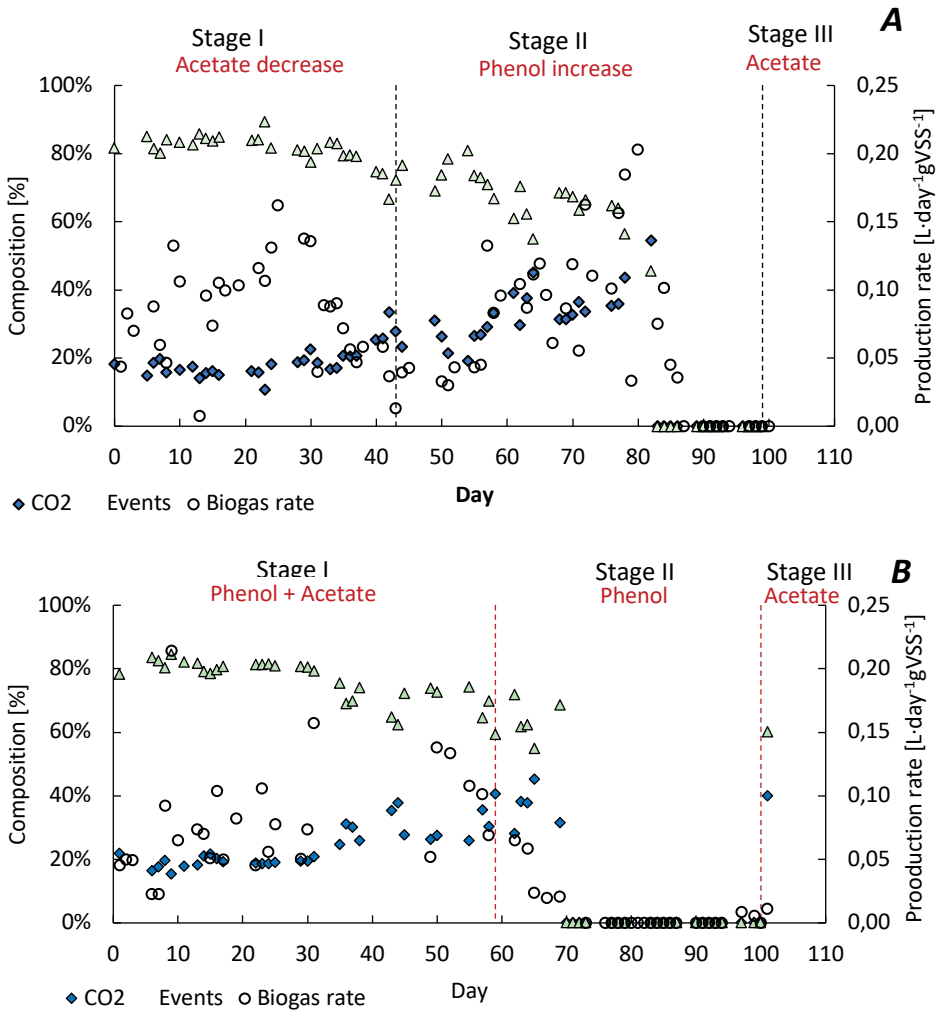


Figure A.2.2. Biogas production rate and composition (CH_4 and CO_2) for R1, and R2(a).

A.2.6 References

- Fang, H.H.P., Chen, T., Li, Y.-Y., Chui, H.-K., 1996. Degradation of phenol in wastewater in an upflow anaerobic sludge blanket reactor. *Water Res.* 30(6), 1353-1360. [https://doi.org/https://doi.org/10.1016/0043-1354\(95\)00309-6](https://doi.org/https://doi.org/10.1016/0043-1354(95)00309-6).
- Kus, F., Wiesmann, U., 1995. Degradation kinetics of acetate and propionate by immobilized anaerobic mixed cultures. *Water Res.* 29(6), 1437-1443. [https://doi.org/https://doi.org/10.1016/0043-1354\(94\)00285-F](https://doi.org/https://doi.org/10.1016/0043-1354(94)00285-F).
- Muñoz Sierra, J.D., Lafita, C., Gabaldón, C., Spanjers, H., van Lier, J.B., 2017. Trace metals supplementation in anaerobic membrane bioreactors treating highly saline phenolic wastewater. *Bioresour. Technol.* 234, 106-114. <https://doi.org/http://dx.doi.org/10.1016/j.biortech.2017.03.032>.
- Suidan, M.T., Najm, I.N., Pfeffer, J.T., Wang, Y.T., 1988. Anaerobic biodegradation of phenols inhibition kinetics and system stability. *Journal of environmental engineering* 114(6), 1359-1376.
- Tay, J.-H., He, Y.-X., Yan, Y.-G., 2000. Anaerobic biogranulation using phenol as the sole carbon source. *Water Environ. Res* 72(2), 189-194.
- Tay, J.-H., He, Y.-X., Yan, Y.-G., 2001. Improved anaerobic degradation of phenol with supplemental glucose. *Journal of environmental engineering* 127(1), 38-45.
- Vavilin, V.A., Lokshina, L.Y., 1996. Modeling of volatile fatty acids degradation kinetics and evaluation of microorganism activity. *Bioresour. Technol.* 57(1), 69-80. [https://doi.org/https://doi.org/10.1016/0960-8524\(96\)00052-1](https://doi.org/https://doi.org/10.1016/0960-8524(96)00052-1).
- Wang, W., Wu, B., Pan, S., Yang, K., Hu, Z., Yuan, S., 2017. Performance robustness of the UASB reactors treating saline phenolic wastewater and analysis of microbial community structure. *J. Hazard. Mater.* 331, 21-27. <https://doi.org/https://doi.org/10.1016/j.jhazmat.2017.02.025>.
- Zhou, G.-M., Fang, H.H.P., 1997. Co-degradation of phenol and m-cresol in a UASB reactor. *Bioresour. Technol.* 61(1), 47-52. [https://doi.org/http://dx.doi.org/10.1016/S0960-8524\(97\)84698-6](https://doi.org/http://dx.doi.org/10.1016/S0960-8524(97)84698-6).



Appendix A3

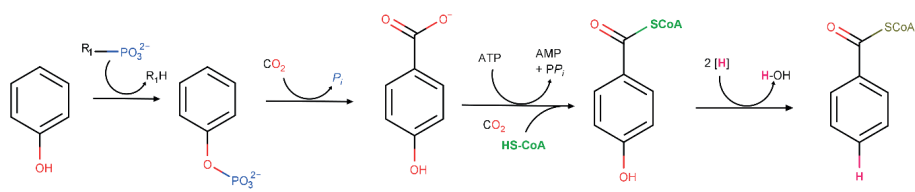
Supplementary material Chapter 3

A.3 Appendix: Syntrophic acetate oxidation having a key role in thermophilic phenol conversion in anaerobic membrane bioreactor under saline conditions

A.3.1 Phenol degradation routes

Via benzoyl-CoA pathway (mesophilic conditions) (Nobu et al., 2015).

A



Via caproate pathway (thermophilic conditions) (Fang et al., 2006).

B

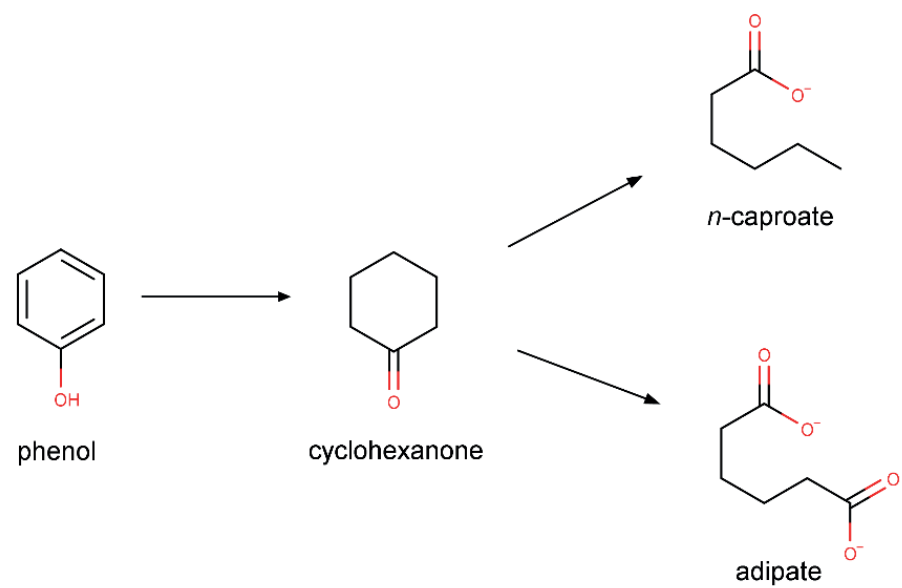


Figure A.3.1. Proposed phenol degradation routes under anaerobic conditions, via benzoyl-CoA (A) or caproate (B) pathways.

A.3.2 Permeability analysis of the membrane

The membrane's permeability was determined as the ratio of the (constant) operational flux (4.0 LMH) and the measured TMP. Figure A.3.2 shows the permeability of the membrane during the different operational stages of the reactor. In general, there is a decreasing trend from $13.1 \pm 1.8 \text{ LMH}\cdot\text{bar}^{-1}$ in Stage A to $8.4 \pm 1.2 \text{ LMH}\cdot\text{bar}^{-1}$ in Stage D which may relate to the generation of a biomass layer on the membrane. Interesting to note the sudden decrease in the permeability in the stage C which follows the decrease in the COD removal efficiency due to the operational conditions applied in Stage B.

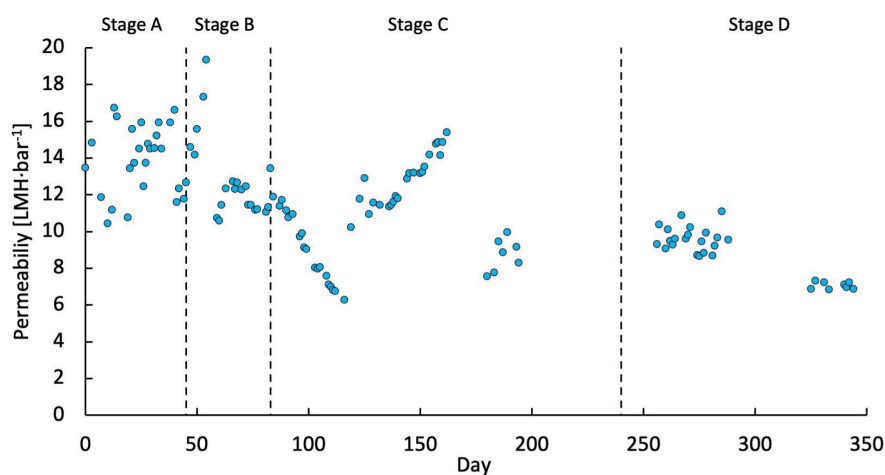


Figure A.3.2. Permeability of the AnMBR's membrane during the reactor operation.

A.3.3 Microscopic imaging membrane analysis

A new and the used membrane were cut both wet and after drying in a vacuum desiccator. Microscope images from the dry tubular membrane were taken by an environmental scanning electron microscope (ESEM) (XL30ESEM, Thermo scientific) (Figure A.3.3 A & B). A surface microscope (VHX- Digital Microscope) was used for taking pictures of the cross-sectional area of the membrane in wet conditions (Figure A.3.3 C & D).

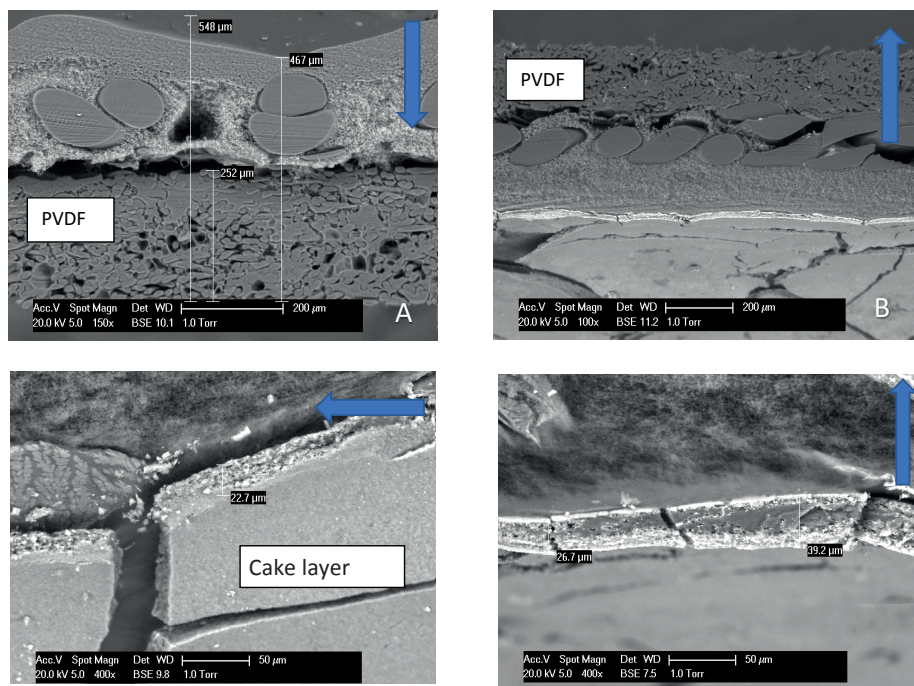


Figure A.3.3. Scanning electron microscope images of a cross-section of the UF PVDF membrane used in the AnMBR. The blue arrows on the right top corner show the direction of the flow of the permeate. A, shows the structure of the new membrane, one can see the mesh of the support material and the PVDF. B-D show the cake layer after the 350 day operation period. The thickness of the dry cake layer is indicated in the images.

A.3.4 References

- Fang, H., Liang, D., Zhang, T., Liu, Y., 2006. Anaerobic treatment of phenol in wastewater under thermophilic condition. *Water Res.* 40(3), 427-434. <https://doi.org/10.1016/j.watres.2005.11.025>.
- Nobu, M.K., Narihiro, T., Hideyuki, T., Qiu, Y.L., Sekiguchi, Y., Woyke, T., Goodwin, L., Davenport, K.W., Kamagata, Y., Liu, W.T., 2015. The genome of *Syntrophorhabdus aromaticivorans* strain UI provides new insights for syntrophic aromatic compound metabolism and electron flow. *Environ. Microbiol.* 17(12), 4861-4872. <https://doi.org/10.1111/1462-2920.12444>.



Appendix A4

Supplementary material Chapter 5

A.4 Appendix: Chemical characterization and anaerobic treatment of bitumen fume condensate using a membrane bioreactor

A.4.1 Bitumen fume condensate generation method

A plastic sampling probe was installed and inserted in the chimney that exhausts the gases generated in the rotary drum. After the bitumen fume production started, the fumes were directed through the probe to a small (approximately 30 L) cubical plastic condensing-device (Figure A.4.1). Inside of the device, two 10 L containers (condensers) connected in series were used. The first one was the main receptor whereas the second one was used as a trap for the remaining vapors. The condensing-device was kept under low temperature conditions by placing ice packs in its interior. The hose coming out from the second condenser in the condensing device was connected to a cylindrical filter. The filter was used to clean any remaining moisture. Lastly, another hose connected the filter to an air pump

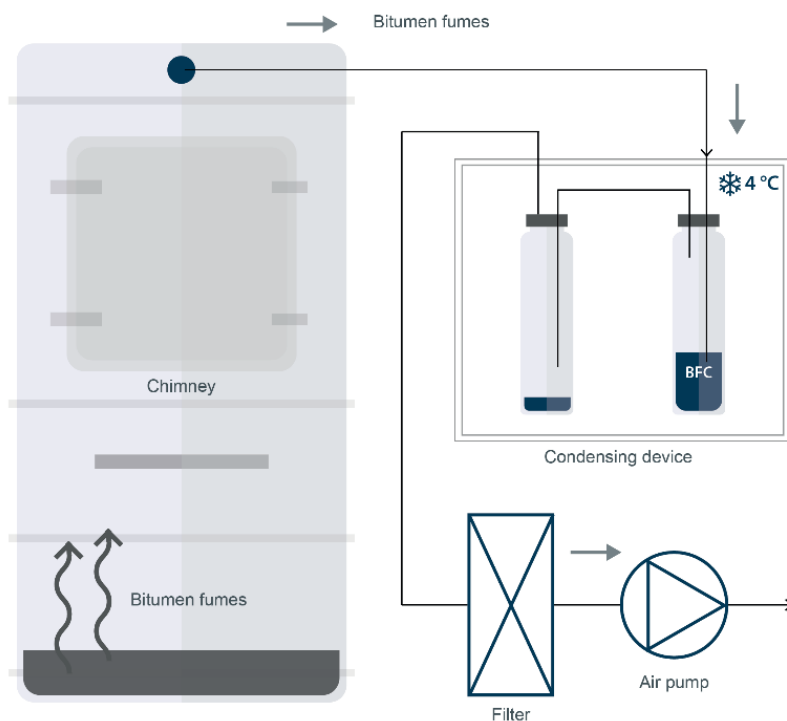


Figure A.4.1. Scheme of the bitumen fumes sampling and condensing system used to collect the BFC.

A.4.2 Volatilization tests

PAHs and fatty acids can be volatilized during the anaerobic digestion process (Van Metre et al., 2012). Therefore, a volatilization test was performed to verify whether the volatilization of the BFC could occur. For that purpose, nine 250 mL Schott Duran bottles with 200 mL of BFC in each were incubated at 35°C and 130 rpm in a temperature-controlled shaker (New Brunswick Scientific, Innova 44). The variation of COD concentration over 10 days was observed. In Figure A.4.2, the COD concentration determined on the first day of the experiment (1), on an intermediate day (7), and the last day (11) are presented. The columns indicate the average of the COD concentration of the nine bottles. No significant changes in the COD concentration were observed over the 10 days as the error bars (representing 95% confidence interval) overlapped. The results indicated that no volatilization of compounds could occur during the anaerobic digestion at the applied temperature of 35°C.

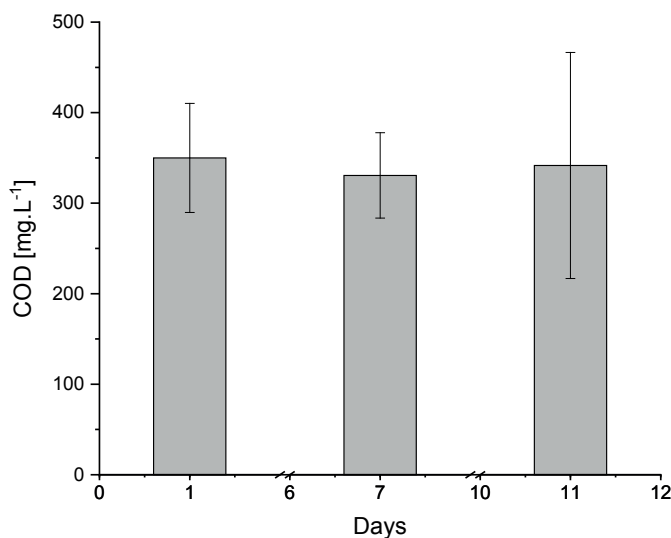


Figure A.4.2. Variation of the COD concentration over the volatilization test. Error bars 95% C.I.

A.4.3 Targeted analysis GC-MS/MS

Table A.4.1. List and concentrations of the 67 compounds analyzed by GC-MS/MS

No. of compound	Compound	ug/L
1	1,2,4-trichloorbenzeen	<0.02
2	1,2-dichlorobenzene	<0.02
3	1,3,5-trichloorbenzeen	<0.02
4	1,3-dichloorbenzeen	<0.02
5	1,4-dichloorbenzeen	<0.02
6	1,2,3-trichloorbenzeen	<0.02
7	pentachloorbenzeen	<0.04
8	1,2,4,5-tetrachloorbenzeen	<0.04
9	1,2,3,4-tetrachloorbenzeen	<0.02
10	hexachloorethaan	<0.02
11	hexachloorbutadien	<0.02
12	fluorantheen	0.02
13	antraceen	<0.004
14	benzo(a)antraceen	<0.01
15	acenaftyleen	0.27
16	benzo(b)fluorantheen	<0.008
17	benzo(ghi)peryleen	<0.008
18	benzo(k)fluoranthene	<0.008
19	acenafteen	0.03
20	fluorine	0.04
21	benzo(a)pyreen	<0.006
22	pyreen	<0.006
23	indeno (1,2,3-cd)pyreen	<0.008
24	naftaleen	0.7
25	chryseen	<0.006
26	fenantreen	0.04
27	2,4,4'-trichloorbifenyl (PCB-28)	<0.04
28	2,5,2',5'-tetrachloorbifenyl (PCB-52)	<0.04
29	2,4,5,2',5'-pentachloorbifenyl (PCB-101)	<0.02
30	2,4,5,3',4'-pentachloorbifenyl (PCB-118)	<0.02
31	2,4,5,2',4',5'-hexachloorbifenyl (PCB-153)	<0.04
32	2,3,4,2',4',5'-hexachloorbifenyl (PCB-138)	<0.04
33	2,3,4,5,2',4',5'-heptachloorbifenyl (PCB-180)	<0.04

Table A.4.1. Continued

No. of compound	Compound	ug/L
34	difenylamine	<0.04
35	fluxapyroxad	<0.06
36	furalaxyl	<0.06
37	sulfotep	<0.06
38	pyrimethanil	<0.04
39	alachloor	<0.02
40	ethofumesaat	<0.04
41	cyprodinil	<0.04
42	diethofencarb	<0.04
43	prosulfocarb	<0.06
44	propyzamide	0.18
45	isopyrazam	<0.08
46	kresoxim-methyl	<0.04
47	procymidon	<0.04
48	piperonyl-butoxide	<0.06
49	amisulbrom	<0.06
50	beta-endosulfan	<0.02
51	vinclozolin	<0.04
52	bupirimaat	<0.04
53	bitertanol	<0.06
54	gamma-hexachloorcyclohexaan	<0.04
55	beta-hexachloorcyclohexaan	<0.04
56	alfa-hexachloorcyclohexaan	<0.04
57	aldrin	<0.04
58	hexachloorbenzeen (HCB)	<0.04
59	alfa-endosulfan	<0.04
60	dichlobenil	<0.04
61	dieldrin	<0.04
62	heptachloor	<0.04
63	endrin	<0.04
64	p,p'-DDE	<0.04
65	p,p'-DDT	0.07



Table A.4.1. Continued

No. of compound	Compound	ug/L
66	p,p'-DDD	<0.04
67	dibenzo(a,h)antracene	<0.008

A.4.4 Organic compound non-targeted analysis GC-MS QTOF

Table A.4.2. Compounds found in the BFC by the GC/MS-QTOF analysis

Retention time	Compound	Formula
7.32	Cyclopentanone	C ₅ H ₈ O
7.57	Urea, propyl-	C ₄ H ₁₀ N ₂ O
7.80	2,5-Hexanedione	C ₆ H ₁₀ O ₂
7.83	Pyridine, 2,5-dimethyl-	C ₇ H ₉ N
8.34	2-Butyn-1-al diethyl acetal	C ₈ H ₁₄ O ₂
8.38	Butane, 2,2,3-trimethyl-	C ₇ H ₁₆
8.66	2,4-Dimethylfuran	C ₆ H ₈ O
8.75	2H-Pyran-2-one	C ₅ H ₄ O ₂
8.86	Methacrylic anhydride	C ₈ H ₁₀ O ₃
9.08	Pentanoic acid, 2-methyl-, anhydride	C ₁₂ H ₂₂ O ₃
9.14	Benzonitrile	C ₇ H ₅ N
9.97	2-Furancarboxylic acid, tetrahydro-3-methyl-5-oxo-	C ₆ H ₈ O ₄
10.21	2-Cyclopenten-1-one, 2,3-dimethyl-	C ₇ H ₁₀ O
10.27	Methacrylic anhydride	C ₈ H ₁₀ O ₃
10.53	Phenol, 2-methyl-	C ₇ H ₈ O
10.73	Benzenemethanol, .alpha.-methyl-, (R)-	C ₈ H ₁₀ O
10.83	Phenacylidene diacetate	C ₁₂ H ₁₂ O ₅
10.93	Ethyl 4-(ethyloxy)-2-oxobut-3-enoate	C ₈ H ₁₂ O ₄
10.95	p-Cresol	C ₇ H ₈ O
11.16	Ethanone, 1-(3-thienyl)-	C ₆ H ₆ OS
11.26	Ethanone, 1-(3-thienyl)-	C ₆ H ₆ OS
11.69	Phenylethyl Alcohol	C ₈ H ₁₀ O
12.05	Phenol, 2-ethyl-	C ₈ H ₁₀ O
12.19	Benzenemethanol, 2-methyl-	C ₈ H ₁₀ O
12.29	Phenol, 3,5-dimethyl-	C ₈ H ₁₀ O

Table A.4.2. Continued

Retention time	Compound	Formula
12.48	Benzenemethanol, .alpha.,4-dimethyl-	C ₉ H ₁₂ O
12.60	Phenol, 2-ethyl-	C ₈ H ₁₀ O
12.73	Phenol, 2,3-dimethyl-	C ₈ H ₁₀ O
12.95	p-Toluic acid, 4-cyanophenyl ester	C ₁₅ H ₁₁ NO ₂
12.99	Phenol, 3,4-dimethyl-	C ₈ H ₁₀ O
13.21	Benzofuran	C ₈ H ₆ O
13.61	Benzothiazole	C ₇ H ₅ NS
13.64	1H-Inden-1-ol, 2,3-dihydro-	C ₉ H ₁₀ O
13.77	Phenol, 2-ethyl-4-methyl-	C ₉ H ₁₂ O
13.79	Benzeneacetonitrile, .alpha.-methylene-	C ₉ H ₇ N
14.15	1-Benzocyclobutenecarbonitrile	C ₉ H ₇ N
14.18	Benzenepropanoic acid, 3-phenylpropyl ester	C ₁₈ H ₂₀ O ₂
14.41	1H-Inden-1-one, 2,3-dihydro-	C ₉ H ₈ O
14.80	2-Propenal, 3-(4-methylphenyl)-	C ₁₀ H ₁₀ O
14.96	1-Methylindan-2-one	C ₁₀ H ₁₀ O
15.15	Isoquinoline, 3-methyl-	C ₁₀ H ₉ N
15.29	Isoquinoline, 1-methyl-	C ₁₀ H ₉ N
15.34	1-Propanone, 3-chloro-1-phenyl-	C ₉ H ₉ ClO
15.42	7-Methylindan-1-one	C ₁₀ H ₁₀ O
15.56	1-Propanone, 3-chloro-1-phenyl-	C ₉ H ₉ ClO
15.79	1(2H)-Naphthalenone, 3,4-dihydro-	C ₁₀ H ₁₀ O
16.00	7-Methylindan-1-one	C ₁₀ H ₁₀ O
16.02	4H-1-Benzopyran-4-one	C ₉ H ₆ O ₂
16.12	Coumarin	C ₉ H ₆ O ₂
16.19	7-Methylindan-1-one	C ₁₀ H ₁₀ O
16.22	7-Methylindan-1-one	C ₁₀ H ₁₀ O
16.27	4-Methylphthalaldehyde	C ₉ H ₈ O ₂
16.45	4'-Methylbutyrophenone	C ₁₁ H ₁₄ O
16.60	2-Propenoic acid, 3-(2-hydroxyphenyl)-, (E)-	C ₉ H ₈ O ₃
16.63	Ethanone, 1-[4-(1-methylethenyl)phenyl]-	C ₁₁ H ₁₂ O
16.89	4'-Methylpropiophenone	C ₁₀ H ₁₂ O

Table A.4.2. Continued

Retention time	Compound	Formula
16.93	4'-Methylpropiophenone	$C_{10}H_{12}O$
17.08	4'-Methylpropiophenone	$C_{10}H_{12}O$
17.27	Benzonitrile, 2-ethoxy-	C_9H_9NO
17.87	1-Propanone, 1-(2,4-dimethylphenyl)-	$C_{11}H_{14}O$
18.09	4-Ethylbenzoic acid, 4-nitrophenyl ester	$C_{15}H_{13}NO_4$
18.34	Benzoic acid, 3,4-dimethyl-, methyl ester	$C_{10}H_{12}O_2$
18.38	2-Naphthalenemethanol	$C_{11}H_{10}O$
18.97	1-Propanone, 1-(2,4-dimethylphenyl)-	$C_{11}H_{14}O$
19.39	1-Acenaphthenol	$C_{12}H_{10}O$
20.26	9H-Fluoren-9-ol	$C_{13}H_{10}O$
20.63	Benzenesulfonamide, N-butyl-	$C_{10}H_{15}NO_2S$
20.70	2-Propanol, 1-chloro-, phosphate (3:1)	$C_9H_{18}C_3O_4P$
22.18	1H,3H-Naphtho[1,8-cd]pyran-1-one	$C_{12}H_8O_2$
22.98	Dibenzothiophene, 4,6-dimethyl-	$C_{14}H_{12}S$
24.60	Hexanoic acid, (2-hexanoylaminoethyl)-amide	$C_{14}H_{28}N_2O_2$

A.4.5 Surrogate organic parameters

Surrogate organic parameters were determined for the BFC. Dissolved organic carbon (DOC) and dissolved nitrogen (DN) samples were filtered through 0.45µm pore size GF/F Whatman and acidified, if needed, with HCl 37% to a pH=3. Analysis was carried out on a Shimadzu TOC-LCSH (Kyoto, Japan) total carbon analyzer which utilizes a high temperature method, in accordance with Standard method 5310B (AWWA, 1999). An Aqualog Horiba (Jobin Ivon) spectrophotometer was used to measure UV absorbance and fluorescence-EEM. Wavelengths from 200 to 800 nm with 4 nm increment for UV absorbance and fluorescence excitation wavelengths from 200 to 450 nm with 5 nm increment were measured. Meanwhile, emission wavelengths from 244.88 nm to 826.96 nm with an increment of 1.16 nm were measured for F-EEM. Data was processed in Matlab to correct for Raleigh/Raman scattering and inner filter effect (i.e., the absorbance of the water matrix) (Park and Snyder, 2018). The intensity of total fluorescence (TF, in Raman units) was integrated and calculated in the scanned area with excitation of 220-450 nm and emission of 240-580 nm wavelengths. Fluorescence in each region was characterized according to Chen et al., (2003) (Chen et al., 2003). BFC showed a strong absorbance at 254 nm as well as fluorescence, therefore bitumen

sample was diluted in DI water. Results shown in Table A.4.3 are already corrected with the dilution factor.

The high content on the UVA_{254} implies a high content of double bond and aromatic moieties compounds. This result can be correlated with the fluorescence-excitation emission matrix (F-EEM). Figure A.4.3 shows a high peak in the region 2 which implies a high content of simple aromatic compounds. Due to the nature of this water, which is industrial and not municipal, it is discarded that aromaticity may come from proteins. Therefore, it can be understanding the high aromaticity content through UVA_{254} belongs to low molecular weight compounds with aromatic and double bonds in their structure.

Table A.4.3. Surrogate organic parameters: UVA_{254} , TF, DOC, DN, and SUVA

Sample	UVA_{254} (cm^{-1})	TF (Raman Units nm^2)	DN (mg N/L)	SUVA (L/mg-m)
Lab blank	0.000017	3514.58	N.D.	1.7
Field Blank	0.002695	8956.76	N.D.	1.88
Bitumen (*)	3.615	10839326.26	46.17	0.74

(*) sample diluted 1:10

N.D.= No detected

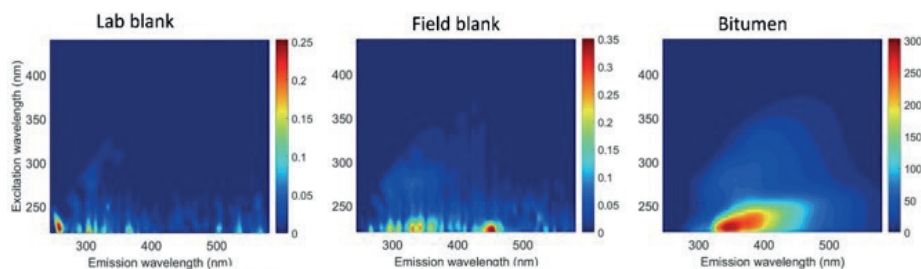


Figure A.4.3. Fluorescence excitation emission matrix (F-EEM) for bitumen sample

A.4.6 Inorganic ions determination in the BFC

Analysis for bromide, bromate, iodide, and iodate were carried out by IC-ICP/MS. For separation of the analytes, a Metrohm 850 professional IC was used. The samples were injected after filtration through a $0.45 \mu\text{m}$ glass fiber filter to eliminate particulate matter. Ion-chromatographic separation was done utilizing a Metrosep A ssup-5

100/4.0 column, eluents were 3.8 mM Na_2CO_3 /1.2 mM NaHCO_3 with 100mM H_2SO_4 for suppression. Analytes detection was carried out by Agilent 8800 ICP-MS Triple quadrupole, whereby the effluent of the suppressor unit was directly coupled to the cross-flow nebulizer system of the ICP/MS unit. Detection of the ions was done via the mass of bromine and iodine (79 and 127 respectively). Data acquisition was done through MassHunter 4.3 Workstation Software for 8800 ICP-QQQ G7201C Version C.01.03 2017. A standard mix of 4 ions was made in MQ water at 100 ppm. For quantification, a calibration curve with 11 levels was made from 1 to 1000 ppb. Samples were run in triplicate. BFC showed content for bromide and iodide (Table A.4.4). These inorganic ions' occurrence may be inherent to the materials used for asphalt production. Metal halides play a key role in bitumen since metal bromide could affect solids yield during thermal conversion (Prado et al., 2018). Nonetheless, this is the first time that iodide is detected on such sort of bitumen.

Table A.4.4. Inorganic ions content in bitumen sample

Sample	Iodate ($\mu\text{g/L}$)	Iodide ($\mu\text{g/L}$)	Bromate ($\mu\text{g/L}$)	Bromide($\mu\text{g/L}$)
Lab blank	N.D.	N.D.	N.D.	N.D.
Field Blank	N.D.	N.D.	N.D.	N.D.
Bitumen	N.D.	7.68	<LOD	355.53

N.D.= No detected

LOD= Level of detection

A.4.7 Principal coordinate analysis of the three biomass sources

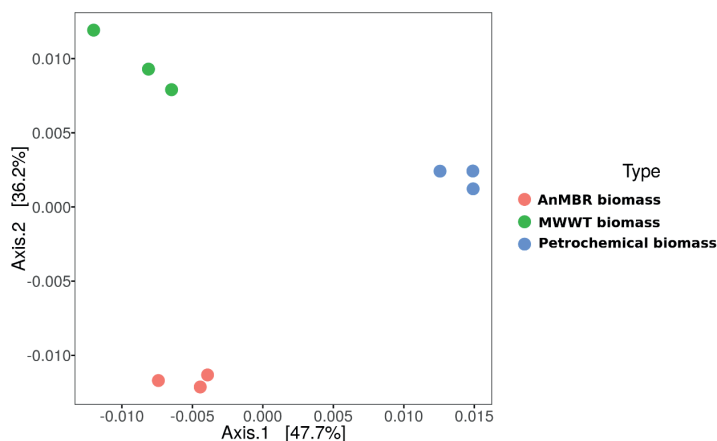


Figure A.4.4. Principal coordinate analysis performed in the three different biomass sources used for the biochemical tests. The graph shows a clear separation between the communities (in triplicate) of each of the sources. Therefore, it is possible to conclude that the samples were significantly ($p < 0.05$) different.

A.4.8 COD-BFC degradation in the AnMBR

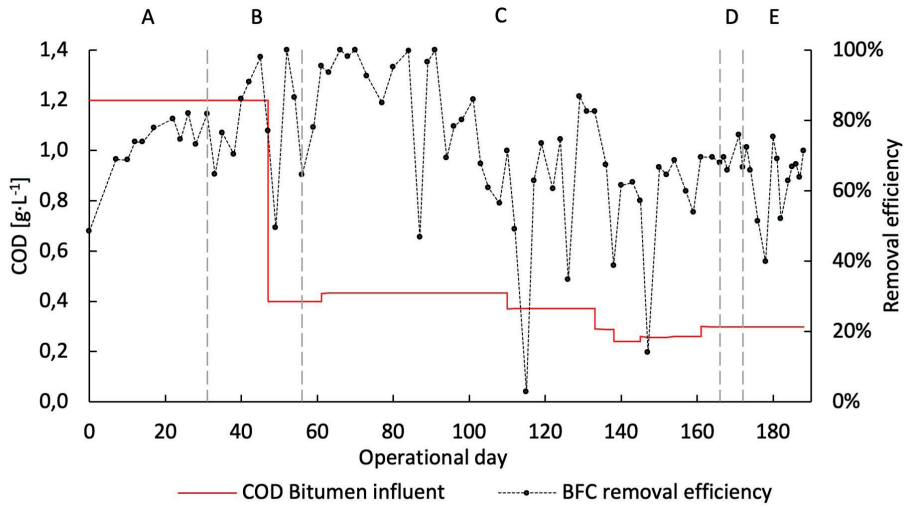


Figure A.4.5. COD-BFC in the influent and calculated COD-BFC removal efficiency during the different stages of the reactor operation.

A.4.9 References

- Almendariz, F.J., Meraz, M., Olmos, A.D., Monroy, O., 2005. Phenolic refinery wastewater biodegradation by an expanded granular sludge bed reactor. *Water Sci. Technol.* 52(1-2), 391-396. <https://doi.org/10.2166/wst.2005.0544> [J Water Science and Technology].
- Bhattacharyya, D., Allison, M.J., Webb, J.R., Zanatta, G.M., Singh, K.S., Grant, S.R., 2013. Treatment of an Industrial Wastewater Containing Acrylic Acid and Formaldehyde in an Anaerobic Membrane Bioreactor. *J. Hazard. Toxic Radioact. Waste* 17(1), 74-79. [https://doi.org/doi:10.1061/\(ASCE\)HZ.2153-5515.0000148](https://doi.org/doi:10.1061/(ASCE)HZ.2153-5515.0000148).
- Chen, W., Westerhoff, P., Leenheer, J.A., Booksh, K., 2003. Fluorescence Excitation–Emission Matrix Regional Integration to Quantify Spectra for Dissolved Organic Matter. *Environ. Sci. Technol.* 37(24), 5701-5710. <https://doi.org/10.1021/es034354c>.
- Garcia-Mancha, N., Puyol, D., Monsalvo, V.M., Rajhi, H., Mohedano, A.F., Rodriguez, J.J., 2012. Anaerobic treatment of wastewater from used industrial oil recovery. *J. Chem. Technol. Biotechnol.* 87(9), 1320-1328. <https://doi.org/10.1002/jctb.3753>.
- Gasim, H., Kutty, S., Isa, M.H., 2012. Anaerobic treatment of petroleum refinery wastewater. *Int. J. Chem. Mol. Eng.* 6(8), 512-515.
- Guyot, J.P., Macarie, H., Noyola, A., 1990. Anaerobic digestion Of a Petrochemical Wastewater using the UASB process. *Appl. Biochem. Biotechnol.* 24(1), 579-589. <https://doi.org/10.1007/BF02920280>.
- Jafarzadeh, M.T., Mehrdadi, N., Hashemian, S.J., 2012. Application of an anaerobic hybrid reactor for petrochemical effluent treatment. *Water Sci. Technol.* 65(12), 2098-2105. <https://doi.org/10.2166/wst.2012.088>.
- Ji, G.D., Sun, T.H., Ni, J.R., Tong, J.J., 2009. Anaerobic baffled reactor (ABR) for treating heavy oil produced water with high concentrations of salt and poor nutrient. *Bioresour. Technol.* 100(3), 1108-1114. <https://doi.org/https://doi.org/10.1016/j.biortech.2008.08.015>.
- Kennes, C., Mendez, R., Lema, J.M., 1997. Methanogenic degradation of p-cresol in batch and in continuous UASB reactors. *Water Res.* 31(7), 1549-1554. [https://doi.org/https://doi.org/10.1016/S0043-1354\(96\)00156-X](https://doi.org/https://doi.org/10.1016/S0043-1354(96)00156-X).
- Kleerebezem, R., Beckers, J., Hulshoff Pol, L.W., Lettinga, G., 2005. High rate treatment of terephthalic acid production wastewater in a two-stage anaerobic bioreactor. *Biotechnol. Bioeng.* 91(2), 169-179. <https://doi.org/10.1002/bit.20502>.
- Kleerebezem, R., Lettinga, G., 2000. High-rate anaerobic treatment of purified terephthalic acid wastewater. *Water Sci. Technol.* 42(5-6), 259-268. <https://doi.org/10.2166/wst.2000.0522> [J Water Science and Technology].
- Kleerebezem, R., Mortier, J., Hulshoff Pol, L.W., Lettinga, G., 1997. Anaerobic pre-treatment of petrochemical effluents: Terephthalic acid wastewater. *Water Sci. Technol.* 36(2), 237-248. [https://doi.org/https://doi.org/10.1016/S0273-1223\(97\)00393-4](https://doi.org/https://doi.org/10.1016/S0273-1223(97)00393-4).
- Noyola, A., Macarie, H., Varela, F., Landrieu, S., Marcelo, R., Rosas, M.A., 2000. Upgrade of a petrochemical wastewater treatment plant by an upflow anaerobic pond. *Water Sci. Technol.* 42(5-6), 269-276. <https://doi.org/10.2166/wst.2000.0523> [J Water Science and Technology].
- Park, M., Snyder, S.A., 2018. Sample handling and data processing for fluorescent excitation-emission matrix (EEM) of dissolved organic matter (DOM). *Chemosphere* 193, 530-537. <https://doi.org/https://doi.org/10.1016/j.chemosphere.2017.11.069>.
- Prado, G.H.C., Riya, Hyrve, M., de Klerk, A., 2018. Role of metal halides in coke formation during bitumen upgrading. *Fuel* 211, 775-782. <https://doi.org/https://doi.org/10.1016/j.fuel.2017.09.052>.

- Ribeiro, R., de Nardi, I.R., Fernandes, B.S., Foresti, E., Zaiat, M., 2013. BTEX removal in a horizontal-flow anaerobic immobilized biomass reactor under denitrifying conditions. *Biodegradation* 24(2), 269-278. <https://doi.org/10.1007/s10532-012-9585-2>.
- Siddique, M.N.I., Sakinah Abd Munaim, M., Zularisam, A.W., 2014. Mesophilic and thermophilic biomethane production by co-digesting pretreated petrochemical wastewater with beef and dairy cattle manure. *J. Ind. Eng. Chem* 20(1), 331-337. <https://doi.org/https://doi.org/10.1016/j.jiec.2013.03.030>.
- Van Metre, P.C., Majewski, M.S., Mahler, B.J., Foreman, W.T., Braun, C.L., Wilson, J.T., Burbank, T.L., 2012. Volatilization of polycyclic aromatic hydrocarbons from coal-tar-sealed pavement. *Chemosphere* 88(1), 1-7. <https://doi.org/10.1016/j.chemosphere.2011.12.072>.
- Wang, W., Han, H., Yuan, M., Li, H., 2010. Enhanced anaerobic biodegradability of real coal gasification wastewater with methanol addition. *J. Environ. Sci. (China)* 22(12), 1868-1874. [https://doi.org/https://doi.org/10.1016/S1001-0742\(09\)60327-2](https://doi.org/https://doi.org/10.1016/S1001-0742(09)60327-2).
- Wang, W., Han, H., Yuan, M., Li, H., Fang, F., Wang, K., 2011. Treatment of coal gasification wastewater by a two-continuous UASB system with step-feed for COD and phenols removal. *Bioresour. Technol.* 102(9), 5454-5460. <https://doi.org/https://doi.org/10.1016/j.biortech.2010.10.019>.
- Wang, W., Yang, Q., Zheng, S., Wu, D., 2013. Anaerobic membrane bioreactor (AnMBR) for bamboo industry wastewater treatment. *Bioresour. Technol.* 149, 292-300. <https://doi.org/10.1016/j.biortech.2013.09.068>.



Professional acknowledgments

The successful completion of a PhD is a process that implies not only the work of the PhD candidate, but, it is the sum of the efforts of several people that help the PhD candidate. Therefore, I want to express my gratitude to every person who helped me to fulfill this journey.

First and foremost, I want to thank my promotor, Prof. dr. ir. Jules B. van Lier for accepting me in his research team, for his trust in me, for the freedom that he gave me to conduct my PhD research, for helping me to achieve my goal of becoming an expert in the wastewater treatment, for teaching me to be (self)critical, and for all the knowledge in the academic and professional areas he shared with me. This knowledge has allowed me not only to obtain a PhD degree but also, to acquire a position as a professional of the anaerobic digestion (AD). Jules, as I mentioned recently, for me, it is extremely enjoyable to have conversations with you, as every time we do so, I am still learning something new. It will always be an honor to mention that you are my PhD Promotor. Similarly, I want to thank my second promotor, Dr. ir. Henri Spanjers, for being part of this process, for his input in the academic writing, and for the lessons he gave me on a topic that I find fascinating: mathematical modeling of (anaerobic) bioprocesses.

In addition to my promotors, I thank one person who was crucial in my PhD cycle and development, Dr. ir. Julián D. Muñoz Sierra. Dr. Julian, thanks for all your support, principally during the beginning of the PhD, when everything was new and unknown to me. Upon my arrival in the Netherlands, you could understand me, especially, regarding the cultural shock that implies the change from a Latin American-based working culture to the Dutch one. You taught me a lot, not only about AD, bioprocesses, and the BioXtreme project but also about how to work and conduct myself in a top University and a high-performance environment such as the one at the TU Delft. Even when we were colleagues, I always considered you as my mentor. Thanks for everything.

I thank Ir. Alexander Hendriks and Dr. Xuedong Zhang for all the scientific discussions we had during the shaping of the research plan for my PhD. Thanks for sharing with me your experience as excellent researchers and knowledge in the AD area, your help was extremely useful and appreciated. Similarly, I thank Dr. Ralph Lindeboom for his help, especially, in the last year and half of the experimental period.

I thank all the members who worked together with me during my part of the BioXtreme project, Dr. Beatriz Egerland B., MSc. Daniël Huisman, Dr. Marjet Oosterkamp, MSc.

Laura M. Fonseca A., MSc. Kiyan M. Quchani, Dr. Amer El-Kalliny, MSc. Chang Gao, MSc. Athira Nair, Dr. Ensiyeh Taheri, Dr. Joonyeob Lee, and the internship students: Revathy Nahir, Nicolas Fouchier, Alberto Núñez, Mireya Puig, Yolanda Arruga, and Hemant Arora. Thanks to all of you because of your hard work and commitment to the project. Definitely, I could not have achieved all the results I got without your contribution!

I thank my colleagues Dr. ir. Pamela S. Cerón C., Dr. ir. Magela Odriozola A., and Dr. ir. Niels van Linden for all the discussions we had. I am glad I could share an office with such smart, capable, and successful people as the three of you. Thanks for being a source of inspiration and motivation. Thanks for your time to discuss and understand my research, and mostly, for your effort to provide me with very critical and valuable feedback. Your comments helped me to improve the quality of my research. Similarly, sincere thanks to my colleague MSc. Javier A. Pavez J. for all the interesting discussions we had about bioprocess engineering, statistics, academic writing, science in general, and especially the topics related to mathematical modeling of the AD processes. Thanks for all your help and knowledge shared.

I thank Dr. Daniel Cerqueda-García for all the work we have done together in the area of bioinformatics analyses. It has been a pleasure to cooperate with you for so many years since I was doing my MSc. Internship at the Instituto de Ecología at Ciudad Universitaria.

I want to thank I. D. Flor Arminda García Rea for all the help she provided to me in the graphical design and work not only for the scientific publications but for this thesis also. Thanks for materializing in beautiful figures my ideas. The work you did was of excellent quality as is everything you do in your life.

Thanks to Dr. P. Guillermo Zerón E. for the help sketching the chemical figures used in several of my scientific publications. To Dr. Ingrid Pinel for the help with the flow cytometry determinations.

To Dr. Nadia van Pelt for her help and advice for the editing of the scientific writing of the scientific publications and this thesis.

To the lab technicians Mohammed Jafar, Armand Middeldorp, Thor Reijs, Patricia van den Bos, and Jane Erkemeij. Thanks for all your help and hard work in the laboratory.



I thank Prof. dr. ir. David Weissbrodt and Dr. ir. Robert Kleerebezem. Thanks to both of you for being an important part of my PhD. Prof. dr. ir. David, thanks for your support, advice, interest, and sincere help offered to me during the first stage of my PhD. Dr. ir. Robert, thanks for all the knowledge you gave me! For me, it was a complete delight being present in each one of your courses. Thanks to you, I became a better scientist, with a stronger knowledge of environmental biotechnology and the amazing world of biothermodynamics.

And finally, I want to thank the members of my committee for reading my PhD dissertation and, if applicable, providing their valuable comments for improving my manuscript.

Personal acknowledgements

After some years, my PhD journey is coming to an end. With these lines, I will do my best to thank and acknowledge everyone who has been part of this enterprise.

First of all, I want to thank my Mexican people and my country (still), México, because, without them and their support, my academic life could have not been possible. Thanks to the contribution of all my Mexican people and the Mexican public university, I was able to get my academic formation, from high school to this PhD. I want to thank my University, the UNAM, because it prepared me for more than 11 years, and with the knowledge I acquired there, I was able to develop myself in a world-top university and a highly demanding environment as it is found in the TU Delft.

I thank my second country, the Netherlands. I will be always grateful for what this country has offered and given to me. In the Netherlands, I completed my development, not only in the professional but in the personal aspect of life. The Netherlands has shown me my potential and my limitations, and specially, it taught me to be mature and strong enough to accept and circumvent them.

I thank my new *alma mater*, the TU Delft, for everything it has given to me. I came to the TU following my life goal of becoming a professional and an expert in the application of bioprocesses for wastewater treatment, looking for challenges and ways to continuously improve myself, looking for professional and academic excellence, and I found everything, here, at the TU. Similarly, it taught me to value, treasure, and be grateful for every single moment that one can share with people that one appreciate. I will always strive to conduct myself in a manner that upholds the values, integrity, and academic excellence of the University.

I want to thank my beloved family, my sister, my mom, and my dad. Gracias por su amor incondicional y por todo su apoyo, gracias por siempre estar para mí, por haberme enseñado valores y haberme hecho aprender a creer en mí. Siempre voy a estar agradecido con Dios y el universo por dejarme tenerlos conmigo, los amo con todo mi corazón. A mi primo Salvador que es como un hermano para mí, te amo primito Totis. A mi senséi, el Dr. Armando Romero Díaz, muchas gracias por enseñarme el valor de la disciplina y la constancia, a dejar el alma en lo que hago, a nunca darme por vencido, y a siempre levantarme ante cualquier reto y adversidad. Sin duda, mis logros son en mucha parte gracias a ti, a tus enseñanzas, y al tiempo y al cariño que me diste. And specially, thanks to my sister, thanks for all your help in the PhD related-things,



thanks for all your time and effort to help me to create all the beautiful graphical abstracts, figures, and for the design of my cover page! Te amito mucho hermanita!

I thank Adrián González for our friendship that started many years ago when we were studying our MSc. at Edificio 5. We both started the process of looking for a PhD position abroad and arrived in February 2016 at the TU Delft. Thanks for sharing with me the research projects that were offered by Jules, and, thanks for the years we shared at Laan van Overvest. Such a life-changing experience the one we decided to do... I am glad to see you succeeding in all the areas of your life.

To Jules, for all his support, not only in the professional way but in the personal also. Thanks for all the details that you have had with me, for listening to me and helping me in the difficult moments. I have a lot of respect and appreciation for you Jules, not only as my Promotor and a world-class scientist, but also as a person.

Thanks to my first Colombian friends at the TU, to mis parceros Julian D. (Medellín), Juan Pablo (Cali), and Andrés (Bogotá). Thanks guys for being a support when I started at the TU. Thanks for sharing with me your experience and providing me with advice. Julian and JP, I still remember the visit to Jumbo after the first day at the TU! Thanks for all the nice moments we shared! I really appreciate you guys! And as well, Julian and JP, thanks for the hospitality when visiting Colombia. By the way JP, I definitely agree... "Cali es Cali, lo demás..."

To my "office mates" and friends, Pam, Mage, and Niels. As I always said, I was in an office with such special people! Thanks to the three of you for your friendship and for taking care of me, everyone in your particular way. You are undoubtedly a really important part of my PhD. So many things to remember with you. The congresses, our trips to Ghent (btw, thanks for the second one Mage XD), the dinners, Sinterklass, the lunchtime, football, parties, our whiteboard, scientific and non-scientific discussions, Macumbas, and for making me the responsible for the room-temperature control. Pam, thanks for being such a nice person to me, for always making yourself time to listen to me, and for all the nice tips for all my biochemical analyses. Thanks for introducing me to the fried sweet potatoes, I got addicted! It was always nice to go to Sportscenter and have a burger and a nice talk after such long, and sometimes suffering, days in the lab! Mage, thanks for being my modeling teacher, for the lessons of the membrane course, for the nice time we had at the DAAL, for our clearly defined four talking topics, and for our nice publication! Definitely, you are one of the best modelers (mathematical) but as well... one of the worst (Latin America) geographers I have ever met, just impressive in both of the topics! Compadre, thanks for all the

nice moments and fun we shared, the gezellige avonds op PSOR, the football matches we went to Rotterdam supporting Excelsior and watching “al Chucky”. Thanks for helping me to improve my Dutch and pass my Inburgering tests! For helping me to conduct some additional and non-PhD related research. And for teaching me words such as pizza polo, tekuilya, jorizo, and Coelho. And, sincerely, I directly blame you for suggesting and convincing me (though it was not so difficult) to install “The App”. I knew I should have not started with it, but, I will be completely sincere... It has been a lot of Poke-fun. ¡Los quiero mucho!

To the members of the BioXtreme team - Track II who became more than colleagues. To Beatriz, thanks for all the amazing work you did and for the nice friendship that we began after your internship! To Dani Huisman. Thanks for being such a kind and good person, I am so glad that currently we keep in touch as friends and as colleagues at Econvert, te quiero mucho Dani. To Laura Fonseca, even when we haven't met for a while, you know you will always have a special place for me! To Amer and Ensiyeh. And to Kiyan. Kiyan, as once I told you, never lose the trust in yourself, because you have a big star.

To León González, Tales Abreu, Sebastián Canizales, and Guilhermeinho Gaucho. Guys, your friendship is one of the biggest gifts of the PhD to my life. So glad and honored to be your friend!

To my friends during the beginning of the PhD, Felipe González, Paco Memo, Filip A., el Dr. Michael F., el Pepe, R. de la Garza, and the Catalan crew: Yahuma, Xavi, y Nachi. What a nice time we shared.

Thanks to all my colleagues and friends from the TU Delft: Javier and la Nicole, Sara, and David thanks for all the excellent moments and the fun we shared guys! To Diana Carolina, thanks for all your support, caring, and understanding during this last part of the PhD, thanks for listening to me in the tough moments, you have been really important to keep me motivated at this stage! To Carina, thanks for your sincere friendship, all the deep talks, and the nice (dancing) parties! To Steef, man, really nice times at the TU, not just at the colloquiums and PSOR but as well... Catching ‘em all using the unique and patented van Linden’s technique! Trouwens, send gifts jonge. To Armand, for all the nice time we had training together! To Antonella, and the Uruguasho Bruno Bicudo, Antonia M., Emilien B., Laïs, Hongxiao, Xuedong, Daniel Daniel, Alexander, Lenno, Saqr, Emiu, Maria Lousada, Yazmina, Ran, Peng, Dara, Frans Willem, Magnolia, Miguel Lourenzo, Daniel Dacomba, Nahomi W., Mohammed, Mona, Antonio M., Marjet, Moniquita, Sophie, Les, Dhavissen, Rifki, and Josif.



To Merle de Kreuk! Even when we could not work together and it was not possible to have you in my committee, I want to let you know that for me was amazing to meet you after reading so much about your work during my MSc! I enjoyed every time we discussed any topic. Thanks for being always so kind to me!

To my martial arts and sporting guys! Qichen and Marleen, Dhruv, Bram, and Franco! Guys, it was amazing all the trainings we had together, all the circuit trainings with Dick, all the rounds we fought, and of course, the traditional KFC dinners we shared!

To my friends in Mexico, Guillermo Zerón, Alfonso Osorno, Icken Hernandez, Oscar Ortiz, Emma Ruiz, Davry Aguilar, Desiree Chacón, Miry Arenas, Lucia López, Yessica Gómez, Angélica Martínez, Israel López, Alberto Villa, Liz Arango, Ir. Rodolfo Cortés, and my teacher Gabriel Rojas.

To my ex house mates, Carlos B. Sánchez y Polito di Dalmau. Gracias por su amistad y los excelentes momentos que hemos compartido chicos, se termina por fin esto, los quiero molt y ¡Olei Bichos!

To all the people and friends I met in Delft, el Nacho y la Chio, Mousa, Alina and Matei, Fardin, Rolien, Jessica, Diego, Manju, Marijn, Rebecca, Myrthe, Camila, Rosnelo, Satoshi, Diana Portillo, Elena, Chico G.

To my colleagues from my work with whom I shared this last stage of finalizing the PhD, Luis, Lau, Jeff, Willi, Javier, Santi, Rutger, Benno K., Jacob, Corinna, Dani, Ruben, Les, Lars, Stijn, and Daniek. And to my colleagues at Doetinchem, Emma, Tuur, Ian, Geo, Nadine, Jalmer, Rick, Marijn, and, Iñigo.



About the author

Victor Servando Garcia Rea was born in Mexico City, Mexico, on the 13th of April of 1988. Raised in a very loving and caring family, Victor S. showed since a very young age his concerns about the environment protection, mainly related to water pollution, a situation that he commonly observed during his trips in Mexico with his family. At the age of 12, he realized that through the study of chemistry, he could be able to propose solutions to solve wastewater-related problems. Consequently, he decided to pursue a scientific career with focus on chemistry, biochemistry, and microbiology which would allow him to reach his goal of becoming a wastewater treatment professional.



In 2002, Victor S. started his studies at the National University of Mexico (UNAM), in the high school “Preparatoria 9, Pedro de Alba”. In August 2005, he got accepted at the Chemistry Faculty of the UNAM where he completed a 5-years Bachelor’s degree in Pharmaceutical and Biological Chemistry. In 2013 Victor S. started his MSc. in Biological Sciences with focus on Environmental Biotechnology at the Laboratory for research in advanced process for water treatment (LIPATA), part of the Engineering Institute, at the UNAM. During his MSc project, Victor S. studied the degradation of 4-chlorophenol using a granular-biomass sequencing batch reactor under aerobic conditions. Victor researched the changes in the reactor’s performance and the microbial community of the aerobic granules when the biomass was kept operating at the (expected) maximum activity using a feeding strategy based on the microbial oxygen consumption.

In February 2016, Victor S. moved to Delft, the Netherlands, where he started his PhD in the Sanitary Engineering section at the Delft University of Technology with the support of CONACyT, the Mexican national council for science and technology. Victor S. joined the research group from Prof. dr. ir. Jules B. van Lier and became a member of the team working on the BioXtreme project. In his PhD, and with Prof. Jules B. van Lier and Dr. ir Henri Spanjers as his promoters, Victor studied the application of anaerobic membrane bioreactors for the treatment of chemical (phenolic-containing) and petrochemical wastewater under extreme biological conditions, for example high salinity and high temperature.

Currently, and since 2021, Victor S. is working as process technologist at the company Econvert, located in Heerenveen, in the beautiful Dutch province of Friesland. Econvert is part of the Nijhuis-Saur Industries (NSI) group and is the expert company in the application of anaerobic digestion for the treatment of industrial wastewater. In his position, Victor S. is responsible for studying and determining the feasibility of the application of anaerobic digestion for the treatment of new industrial wastewater types. In addition, he is part of the Econvert's innovation and development team and the NSI global research and development team where he applies his academic experience and knowledge for the development of new reactor types and processes for the treatment of wastewater.

Victor S. is, and will remain, eager on keep learning about biotechnological and biochemical processes that can be applied for the solution of environmental problems. His goal is to become an expert for the application of environmental biotechnology for the improvement of the environmental health.



List of Publications

Peer reviewed journal publications

Garcia Rea V. S., Muñoz Sierra J. D., Fonseca Aponte L. M., Cerqueda-Garcia D., Quchani K. M., Spanjers H., van Lier J. B. (2020). Enhancing Phenol Conversion Rates in Saline Anaerobic Membrane Bioreactor Using Acetate and Butyrate as Additional Carbon and Energy Sources. *F. Microbiol.*, 11. DOI: 10.3389/fmicb.2020.604173.

Garcia Rea V. S., Egerland Bueno B., Cerqueda-Garcia D., Muñoz Sierra J. D., Spanjers H., van Lier J. B. (2022). Degradation of p-cresol, resorcinol, and phenol in anaerobic membrane bioreactors under saline conditions. *Chem. Eng. J.*, 430. DOI: <https://doi.org/10.1016/j.cej.2021.132672>.

Garcia Rea V. S., Muñoz Sierra J. D., El-Kalliny A. S., Cerqueda-Garcia D., Lindeboom R. E.F., Spanjers H., van Lier J. B. (2023). Syntrophic acetate oxidation having a key role in thermophilic phenol conversion in anaerobic membrane bioreactor under saline conditions, *Chem. Eng. J.*, 455. DOI: <https://doi.org/10.1016/j.cej.2022.140305>.

Garcia Rea V. S., Egerland Bueno B., Muñoz Sierra J. D., Nair A., Lopez Prieto I. J., Cerqueda-Garcia D., van Lier J. B., Spanjers H. (2023). Chemical characterization and anaerobic treatment of bitumen fume condensate using a membrane bioreactor. *J. Hazard. Mater.*, 477. DOI: <https://doi.org/10.1016/j.jhazmat.2022.130709>.

Muñoz Sierra, J.D., **García Rea, V.S.**, Cerqueda-García, D., Spanjers, H., and van Lier, J.B. (2020) Anaerobic Conversion of Saline Phenol-Containing Wastewater Under Thermophilic Conditions in a Membrane Bioreactor. *Frontiers in Bioengineering and Biotechnology*, 8, art. no. 565311, DOI: 10.3389/fbioe.2020.565311

Muñoz Sierra, J.D., Garcia-Rea, V.S., Spanjers, H., and van Lier, J.B. Recent progress in chemical wastewater treatment by anaerobic membrane bioreactors. *In preparation*.

Garcia Rea, V.S., Huisman, D., Egerland Bueno, B., Muñoz Sierra, J.D., Cerqueda Garcia, D., Spanjers, H., and van Lier, J. B. Biodegradability assessment of aniline under methanogenic and saline conditions in anaerobic membrane bioreactor. *In preparation*

Book Chapters

van Lier, J.B., Mahmoud, N., **Garcia Rea V.S.**, 2023. Anaerobic wastewater treatment, in: Lopez-Vazquez, C.M., Damir, B., Volcke, E.I.P., van Loosdrecht, M.C.M., Wu, D., Chen, G. (Eds.), Biological Wastewater Treatment: Examples and Exercises. IWA Publishing, p. o. https://doi.org/10.2166/9781789062304_0507.

Conference presentations

Garcia Rea V.S., Munoz Sierra J. D., Oosterkamp M.J., Spanjers H. and van Lier J. B.. Phenol degradation by anaerobic membrane bioreactor. in 15th World Conference in Anaerobic Digestion. Beijing, 2017. *Poster*.

Garcia Rea V.S., J. D. Munoz Sierra, M.J. Oosterkamp, R. Lindeboom, H. Spanjers and J. B. van Lier. Enhancement of phenol conversion rate by addition of acetate in a thermophilic anaerobic membrane bioreactor. in XIII Latin American Workshop and Symposium on Anaerobic Digestion. Medellin, 2018. *Oral presentation*.

Garcia Rea V.S., Fonseca Aponte L.M., Muñoz Sierra J.D., Garcia-Cerqueda D., Spanjers H. and van Lier J.B. Enhanced phenol conversion rate and recovery time after phenol shock load in anaerobic membrane bioreactors by the dosage of acetate. in 16th IWA World Congress on Anaerobic Digestion Delft, The Netherlands, 2019. *Poster*.

Garcia Rea V. S., El-Kalliny A., Muñoz-Sierra J. D., Cerqueda-Garcia D., Lindeboom R., Spanjers H., van Lier J. B. Microbial community dynamics during enhanced phenol conversion rate in a thermophilic saline anaerobic membrane bioreactor. in 6th IWA Young Water Professionals Benelux Conference (Luxemburg), 2020. *Oral presentation*.

Garcia Rea V. S., Egerland Bueno B., Muñoz Sierra J. D., Nair A., Lopez Prieto I. J., CerquedaGarcia D., Spanjers H. and van Lier J. B.. Degradation of Phenolic Mixtures under Saline Conditions and Bitumen Fume Condensate wastewater in Anaerobic Membrane Bioreactor. in 17th World Conference in Anaerobic Digestion. Ann Arbor, Michigan, USA, 2022. *Oral presentation*.



